



PONTIFICIA UNIVERSIDAD CATOLICA DE CHILE
SCHOOL OF ENGINEERING

SPECTRAL METHODS FOR BOUNDARY INTEGRAL EQUATIONS IN COMPLEX MEDIA

JOSÉ ANDRÉS PINTO DENEGRI

Thesis submitted to the Office of Graduate Studies in partial fulfillment of
the requirements for the Degree of Doctor in Engineering Sciences

Advisors:

CARLOS JEREZ-HANCKES

MIGUEL TORRES

Santiago de Chile, April 2021

© MMXIX, JOSÉ ANDRÉS PINTO DENEGRI



PONTIFICIA UNIVERSIDAD CATOLICA DE CHILE
SCHOOL OF ENGINEERING

SPECTRAL METHODS FOR BOUNDARY INTEGRAL EQUATIONS IN COMPLEX MEDIA

JOSÉ ANDRÉS PINTO DENEGRI

Members of the Committee:

CARLOS JEREZ-HANCKES

DocuSigned by:

Carlos Jerez-Hanckes

4E8321EF7280451...

DocuSigned by:

Miguel Torres

1AFF1D517681434...

DocuSigned by:

Norbert Heuer

7BDD9167921C434...

DocuSigned by:

Daniel Hurtado S.

4AD1C27AD19B480...

DocuSigned by:

Michael Karkulik

D2B2FA78775540A...

DocuSigned by:

Andrea Moiola

F06E79C138C940E...

DocuSigned by:

Héctor Jorquera G.

EAF806E0AA12408...

MIGUEL TORRES

NORBERT HEUER

DANIEL HURTADO

MICHAEL KARKULIK

ANDREA MOIOLA

HÉCTOR JORQUERA

Thesis submitted to the Office of Graduate Studies in partial fulfillment
of the requirements for the Degree Doctor in Engineering Sciences

Santiago de Chile, April, 2021

*In memory of Rush Limbaugh &
Ashli Babbitt*

ACKNOWLEDGEMENTS

Always in the first place to God, my work and life belong to Him. To quote the great Rush Limbaugh -talent on loan from God- in other words, this thesis is a product of the gifts of the Lord.

To my family, Jose sr, Maria Angelica, Carlos, and my girlfriend Alejandra without their continuous support this would have been impossible.

To my advisor Carlos, whom I have the pleasure to know for eight years and has been a very special person in my growth in different aspects of life.

To the professors Norber Heuer, and Andrea Moila for their good recommendations which play a big role in this thesis. Also for the same reason to the reviewers, of the associated publications, who took the time to read and make very good suggestions.

To my friend and co-author in some publications Ruben, has been interesting four years I only wish you the best in whatever path in life you decide to take.

To my longtime friend Fernando who has endured more than almost every person coursing a doctoral program and has been a terrific friend in every stage of my life.

To my regular office mate Paul, and the not-so-regular Ignacio, Ignacia, and Isabel.

To the university futsal team, coaches, and companions. It was a long ride and I wish that future generations will make the team greater.

Special mention to Pumas futsal team, and the workers of SIEB who welcomed me in their football team every Wednesday. Words are not enough to express my gratitude for these two institutions.

Finally to two-person whom I do not know personally. First, to Eduardo Bonvallet, he was an inspiring figure that I started hearing on the radio back in the 90s and had a strong presence in different medias until his tragic death in 2015. His words helped me in many turbulent times and contribute greatly to the person I have grown to be. Rest in peace Guru.

Secondly, to president Donald Trump, I have never seen someone who works hard as him. His unapologetic willingness to fight for the Judeo-Christian and conservative principles is something that I admire deeply.

Contents

ACKNOWLEDGEMENTS	ii
List of Figures	ix
List of Tables	xii
ABSTRACT	xiii
RESUMEN	xv
Journal Publications	1
Chapter 1. GENERAL INTRODUCTION	3
1.1. Motivation	3
1.1.1. Mathematical Motivation	3
1.1.2. Physical motivation	8
1.2. Objective and Outline of the thesis	11
Chapter 2. High-order Galerkin Method for Helmholtz and Laplace Problems on Multiple Open Arcs	13
2.1. Introduction	13
2.2. Mathematical tools	16
2.2.1. General notation	16
2.2.2. Arcs	17
2.2.3. Sobolev spaces and trace operators	18
2.3. Boundary integral problem formulation	20
2.4. Numerical Analysis	27
2.4.1. Approximation Spaces	28
2.4.2. Convergence Results	30
2.5. Matrix computations	44
2.5.1. Fourier-Chebyshev expansions	45

2.5.2.	Kernel expansion	46
2.5.3.	Computations for $i \neq j$	46
2.5.4.	Computations for $i = j$	47
2.6.	Compression Algorithm	47
2.7.	Numerical Results	51
2.7.1.	Convergence Results	51
2.7.2.	Compression Results	52
2.8.	Concluding remarks	54
Chapter 3. Fast Solver for Quasi-Periodic 2D-Helmholtz Scattering in Layered Media		56
3.1.	Introduction	56
3.2.	Notation and Functional Space Setting	58
3.2.1.	General Notation	58
3.2.2.	Quasi-periodic Sobolev Spaces	59
3.2.3.	Quasi-periodic Sobolev Spaces on Boundaries and Traces	60
3.3.	Helmholtz problem in periodic layered media	63
3.3.1.	Geometric Setting	63
3.3.2.	Helmholtz transmission problem on periodic media	64
3.4.	Boundary integral equations	66
3.4.1.	Quasi-Periodic Fundamental Solution	66
3.4.2.	Layer Potentials and Boundary Integral Operators	68
3.4.3.	Boundary Integral Formulation	77
3.5.	Spectral Galerkin Method	83
3.5.1.	Discrete Spaces	84
3.5.2.	Discrete Problem	84
3.5.3.	Implementation	87
3.6.	Numerical Examples	89
3.6.1.	Code Validation	90
3.6.2.	Convergence results	91
3.7.	Conclusions	92

Chapter 4. Fast Galerkin Method for Solving Helmholtz Boundary Integral Equations	
on Screens	96
4.1. Introduction	96
4.2. Mathematical Tools	98
4.2.1. Geometry	99
4.2.2. Classical Functional Spaces	99
4.2.3. Spherical Harmonics and Projected Basis	101
4.2.4. Auxiliary Functional Spaces	103
4.3. Boundary Integral Formulation	106
4.3.1. Boundary Integral Operators	106
4.3.2. Boundary Integral Equations	107
4.4. Spectral Discretizations	108
4.4.1. Discrete Problem	109
4.4.2. Matrix Computation	111
4.4.3. Numerical Implementation	119
4.5. Full Discretization Error Analysis	119
4.5.1. Quadrature Error	120
4.5.2. Fully Discrete Error Analysis:	124
4.6. Numerical Results	128
4.6.1. Quadrature Results	129
4.6.2. Code Validation	130
4.6.3. More complex screens	131
4.7. Concluding Remarks	133
Chapter 5. Final Conclusions	135
References	137
APPENDIX A. Technical Results for Multiple Open Arcs Problems	156
A.1. Laplace Uniqueness Result	156
A.2. Technical Lemmas	157

A.2.1.	Proof of Lemma 2.2.1	157
A.2.2.	Proof of Lemma 2.4.6	158
A.2.3.	Proof of Lemma 2.4.7	159
A.3.	Basic Approximation properties	160
A.3.1.	Proof of Lemma 2.4.14	162
A.4.	Some properties of Chebyshev polynomials	164
APPENDIX B.	On the properties of quasi-periodic boundary integral operators for the Helmholtz equation	166
B.1.	Introduction	166
B.2.	Functional space framework	168
B.2.1.	General notation	168
B.2.2.	Quasi-periodic functions and distributions	170
B.2.3.	Quasi-periodic Sobolev spaces	173
B.3.	Time-Harmonic wave scattering by periodic surfaces in \mathbb{R}^2	188
B.3.1.	Unbounded wave scattering	188
B.3.2.	Quasi-periodicity of the solution and radiation condition	189
B.3.3.	Dirichlet-to-Neumann (DtN) maps	193
B.4.	Boundary integral operators	195
B.5.	Concluding remarks	203
B.6.	Proof of Theorem B.9	204
B.7.	Regularity of solutions and continuity of BIOs	207
APPENDIX C.	Technical Results for 3D-Screen Problems	223
C.1.	Proof of Lemma 4.3	223
C.2.	Singular Integrals Analysis	224
C.2.1.	General idea	224
C.2.2.	Integral I^c	225
C.2.3.	Integral I^d	228
C.2.4.	Integral I^e	229

APPENDIX D. Implementation Details for 3D Spectral Screen Solver	231
D.0.1. Screen Class	231
D.0.2. Green Function Class	232
D.0.3. Disk Function Class	232
D.0.4. Quadratures	233
D.0.5. Integration and Inside Integrator Class	233

List of Figures

- 1.1 Error of different approximation methods. In red with big circles, the approximation by piece-wise constant functions, and in green with small circles the spectral method approximation. The x-axis represents the number of functions (piece-wise constant or orthogonal polynomials) used to construct the approximation. 4

- 2.1 $\tilde{H}^{-\frac{1}{2}}(\hat{\Gamma})$ errors, for $g(t) = |t|^p$. Values m are slopes of $\log_{10}(\text{Error})$ with respect to $\log_{10} N$. Errors are computed with respect to an overkill solution with $N = 440$ 51

- 2.2 $\tilde{H}^{-\frac{1}{2}}(\Gamma)$ errors, for Γ given by $\mathbf{r}(t) = (t, |t|^p)$ and $g(t) = t^2$. Values m are slopes of $\log_{10}(\text{Error})$ with respect to $\log_{10} N$. Errors are computed with respect to an overkill solution with $N = 440$ 52

- 2.3 In (a), a smooth geometry with $M = 28$ open arcs, each with a parametrization $(at, c \sin(bt)) + \mathbf{d}$, where $a \in [0.45, 0.50]$, $b \in [1.0, 1.5]$, $c \in [1.0, 1.3]$, $\mathbf{d} \in [2, 3.5] \times [11, 25]$, and $t \in [-1, 1]$. In (b), convergence for the corresponding geometry and different wavenumbers using as right-hand side the trace of $g(\mathbf{x}) = \exp(-i\hat{\kappa}\mathbf{x} \cdot \mathbf{y})$, where $\hat{\kappa} = \kappa$ for $k > 0$, $\hat{0} = 5$, $\mathbf{y} = (\cos \alpha, \sin \alpha)$, and $\alpha = \pi/4$. The x-axis denotes the number of polynomials used per arc. Errors are computed with respect to an overkill solution with $N = 500$ per arc. The mean arc lengths in terms of the wavelength are $8\lambda, 16\lambda, 32\lambda$ for $\kappa = 25, 50, 100$ respectively. In (c) the error in the solution of the linear system for the different cases, and in (d) the corresponding conditioning number (in norm 2) for the linear systems. . . 53

- 3.1 Example of a multi-layered grating. \mathcal{G} is highlighted and the dotted lines represent its boundaries at 0 and 2π 64

- 3.2 Subfigure (a) shows the problem geometry. Subfigure (b) shows the error in the $\mathcal{V}_{\theta}^{\frac{1}{2}, -\frac{1}{2}}$ norm with respect to the analytic solution. We have included results for different numbers ghost layers (1,2 and 3, respectively), i.e., the first experiment

	considers only the first 3 layers (counting downwards), the second one considers the first 4 layers and the third considers all 5 layers.	91
3.3	Error in the $\mathcal{V}_{\theta}^{\frac{1}{2}, -\frac{1}{2}}$ norm with respect to the analytic solution. The legend indicates an estimate of the slope of the error convergence curves for different values of p (degrees of smoothness). Classically, error convergence estimates for spectral methods indicate the slope to be at least equal to p . We also consider the case $p = 2$, where the extra layer is \mathcal{C}^{∞} and the super-algebraic convergence rate is observed.	92
3.4	Subfigure (a) shows the problem geometry (with 12 layers). Subfigures (b), (c) and (d) display the errors (in the corresponding energy norm) for the different values of k_0 , i.e., 2.8, 14 and 28, respectively. Each of these subfigures present error convergence curves for the two scenarios of refraction indices considered and specified in Table 3.1. Notice that the curves in red—corresponding to parameters η_i^2 in Table 3.1, with higher discrepancy between layers—display a longer preasymptotic regime before convergence is observed for all considered values of k_0	93
3.5	Real part of the total wave ($u^{(\text{tot})} = u^{(\text{sc})} + u^{(\text{inc})}$) for each different value of k_0 , namely 2.8, 14 and 28. The refraction indices on each layer are those indicated on Table 3.1. The incidence angle is again 0.47.	95
4.1	Polar change of variables performed in (4.16).	113
4.2	Quadrature errors for $k = 2.8$, computed against an overkill with $N_q = 76$. The error is computed by taking the 2-norm ($\ A\ _2 = \sup_{\mathbf{v} \neq 0} \frac{\mathbf{v} \cdot A \mathbf{v}}{\ \mathbf{v}\ }$) we fix $N = 8$, (45 degrees of freedom).	129
4.3	(a) Convergence curves for the Laplace problems on the disk. Parameters for the plane wave are $k_0 = 2.8$, $\theta_0 = \pi/3$, $\varphi_0 = \frac{\pi}{4}$. Running times for $N = 14$ are 181s, 730s for Dirichlet and Neumann cases, respectively. (b) Maximum of the absolute values in the right-hand side for each of the corresponding levels N , i.e. for $N = 4$ are the maximum value between the terms $m = -4, -2, 0, 2, 4$. . .	131

4.4	Error in the $Q_e^{-\frac{1}{2}}$ -Norm for the Dirichlet problems, and $P_o^{\frac{1}{2}}$ for the Neumann problems. Overkill solutions are computed using $N = 20$. Run times for Dirichlet and Neumann problems (with $N = 20$) are 749s, 2087s respectively.	132
4.5	Geometry of Γ_3 , and Γ_4 .	133
4.6	Error in the $Q_e^{-\frac{1}{2}}$ -Norm for the Dirichlet problems, and $P_o^{\frac{1}{2}}$ for the Neumann. Overkill solutions are computed using $N = 28$. Run times for Dirichlet and Neumann problem (with $N = 28$) are 2800s, 6198s respectively.	133
4.7	(a)-(b) Screen Γ_5 profiles. (c) Convergence plots for Dirichlet and Neumann problems computed against an overkill solution computed with $N = 28$, for $k = 2.8$, $k_0 = k$, $\theta_0 = \frac{\pi}{2}$, and $\phi_0 = 0$. (d) Plot of the volume solution for the Dirichlet problem.	134
B.1	Sinusoidal grating	180
B.2	Square grating	180
B.3	Example of possible curves. Dotted lines represent periodic boundaries.	180
B.4	Periodic cell. Dotted and dashed lines represent periodic and fictitious boundaries Γ and Γ_H , respectively. Ω_H is domain enclosed by Γ and Γ_H whereas Ω lies above Γ .	189

List of Tables

2.1	Compression performance $\epsilon = 1e - 10, \kappa = 100$	54
2.2	Compression performance $\epsilon = 1e - 14, \kappa = 100$	55
3.1	Value of the refraction indices $\{\eta_i^1\}_{i=1}^{12}$ and $\{\eta_i^2\}_{i=1}^{12}$ (corresponding to the two considered cases) for the grating in Figure 3.5 (counting downwards).	92
4.1	Quadrature error for the weakly-singular operator with $k = 2.8$ computed against an overkill with $N_q = 92, N = 24$. The rule for increasing the quadrature points with N is $N_q(N) = 1.75N + 50$. The error again is computed as the 2-norm of the approximation of the weakly-singular operator matrix.	130
A.1	Coefficients used in Lemma A.4.1.	164
D.1	Computational cost in terms of number of multiplications.	237

ABSTRACT

The simulation of physical problems utilizing mathematical models traditionally leads to a system of partial differential equations whose solution describes the behavior of the physical quantities in consideration. Although the underlying mathematical theory provides results on the existence, uniqueness, and asymptotic behaviors of the solutions, explicit forms for the latter are known for relatively few cases. For this reason, different methods of approximation have been developed.

The most conventional methods of approximation consist of using local functions (typically defined over a mesh) in conjunction with a numerical method. The latter converts the system of partial differential equations into a linear system, whose solution gives the values to the local functions for the construction of the approximation.

On the other hand, it is well known that the use of high-order global functions (spectral methods) can approximate the solutions of standard partial differential equations more efficiently (in terms of accuracy achieved versus the number of degrees of freedom used). However, their use has traditionally been limited by the difficulties that arise when implementing these methods.

The objective of this thesis is to show that, in certain circumstances, spectral methods can be implemented efficiently, and we can rigorously show the properties of rapid convergence.

In particular, we will focus on the Helmholtz equation, which has applications to electromagnetic and acoustic wave scattering diffraction problems. More in detail, we will consider boundary integral formulations of the Helmholtz equation for three different problems, which are:

- (i) Problems of multiple open arcs in two dimensions.
- (ii) Quasi-periodic problems in two dimensions.
- (iii) Problems of open surfaces in three dimensions.

In each one of these problems we will: adequately describe the corresponding spectral method, analyze its mathematical properties, and detail how they can be implemented.

Keywords: spectral methods, boundary integral formulations, wave diffraction problems, open arc, quasi-periodic problems, open surfaces.

RESUMEN

La simulación de problemas físicos por medio de modelos matemáticos, tradicionalmente, se traduce en un sistema de ecuaciones diferenciales parciales cuya solución describe el comportamiento de las cantidades físicas en consideración. Pese a que la teoría matemática provee resultados sobre la existencia, unicidad, y comportamientos asintóticos de las soluciones, solo en relativamente pocos casos se cuentan con una forma explícita para estas últimas. Por esta razón se han desarrollado diversos métodos de aproximación.

Los métodos más convencionales de aproximación consisten en usar funciones locales (típicamente definidas sobre una malla) junto con un método numérico. Este último, convierte el sistema de ecuaciones diferenciales parciales en un sistema lineal, cuya solución da los valores a las funciones locales para construir la aproximación.

Por otra parte se sabe que la utilización de funciones globales de alto orden (métodos espectrales) pueden aproximar las soluciones de las ecuaciones más rápidamente. Sin embargo, su uso ha sido tradicionalmente limitado por las dificultades que surgen al implementar estos métodos.

El objetivo de esta tesis es mostrar que en ciertas circunstancias los métodos espectrales pueden ser implementados de manera eficaz y podemos mostrar rigurosamente las propiedades de convergencia rápida.

En particular nos centraremos en problemas de difracción de ondas acústicas (o electromagnéticas en ciertas polarizaciones) los cuales pueden ser modelados utilizando una formulación de integrales de frontera. Más específicamente consideramos tres casos:

- (i) Problemas de múltiples arcos abiertos en dos dimensiones.
- (ii) Problemas cuasi-periódicos en dos dimensiones.
- (iii) Problemas de superficies abiertas en tres dimensiones.

En cada uno de estos problemas describiremos adecuadamente el método espectral correspondiente, analizaremos sus propiedades desde un punto de vista matemático, y detallaremos como pueden ser implementados.

Palabras claves: métodos espectrales, formulación de integrales de frontera, problemas de difracción de ondas, arco abiertos, problemas cuasi-periódicos, superficies abiertas.

JOURNAL PUBLICATIONS

- (i) Chapter 2: Jerez-Hanckes, C., & Pinto J. (2020) High-order Galerkin method for Helmholtz and Laplace problems on multiple open arcs. *ESAIM: M2AN*, 54(6), 1975-2009.

Main scientific contributions:

- Semi-discrete analysis for limited regularity data based on Fourier-Chebyshev transforms without any assumption of the behavior of the solution.
- Efficient compression algorithm for the computation and storage of cross-interaction matrices.

- (ii) Chapter 3: Aylwin, R., Jerez-Hanckes, C., Pinto J. (2020) Fast Solver for Quasi-Periodic 2D-Helmholtz Scattering in Layered Media. *submitted*.

Main scientific contributions:

- Regularity of quasi-periodic integral operator on the corresponding Sobolev spaces for smooth grating interfaces.
- Efficient implementation of the integral operator with an adequate handling of the singularities.

- (iii) Chapter 4: Jerez-Hanckes, C., & Pinto J. (2020) Fast Galerkin Method for Solving Helmholtz Boundary Integral Equations on Screens. *submitted*.

Main scientific contributions:

- Definition of an adequate family of functional spaces that lead to a straightforward semi-discrete analysis.
- Detailed analysis of the integration of the associated singular functions that leads to an efficient implementation.
- Fully discrete error analysis through bounds of the complex extension of the spectral basis.

- (iv) Appendix B. Aylwin, R., Jerez-Hankes, C., Pinto J. (2019) On the Properties of Quasi-periodic Boundary Integral Operators for the Helmholtz Equation. Integral Equations and Operator Theory, 92.

Main scientific contributions:

- Definition of Sobolev quasi-periodic spaces, and extension of classical results for the quasi-periodic framework.
- Well-posedness of indirect Dirichlet and Neumann boundary integral formulations for Lipschitz gratings.

Chapter 1. GENERAL INTRODUCTION

1.1. Motivation

This thesis has two ideas as main motivation points, consequently, we will present each of them separately.

First, we will consider a pure mathematical motivation. We explain the principles behind spectral methods in a general sense and try to convince the reader why, in the right circumstances, they are an attractive alternative to the more widely used low order methods. We will also make a brief presentation of the state of the art of spectral methods, especially those works that are closely related to the topics of this thesis.

In the second part of the motivation, we will present the class of electromagnetic and acoustic problems that concern us and show the advantages of the spectral methods in this context.

1.1.1. Mathematical Motivation

Spectral methods, in a nutshell, are methods to approximate a given function by a linear combination of known functions (belonging to a particular family) that share the same domain and support of the original function. Different spectral methods differ in the family of functions used as bases. Examples of non-spectral methods are the approximation by means of locally supported function, or point-wise approximations.

Lets consider an example of an infinitely smooth function $f(x) = 0.28 \sin(2.8x) + 0.28 \sin(7x) + 0.7$ with domain in $[0, 1]$, and two approximations. First, by means of piece-wise constant functions, and secondly, by orthogonal polynomials (spectral approximation). We will compare them in terms of their L^2 error, ie.

$$\sqrt{\int_0^1 |f(x) - f_n(x)|^2 dx}$$

where f_n is the approximation (with $n \in \mathbb{N}$ denoting the number of basis used to construct the approximation), against the number of basis, n . The results are reported in Figure 1.1.

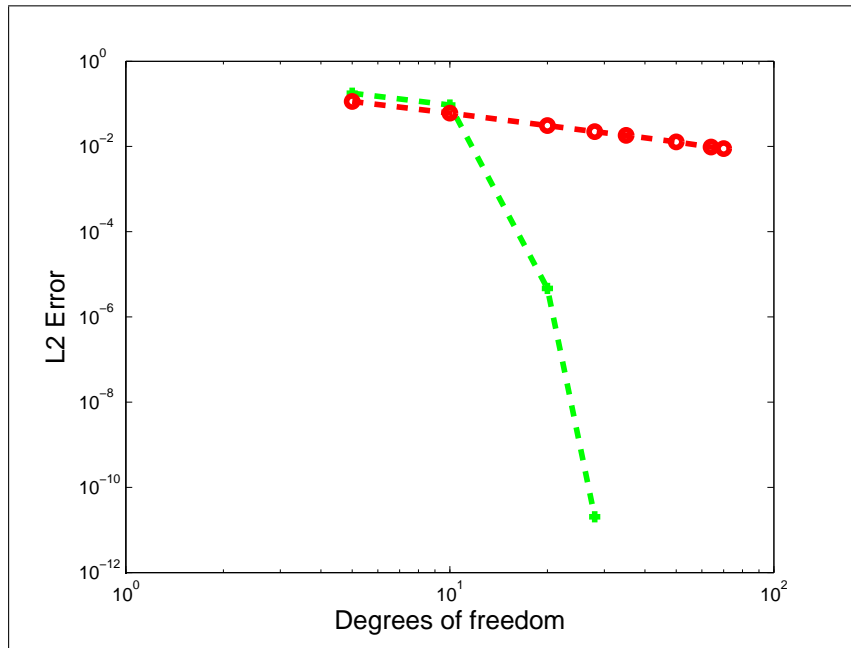


FIGURE 1.1. Error of different approximation methods. In red with big circles, the approximation by piece-wise constant functions, and in green with small circles the spectral method approximation. The x-axis represents the number of functions (piece-wise constant or orthogonal polynomials) used to construct the approximation.

A simple look at the figure shows that with the same number of piece-wise constant functions and orthogonal polynomials, the error in the spectral method is drastically inferior to the one of the local method. In fact, it can be rigorously proved that, for a class of smooth functions, the approximation error of the spectral method decays exponentially in the number of functions used. In contrast, the error for the piece-wise constant approximation decays as the inverse of the number functions. We refer to (L. Trefethen, 2013) for a more detailed discussion on the topic.

Generalizing the conclusion of our example, the spectral approximation performs exponentially better than the local alternative, but it is also more expensive (in terms of the number of operations) than using local low order functions. However, as we will see throughout this thesis, in many contexts the cost of the implementation is not extraordinarily high, and the benefits of using a small number of functions (which will be explained in the next section) make up for the more expensive implementation.

For the remainder of this thesis, our focus is to approximate a function which is the unique solution of a given partial differential equation¹, shortened as PDE. In this context, we can classify the spectral methods into two classes. First, and more classical, are the pseudo-spectral methods, also known as spectral collocation methods, in which the solution of a given PDE is expanded in terms of a global basis, and a system of equations is obtained by imposing equality in a grid of points. We refer to (L. N. Trefethen, 2000) and references therein for more details on this topic.

Secondly are the spectral Galerkin methods, the actual framework of this thesis. In general terms, the Galerkin methods do not obtain the system of equations by imposing the equality to hold on a set of points, but instead uses a scalar product and find the approximation as a projection on a finite-dimensional space. Spectral Galerkin methods use a finite-dimensional space spanning from the basis of a spectral method and the Galerkin method to construct the approximation.

While our focus is on the approximation of a solution of a PDE, in many situations it is convenient to transform the latter into a boundary integral equation (see (Sauter & Schwab, 2011), (McLean, 2000) for details on the equivalence of the two). More details on the situations in which this equivalence is convenient will be covered in the next section, but the premise of this thesis is that we are working on problems where it is convenient to use boundary integrals equations². In this context, spectral Galerkin methods (as well as spectral collocation, low order Galerkin, among others) are employed to approximate the solution of the associated boundary integral equation, which then yields an approximation of the solution of the PDE which will inherit the accuracy of the underlying approximation method.

The advantages of using a spectral Galerkin discretization for the approximation of a boundary integral equation are inherited from the Galerkin theory and the fast convergence of the spectral method. To be more precise these include:

¹We refer to the classical textbook (Evans, 2010) for a detailed review on the theory of partial differential equations, and to (Epstein, 2017) for a presentation of the importance of this kind of equations in the constructions of mathematical models.

²Also referenced as the boundary integral formulation.

- (i) Error bounds easily obtained using functional analysis tools (Lax-Milgram Lemma, or compact perturbation theory).
- (ii) Fast convergence whenever the real solution is smooth, which can be assured using PDE theory.
- (iii) Smaller linear system compared to low order Galerkin methods.

As for the drawbacks we can enumerate,

- (i) More expensive implementation compared to collocation and low order approximations.
- (ii) Lack of any fast compression algorithm in comparison to low order Galerkin method.
- (iii) Their utility is in general restricted to problems with smooth solutions.

This thesis will show how some of the drawbacks can be overcome in different contexts, but for now, let us present some previous works that have used spectral Galerkin methods in the context of boundary integral equations.

For two-dimensional problems, the work of (Fang, 1995) uses Fourier bases for the approximation of scattering problems of closed smooth objects. Same ideas were later used in (Thierry, Antoine, Chniti, & Alzubaidi, 2015) and in (Henríquez & Jerez-Hanckes, 2018). The method is also explained and analyzed in detail in (Saranen & Vainikko, 2013, Chapter 9). In the latter, a common feature of spectral methods is explained, that is the connection between spectral methods and pseudodifferential-operators theory³. The link between the two consists in that the basis of a given spectral discretization is the truncation to finite-dimension of the functions in which the action of pseudo-differential operators is well understood.

³A general class of operator which include integral and differential operators.

While smooth domains with closed boundary the solution of PDEs is known to be smooth, this does not follow if we consider infinite domains in which an open arc (or surface in three dimensions) is subtracted. For this class of problem, the solution exhibits singular behavior⁴ near the edges of the arc (or boundary of the surface in three dimensions). To achieve an efficient approximation, the basis of the spectral method has to explicitly include the singular behavior. This kind of problem has been studied in (Frenkel, 1983), and in (K. E. Atkinson & Sloan, 1991).

It is worth mentioning that if the solution is not smooth and this is not reflected by a special selection of the spectral basis, the spectral method will still converge faster than a standard local low order alternative, see (E. Stephan & Suri, 1989). In fact, it converges twice as fast (with respect to the number of functions used to construct the approximation) in the worst case. However, the difficulties that arise on the implementation overshadow the benefits for these cases.

In three dimensions, spectral methods are less common. However, for scattering problems on domains which are smooth deformations of the unitary sphere a spectral method based on spherical harmonics was implemented and analyzed in (Graham & Sloan, 2002).

Finally, we wish to mention a family of methods that are closely related to the spectral methods, known as hp-methods. The hp-methods are an extension of the low order methods in which local high order bases are used. While they benefit from the fast convergence of the spectral method and the flexibility of the low-order alternatives, they are typically restricted to the usage of polynomials only. A subfamily of these methods are the p-methods, where the supports (h-discretization) are fixed and only the polynomials degree are increased. When only one support is used, we get a spectral method with a polynomial basis. The topic is vast, so we include only a few references that explore problems similar to the ones presented in this thesis.

⁴the derivative of the solution is not bounded

For three-dimensional open surfaces, the work (Heuer, Maischak, & Stephan, 1999), shows that similar rates as the one obtained by a pure spectral method are achieved by hp-methods, but special care has to be taken on the refinement of the discretization near the boundary of the screens. The p-version was analyzed for 2d-polygons in (Guo & Heuer, 2004), and in (Bespalov & Heuer, 2005) for three-dimensional open surfaces.

1.1.2. Physical motivation

Let us now consider a direct scattering problem. In this problem, a known object is illuminated by an incident wave⁵. As a result, part of the wave penetrates the object, and the remaining part is scattered back to the medium.

The applications of this problem range from the design of electric hardware to medical imaging, including areas such as military design or cancer treatment.

Consider an open domain $\Omega \subset \mathbb{R}^d$, with $d \in \{2, 3\}$ whose boundary is denoted $\partial\Omega$. Under the assumption that the temporal component of the incident and scattered waves is an oscillatory function with a fixed frequency (time-harmonic), we will name u^{scat} , u^{inc} the spatial component of the scattered and incident wave respectively. With this notations the PDE model is to find u^{scat} such that

$$\begin{aligned} -\Delta u^{\text{scat}} - k^2 u^{\text{scat}} &= 0, \quad \text{in } \mathbb{R}^d \setminus \partial\Omega \\ \text{Transmission Conditions}(u^{\text{scat}}, u^{\text{inc}}), &\quad \text{on } \partial\Omega \\ \text{Radiation Condition}(u^{\text{scat}}), & \end{aligned}$$

where $k \in \mathbb{R}$ is the piece-wise constant wave-number function which depends on the materials, and the frequency of the incident wave. The transmission conditions ensure the continuity of the total wave across the interface $\partial\Omega$, while the radiation condition implies that the scattered wave radiates from the object to the free space and not the other way around. As in most PDE models, a closed form for the solution is only known for a few possibilities of Ω . Hence, numerical methods are needed to approximate the solution for

⁵We will limit ourselves to waves of acoustic or electric nature, but an extension to other cases is possible

general geometries. We notice that the actual domain of the problem is unbounded, and so the classical methods such as finite differences, finite elements methods, or pseudo-spectral methods are unsuited ⁶. In contrast, the boundary integral formulation reduces the PDE model to a system of integral equations defined on $\partial\Omega$ (which is finite). Thus the obtained formulation is especially attractive for the problem under consideration. We again refer to (Sauter & Schwab, 2011), and (McLean, 2000) for the equivalence of boundary integral formulations and the presented problem.

As it was mentioned in the previous section, we can use different methods to approximate the solution of the boundary integral equation. To understand how the spectral method compares to other discretizations is it important to know how expensive are the implementations of the methods under consideration.

We will focus only on Galerkin discretizations, in this framework, we recognize two main stages in the implementation:

- (i) First is the assembly process, where the boundary operators are transformed into finite-dimensional matrices by computing the action of the operators on the discretization basis. This process is similar to the construction of the matrices of the finite element method, however, the integrals are now singular and the resulting matrix is not sparse which leads to a more expensive process ⁷.
- (ii) Secondly, once the matrices are obtained a linear system needs to be solved. Since the matrix is not sparse, and for scattering problems is not even positive-definite, the process is more costly in comparison to other methods ⁸.

While the drawbacks in the implementation could be discouraging, it is also true that the involved matrices are much smaller as they only require bases in the boundary $\partial\Omega$ instead of the domain Ω .

⁶All these methods could be used if special conditions to create approximations to the radiation condition on a finite artificial boundary are added.

⁷What we mean with more expensive is that the number of operations to assembly a matrix coming from a boundary integral operator, is much greater compared with a matrix of same dimensions coming from a traditional finite element discretization.

⁸Again costly in terms of operations when the dimension is the same.

In the most classical implementation, the matrices are computed using Gaussian quadrature with a special change of variable to take care of the singularities, and the linear system is solved using an iterative method (typically GMRES, see (Saad, 2003) for details).

For low order Galerkin methods, if we denote by N the number of functions (and thus the operator matrices are of dimension N^2), and N_L the number iterations needed for the linear system solver (which itself depends on N). The cost, in terms of arithmetic operations, is dominated by the second stage and is proportional to $N^2 N_L$. This can be reduced using compression algorithms (see (Bebendorf, 2008), or (Yijun, 2009)) to $NN_L \log N$.

While such analysis is not straightforward for spectral Galerkin methods, and no compression algorithms are generally available, the convergence of spectral method suggests that if for a fixed accuracy N low order basis are needed, the same accuracy could be achieved by a number proportional to $\log N$ spectral basis, drastically reducing the cost of the second stage. We again refer to the works presented in the previous section for a detailed analysis of the cost of specific spectral Galerkin methods.

The question now is how big should N and N_L be, for a desire accuracy level. The answer depends on the geometry and the wave-number k in consideration. While this is still a topic under active investigation, at least under some assumptions very interesting results are available. We refer to (Galkowski, Müller, & Spence, 2016), (Graham, Löhndorf, Melenk, & Spence, 2014), (Chandler-Wilde, Graham, Langdon, & Spence, 2012) for a detailed discussion on the topic.

Formally speaking what has been observed, and in some cases rigorously proved, is that as the frequency increases the number of degrees of freedom and iterations of the linear solver also increase. The detailed dependency is hard to establish, but for low order, Galerkin discretizations it is known that for some simple objects (typically called non-trapping domains) the increase is moderate, and is proportional to a low order power of k . However, for other domains, the effect could be as bad as exponentially increasing.

The big potential of spectral methods is that it makes problems of high frequency treatable, as the involved matrices will be small enough to be stored in current generation hardware. However, this will only be practical if the cost of the first step (assembly of the operators' matrices) is reasonably small.

Finally, to close this section we remark that high-frequency scattering problems are of practical interest. Applications such as radars and sonars could benefit from the higher frequency in various situations, see for example (Sukharevsky, Vasilets, Nechitailo, & Khlopov, 2016; Walsh & Gill, 2000). Similarly, when used in medical-image high frequencies provide greater details that could reveal abnormalities that are not detected with lower frequencies. For example, in (Bisciotti & Eirale, 2013) the authors report that in many cases muscle injuries are only detected when high-frequency ultrasound is used.

1.2. Objective and Outline of the thesis

The main objective of this thesis is to show the effectiveness of spectral Galerkin methods for boundary integral formulations in different contexts. With this in mind, we will analyze and implement spectral Galerkin methods for three different problems.

Chapter 2 focuses on problems of multiple arcs in two dimensions. While this problem is the most documented in the literature of boundary spectral Galerkin methods (of the three in consideration), we generalize the convergence analysis with non-smooth arcs and also provide a compression algorithm. Technical results of this chapter are relegated to Appendix A.

Chapter 3 is an extension of the classical spectral methods on closed objects of two dimensions to periodic gratings. The periodic gratings are relevant structures as they have many engineering applications (see (E. Loewen & Popov, 1997) and reference therein for details), hence an accurate and fast solver is of great importance. This chapter is complemented with Appendix B, in which the functional setting for this problem is discussed in detail.

Chapter 4 is concerned with the problem of open surfaces in \mathbb{R}^3 , with technical results relegated to Appendix C. While many ideas could be carried from the two-dimension presentation in Chapter 2, the implementation is much more complicated and special efforts have to be done to optimize the algorithm. For this reason, the mathematical analysis performed in this chapter is complemented by Appendix D, which presents some special considerations for the implementation.

Finally, general conclusions and comparison between Chapters are addressed in Chapter 5.

Chapter 2. HIGH-ORDER GALERKIN METHOD FOR HELMHOLTZ AND LAPLACE PROBLEMS ON MULTIPLE OPEN ARCS

2.1. Introduction

We present a spectral Galerkin method for solving weakly singular boundary integral equations (BIEs) arising from Laplace or Helmholtz Dirichlet problems on unbounded domains with boundaries composed of finite collections of disjoint finite open arcs in \mathbb{R}^2 . Such problems are of particular interest in multiple contexts: in structural and mechanical engineering, wherein fractures or cracks are represented as slits (Tanaka, Okada, Okazawa, & Fujikubo, 2013; Tanaka, Suzuki, Ueda, & Sannomaru, 2015; Bittencourt, Wawrzynek, Ingrassia, & Sousa, 1996; Liew, Cheng, & Kitipornchai, 2007); in the detection of microfractures (Abda, Ameer, & Jaoua, 1999; Andrieux & Abda, 1996) and even for the imaging of muscular strains due to sport injuries (Verrall, Slavotinek, Barnes, Fon, & Spriggins, 2001). For these applications, one is interested in developing a numerical scheme that can robustly deal with large numbers of arcs –from tens to thousands– for a broad range of wavelengths –ranging from zero to several hundred times the length of the arcs.

For a single arc, wellposedness of these problems was studied in (E. P. Stephan & Wendland, 1984). Here, we only perform minor extensions to ensure uniqueness and existence of solutions for the multiple arcs case. In particular, volume solutions are shown to be constructed as superpositions of single layer potentials applied to surface densities over each arc; these layer densities are derived from solving a system of BIEs. Numerical approximations of these boundary unknowns are traditionally obtained via either variational methods such as the boundary element method (BEM) (Sauter & Schwab, 2011) or Nyström-type strategies (Bruno & Lintner, 2012; Domínguez, 2003). In this work, we opt for the former.

Still, for the type of applications considered, several issues hinder the standard low-order BEM performance. On one hand, solutions at the continuous level are well known

to exhibit square-root singularities at the arcs' endpoints (Costabel & Dauge, 2002; Grisvard, 2011; Krutitskii, 2000). Consequently, convergence of low-order uniform-mesh discretizations is suboptimal with improvements relying on either graded (Von Petersdorff & Stephan, 1990) or adaptive mesh refinement (Feischl, Führer, Heuer, Karkulik, & Praetorius, 2015), or on augmenting the approximation space (E. P. Stephan & Wendland, 1984). Also, the Galerkin matrices derived from first kind Fredholm formulations are intrinsically ill-conditioned, thus heavily requiring preconditioning (Hiptmair, Jerez-Hanckes, & Urzua-Torres, 2014; McLean & Steinbach, 1999). Moreover, the minimal number of unknowns to ensure asymptotic convergence increases with the wavenumber (Melenk & Sauter, 2011) while the number of matrix entries grow quadratically with the number of arcs in order to account for cross-interactions. Hence, for the present problems of interest, one can expect extremely large numbers of degrees of freedom (dofs) when using mesh-dependent methods and alternative ones must be sought.

In (K. E. Atkinson & Sloan, 1991; Jerez-Hanckes, Nicaise, & Urzúa-Torres, 2018) a spectral Galerkin-Bubnov discretization for a single arc was shown to greatly reduce the number of dofs in comparison to the case of locally defined low-order bases. Specifically, the approximation basis employed is given by weighted first kind Chebyshev polynomials, where the weight mimics the singular behavior at the endpoints. Our work expands the use of such bases to multiple arcs and Helmholtz cases providing also a rigorous convergence analysis. The analysis presented here is based in the asymptotic decay of the Fourier-Chebyshev expansions coefficients of the solutions. With these tools, one can derive convergence rates for order p polynomial approximations that only depend on smoothness of the excitations and of the arcs itself, with constants that may depend on the wavenumber. In particular, one obtains super-algebraic convergence when both arcs and sources can be represented by analytic functions.

Alternatively, for two-dimensional problems, the BIEs for open arcs can be recasted as a problem of integral equations on closed boundaries for even functions. This is done using a cosine change of variables (*cf.* (K. E. Atkinson & Sloan, 1991) or (Saranen & Vainikko, 2013, Chapter 11)). Using this property along with classical Fourier analysis, we retrieve

convergence rates given in (K. E. Atkinson & Sloan, 1991) for single arc. Thus, our proof of convergence can be seen as the Fourier-Chebyshev version of those results, with the additional extension to the Helmholtz case.

For implementation purposes, we follow the scheme introduced in (Hu, 1994) wherein all integral kernel singularities are subtracted. This gives rise to smooth functions and singular functions whose integrals are respectively computed via the Fast Fourier Transform (FFT) (Jerez-Hanckes, Pinto, & Tournier, 2015) or analytically using a Chebyshev polynomial expansion of the fundamental solution (Frenkel, 1983). Recently, Slevinsky and Olver (Slevinsky & Olver, 2017) devised a similar construction based on Chebyshev polynomials for more general integral equations, but limited to line segments and focused exclusively on the spectral properties of collocation method. Though the authors also provide ideas on how to extend their method to more general arcs, the focus remains in solving a linear system. Hewett *et al.* (Hewett, Langdon, & Chandler-Wilde, 2014) propose a different numerical method for which they also obtain super-convergence. Their discretization basis captures explicitly the oscillatory behavior on a segment while employing a low polynomial order adaptive bases for the slow but singular part. Though this splitting leads to impressive results especially for high-frequency, its use is restricted to collinear segments and not for general arcs. Still, our approach could be combined with this one but this would require significant work beyond the scope of the present manuscript.

The structure of a problem with multiple arcs implies that many of the interactions, in the BIE system, are characterized by a smooth kernel functions. Thus, one can generally compress these interactions by considering fewer functions than in the self-interaction case. This hints at a compression algorithm, in the same spirit of (Jiang & Xu, 2010). Here, the implementation is performed by a bisection algorithm which allows to reuse the integration routines of self-interactions terms. Moreover, we obtain bounds on how the introduction of this compression algorithm affects the accuracy of the numerical solution.

It is also well known that first kind formulations for open arc problems suffer from poor performance when solving the associated linear system via iterative methods. Many

remedies for this issue have been proposed, among which the construction of preconditioners has received attention in recent years (*cf.* (S. Lintner, 2012; Jerez-Hanckes & Nédélec, 2012; Hiptmair et al., 2014) for detailed reviews). These preconditioning techniques could be combined with our spectral solver. Indeed, as spectral methods entail significantly fewer dofs in comparison to low-order methods for a fixed accuracy, it is feasible to invert self-interaction parts of the matrix using a direct method and, by doing so, obtain a better preconditioner. Since the multiple scattering problem requires a large amount of memory to store the problem matrix, direct methods for the full matrix could only be used when the product of frequency and total length of the arcs is small. Moreover, contrary to what one could think the direct method also suffers from numerical cancellation/round-off errors (see Section 2.7.1 for an illustration). Hence the need of iterative solvers is mandatory, and to be able to use it effectively we need to accelerate the matrix-vector product.

The paper is organized as follows. Section 2.2 puts forward formal definitions and properties needed throughout. In Section 2.3, we formulate the problem as a system of BIEs and show that these are well posed. Section 2.4 gives details on the Galerkin discretization method; in particular, we establish error convergence rates for the discrete problem assuming regularity conditions on the data. Employed quadrature schemes are detailed in Section 2.5. Our proposed compression algorithm is given in Section 2.6. Numerical results illustrating the accuracy of the method as well as the performance of the compression algorithm are presented in Section 2.7. Finally, conclusions are drawn along with appendices for completeness.

2.2. Mathematical tools

2.2.1. General notation

We employ the standard $\mathcal{O}(\cdot)$ and $o(\cdot)$ notation for asymptotics. We also use the notation $a_n \lesssim b_n$ if there exists a positive constant C and an integer $N > 0$ such that $a_n \leq Cb_n$ for all $n > N$.

Vectors are indicated by boldface symbols with Euclidean norm written as $\|\cdot\|_2$; other norms are signaled by subscripts. Quantities defined over volume domains will be written in capital case whereas those on boundaries in normal one, e.g., $U : G \rightarrow \mathbb{C}$ while $u : \partial G \rightarrow \mathbb{C}$.

Let $G \subseteq \mathbb{R}^d$, $d = 1, 2$, be an open domain. For $k \in \mathbb{N} \cup \{0\}$, $\mathcal{C}^k(G)$ denotes the set of k -times continuously differentiable functions over G . Compactly supported $\mathcal{C}^k(G)$ functions are designated by $\mathcal{C}_0^k(G)$. Denote by $\mathcal{D}(G) \equiv \mathcal{C}_0^\infty(G)$ the space of infinitely differentiable functions with compact support on a open set G . Duals are indicated by asterisks, e.g., the space of distributions is $\mathcal{D}^*(G)$. The class of p -integrable functions over G is written $L^p(G)$. Duality pairings and inner products are written as $\langle \cdot, \cdot \rangle$ and (\cdot, \cdot) , respectively, with subscripts declaring the domain involved, if not clear from the context.

We say that $g : (-1, 1) \rightarrow \mathbb{C}$ is in $\mathcal{C}_v^m(-1, 1)$, if it is in $\mathcal{C}^m(-1, 1)$ and its m th derivative has bounded variation, i.e. the distributional derivative $g^{(m+1)}$ is Lebesgue integrable. Notice that $\mathcal{C}^{m+1}(-1, 1) \subset \mathcal{C}_v^m(-1, 1)$. Also we say g (a function as before) is ρ -analytic, if there exists a Bernstein ellipse of parameter $\rho > 1$, such that g can be extended to an analytic function in the complex ellipse containing the interval $(-1, 1)$ (cf. (L. Trefethen, 2013, Chapter 8)). Lastly, throughout we will claim a sesquilinear form to be *coercive* if it is the addition of a positive definite form and a compact one; similarly for induced operators.

2.2.2. Arcs

We call $\Lambda \subset \mathbb{R}^2$ a regular Jordan arc of class \mathcal{C}^m (resp. \mathcal{C}_v^m), for $m \in \mathbb{N}$, if there exists a bijective parametrization denoted by $\mathbf{r} : (-1, 1) \rightarrow \Lambda$, such that its components are $\mathcal{C}^m(-1, 1)$ -functions (resp. $\mathcal{C}_v^m(-1, 1)$ -functions) and $\inf_{t \in (-1, 1)} \|\mathbf{r}'(t)\|_2 > 0$. Analogously, we say that Λ is ρ -analytic, if there is a corresponding parametrization that is ρ -analytic. Henceforth, we assume all arcs to be Jordan arcs of a given regularity and we will refer to them as open arcs or just arcs.

ASSUMPTION 2.1. *For any Λ open arc, there exists an extension to $\tilde{\Lambda}$ which is a simple closed curve containing and having the same regularity of Λ .*

We consider a finite number $M \in \mathbb{N}$ of open arcs $\{\Gamma_i\}_{i=1}^M$, such that under Assumption 2.1 their extensions $\{\tilde{\Gamma}_i\}_{i=1}^M : \tilde{\Gamma}_i \supset \Gamma_i, i = 1, \dots, M$, are mutually disjoint. We define

$$\Gamma := \bigcup_{i=1}^M \Gamma_i \quad \text{and} \quad \Omega := \mathbb{R}^2 \setminus \bar{\Gamma}.$$

ASSUMPTION 2.2. *There are M domains Ω_i whose boundaries are given by $\partial\Omega_i = \tilde{\Gamma}_i$, for $i = 1, \dots, M$, and their closures $\bar{\Omega}_i$ are disjoint.*

For $m \in \mathbb{N}$, we say that the family of arcs Γ is of class \mathcal{E}^m (resp. \mathcal{E}_v^m), if each arc Γ_i is of class \mathcal{E}^m (resp. \mathcal{E}_v^m), and write $\Gamma \in \mathcal{E}^m$ (resp. $\Gamma \in \mathcal{E}_v^m$); similarly for ρ -analytic arcs. Denote by \mathbf{r}_i a parametrization of the corresponding regularity mapping $(-1, 1)$ to an arc $\Gamma_i, i \in \{1, \dots, M\}$. For a vector function $\mathbf{g} = (g_1, \dots, g_M)$ such that $g_i : \bar{\Gamma}_i \rightarrow \mathbb{C}$, for $i \in \{1, \dots, M\}$, we state that \mathbf{g} is of class $\mathcal{E}^m(\Gamma)$ (resp. $\mathcal{E}_v^m(\Gamma)$), if $g_i \circ \mathbf{r}_i \in \mathcal{E}^m(-1, 1)$ (resp. $g_i \circ \mathbf{r}_i \in \mathcal{E}_v^m(-1, 1)$), for $i \in \{1 \dots M\}$, and denote $\mathbf{g} \in \mathcal{E}^m(\Gamma)$ (resp. $\mathbf{g} \in \mathcal{E}_v^m(\Gamma)$), and again the ρ -analytic case is defined analogously.

Finally, we will identify every open arc with a given parametrization so that for example $\Lambda_1 := \{(t^3, 1), t \in (-1, 1)\}$ and $\Lambda_2 := \{(t, 1), t \in (-1, 1)\}$ are different arcs, even if they are the same set of points in \mathbb{R}^2 . We will frequently refer to the canonical open arc:

$$\hat{\Gamma} := \{(t, 0), t \in (-1, 1)\}.$$

2.2.3. Sobolev spaces and trace operators

Let $G \subseteq \mathbb{R}^d, d = 1, 2$, be an open domain. For $s \in \mathbb{R}$, we denote by $H^s(G)$ the standard Sobolev spaces in $L^2(G)$ and by $H_{loc}^s(G)$ their locally integrable counterparts (Sauter & Schwab, 2011, Section 2.3). We also use the following Hilbert space:

$$W(G) := \left\{ U \in \mathcal{D}'(G) : \frac{U(\mathbf{x})}{\sqrt{1 + \|\mathbf{x}\|_2^2} \log(2 + \|\mathbf{x}\|_2^2)} \in L^2(G), \nabla U \in L^2(G) \right\},$$

which is a subspace of $H_{loc}^1(G)$. Under Assumption 2.1 for an open arc Λ , we define

$$\tilde{H}^s(\Lambda) := \{u \in \mathcal{D}^*(\Lambda) : \tilde{u} \in H^s(\tilde{\Lambda})\}, \quad s > 0,$$

wherein \tilde{u} denotes the extension by zero of u to $\tilde{\Lambda}$. For $s > 0$, we can identify

$$\tilde{H}^{-s}(\Lambda) = (H^s(\Lambda))^* \quad \text{and} \quad H^{-s}(\Lambda) = (\tilde{H}^s(\Lambda))^*.$$

We will also need the family of mean-zero Sobolev spaces:

$$\tilde{H}_{(0)}^s(\Lambda) = \{u \in \tilde{H}^s(\Lambda) : \langle u, 1 \rangle = 0\}, \quad s \in \mathbb{R}.$$

The following result will be used to establish convergence rates and error computations in our numerical experiments (cf. Section 2.7) with proof given in Appendix A.2.

LEMMA 2.2.1. *Let $\zeta \in H^{\frac{1}{2}}(\Gamma_i)$, $\psi \in \tilde{H}^{-\frac{1}{2}}(\Gamma_i)$, and $\mathbf{r}_i : (-1, 1) \rightarrow \Gamma_i$, the parametrization of Γ_i . Then, we have the norm equivalences:*

$$\begin{aligned} c \|\zeta\|_{H^{\frac{1}{2}}(\Gamma_i)} &\leq \|\zeta \circ \mathbf{r}_i\|_{H^{\frac{1}{2}}(\hat{\Gamma})} \leq C \|\zeta\|_{H^{\frac{1}{2}}(\Gamma_i)}, \\ c \|\psi\|_{\tilde{H}^{-\frac{1}{2}}(\Gamma_i)} &\leq \|\psi \circ \mathbf{r}_i\|_{\tilde{H}^{-\frac{1}{2}}(\hat{\Gamma})} \leq C \|\psi\|_{\tilde{H}^{-\frac{1}{2}}(\Gamma_i)}, \end{aligned}$$

where the pullbacks for negative order are defined by duality, with generic positive constants c and C depending on Γ_i .

For the finite union of disjoint open arcs Γ , we define piecewise spaces as

$$\mathbb{H}^s(\Gamma) := H^s(\Gamma_1) \times H^s(\Gamma_2) \times \cdots \times H^s(\Gamma_M).$$

Norms and dual products are naturally extended by the previous identification, similarly for spaces $\tilde{\mathbb{H}}^s(\Gamma)$ and $\tilde{\mathbb{H}}_{(0)}^s(\Gamma)$, while $\mathbb{H}^s(\hat{\Gamma})$ is understood as the Cartesian product $\prod_{i=1}^M H^s(\hat{\Gamma})$.

For $U \in \mathcal{C}^\infty(\overline{\Omega_i})$ (resp. $U \in \mathcal{C}^\infty(\mathbb{R}^2 \setminus \Omega_i)$), we can set the interior (-) (resp. exterior (+)) Dirichlet traces:

$$\gamma_i^\pm U(\mathbf{x}) := \lim_{\epsilon \downarrow 0} U(\mathbf{x} \pm \epsilon \mathbf{n}_i) \quad \forall \mathbf{x} \in \Gamma_i,$$

where \mathbf{n}_i denotes the unitary normal vector with direction of $(r'_{i,2}, -r'_{i,1})$. If $\gamma_i^+ U = \gamma_i^- U$, we denote $\gamma_i U := \gamma_i^\pm U$. These definitions can be extended to more general Sobolev spaces by density, in particular, we have that $\gamma_i^\pm : H_{loc}^1(\Omega) \rightarrow H^{1/2}(\Gamma_i)$, as a bounded linear operator (see (McLean, 2000, Theorem 3.37)). Neumann traces can be defined for smooth functions U as

$$\gamma_{N,i}^\pm U := \lim_{\epsilon \downarrow 0} \mathbf{n}_i \cdot \nabla U(\mathbf{x} \pm \epsilon \mathbf{n}_i), \quad \forall \mathbf{x} \in \Gamma_i.$$

In contrast to the Dirichlet trace, the extension to Sobolev spaces is carried out using Green's formula in Ω_i along with the restriction operator. For $U \in H_{loc}^1(\Omega_i)$ and $\Delta U \in L_{loc}^2(\Omega_i)$, then $\gamma_{N,i}^\pm U \in H^{-1/2}(\Gamma_i)$ (cf. (McLean, 2000, Lemma 4.3)). Finally, traces taken with respect to the domains $\Omega_i, i \in \{1, \dots, M\}$ will be denoted $\tilde{\gamma}_i^\pm$ and $\tilde{\gamma}_{N,i}^\pm$ respectively.

2.3. Boundary integral problem formulation

As explained, we are interested in solving the families of boundary value problems in Ω via suitable integral representations with unknown densities over the boundaries Γ .

PROBLEM 2.3.1 (Volume Problem). Let $\mathbf{g} = (g_1, \dots, g_M) \in \mathbb{H}^{\frac{1}{2}}(\Gamma)$ and consider a real wavenumber $\kappa \geq 0$. We seek $U \in H_{loc}^1(\Omega)$ such that

$$-\Delta U - \kappa^2 U = 0 \quad \text{in } \Omega, \quad (2.1)$$

$$\gamma_i^\pm U = g_i \quad \text{for } i = 1, \dots, M, \quad (2.2)$$

$$\text{condition at infinity}(\kappa). \quad (2.3)$$

The case $\kappa = 0$ corresponds to the Laplace operator whereas $\kappa > 0$ to the Helmholtz one. The behavior at infinity (2.3) depends on κ in the following way: if $\kappa > 0$, we employ the classical Sommerfeld condition:

$$\lim_{R \rightarrow \infty} \int_{\|\mathbf{x}\|_2=R} \left| \frac{\partial U}{\partial r}(\mathbf{x}) - i\kappa U(\mathbf{x}) \right|^2 d\Gamma_{\mathbf{x}} = 0,$$

If $\kappa = 0$, we seek solutions $U \in W(\Omega)$. For $\kappa > 0$ the existence and uniqueness of Problem 2.3.1 can be obtained from (E. P. Stephan & Wendland, 1984, Lemma 1.2), while

for $\kappa = 0$ although very similar to (E. P. Stephan & Wendland, 1984, Lemma 1.1), the result is slightly different as we need to use the space $W(\Omega)$. For sake of completeness, uniqueness is addressed in Appendix A.1. We can express the volume solution U as

$$U(\mathbf{x}) = \sum_{i=1}^M (\text{SL}_i[\kappa]\lambda_i)(\mathbf{x}), \quad \forall \mathbf{x} \in \Omega, \quad (2.4)$$

where

$$(\text{SL}_i[\kappa]\lambda_i)(\mathbf{x}) := \int_{\Gamma_i} G_\kappa(\mathbf{x}, \mathbf{y}) \lambda_i(\mathbf{y}) d\Gamma_i(\mathbf{y}),$$

denotes the single layer potential generated at a curve Γ_i with fundamental solution:

$$G_\kappa(\mathbf{x}, \mathbf{y}) = \begin{cases} \frac{-1}{2\pi} \log \|\mathbf{x} - \mathbf{y}\|_2 & k = 0, \\ \frac{i}{4} H_0^1(\kappa \|\mathbf{x} - \mathbf{y}\|_2) & k > 0. \end{cases} \quad (2.5)$$

Here, $H_0^1(\cdot)$ denotes the zeroth-order first kind Hankel function (Abramowitz & Stegun, 1965, Chapter 9). From the properties of the single layer potential on closed domains (McLean, 2000, Chapter 7) and the completion $\tilde{\Gamma}_i$ for each arc, one can see that

$$\text{SL}_i[\kappa] : H^{-1/2}(\Gamma_i) \rightarrow H_{loc}^1(\mathbb{R}^2),$$

as a bounded linear map. Moreover, if U is expressed as in (2.4), then it solves (2.1). By (McLean, 2000, Theorem 9.6) for $\kappa > 0$, the representation (2.4) satisfies the Sommerfeld condition. The case $\kappa = 0$ is given by the following result.

LEMMA 2.3.2. *The single layer potential $\text{SL}_i[0]$ is a bounded linear map between the spaces $\tilde{H}_{\langle 0 \rangle}^{-\frac{1}{2}}(\Gamma_i)$ and $W(\mathbb{R}^2 \setminus \bar{\Gamma}_i)$.*

PROOF. As $\tilde{H}_{\langle 0 \rangle}^{-\frac{1}{2}}(\Gamma_i) \subset \tilde{H}^{-\frac{1}{2}}(\Gamma_i)$ we have that $\text{SL}_i[0] : \tilde{H}_{\langle 0 \rangle}^{-\frac{1}{2}}(\Gamma_i) \rightarrow H_{loc}^1(\mathbb{R}^2)$. Hence, we only need to verify the conditions:

$$\frac{(\text{SL}_i[0]u)(\mathbf{x})}{\sqrt{1 + \|\mathbf{x}\|_2^2 \log(2 + \|\mathbf{x}\|_2^2)}} \in L^2(\mathbb{R}^2 \setminus \bar{\Gamma}_i), \quad \text{and} \quad \nabla (\text{SL}_i[0]u) \in L^2(\mathbb{R}^2 \setminus \bar{\Gamma}_i).$$

For every $u \in \widetilde{H}_{(0)}^{-\frac{1}{2}}(\Gamma_i)$. From (McLean, 2000, Corollary 8.11), we know that the asymptotic behavior of the single layer potential for large arguments is

$$(\text{SL}_i[0]u)(\mathbf{x}) = -\frac{1}{2\pi} \langle u, 1 \rangle \log \|\mathbf{x}\|_2 + \mathcal{O}(\|\mathbf{x}\|_2^{-1}), \quad \text{for } \|\mathbf{x}\|_2 \rightarrow \infty.$$

Thus, if $u \in \widetilde{H}_{(0)}^{-\frac{1}{2}}(\Gamma_i)$ then

$$(\text{SL}_i[0]u)(\mathbf{x}) = \mathcal{O}(\|\mathbf{x}\|_2^{-1}), \quad \text{for } \|\mathbf{x}\|_2 \rightarrow \infty. \quad (2.6)$$

Using polar coordinates and the above bound, we can verify that the first condition. The proof of that the gradient is in $L^2(\mathbb{R} \setminus \overline{\Gamma_i})$ is obtained by using the Taylor expansion of the gradient of the logarithmic term. \square

In order to find the boundary unknowns λ_i , we take Dirichlet traces of the single layers potentials and impose (2.2). This induces the definition of weakly singular boundary integral operators (BIOs) as

$$\mathcal{L}_{ij}[\kappa] := \frac{1}{2} (\gamma_i^+ \text{SL}_j[\kappa] + \gamma_i^- \text{SL}_j[\kappa]) = \gamma_i \text{SL}_j[\kappa],$$

the last equation resulting from the continuity properties of the SL_i across Γ_i for each $i = 1, \dots, M$.

PROBLEM 2.3.3. For $\kappa > 0$ and $\mathbf{g} \in \mathbb{H}^{\frac{1}{2}}(\Gamma)$, we seek $\boldsymbol{\lambda} = (\lambda_1, \dots, \lambda_M) \in \widetilde{\mathbb{H}}^{-\frac{1}{2}}(\Gamma)$ such that

$$\mathcal{L}[\kappa] \boldsymbol{\lambda} = \mathbf{g},$$

or equivalently,

$$\langle \mathcal{L}[\kappa] \boldsymbol{\lambda}, \phi \rangle_\Gamma = \langle \mathbf{g}, \phi \rangle_\Gamma, \quad \forall \phi \in \widetilde{\mathbb{H}}^{-\frac{1}{2}}(\Gamma),$$

where

$$\mathcal{L}[\kappa] := \begin{bmatrix} \mathcal{L}_{11}[\kappa] & \mathcal{L}_{12}[\kappa] & \dots & \mathcal{L}_{1M}[\kappa] \\ \mathcal{L}_{21}[\kappa] & \mathcal{L}_{22}[\kappa] & \dots & \mathcal{L}_{2M}[\kappa] \\ \vdots & \vdots & \ddots & \vdots \\ \mathcal{L}_{M1}[\kappa] & \mathcal{L}_{M2}[\kappa] & \dots & \mathcal{L}_{MM}[\kappa] \end{bmatrix} : \widetilde{\mathbb{H}}^{-\frac{1}{2}}(\Gamma) \rightarrow \mathbb{H}^{\frac{1}{2}}(\Gamma).$$

In the case $\kappa = 0$, we need $\mathbf{g} \in (\widetilde{\mathbb{H}}_{(0)}^{-\frac{1}{2}}(\Gamma))^*$ and restrict $\boldsymbol{\lambda}$ to $\widetilde{\mathbb{H}}_{(0)}^{-\frac{1}{2}}(\Gamma)$.

REMARK 2.3.4. Problem 2.3.3 can be recast in the reference space $\widetilde{\mathbb{H}}^{-\frac{1}{2}}(\widehat{\Gamma})$ or $\widetilde{\mathbb{H}}_{(0)}^{-\frac{1}{2}}(\widehat{\Gamma})$ for $\kappa = 0$ so as to find $\widehat{\boldsymbol{\lambda}}$ such that

$$\widehat{\mathcal{Z}}[\kappa]\widehat{\boldsymbol{\lambda}} = \widehat{\mathbf{g}},$$

wherein $\widehat{g}_j := g_j \circ \mathbf{r}_j$, $\widehat{\mathcal{L}}_{ij}$ are the BIOs defined over the reference arc $\widehat{\Gamma}$ with integral kernel $G_\kappa(\mathbf{r}_i(t), \mathbf{r}_j(s))$ and the unknowns $\widehat{\lambda}_j := (\lambda_j \circ \mathbf{r}_j)/\|\mathbf{r}'_j\|_2$.

REMARK 2.3.5. Later on we will use the operator $\mathcal{L}_{ii}[\kappa]$ for the choice $\Gamma_i = \widehat{\Gamma}$, which we denote by $\check{\mathcal{L}}[\kappa]$. The difference with respect to $\widehat{\mathcal{L}}_{ii}[\kappa]$ relies on the absence of parametrizations \mathbf{r}_i involved in the kernel. In the case of a single open arc with parametrization \mathbf{r} , we will write $\widehat{\mathcal{L}}[\kappa] \equiv \widehat{\mathcal{L}}_{ii}[\kappa]$. In this case, and for $\kappa = 0$, one can deduce that the kernel function of the integral operator $\check{\mathcal{L}}[0] - \widehat{\mathcal{L}}[0]$ is given by

$$E_{\mathbf{r}}(t, s) := -\frac{1}{2\pi} \log \left(\frac{\|\mathbf{r}(t) - \mathbf{r}(s)\|_2}{|t - s|} \right)$$

for which we have the following result.

LEMMA 2.3.6. *Let $m \in \mathbb{N}$ and Λ be a single \mathcal{C}_v^m -arc. Then the function $E_{\mathbf{r}}(t, s)$ is a $\mathcal{C}_v^m(-1, 1)$ -function in each of its components. If Γ is a ρ -analytic arc, $E_{\mathbf{r}}(t, s)$ is a bivariate ρ -analytic function.*

PROOF. By performing a Taylor expansion in t , we can write

$$\Theta_{\mathbf{r}}(t, s) := \frac{\mathbf{r}(t) - \mathbf{r}(s)}{t - s} = \sum_{j=1}^{m-1} \frac{(t - s)^{j-1} \mathbf{r}^{(j)}(s)}{j!} + \frac{1}{t - s} \int_s^t \frac{(t - \xi)^m \mathbf{r}^{(m)}(\xi)}{m!} d\xi.$$

This function admits m continuous derivatives in the t variable. As mentioned at the beginning of Section 2.2.2, open arc parametrizations are injective, and thus, the function can only be zero if $t = s$. However, as t approaches s , the above function behaves as $\mathbf{r}'(s)$, which is not zero. Hence, $\Theta_{\mathbf{r}}(t, s)$ does not vanish and so $E_{\mathbf{r}}(t, s)$ is the composition of \mathcal{C}_v^m -functions, despite there being an absolute value. The ρ -analytic case follows from the same argument. \square

REMARK 2.3.7. One should fully understand the differences between the cases $\kappa = 0$ and $\kappa > 0$. The first one is posed over the smaller space $\widetilde{\mathbb{H}}_{(0)}^{-\frac{1}{2}}(\Gamma)$, and the right-hand side must be in the dual of this space, which is bigger than $\mathbb{H}^{\frac{1}{2}}(\Gamma)$ under the identification of $L^2(\Gamma)$ with its own dual. However, one has to be careful with the identifications that occur as many elements of $\mathbb{H}^{\frac{1}{2}}(\Gamma)$ are identifiable with one element of $(\widetilde{\mathbb{H}}_{(0)}^{-\frac{1}{2}}(\Gamma))^*$: for example, all constants are equivalent to the zero function. A more general formulation for the $\kappa = 0$ case can be found in (E. P. Stephan & Wendland, 1984).

Now, we show that Problem 2.3.3 is well posed. First, we prove that the diagonal operators $\mathcal{L}_{ii}[k]$ are coercive and use ideas from (E. P. Stephan & Wendland, 1984) to transform the problem into a closed domain one.

LEMMA 2.3.8. *For $i \in \{1, \dots, M\}$, $k \geq 0$, there exist a constant $c_{e,i}$ such that*

- *if $\kappa = 0$, it holds*

$$\langle \mathcal{L}_{ii}[0]u, u \rangle_{\Gamma_i} \geq c_{e,i} \|u\|_{\widetilde{H}^{-\frac{1}{2}}(\Gamma_i)}^2, \quad \forall u \in \widetilde{H}^{-1/2}(\Gamma_i)$$

- *if $\kappa > 0$, then there are compact BIOs $\mathcal{K}_{ii}[\kappa] : \widetilde{H}^{-\frac{1}{2}}(\Gamma_i) \rightarrow H^{\frac{1}{2}}(\Gamma_i)$, such that*

$$\langle (\mathcal{L}_{ii}[\kappa] + \mathcal{K}_{ii}[\kappa])u, u \rangle_{\Gamma_i} \geq c_{e,i} \|u\|_{\widetilde{H}^{-\frac{1}{2}}(\Gamma_i)}^2, \quad \forall u \in \widetilde{H}^{-\frac{1}{2}}(\Gamma_i).$$

PROOF. Given u and v in $\widetilde{H}^{-1/2}(\Gamma_i)$, consider their respective zero extension \widetilde{u} and \widetilde{v} to $\partial\Omega_i$. Denote by $\mathcal{V}_{ii}[k]$ the weakly singular integral operator given by taking the trace over $\partial\Omega_i$ of the single layer potential in $\partial\Omega_i$. Then, we have that

$$\langle \mathcal{L}_{ii}[\kappa]u, u \rangle_{\Gamma_i} = \langle \mathcal{V}_{ii}[\kappa]\widetilde{u}, \widetilde{u} \rangle_{\partial\Omega_i}.$$

The results then follows from the closed curves case (cf. (Costabel, 1988, Theorem 2)). \square

REMARK 2.3.9. Continuity of operators \mathcal{L}_{ij} , $i, j \in \{1, \dots, M\}$, can be proved by using the same arguments as those for Lemma 2.3.8. Then, one can easily show that

$$\mathcal{L}_{ij}[\kappa] : \widetilde{H}^{-1/2}(\Gamma_j) \rightarrow H^{1/2}(\Gamma_i)$$

as a bounded operator. Moreover, if $i \neq j$ the operator is compact as the kernel function is at least \mathcal{C}^1 in each component.

THEOREM 2.3.10. *For $\kappa > 0$, Problem 2.3.3 has a unique solution $\boldsymbol{\lambda} \in \widetilde{\mathbb{H}}^{-\frac{1}{2}}(\Gamma)$, whereas for $\kappa = 0$ a unique solution exists in the subspace $\boldsymbol{\lambda} \in \widetilde{\mathbb{H}}_{(0)}^{-\frac{1}{2}}(\Gamma)$. Also, we have the continuity estimate*

$$\|\boldsymbol{\lambda}\|_{\widetilde{\mathbb{H}}^{-\frac{1}{2}}(\Gamma)} \leq C(\Gamma, \kappa) \|\mathbf{g}\|_{\mathbb{H}^{\frac{1}{2}}(\Gamma)}.$$

PROOF. By compactness of the cross-interaction BIOs and the coercivity result of Lemma 2.3.8, the Fredholm alternative (McLean, 2000, Theorem 2.33) indicates that we only need to prove injectivity to ensure existence. First, consider the case $M = 1$: for $\kappa = 0$, the result is obtained from Lax-Milgram lemma while for $\kappa > 0$, we obtain the result from (E. P. Stephan & Wendland, 1984, Theorem 1.7).

Now, we focus in the case $M > 1$. Let $\boldsymbol{\lambda} = (\lambda_1, \dots, \lambda_M)$ be such that

$$\sum_{j=1}^M \mathcal{L}_{ij}[\kappa] \lambda_j = 0 \quad \forall i = 1, \dots, M.$$

For $j \in \{1, \dots, M\}$, let us define volume potentials $U_j := \text{SL}_j[k] \lambda_j$, solutions of individual homogenous Helmholtz problems over $\mathbb{R}^2 \setminus \overline{\Gamma}_j$ as well as the superposition $U_\sigma := \sum_{j=1}^M U_j$ defined over Ω . Then, it holds

$$\gamma_i U_\sigma = \gamma_i \sum_{j=1}^M U_j = \sum_{i=1}^M \mathcal{L}_{ij}[k] \lambda_j = 0, \quad \forall i = 1, \dots, M.$$

However, U_σ is also the solution of Problem 2.3.1, with zero Dirichlet boundary condition. Hence, as this problem has at most one solution we conclude that

$$U_\sigma = \sum_{j=1}^M \text{SL}_j[k] \lambda_j = 0,$$

and consequently, for all $i = 1, \dots, M$, it holds

$$U_i = \text{SL}_i[k] \lambda_i = - \sum_{j \neq i} \text{SL}_j[k] \lambda_j. \quad (2.7)$$

Let us now consider the closed curve $\tilde{\Gamma}_i = \partial\Omega_i$, and denote by $\tilde{\lambda}_i \in \tilde{H}^{-\frac{1}{2}}(\tilde{\Gamma}_i)$ the extension by zero of λ_i . It holds,

$$U_i(\mathbf{x}) = \text{SL}_i[k](\mathbf{x})\lambda_i = \text{SL}_{\tilde{\Gamma}_i}[k](\mathbf{x})\tilde{\lambda}_i \quad \forall \mathbf{x} \in \Omega,$$

where the last potential is defined on the closed curve $\tilde{\Gamma}_i$. If we take normal jumps, defined as $[\gamma_N U] = \gamma_N^+ U - \gamma_N^- U$, by (Sauter & Schwab, 2011, Theorem 3.3.1), we obtain

$$[\tilde{\gamma}_{N,i} U_i]_{\tilde{\Gamma}_i} = [\tilde{\gamma}_{N,i} \text{SL}_{\tilde{\Gamma}_i}[k]\tilde{\lambda}_i]_{\tilde{\Gamma}_i} = -\tilde{\lambda}_i.$$

Using (2.7) in the expression above yields

$$[\tilde{\gamma}_{N,i} U_i]_{\tilde{\Gamma}_i} = - \left[\tilde{\gamma}_{N,i} \sum_{j \neq i} \text{SL}_j[k]\lambda_j \right]_{\tilde{\Gamma}_i} = 0$$

where the last equality comes from the smoothness of the integral kernel since $\tilde{\Gamma}_i \cap \tilde{\Gamma}_j = \emptyset$, for $j \neq i$. Thus, we can conclude that $\lambda_j = 0$ and the same follows for the other components. \square

REMARK 2.3.11. Much of the ideas presented in this section can be used in a more general context. In a more abstract setting the notion of open arcs Γ_i has to be changed by a proper connected Lipschitz subsets of the boundary of a domain $\Omega_i \in \mathbb{R}^d$, for $d = 2, 3$, and whose normal vector is continuous. Define Ω as the exterior of a finite set of generalized open arcs Γ . As in (McLean, 2000, Chapter 4), consider any strongly elliptic second-order self-adjoint partial differential operator, denoted by \mathcal{P} , with smooth \mathbb{C}^m -valued vector fields coefficients. Thus, for a given Dirichlet or Neumann datum, $\mathbf{g} \in [\mathbb{H}^{\frac{1}{2}}(\Gamma)]^m$ or $\mathbf{h} \in [\mathbb{H}^{-\frac{1}{2}}(\Gamma)]^m$, respectively, we seek for $\mathbf{U} \in [H_{loc}^1(\Omega)]^m$ such that,

$$\begin{aligned} \mathcal{P}\mathbf{U} &= 0 \quad \text{in } \Omega, \\ \gamma\mathbf{U} &= \mathbf{g} \quad \text{or} \quad B_{\mathbf{n}}\mathbf{U} = \mathbf{h} \quad \text{on } \Gamma, \end{aligned}$$

with the conormal trace $B_{\mathbf{n}}$ defined as in (McLean, 2000, Chapter 4). The following points are needed in order to establish the existence and uniqueness of an equivalent boundary integral formulation for Cauchy data.

- (i) An adequate condition at infinity that ensures the uniqueness of the boundary value problem.
- (ii) A fundamental solution $G(\mathbf{x}, \mathbf{y})$, such that $\mathcal{P}_{\mathbf{x}}G(\mathbf{x}, \mathbf{y}) = \delta_{\mathbf{x}-\mathbf{y}}\mathbf{l}$, where \mathbf{l} is the identity operator in $\mathbb{R}^{m \times m}$.
- (iii) Layer potentials:

$$(\mathbf{SL}_i \boldsymbol{\lambda})(\mathbf{x}) := \int_{\Gamma_i} G(\mathbf{x}, \mathbf{y}) \boldsymbol{\lambda}(\mathbf{y}) d\Gamma_i(\mathbf{y}) \quad (\text{Dirichlet trace}),$$

$$(\mathbf{DL}_i \boldsymbol{\lambda})(\mathbf{x}) := \int_{\Gamma_i} B_{\mathbf{n}(\mathbf{y})} G(\mathbf{x}, \mathbf{y}) \boldsymbol{\lambda}(\mathbf{y}) d\Gamma_i(\mathbf{y}) \quad (\text{conormal trace}),$$

that display the adequate behavior at infinity specified by the first point in the trace spaces. Specifically, $\boldsymbol{\lambda} \in \left[\widetilde{\mathbb{H}}^{-\frac{1}{2}}(\Gamma) \right]^m$ for the Dirichlet problem and $\boldsymbol{\lambda} \in \left[\widetilde{\mathbb{H}}^{\frac{1}{2}}(\Gamma) \right]^m$ for the conormal trace case.

With the above, the integral equation is constructed by imposing the boundary condition to the following representations:

$$\mathbf{U} = \sum_{i=1}^M \mathbf{SL}_i \boldsymbol{\lambda}_i \quad (\text{Dirichlet trace}),$$

$$\mathbf{U} = \sum_{i=1}^M \mathbf{DL}_i \boldsymbol{\lambda}_i \quad (\text{conormal trace}).$$

If the previously stated conditions are satisfied, then the construction of the arising BIEs as well as their wellposedness proof is done as in the cases that we presented in detail. It is worth noticing that the 2D-Laplace case is slightly different as the condition at infinity of the potential only holds in a subspace.

2.4. Numerical Analysis

We now describe a spectral Galerkin numerical scheme for solving Problem 2.3.3 and establish specific convergence rates.

2.4.1. Approximation Spaces

Our aim is to construct a dense conforming discretization of the spaces $\tilde{H}^{-1/2}(\Gamma_i)$ and $\tilde{H}_{\langle 0 \rangle}^{-1/2}(\Gamma_i)$, for $i \in \{1, \dots, M\}$. Certainly, one could use traditional low-order bases built on arc meshes for which approximation properties are well known. However, this would imply large numbers of dofs to solve problems with many arcs and/or large values of κ . Thus, we opt for high-order global polynomial bases such as weighted Chebyshev polynomials per arc.

2.4.1.1. Single Arc Approximation

We denote by $\{T_n\}_{n=0}^N$ the set of first $N+1$ first-kind Chebyshev polynomials, orthogonal under the weight w^{-1} with $w(t) := \sqrt{1-t^2}$. Consider the elements $p_n^i = T_n \circ \mathbf{r}_i^{-1}$ over each arc Γ_i , the space they span is denoted $\mathbb{T}_N(\Gamma_i)$, and define the normalized space:

$$\bar{\mathbb{T}}_N(\Gamma_i) := \left\{ \bar{p}^i \in C(\Gamma_i) : \bar{p}^i := \frac{p^i}{\|\mathbf{r}'_i \circ \mathbf{r}_i^{-1}\|_2}, \quad p^i \in \mathbb{T}_N(\Gamma_i) \right\}.$$

We account for edge singularities by multiplying by a suitable weight:

$$\mathbb{Q}_N(\Gamma_i) := \{q^i := w_i^{-1} \bar{p}^i : \bar{p}^i \in \bar{\mathbb{T}}_N(\Gamma_i)\},$$

wherein $w_i := w \circ \mathbf{r}_i^{-1}$. The corresponding bases for $\mathbb{Q}_N(\Gamma_i)$ will be denoted $\{q_n^i\}_{n=0}^N$, and are characterized by $q_n^i = w_i^{-1} \|\mathbf{r}'_i \circ \mathbf{r}_i^{-1}\|_2^{-1} T_n \circ \mathbf{r}_i^{-1}$. By Chebyshev orthogonality, we can easily define the mean-zero subspace:

$$\mathbb{Q}_{N,\langle 0 \rangle}(\Gamma_i) := \mathbb{Q}_N(\Gamma_i) / \mathbb{Q}_0(\Gamma_i),$$

spanned by $\{q_n^i\}_{n=1}^N$. Basic approximation properties of the spaces $\mathbb{Q}_N(\Gamma_i)$ are detailed in Appendix A.3.

2.4.1.2. Multiple Arcs Approximation

Let us define the approximation product spaces:

$$\mathbb{H}^N := \prod_{i=1}^M \mathbb{Q}_N(\Gamma_i), \quad \mathbb{H}_{\langle 0 \rangle}^N := \prod_{i=1}^M \mathbb{Q}_{N,\langle 0 \rangle}(\Gamma_i).$$

With the previously defined discrete spaces, we can find an approximation to the solution of Problem 2.3.3 by solving the following linear system.

PROBLEM 2.4.1 (Linear System). Let $m, N \in \mathbb{N}$, $\Gamma \in \mathcal{C}_v^m$, $\kappa > 0$, and $\mathbf{g} \in \mathbb{H}^{\frac{1}{2}}(\Gamma)$, we seek coefficients $\mathbf{u} = (\mathbf{u}_1, \dots, \mathbf{u}_M) \in \mathbb{C}^{M(N+1)}$, such that

$$\mathbf{L}[\kappa]\mathbf{u} = \mathbf{g},$$

wherein we have defined the Galerkin matrix $\mathbf{L}[\kappa] \in \mathbb{C}^{M(N+1) \times M(N+1)}$ with matrix blocks $\mathbf{L}_{ij} \in \mathbb{C}^{(N+1) \times (N+1)}$ whose entries are

$$(\mathbf{L}_{ij}[\kappa])_{lm} = \langle \mathcal{L}_{ij}[\kappa]q_m^j, q_l^i \rangle_{\Gamma_i}, \quad \forall i, j = 1, \dots, M, \text{ and } \forall l, m = 0, \dots, N. \quad (2.8)$$

The right-hand $\mathbf{g} = (\mathbf{g}_1, \dots, \mathbf{g}_M) \in \mathbb{C}^{M(N+1)}$ has components $(\mathbf{g}_i)_l = \langle g_i, q_l^i \rangle_{\Gamma_i}$.

For $\kappa = 0$ we impose $g \in (\widetilde{\mathbb{H}}_{(0)}^{-\frac{1}{2}}(\Gamma))^*$, and the spaces $\mathbb{Q}_N(\Gamma_j)$ have to be changed to $\mathbb{Q}_{N, \langle 0 \rangle}(\Gamma_j)$.

Approximations to solutions of Problem 2.3.3 are constructed using the solution \mathbf{u} of Problem 2.4.1 as follows

$$(\lambda_N)_i = \sum_{l=0}^N (\mathbf{u}_i)_l q_l^i \text{ in } \Gamma_i, \quad \text{for all } i \in \{1, \dots, M\}.$$

Observe that the sum starts with $l = 1$ if $\kappa = 0$.

REMARK 2.4.2. By performing a change of variables, we can recast Problem 2.4.1 on $\widehat{\Gamma}$ with matrix terms given by

$$(\mathbf{L}_{ij}[\kappa])_{lm} = \left\langle \widehat{\mathcal{L}}_{ij} w^{-1} T_m, w^{-1} T_l \right\rangle_{\widehat{\Gamma}}, \quad \forall i, j = 1, \dots, M, \text{ and } \forall l, m = 0, \dots, N,$$

with $w(t) = \sqrt{1 - t^2}$, and the right hand side $\mathbf{g} = (\mathbf{g}_1, \dots, \mathbf{g}_M) \in \mathbb{C}^{M(N+1)}$ with components $(\mathbf{g}_i)_l = \langle g \circ \mathbf{r}_i, w^{-1} T_l \rangle_{\widehat{\Gamma}}$. We have the corresponding approximation of the pulled back solution $\widehat{\lambda}$:

$$(\widehat{\lambda}_N)_i = \sum_{l=0}^N (\widehat{\mathbf{u}}_i)_l w^{-1} T_l \text{ in } \widehat{\Gamma}, \quad \text{for all } i \in \{1, \dots, M\}$$

The following result is a direct consequence of the coercivity of $\mathcal{L}[\kappa]$ and the basic approximation properties presented in Appendix A.3 (see (Sauter & Schwab, 2011, Theorem 4.29) for a detailed proof).

THEOREM 2.4.3. *For $\kappa > 0$, given $\mathbf{g} \in \mathbb{H}^{\frac{1}{2}}(\Gamma)$, there exist $N_0 \in \mathbb{N}$, and $C > 0$, both depending of Γ , \mathbf{g} , and κ such that for any $N \in \mathbb{N} : N > N_0$ there exist only one solution \mathbf{u} of Problem 2.4.1. Moreover, for the approximation $\boldsymbol{\lambda}_N \in \mathbb{H}^N$ we can bound the error as*

$$\|\boldsymbol{\lambda}_N - \boldsymbol{\lambda}\|_{\widetilde{\mathbb{H}}^{-\frac{1}{2}}(\Gamma)} \leq C \inf_{\mathbf{v}_N \in \mathbb{H}^N} \|\mathbf{v}_N - \boldsymbol{\lambda}\|_{\widetilde{\mathbb{H}}^{-\frac{1}{2}}(\Gamma)}.$$

For $\kappa = 0$ we need to take $\mathbf{g} \in (\widetilde{\mathbb{H}}_{\langle 0 \rangle}^{-\frac{1}{2}}(\Gamma))^$, and $\mathbb{H}_{\langle 0 \rangle}^N$ as the discrete space, for the result to hold.*

2.4.2. Convergence Results

The density of the family of spaces $\{\mathbb{H}^N\}_{N \in \mathbb{N}}$ in $\mathbb{H}^{-\frac{1}{2}}(\Gamma)$ (resp. $\{\mathbb{H}_{\langle 0 \rangle}^N\}_{N \in \mathbb{N}}$ in $\widetilde{\mathbb{H}}_{\langle 0 \rangle}^{-\frac{1}{2}}(\Gamma)$) shown in Appendix A.3 combined with Theorem 2.4.3 allows to conclude that when N goes to infinity convergence occurs in the general context. However, this does not provide any insight on convergence rates.

In this section, we will bound the error in terms of the dimension N , the degree of polynomials used in each arc. Explicit convergence rates with respect to κ are not analyzed and we leave this as future work. Similar bounds for error convergence rates were established in (Jerez-Hanckes et al., 2018) (for $\kappa = 0$ on an interval) and in (K. E. Atkinson & Sloan, 1991). This last work while only shows the Laplace case for one arc, could be extended for multiple arcs easily. The authors also consider the error introduced by the quadrature scheme. However, the extension to Helmholtz does not appear to be straightforward, as it is hard to argue data regularity is preserved. In fact, proving this last point takes significant effort. The effect of numeric integration will not be considered here but one can easily show that it introduces an extra error which decays as fast as the Fourier-Chebyshev coefficients of the (regular) right-hand side and the geometry (*cf.* Section 2.5).

Before carrying on, we review the general idea presented in this section. In Sections 2.4.2.1, and 2.4.2.2 we characterize the decay of Chebyshev coefficients $\{\lambda_n\}_{n \in \mathbb{N}}$ appearing in the solution of the single scatter problem. This is done in a constructive way: we start with the most simple case ($\kappa = 0, \Gamma = \widehat{\Gamma}$) Lemma 2.4.5, and finalize with a general arc for non-zero frequency in Lemma 2.4.16 (Lemmas 2.4.9, and 2.4.13 are intermediate results). Once the coefficients' decay is characterized, we use it in conjunction with the quasi-optimality result to establish the error convergence of a single arc problem (Theorem 2.4.17). Finally, in Section 2.4.2.4 we generalize the results for multiple arcs. For this, we first establish the decay of the coefficients (Lemma 2.4.20) and conclude, as in the single arc case, in Theorem 2.4.21 which gives the rate of convergence for general multiple arcs and $\kappa \geq 0$.

We start by analyzing the most simple problem $-\kappa = 0$ and a single interval—, and from there we gradually consider more generalities until we arrive to the most complex case ($\kappa > 0$ for multiple arcs). Every function $\widehat{\lambda}$ in $\widetilde{H}^{-\frac{1}{2}}(\widehat{\Gamma})$, can be expressed as a convergent series:

$$\widehat{\lambda}(s) = w^{-1} \sum_{n \geq 0} \lambda_n T_n(s), \quad s \in (-1, 1).$$

Furthermore, we have an explicit expression for the $\widetilde{H}^{-\frac{1}{2}}(\widehat{\Gamma})$ -norm when such representation is used

$$\left\| \widehat{\lambda} \right\|_{\widetilde{H}^{-\frac{1}{2}}(\widehat{\Gamma})}^2 = \sum_{n \geq 0} |\lambda_n|^2 d_n, \quad (2.9)$$

where $d_0 = 1$, and $d_n = n^{-1}$ for $n > 0$ (Jerez-Hanckes & Nédélec, 2011, proof of Proposition 3.5).

2.4.2.1. Chebyshev Coefficients Behavior: Laplace Case

We recall operators $\check{\mathcal{L}}[0]$ and $\widehat{\mathcal{L}}[0]$ defined over $\widehat{\Gamma}$ (cf. Remark 2.3.5). In this section, we consider the pullback problem:

PROBLEM 2.4.4. For $m \in \mathbb{N}$ given $\Gamma \in \mathcal{C}_v^m$, and $g \in \mathcal{C}_v^m(\Gamma) \cap (\widetilde{H}_{(0)}^{-\frac{1}{2}}(\Gamma))^*$, we seek $\widehat{\lambda} \in \widetilde{H}_{(0)}^{-\frac{1}{2}}(\widehat{\Gamma})$ such that

$$\widehat{\mathcal{L}}[0]\widehat{\lambda} = \widehat{g} \quad \text{on } \widehat{\Gamma},$$

which is equivalent to Problem 2.3.3 with $\kappa = 0$ and $M = 1$.

We aim to characterize the mapping properties of these weakly singular BIOs (defined as in Section 2.3) acting on weighted Chebyshev polynomials.

LEMMA 2.4.5. *For n and l in \mathbb{N} , it holds*

$$\left\langle \check{\mathcal{L}}[0] \frac{T_n}{w}, \frac{T_l}{w} \right\rangle = \frac{\pi}{4n} \delta_{nl}.$$

PROOF. Direct consequence of the kernel expansion ((Jerez-Hanckes & Nédélec, 2012, Theorem 4.4)):

$$G_0(\mathbf{x}, \mathbf{y}) = -\frac{1}{2\pi} \log |t - s| = \frac{1}{2\pi} \log 2 + \sum_{n \geq 1} \frac{1}{\pi n} T_n(t) T_n(s), \quad \forall s \neq t.$$

and the orthogonality property of Chebyshev polynomials. \square

One can interpret this result as follows: given an element in $\widehat{\lambda} \in \widetilde{H}^{-\frac{1}{2}}(\widehat{\Gamma})$, its image by $\check{\mathcal{L}}[0]$ is a function whose Chebyshev coefficients decay as $\mathcal{O}(n^{-1})$. The rest of this section extends this idea to more general arcs.

LEMMA 2.4.6. *For $m \in \mathbb{N}$, let $h : [-1, 1]^2 \rightarrow \mathbb{C}$ be such that $h(t, \cdot)$ and $h(\cdot, s)$ are $\mathcal{C}_v^m(-1, 1)$ -functions as functions of s and t , respectively. Thus, we can write h as*

$$h(t, s) = \sum_{n=0}^{\infty} \sum_{k=0}^{\infty} b_{nk} T_n(t) T_k(s),$$

with coefficients decaying as follows:

$$b_{nk} = \mathcal{O} \left(\min \{ n^{-m-1}, k^{-m-1} \} \right).$$

If h is ρ -analytic in both variables

$$b_{nk} = \mathcal{O} \left(\rho^{\min \{-n, -k\}} \right).$$

PROOF. This is just the bivariate version of (L. Trefethen, 2013, Theorem 7.1) and (L. Trefethen, 2013, Theorem 8.1) (see Appendix A.2 for a detailed proof). \square

LEMMA 2.4.7. *Let $m \in \mathbb{N}$ and $h : [-1, 1]^2 \rightarrow \mathbb{C}$ be a $\mathcal{C}_v^m(-1, 1)$ -function in both arguments. Consider the integral operator taking as kernel the bivariate function h :*

$$(\mathcal{H}f)(s) := \int_{\widehat{\Gamma}} h(t, s) f(t) dt,$$

Let $f \in \widetilde{H}^{-1/2}(\widehat{\Gamma})$, then for $\epsilon \in \mathbb{R}$ such that $0 < \epsilon < 1$, we have that the Fourier-Chebyshev coefficients of $\mathcal{H}f$, denoted $\{v_l\}_{l \in \mathbb{N}_0}$, decay as

$$v_l = \mathcal{O}(l^{(-1+\epsilon)m}).$$

Moreover, if the kernel is ρ -analytic we have that

$$v_l = \mathcal{O}(\rho^{-l}).$$

PROOF. See Appendix A.2. □

REMARK 2.4.8. The previous result is by no means sharp. In the context of pseudo-differential operators using Fourier expansion for the norms one could obtain better bounds, see for example (Saranen & Vainikko, 2013, Chapter 7). Results for open arcs in terms of Fourier-Chebyshev expansions can be obtained using the cosine change of variables.

We continue by estimating bounds for the Chebyshev coefficients of solutions of the BIE associated to the Laplace problem for any sufficiently smooth single arc.

LEMMA 2.4.9. *Let $\widehat{\lambda} \in \widetilde{H}_{(0)}^{-\frac{1}{2}}(\widehat{\Gamma})$ be the unique solution of Problem 2.4.4, with $m \geq 2$. If we expand $\widehat{\lambda}$ as*

$$\widehat{\lambda} = w^{-1} \sum_{n=1}^{\infty} a_n T_n,$$

we obtain the following coefficient asymptotic behaviors:

$$a_n = \mathcal{O}(n^{-m}).$$

Moreover, if Γ is a ρ -analytic arc and g is also ρ -analytic, we obtain

$$a_n = \mathcal{O}(n\rho^{-n}).$$

PROOF. Since $\widehat{g} = g \circ \mathbf{r}$, we can expand it as a Fourier-Chebyshev series with coefficients \widehat{g}_l leading to

$$(\widehat{\mathcal{L}}[0]\widehat{\lambda})_l = \widehat{g}_l, \quad \forall l \in \mathbb{N}.$$

The coefficients of the left-hand side of the latter equation can be computed by adding and subtracting the term $\check{\mathcal{L}}[0]\widehat{\lambda}$. By doing so and combining Lemmas 2.4.5, 2.4.6, 2.4.7 and 2.3.6, we obtain the following expression:

$$\frac{\pi}{4} \frac{a_l}{l} + v_l = \widehat{g}_l, \quad \forall l \in \mathbb{N},$$

where the coefficient v_l corresponds to that in the expansion of $(\widehat{\mathcal{L}}[0] - \check{\mathcal{L}}[0])\widehat{\lambda}$. By the regularity conditions, it holds $\widehat{g}_l = \mathcal{O}(l^{-m-1})$, and therefore,

$$\frac{\pi}{4} a_l l^{-1} + v_l = \mathcal{O}(l^{-m-1}).$$

Hence, there are two alternatives: either (i) $a_l = \mathcal{O}(l^{-m})$ and $v_l = \mathcal{O}(l^{-m-1})$, or (ii) both have the same decay order. As the first implies the result directly, we assume the second alternative in what follows.

Let $2 < m < \infty$. By Lemma 2.4.7 (i), we have that $v_l = \mathcal{O}(l^{(-1+\epsilon')m})$, and under our current assumption, this implies that

$$a_l = \mathcal{O}(l^{(-1+\epsilon')m}).$$

Since $m > 2$, we can choose ϵ such that $\sum_{n=1}^{\infty} a_n$ is finite and a new estimate for v_l holds

$$v_l = \sum_{n=1}^{\infty} b_{nl} a_n \lesssim l^{-m-1}.$$

Here, b_{nl} are the coefficients detailed in Lemma 2.4.6 for the function $E_{\mathbf{r}}$ defined in Remark 2.3.5. This last equality implies the result directly. The case $m = 2$ is slightly more complicated as one can not directly ensure that the coefficients a_l are summable. However, by Lemma 2.4.7, for a small $\delta > 0$, then $v_l = \mathcal{O}(l^{-2+\delta})$, which implies that $a_l = \mathcal{O}(l^{-1+\delta})$. By re-estimating bounds on v_l , we now obtain that $v_l = \mathcal{O}(l^{-3+2\delta})$. Hence, $a_l = \mathcal{O}(l^{-2+2\delta})$ which are summable from where one can argue as before. For the

ρ -analytic, the result is direct as the v_l already has a decay that implies the corresponding behavior of the coefficients a_l . \square

2.4.2.2. Chebyshev Coefficients Behavior: Helmholtz Case

We now consider the following single arc problem:

PROBLEM 2.4.10. For $m \in \mathbb{N}$, $\kappa > 0$, given $\Gamma \in \mathcal{C}_v^m$, and $g \in \mathcal{C}_v^m(\Gamma)$, we seek $\hat{\lambda} \in \tilde{H}_{(0)}^{-\frac{1}{2}}(\hat{\Gamma})$ such that

$$\hat{\mathcal{L}}[\kappa]\hat{\lambda} = \hat{g} \quad \text{on } \hat{\Gamma}, \quad (2.10)$$

which is equivalent to Problem 2.3.3 with $\kappa > 0$ and $M = 1$.

One could see the Helmholtz case as a perturbation of the previous one, but this perturbation is not smooth as the operator difference $\hat{\mathcal{L}}[\kappa] - \check{\mathcal{L}}[0]$ (cf. Remark 2.3.5) only has a \mathcal{C}^1 -kernel, even for smooth arcs. Thus, we can not replicate the previous arguments and need to examine in depth $\hat{\mathcal{L}}[\kappa] - \check{\mathcal{L}}[0]$ in terms of Chebyshev coefficients.

Using (Abramowitz & Stegun, 1965, Formula 9.1.13), the kernel of $\hat{\mathcal{L}}[\kappa]$, given in (2.5), can be also be written as

$$\hat{G}_k(t, s) = \frac{i}{4} H_0^1(k \|\mathbf{r}(t) - \mathbf{r}(s)\|_2) = \sum_{p=0}^{\infty} z_p R_p(t, s) |t - s|^{2p} \log |t - s| + \psi_R(t, s),$$

wherein $\mathbf{r} : (-1, 1) \rightarrow \Gamma_i$ is a suitable parametrization,

$$z_p := \frac{1}{2\pi} (-1)^p \left(\frac{k}{2}\right)^{2p} (p!)^{-2}, \quad (2.11)$$

$$R_p(t, s) := \left(\frac{\|\mathbf{r}(t) - \mathbf{r}(s)\|_2}{|t - s|} \right)^{2p}, \quad (2.12)$$

and ψ_R is $C_v^m(-1, 1)$ -regular in each component. Notice that the term $|t - s|^{2p} \log |t - s|$ is a $\mathcal{C}^{2p-1}(-1, 1)$ -function in each component.

We begin by analyzing the Helmholtz case for $\hat{\Gamma}$ following similar techniques to those in (Frenkel, 1983). To simplify notation, we define kernels $\hat{G}_k^p(t, s) := z_p R_p(t, s) |t -$

$s|^{2p} \log |t - s|$ and their corresponding BIOs:

$$\widehat{\mathcal{L}}^p[\kappa]f := \int_{-1}^1 \widehat{G}_k^p(t, s) f(t) dt.$$

Extensive use will be given to the following lemma:

LEMMA 2.4.11. *For $p \in \mathbb{N}_0$, we have*

$$|t - s|^{2p} \log |t - s| = \sum_{n=0}^{\infty} \sum_{l=0}^{\infty} b_{nl}^p T_n(t) T_l(s)$$

where

$$b_{nl}^p = \begin{cases} \mathcal{O}(l^{-(2p+1)}) & n = l, l \pm 2, \dots, l \pm 2p \\ 0 & \text{any other case.} \end{cases}$$

PROOF. We proceed by induction. As the case $p = 0$ was proven in Lemma 2.4.5, we start by setting $p = 1$. By Lemma A.4.2, it holds

$$|t - s|^2 \log |t - s| = \sum_{j \in \{-1, 0, 1\}} \sum_{n=0}^{\infty} \beta_n^{(j)} T_n(t) T_{|n+2j|}(s).$$

Moreover, bounds for coefficients $\beta_n^{(j)}$ are found by using Lemma A.4.2. Since in this case $a_n := b_n^0 = \mathcal{O}(\frac{2}{n})$ (cf. Lemma 2.4.5), we obtain the stated result.

Assuming now that the result holds for $p \geq 2$, we prove it for $p + 1$. Indeed,

$$\begin{aligned} |t - s|^2 (|t - s|^{2p} \log |t - s|) &= |t - s|^2 \sum_{n=0}^{\infty} \sum_{l=0}^{\infty} b_{nl}^p T_n(t) T_l(s) \\ &= |t - s|^2 \sum_{j \in \{-1, 0, 1\}^n} \sum_{n=0}^{\infty} \beta_n^{(j)} T_n(t) T_{|n+2 \sum j|}(s) \end{aligned}$$

and we proceed as in the proof of Lemma A.4.2 to obtain the expansion. The asymptotic behavior is obtained by a direct computation using expressions of Lemma A.4.2. \square

LEMMA 2.4.12. *Let $\widehat{\lambda} \in \widetilde{H}^{-\frac{1}{2}}(\widehat{\Gamma})$ with expansion*

$$\widehat{\lambda} = w^{-1} \sum_{n=0}^{\infty} a_n T_n.$$

Then, the Fourier-Chebyshev coefficients of $\widehat{\mathcal{L}}^p[\kappa]\widehat{\lambda}$, denoted $\{v_l^p\}_{l \in \mathbb{N}_0}$, are given by

$$v_l^p = z_p \sum_{n=0}^{\infty} b_{nl}^p a_n,$$

where the coefficients b_{nl}^p are given by Lemma 2.4.11, and terms z_p are defined in (2.11).

Moreover, it holds

$$v_l^p = \mathcal{O}(l^{-2p-\frac{1}{2}}).$$

PROOF. The representation is a direct consequence of the Fourier-Chebyshev expansion of $\widehat{\lambda}$ and the kernel function given by Lemma 2.4.11. The asymptotic behavior is deduced as follows

$$|v_l^p| \sim \left| \sum_{n=0}^{\infty} b_{nl}^p a_n \right| \leq \|\widehat{\lambda}\|_{\widetilde{H}^{-\frac{1}{2}}(\widehat{\Gamma})} \left| \sum_{n=0}^{\infty} (b_{nl}^p)^2 d_n^{-1} \right|^{\frac{1}{2}}, \lesssim l^{-2p-\frac{1}{2}},$$

with d_n coming from (2.9) and where the last inequality is obtained using Lemma 2.4.11. \square

With the above results, we can estimate the asymptotic order of the Chebyshev coefficients of $\check{\mathcal{L}}[\kappa] - \check{\mathcal{L}}[0]$, where $\check{\mathcal{L}}[\kappa]$ is the weakly singular Helmholtz operator for the special case $\Gamma \equiv \widehat{\Gamma}$. This bound turns out to be crucial in proving the convergence of the proposed method.

LEMMA 2.4.13. Let $\widehat{\lambda} \in \widetilde{H}^{-\frac{1}{2}}(\widehat{\Gamma})$ be the only solution of Problem 2.4.10, with $\Gamma = \widehat{\Gamma}$, and expand it as

$$\widehat{\lambda} = w^{-1} \sum_{n=0}^{\infty} a_n T_n$$

Then, the coefficients a_n decay as

$$a_n = \mathcal{O}(n^{-m}).$$

Moreover, if g is ρ -analytic, we have that

$$a_n = \mathcal{O}(n\rho^{-n}).$$

PROOF. By the regularity of g , we have

$$(\check{\mathcal{L}}[\kappa]\lambda)_l = g_l = \mathcal{O}(l^{-m-1}).$$

On the other hand, using the integral kernel expansion and Lemma 2.4.5, for any $Q \in \mathbb{N}$, with $Q > 1$, we derive

$$(\check{\mathcal{L}}[\kappa]\lambda)_l = \frac{\pi^2}{4} \frac{a_l}{l} + \sum_{j=1}^{Q-1} v_l^j + v_l^{R(Q)},$$

where coefficients v_l^j are given by Lemma 2.4.12 and $v_l^{R(Q)}$ is the remainder of order $\mathcal{O}(l^{-2Q-\frac{1}{2}})$. Thus, if we choose Q as the upper integer part of $\frac{m+1}{2}$, we have that

$$\frac{\pi}{4} \frac{a_l}{l} + \sum_{j=1}^{Q-1} v_l^j = \mathcal{O}(l^{-m-1}).$$

From the latter equation we need to deduce the behavior of the coefficients a_l given the value of m . We proceed by induction, if $m = 1$ we have that

$$\frac{\pi^2}{4} \frac{a_l}{l} = \mathcal{O}(l^{-2}),$$

which directly implies $a_l = \mathcal{O}(l^{-1})$. For the induction hypothesis we denote $Q(r)$ the corresponding value of Q given a natural number $r < m$. Then, the induction hypothesis reads as: if

$$\frac{\pi}{4} \frac{a_l}{l} + \sum_{j=1}^{Q(r)-1} v_l^j = \mathcal{O}(l^{-r-1}), \quad (2.13)$$

then $a_l = \mathcal{O}(l^{-r})$. Now, we prove for $r + 1$, since we do not assume that r is even or odd we have two options: $Q(r + 1) = Q(r)$ or $Q(r + 1) = Q(r) + 1$. If the latter is true, there is a new term of order $-r - 1$. Thus, without loss of generality we can assume that

$$\frac{\pi}{4} \frac{a_l}{l} + \sum_{j=1}^{Q(r)-1} v_l^j = \mathcal{O}(l^{-r-1}).$$

By the induction hypothesis, $a_l = O(l^{-r})$. Then, by definition of coefficients v_l^j as in Lemma 2.4.12, and Lemma 2.4.11 one has

$$\begin{aligned} v_l^1 &= \mathcal{O}(l^{-r-3}) \\ v_l^2 &= \mathcal{O}(l^{-r-5}) \\ &\vdots \\ v_l^{Q(n)-1} &= \mathcal{O}(l^{-r-1-2(Q(r)-1)}), \end{aligned}$$

and so from (2.13) we obtain the correct order for a_l .

The ρ -analytic case employs the same argument. As $a_l l^{-1}$ and $\sum_{j=1}^{\infty} v_l^j$ cannot have the same decay order, the only option is for both terms to decay geometrically. \square

To end this section, we consider the Helmholtz case for general arcs. Our main ingredients here are the bounds for Chebyshev coefficients of the product of two functions. For one-dimensional \mathcal{C}^1 -functions, this can be done easily: let $f(t) = \sum_{k \in \mathbb{N}_0} f_k T_k(t)$ and $g(t) = \sum_{l \in \mathbb{N}_0} g_l T_l(t)$. One can write

$$f(t)g(t) = \sum_{n \in \mathbb{N}_0} e_n c_n T_n(t), \quad \text{where } e_n = \int_{-1}^1 f(t)g(t) \frac{T_n(t)}{w(t)} dt,$$

and $c_0 = \pi^{-1}$, $c_n = 2\pi^{-1}$, for $n > 0$. By replacing the series expansion for f above, we derive

$$e_n = \sum_{k \in \mathbb{N}_0} f_k \int_{-1}^1 g(t) T_k(t) \frac{T_n(t)}{w(t)} dt,$$

Using now Lemma A.4.1 and Chebyshev orthogonality, it holds

$$e_n = \sum_{k \in \mathbb{N}_0} f_k \int_{-1}^1 g(t) \frac{T_{k+n}(t) + T_{|k-n|}(t)}{2w(t)} dt = \sum_{k \in \mathbb{N}_0} \frac{f_k}{2} \left(\frac{g_{k+n}}{c_{k+n}} + \frac{g_{|k-n|}}{c_{|k-n|}} \right).$$

Consequently, we can estimate the decay of e_n by the properties of f_n and g_n . In two dimensions we have a similar result.

LEMMA 2.4.14. *Let $m \in \mathbb{N}$, $p \in \mathbb{N}$, and recall the definition of $R_p(t, s)$ given in (2.12). Then, the series*

$$R_p(t, s)|t - s|^{2p} \log |t - s| = \sum_{i=0}^{\infty} \sum_{j=0}^{\infty} C_{ij}^p T_i(t) T_j(t), \quad \forall (t, s) \in [-1, 1]^2,$$

holds, with coefficients

$$C_{ij}^p = \sum_{n=0}^{\infty} \sum_{l=0}^{\infty} \frac{b_{nl}^p}{4} (r_{n+i, l+j} + r_{n+i, |l-j|} + r_{|n-i|, l+j} + r_{|n-i|, |l-j|})$$

with coefficients b_{nl}^p being those of Lemma 2.4.11 and $r_{i,j}$ the Chebyshev coefficients of $R_p(t, s)$. Moreover, the following asymptotic behavior hold

$$C_{ij}^p = \mathcal{O}(\min\{i^{-\min(m+1, 2p+1)}, j^{-\min(m+1, 2p+1)}\}).$$

If we consider a ρ -analytic arc we have

$$C_{ij}^p = \mathcal{O}(\min\{i^{-(2p+1)}, j^{-(2p+1)}\}).$$

PROOF. See Appendix A.2. □

LEMMA 2.4.15. *For $m \in \mathbb{N}$, let $\Gamma \in \mathcal{C}_v^m$ and $\hat{\lambda} \in \tilde{H}^{-\frac{1}{2}}(\hat{\Gamma})$ have the representation:*

$$\hat{\lambda} = w^{-1} \sum_{n=0}^{\infty} a_n T_n.$$

Then, the Fourier-Chebyshev coefficients of $\hat{\mathcal{L}}^p[\kappa]\hat{\lambda}$, denoted $\{v_l^p\}_{l \in \mathbb{N}_0}$, satisfy

$$v_l^p = z_p \sum_{n=0}^{\infty} C_{nl}^p a_n,$$

where the coefficients C_{nl}^p are given in Lemma 2.4.14, z_p are defined in (2.11), and the asymptotic behaviors hold

- (i) *If $m \leq 2p$ and for $\epsilon \in \mathbb{R}$ such that $0 < \epsilon < 1 - \frac{1}{m+1}$, $v_l^p = \mathcal{O}(l^{-m+(m+1)\epsilon})$*
- (ii) *If $m > 2p$ and for $\epsilon \in \mathbb{R}$ such that $0 < \epsilon < 1 - \frac{1}{2p+1}$, $v_l^p = \mathcal{O}(l^{-2p+(2p+1)\epsilon})$.*

PROOF. The proof follows the steps of Lemma 2.4.7 but by using Lemma 2.4.14 instead of Lemma 2.4.11. \square

LEMMA 2.4.16. *For $m \in \mathbb{N}$ with $m \geq 2$, let $\widehat{\lambda} \in \widetilde{H}^{-\frac{1}{2}}(\widehat{\Gamma})$ be the unique solution of Problem 2.4.10. Then, if the solution is expanded as $\widehat{\lambda} = \sum_{n=0}^{\infty} a_n w^{-1} T_n$, the following asymptotic behaviors for coefficients a_n holds*

$$a_n = \mathcal{O}(n^{-m}).$$

Moreover, if Γ and g are ρ -analytic

$$a_n = \mathcal{O}(n\rho^{-n}).$$

PROOF. We follow similar steps of those for Lemmas 2.4.13 and 2.4.9, the integral equation reads as

$$(\widehat{\mathcal{L}}[\kappa]\widehat{\lambda})_l = \frac{\pi}{4} \frac{a_l}{l} + \sum_{j=1}^Q v_l^j + v_l^R = \mathcal{O}(l^{-m-1}),$$

where v_l^j are defined as in Lemma 2.4.15, and Q is fixed such that the remainder is given by a $\mathcal{C}_v^m(-1, 1)$ -function. Thus, for $\epsilon \in (0, 1 - \frac{1}{m+1})$, $v_l^R = \mathcal{O}(l^{-m+(m+1)\epsilon})$. Moreover, we can assume that, for $\delta \in (0, 1 - \frac{1}{3})$, by Lemma 2.4.15, it holds $v_l^j = \mathcal{O}(l^{-2j+(2j+1)\delta})$, for all $j = 1, \dots, Q$. The rest of the proof is the same as in Lemma 2.4.9, as standard, the ρ -analytic case follows the same arguments. \square

2.4.2.3. Convergence rates for a single arc

From the decay properties of Chebyshev coefficients, we can obtain bounds for the approximation error. First, notice that, by norm equivalences (cf. Lemma 2.2.1), we can do all the estimates in $\widehat{\Gamma}$ and transform $\lambda \mapsto \widehat{\lambda}$. On the other hand, we have the quasi-optimality result (cf. Theorem 2.4.3): there exists $N_0 > 0$ and a constant $C(\Gamma, \kappa) > 0$, such that for all $N > N_0$:

$$\|\lambda - \lambda_N\|_{\widetilde{H}^{-1/2}(\Gamma)} \leq C(\Gamma, \kappa) \inf_{q_N \in \mathbb{Q}_N(\widehat{\Gamma})} \left\| \widehat{\lambda} - q_N \right\|_{\widetilde{H}^{-1/2}(\widehat{\Gamma})}.$$

For $\hat{\lambda}$ we have an expansion of the form $\hat{\lambda} = \sum a_n w^{-1} T_n$. Hence, we can choose $q_N = \sum_{n \leq N} a_n w^{-1} T_n$, and use the norm representation to estimate the error as

$$\left\| \hat{\lambda} - q_N \right\|_{\tilde{H}^{-1/2}(\hat{\Gamma})}^2 = \sum_{n > N} \frac{|a_n|^2}{n}.$$

Finally, using the bounds from Lemmas 2.4.16, and 2.4.9 for the behavior of coefficients a_n , we can establish convergence rates.

THEOREM 2.4.17. *Let $\kappa > 0$, $m \in \mathbb{N}$ with $m \geq 2$, $\Gamma \in \mathcal{C}_v^m$. For $g \in \mathcal{C}_v^m(\Gamma)$, let λ be the unique solution of Problem 2.3.3, and λ_N the approximation obtained from the solution of 2.4.1, with $N > N_0$ according to Theorem 2.4.3. Then there is a constant $C(\Gamma, \kappa)$, such that*

$$\|\lambda - \lambda_N\|_{\tilde{H}^{-1/2}(\Gamma)} \leq C(\Gamma, \kappa) N^{-m}.$$

Moreover, if Γ and g are ρ -analytic we have that

$$\|\lambda - \lambda_N\|_{\tilde{H}^{-1/2}(\Gamma)} \leq C(\Gamma, \kappa) \rho^{-N+2} \sqrt{N}.$$

If $\kappa = 0$ we need also that $g \in (\tilde{H}_{(0)}^{-1/2}(\Gamma))^*$, for the result to hold true.

PROOF. Following the above discussion, we have to estimate $\sum_{n > N} \frac{|a_n|^2}{n}$, where the a_n are characterized in Lemmas 2.4.9 and 2.4.16. Since these are decreasing, the results follows from the following elementary estimation:

$$\sum_{n > N} \frac{|a_n|^2}{n} \leq \int_N^\infty \frac{a(\xi)^2}{\xi} d\xi,$$

where $a(\xi)$ is a monotonously continuous decreasing function such that $a(n) = |a_n|$. \square

REMARK 2.4.18. Even though N_0 and $C(\Gamma, \kappa)$ depend on the geometry and wave-number κ , the decay rates do not depend on any of these two.

2.4.2.4. Multiple arcs approximation

Since the existence of more than one arc translates into perturbations of the Chebyshev coefficients with decay rates given by arc regularity, convergence rates for the case of multiple arcs are given by those of the single arc case. To see this, let us recall Problem 2.3.3 for the case of two \mathcal{C}_v^m -arcs pullbacked onto $\widehat{\Gamma}$: for $g_1, g_2 \in C_v^m(\widehat{\Gamma})$, find $\widehat{\lambda}_1, \widehat{\lambda}_2 \in \widetilde{H}^{-\frac{1}{2}}(\widehat{\Gamma})$ such that

$$\begin{aligned}\widehat{\mathcal{L}}_{11}[\kappa]\widehat{\lambda}_1 + \widehat{\mathcal{L}}_{12}[\kappa]\widehat{\lambda}_2 &= \widehat{g}_1, \\ \widehat{\mathcal{L}}_{21}[\kappa]\widehat{\lambda}_1 + \widehat{\mathcal{L}}_{22}[\kappa]\widehat{\lambda}_2 &= \widehat{g}_2.\end{aligned}$$

By Assumption 2.2, the arcs cannot touch nor intersect. Hence, there is always $d > 0$ such that for all $(\mathbf{x}, \mathbf{y}) \in \Gamma_1 \times \Gamma_2$, $\|\mathbf{x} - \mathbf{y}\|_2 > d$. This leads to the next result.

LEMMA 2.4.19. *Let $m \in \mathbb{N}$ consider two open \mathcal{C}_v^m -arcs fulfilling Assumption 2.2. Then, if we write the pulled back solutions as*

$$\widehat{\lambda}_i = \sum a_n^i \frac{T_n}{w},$$

for $i \neq j$, it holds

$$(\widehat{\mathcal{L}}_{ij}[\kappa]\widehat{\lambda})_l = \sum_n b_{nl} a_n,$$

with asymptotic decay rate:

$$b_{nl} = \mathcal{O}(\min\{n^{-m-1}, l^{-m-1}\}).$$

Moreover, if the arcs Γ_1, Γ_2 and \mathbf{g} are ρ -analytics we have that

$$b_{nl} = \mathcal{O}(\rho^{\min\{-m, -l\}}).$$

PROOF. As the distance between two disjoint arcs is strictly positive, the kernel $G_\kappa(\mathbf{r}_i(t), \mathbf{r}_j(s))$ belongs to \mathcal{C}_v^m and the proof follows verbatim that of Lemma 2.4.6.

□

LEMMA 2.4.20. *Let $m \in \mathbb{N}$ with $m \geq 2$, and λ be the only solution of Problem 2.3.3, whose pullback is expanded as $\sum_{n \geq \mathbb{N}_0} a_n^j w^{-1} T_n$, it holds*

$$a_n^j = \mathcal{O}(n^{-m}).$$

Moreover, for the ρ -analytic case we have that

$$a_n^j = \mathcal{O}(n\rho^{-n}).$$

PROOF. The proof is similar to that of Lemma 2.4.16, now taking care of cross-interaction terms by Lemma 2.4.19 and using the same arguments from Lemma 2.4.9. \square

THEOREM 2.4.21. *Let $m \in \mathbb{N}$ with $m > 2$, $\kappa > 0$, $\Gamma \in \mathcal{C}_v^m$, $\mathbf{g} \in \mathcal{C}_v^m(\Gamma)$, λ the only solution of Problem 2.3.3 and λ_N approximation constructed from 2.4.1, then we have the*

$$\|\lambda - \lambda_N\|_{\tilde{\mathbb{H}}^{-\frac{1}{2}}(\Gamma)} \leq C(\Gamma, \kappa) N^{-m+1},$$

and for the ρ -analytic case

$$\|\lambda - \lambda_N\|_{\tilde{\mathbb{H}}^{-\frac{1}{2}}(\Gamma)} \leq C(\Gamma, \kappa) \rho^{-N+2} \sqrt{N}.$$

For $\kappa = 0$ we need to impose the condition $\mathbf{g} \in (\tilde{\mathbb{H}}_{(0)}^{-\frac{1}{2}}(\Gamma))^$.*

PROOF. The proof follows that of Theorem 2.4.17 as the $\tilde{\mathbb{H}}^{-\frac{1}{2}}(\Gamma)$ -norm is equivalent to the Cartesian product of M times the space $\tilde{H}^{-\frac{1}{2}}(\hat{\Gamma})$ with corresponding bounds for the coefficients established in Lemma 2.4.20. \square

2.5. Matrix computations

We now explicitly describe numerically how to solve Problem 2.4.1 using the discrete spaces defined in Section 2.4.1. By definition (2.8), the matrix entries are

$$(\mathbf{L}_{ij}[\kappa])_{ln} = \langle \mathcal{L}_{ij}[\kappa] q_n^j, q_l^i \rangle_{\Gamma_i}.$$

In Remark 2.4.2, we showed that this can be computed as

$$(\mathbb{L}_{ij}[\kappa])_{ln} = \left\langle \widehat{\mathcal{L}}_{ij}[\kappa] w^{-1} T_n, w^{-1} T_l \right\rangle_{\widehat{\Gamma}}.$$

First, we review how the integrals involving the functions $w^{-1} T_n$ can be approximated.

2.5.1. Fourier-Chebyshev expansions

Every function in $\mathcal{C}^1([-1, 1])$ can be expanded as a Chebyshev series (cf. (L. Trefethen, 2013, Theorem 3.1)),

$$f(s) = \sum_{n=0}^{\infty} f_n T_n(s), \quad \forall s \in [-1, 1] \quad \text{with} \quad f_n := c_n \langle f, w^{-1} T_n \rangle_{\widehat{\Gamma}},$$

with $c_0 = \pi$ and $c_n = \pi/2$ for $n > 0$. For a given $N \in \mathbb{N}$, the Fourier-Chebyshev coefficients $\{f_n\}_{n \in \mathbb{N}_0}$ can be approximated using the FFT as follows:

- (i) Construct a vector $\mathbf{v}^N \in \mathbb{C}^{N+1}$ with entries $f(s_n^N)$, for $n = 0, \dots, N$, and where the $s_n^N = \cos(n\pi/N)$ correspond to the Chebyshev points of order N .
- (ii) Apply the FFT to a periodic extension of the vector \mathbf{f}^N ,

$$\widetilde{\mathbf{f}}^N := FFT(v_N^N, v_{N-1}^N, \dots, v_1^N, v_0^N, v_1^N, \dots, v_N^N).$$

- (iii) Define the approximations as

$$f_n^N := \widetilde{f}_n^N, \quad n = 1, \dots, N-1, \quad f_0^N = \frac{1}{2} \widetilde{f}_0^N, \quad f_N^N = \frac{1}{2} \widetilde{f}_N^N.$$

REMARK 2.5.1. Notice that Fourier-Chebyshev expansions correspond to the expansions of even functions in Fourier basis under a cosine change of variable.

Using aliasing properties of Chebyshev series, one can easily see that for $f \in \mathcal{C}_v^m(-1, 1)$,

$$|f_n - f_n^N| = \mathcal{O}(N^{-m-1}),$$

while for ρ -analytic functions, it holds

$$|f_n - f_n^N| = \mathcal{O}(\rho^{-N}).$$

For more details see (L. Trefethen, 2013, Chapter 4).

2.5.2. Kernel expansion

An expansion similar to the one above holds for the fundamental solution $G_0(\mathbf{x}, \mathbf{y})$ when $\kappa = 0$ over $\widehat{\Gamma}$. Specifically, for collinear vectors, i.e. $\mathbf{x} = (t, 0)$ and $\mathbf{y} = (s, 0)$, $(s, t) \in [-1, 1]^2$, it holds (*cf.* (Reade, 1979) and (Jerez-Hanckes & Nédélec, 2012, Theorem 4.4)):

$$G_0(\mathbf{x}, \mathbf{y}) = -\frac{1}{2\pi} \log |t - s| = \frac{1}{2\pi} \log 2 + \sum_{n \geq 1} \frac{1}{\pi n} T_n(t) T_n(s), \quad \forall s \neq t. \quad (2.14)$$

This series expansion converges point-wise for $t \neq s$ as the fundamental solution is then smooth.

2.5.3. Computations for $i \neq j$

We consider cross-interactions given by blocks $L_{ij}[\kappa]$. The associated kernel is smooth, and consequently, we can expand it as a Chebyshev series using the FFT. To this end, we consider a bivariate version of the procedure presented in Section 2.5.1 :

- (i) Evaluate the function $F(t, s) := G_\kappa(\mathbf{r}_i(t), \mathbf{r}_j(s))$ in a grid of Chebyshev points (t_i^N, s_j^N) , obtaining a matrix $F \in \mathbb{C}^{(N+1) \times (N+1)}$.
- (ii) For each row, we follow steps (i) and (ii) of the one-dimensional procedure detailed in Section 2.5.1. This leads to the following expansion:

$$F(t, s) = \sum_{n \geq 0} a_n(s) T_n(t),$$

where the coefficients of the matrix are approximations at the Chebyshev points, i.e. $F_{jn} \approx a_n(x_j^N)$, $n = 0, \dots, N$.

- (iii) We repeat the last step but with the columns of the new matrix F , i.e. the same one-dimensional procedure for the functions $a_n(s)$, $n = 0, \dots, N$. The matrix F

is updated such that $F_{ln} \approx a_{ln}$, where

$$F(t, s) = \sum_{l \geq 0} \sum_{n \geq 0} a_{ln} T_l(s) T_n(t).$$

Notice that this procedure requires $2(N + 1)$ FFTs. Once the expansion is obtained, the integrals are computed directly using the orthogonality property of Chebyshev polynomials.

2.5.4. Computations for $i = j$

In this setting, we extract singularities by subtracting the purely logarithmic term:

$$R_k^i(t, s) := -\frac{1}{2\pi} \log |t - s| J_0(\kappa \|\mathbf{r}_i(t) - \mathbf{r}_i(s)\|_2),$$

and obtain two families of integrals:

$$\begin{aligned} I_{ln}^1 &:= \int_{-1}^1 \int_{-1}^1 (G_\kappa(\mathbf{r}_i(t), \mathbf{r}_i(s)) - R_k^i(t, s)) w^{-1} T_n(t) w^{-1} T_l(s) dt ds, \\ I_{ln}^2 &:= \int_{-1}^1 \int_{-1}^1 R_k^i(t, s) w^{-1} T_n(t) w^{-1} T_l(s) dt ds. \end{aligned}$$

Using the expansion (Abramowitz & Stegun, 1965, 9.1.13), we find that $G_\kappa(\mathbf{r}_i(t), \mathbf{r}_i(s)) - R_k^i(t, s)$ has the same regularity of \mathbf{r}_i , and thus, we can compute I_{ln}^1 as in the case $i \neq j$. For I_{ln}^2 , we notice that $R_k^i(t, s)$ is a product of two functions: $-\frac{1}{2\pi} \log |t - s|$, with known Chebyshev expansion (2.14) and $J_0(\kappa \|\mathbf{r}_i(t) - \mathbf{r}_i(s)\|_2)$, which by (Abramowitz & Stegun, 1965, 9.1.12) has the same regularity of \mathbf{r}_i . Consequently, its Chebyshev expansion can be computed using the FFT. Finally, the Chebyshev expansion of $R_k^i(t, s)$ is computed using the technique shown in Lemma 2.4.14.

REMARK 2.5.2. The evaluation of the Chebyshev expansion of $R_k^i(t, s)$ can be accelerated by extrapolation techniques like de-aliasing (Hu, 1994).

2.6. Compression Algorithm

While the presented spectral algorithm reduces the number of dofs needed to obtain a desired accuracy with respect the most common low order h -refinement schemes, we

lack any form of matrix compression such as Fast Multipole Method or Hierarchical Matrices (Sauter & Schwab, 2011, Chapter 7). In what follows, we present a compression algorithm specially designed for problems with multiples arcs. The key idea is to recognize that the entries of the matrix $\mathbf{L}[\kappa]$ correspond to Fourier-Chebyshev coefficients of the kernel function. Hence, for smooth kernels, we observe fast decaying entries, and thus it can be approximated by just considering the first coefficients and setting others to zero. Specifically, the kernel function is smooth when we compute cross-interactions blocks.

Let the routine $\text{Quadrature}(l, m)$ compute the term (l, m) of this interaction matrix using a two-dimensional Gauss-Chebyshev quadrature ¹. Given a tolerance ϵ , we reduce the amount of computations needed by performing the following binary search:

ALGORITHM 2.6.1 (H). 1: *INPUT: Tolerance ϵ , Max Level of search L_{max}*
2: *OUTPUT: Number of columns to use N_{cols}*
3: *INITIALIZE: $N_{cols} = N$, level = 0, $a = 0$, $b = N$*
4: **while** level < L_{max} **do**
5: $m = (a + b)/2$
6: $T_{left} = m - 1$
7: $T_{center} = m$
8: $T_{right} = m + 1$
9: $V_{left} = \text{abs}(\text{Quadrature}(0, T_{left}))$
10: $V_{center} = \text{abs}(\text{Quadrature}(0, T_{center}))$
11: $V_{right} = \text{abs}(\text{Quadrature}(0, T_{right}))$
12: **if** $\{V_{right} \& V_{center} < 0.5 * \epsilon\}$ **or** $\{V_{left} \& V_{center} < 0.5 * \epsilon\}$ **then**
13: $b = m$
14: **else**
15: $a = m$
16: **end if**

¹We make the following approximation $\int_{\Gamma_i} \int_{\Gamma_j} G_\kappa(\mathbf{x}, \mathbf{y}) q_m^j(\mathbf{x}) q_l^i(\mathbf{y}) d\mathbf{x} d\mathbf{y} \approx \sum_{p=1}^{N_q} \sum_{r=1}^{N_q} \omega_p \omega_r G_\kappa(\mathbf{r}_i(x_p), \mathbf{r}_j(x_r)) T_m(x_r) T_l(x_p)$, where ω_p, x_p denote the Gauss-Chebyshev quadrature weights and points respectively, and N_q is the number of points to use.

17: $level++$
 18: **end while**
 19: $N_{cols} = b$

The algorithm returns the minimum number of columns N_{cols} to be used, by searching in the first row the minimum index such that the absolute value of the matrix entries is lower than ϵ . The binary search is restricted to a depth $L_{\max} \in \mathbb{N}$. The same procedure is used to estimate the number of rows, N_{rows} , by executing a binary search in the first column. Once N_{cols} and N_{rows} are selected, we define $N_\epsilon := \max\{N_{rows}, N_{cols}\}$ and compute the block of size $N_\epsilon \times N_\epsilon$ as in the full implementation.

Matrix compression also induces an extra error as it perturbs the original linear system in Problem 2.4.1. We can bound this error using the standard theory of perturbed linear systems, to that end denote by $\mathbf{L}_\epsilon[\kappa]$ the matrix generated by the compression algorithm with tolerance ϵ , and define the matrix difference $\Delta\mathbf{L}_\epsilon[\kappa] := \mathbf{L}_\epsilon[\kappa] - \mathbf{L}[\kappa]$. We seek to control the solution $\mathbf{u}^\epsilon = \mathbf{u} + \Delta\mathbf{u}$ of

$$(\mathbf{L}[\kappa] + \Delta\mathbf{L}_\epsilon[\kappa])\mathbf{u}^\epsilon = \mathbf{g},$$

where \mathbf{u} and \mathbf{g} are the same as in Problem 2.4.1. In order to bound this error, we will assume that, for every pair of indices (i, j) in the matrix $\mathbf{L}[\kappa]$, we have,

$$|(\Delta\mathbf{L}_\epsilon[\kappa])_{ij}| < \epsilon. \quad (2.15)$$

THEOREM 2.6.2. *Let $N \in \mathbb{N}$ be such there is only one solution of Problem 2.4.1. Then, there is a constant $C(\Gamma, \kappa) > 0$ such that*

$$\frac{\|\Delta\mathbf{u}\|_2}{\|\mathbf{u}\|_2} \leq \left| \frac{N\epsilon}{C(\kappa, \Gamma) - N\epsilon} \right|.$$

PROOF. By (Saad, 1996, Section 1.13.2) we have that

$$\frac{\|\Delta\mathbf{u}\|_2}{\|\mathbf{u}\|_2} \leq \frac{\|\Delta\mathbf{L}_\epsilon[\kappa]\|_2}{\|(\mathbf{L}[\kappa])^{-1}\|_2 - \|\Delta\mathbf{L}_\epsilon[\kappa]\|_2},$$

and thus, we need to estimate $\|\Delta \mathbf{L}_\epsilon[\kappa]\|_2$ and $\|(\mathbf{L}[\kappa])^{-1}\|_2$. The bound for the first term can be obtained as

$$\begin{aligned} \|\Delta \mathbf{L}_\epsilon[\kappa]\|_2 &= \sup_{\mathbf{x} \neq 0} \frac{\|\Delta \mathbf{L}_\epsilon[\kappa] \mathbf{x}\|_2}{\|\mathbf{x}\|_2} = \sup_{\mathbf{x} \neq 0} \frac{\left(\sum_{i=0}^N \left(\sum_{j=0}^N \Delta \mathbf{L}_\epsilon[\kappa]_{ij} x_j \right)^2 \right)^{1/2}}{\|\mathbf{x}\|_2} \\ &\leq \sup_{\mathbf{x} \neq 0} \frac{\left(\sum_{i=0}^N \|\mathbf{x}\|_2^2 N \epsilon^2 \right)^{1/2}}{\|\mathbf{x}\|_2} \leq N \epsilon. \end{aligned}$$

To estimate $\|(\mathbf{L}[\kappa])^{-1}\|_2$, we have on one hand the classical result $\|(\mathbf{L}[\kappa])^{-1}\|_2 \geq \|(\mathbf{L}[\kappa])\|_2^{-1}$. On the other hand, by the operator continuity it is easy to see that

$$\|(\mathbf{L}[\kappa])\|_2 \leq C(\kappa, \Gamma),$$

the results follows directly from the latter estimation. For $\kappa = 0$, the proof is analogous with the corresponding change in the spaces. \square

We can also estimate the error introduced by the compression algorithm in terms of the energy norm. In order to do so, define $(\boldsymbol{\lambda}_N^\epsilon)_i := \sum_{m=0}^N (\mathbf{u}_i^\epsilon)_m q_m^i$ in Γ_i . By the same arguments in the above proof, we obtain

$$\|\boldsymbol{\lambda}_N - \boldsymbol{\lambda}_N^\epsilon\|_{\tilde{\mathbb{H}}^{-\frac{1}{2}}(\Gamma)} \leq C_1(\kappa, \Gamma) \|\mathbf{g}\|_{\mathbb{H}(\Gamma)^{\frac{1}{2}}} \frac{\epsilon N^{3/2}}{C(\kappa, \Gamma) - \epsilon N},$$

where \mathbf{g} is the same that in Problem 2.3.3, C_1 is the constant of Theorem 2.4.3, and an extra factor $N^{1/2}$ appears as $\|\mathbf{u}\|_2 \leq N^{1/2} \|\boldsymbol{\lambda}_N\|_{\tilde{\mathbb{H}}^{-\frac{1}{2}}(\Gamma)} \leq C_1 N^{1/2} \|\mathbf{g}\|_{\mathbb{H}^{\frac{1}{2}}(\Gamma)}$.

REMARK 2.6.3. We can use the compression algorithm to make a fast version of the matrix-vector product, by splitting the product into blocks, and using the sparse representation for the cross interaction blocks.

REMARK 2.6.4. For the Laplace case $\kappa = 0$, it is also possible to obtain sparse approximations of the self-interaction blocks. We refer to (Jiang & Xu, 2010), for details, and also for a more complete analysis of similar the compression algorithm.

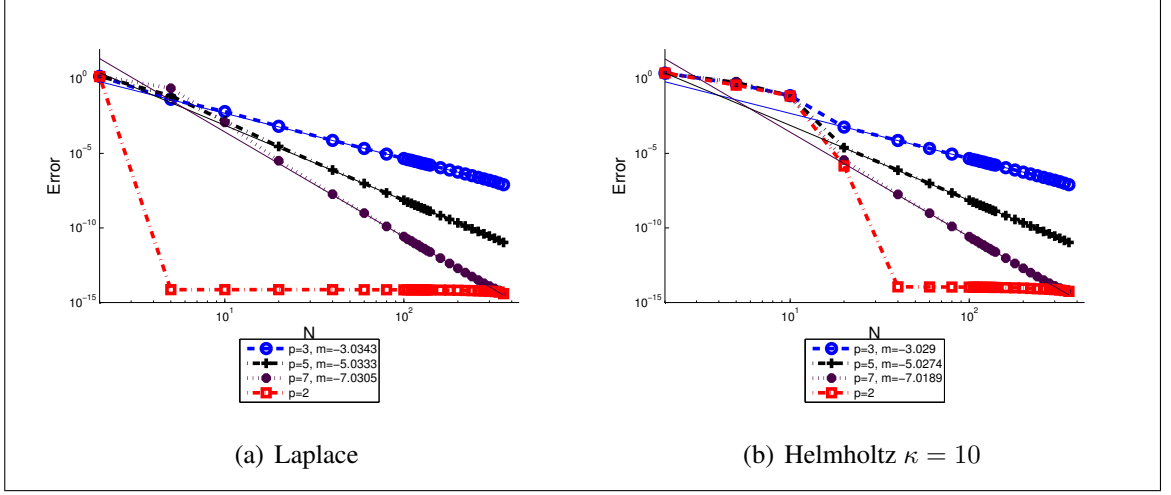


FIGURE 2.1. $\tilde{H}^{-\frac{1}{2}}(\hat{\Gamma})$ errors, for $g(t) = |t|^p$. Values m are slopes of $\log_{10}(\text{Error})$ with respect to $\log_{10} N$. Errors are computed with respect to an overkill solution with $N = 440$.

2.7. Numerical Results

2.7.1. Convergence Results

In what follows, we show experimental results confirming the convergence rates proven in Theorem 2.4.21. Let us first consider the case of a single arc $\hat{\Gamma}$ and an excitation g with limited regularity. Figure 2.1 presents convergence results for different excitation functions. The first three are of the form $g(t) = |t|^p$, with $p = 3, 5, 7$. For these, g is in $\mathcal{C}_v^p(\hat{\Gamma})$. Hence, by Theorem 2.4.21, we should observe the following error bounds:

$$\text{Error} := \|\lambda - \lambda_N\|_{\tilde{H}^{-\frac{1}{2}}(\hat{\Gamma})} = \mathcal{O}(N^{-p}).$$

Thus, we have that the error as a function of N has a slope of $-p$ in logarithmic scale. The fourth case has as right-hand side $g(t) = t^2$, and, being an entire function, we observe the corresponding super-algebraic convergence. Figure 2.2 shows convergence results for geometries with limited regularity and smooth excitation. Just as in the case of source terms of limited regularity, we obtain the convergence rates stated in Theorem 2.4.21. Lastly, we consider the case of multiple arcs and where the excitation function and the geometry are smooth (see Figure 2.3). We observe exponential error convergence in the polynomial

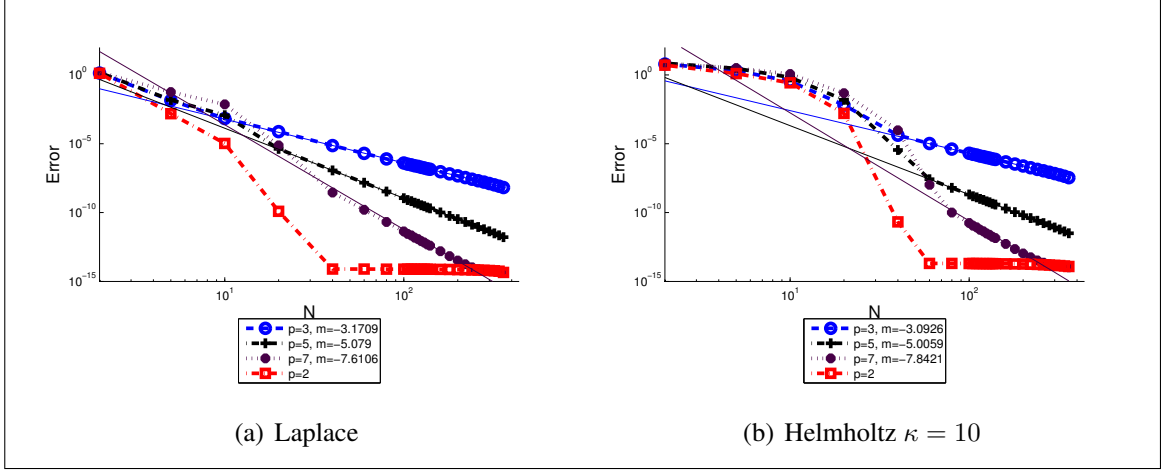


FIGURE 2.2. $\tilde{H}^{-\frac{1}{2}}(\Gamma)$ errors, for Γ given by $\mathbf{r}(t) = (t, |t|^p)$ and $g(t) = t^2$. Values m are slopes of $\log_{10}(\text{Error})$ with respect to $\log_{10} N$. Errors are computed with respect to an overkill solution with $N = 440$.

degree, which is the same for each arc, as predicted. We also observe that, as a function of κ , the errors are increasingly bounded by below. Our experiments shows that this effect is caused by errors in the solution of the linear system, which is currently solved by a direct method (the residual $\|\mathbf{L}[\kappa]\lambda - b\|_2$ dominates the convergence error, see Figure 2.3(C)). For the sake of brevity, we will not attempt to solve this anomaly, as it is a common issue when computing waves scattered by disjoint domains (*cf.* (Ganesh & Hawkins, 2011)). We remark that the $\tilde{H}^{-1/2}$ norms are computed using expression (2.9).

2.7.2. Compression Results

We considered the test cases presented in Figure 2.3. Tables 2.1, 2.2 showcase different measurements of the performance of the compression algorithm. We denote by: % NNZ, the percentage of non zero entries of the compressed matrix; Rel. Error, to the maximum absolute value between of the difference of uncompressed and compressed matrices; GMRES Full, the time (in seconds) that takes to solve the full linear system using GMRES with a tolerance of $1e - 8$; and, GMRES Sparse, same as last but with compressed matrix and an optimized version of the matrix vector product. For the sake of completeness, we have also included the assembly times (in seconds) for the full matrix (Full Assembly), and the

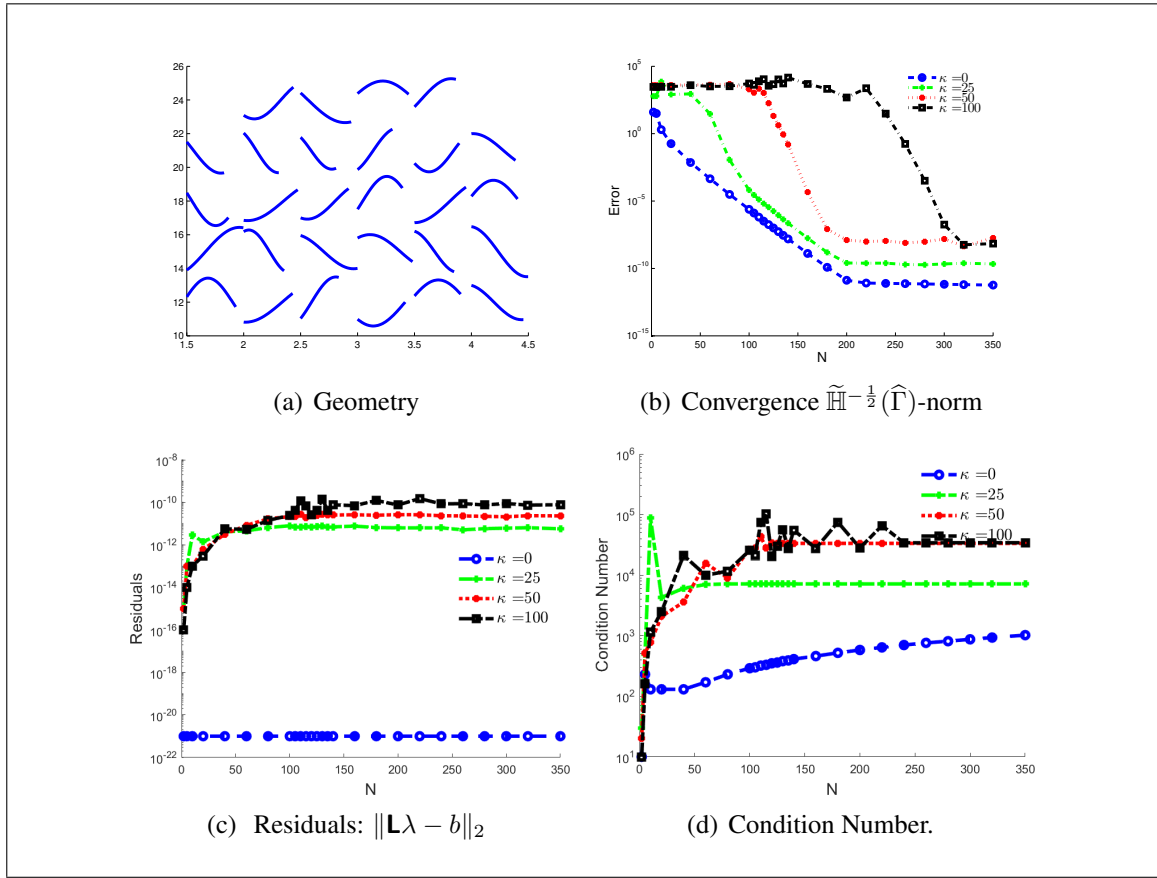


FIGURE 2.3. In (a), a smooth geometry with $M = 28$ open arcs, each with a parametrization $(at, c \sin(bt)) + \mathbf{d}$, where $a \in [0.45, 0.50]$, $b \in [1.0, 1.5]$, $c \in [1.0, 1.3]$, $\mathbf{d} \in [2, 3.5] \times [11, 25]$, and $t \in [-1, 1]$. In (b), convergence for the corresponding geometry and different wavenumbers using as right-hand side the trace of $g(\mathbf{x}) = \exp(-i\hat{\kappa}\mathbf{x} \cdot \mathbf{y})$, where $\hat{\kappa} = \kappa$ for $k > 0$, $\hat{0} = 5$, $\mathbf{y} = (\cos \alpha, \sin \alpha)$, and $\alpha = \pi/4$. The x-axis denotes the number of polynomials used per arc. Errors are computed with respect to an overkill solution with $N = 500$ per arc. The mean arc lengths in terms of the wavelength are $8\lambda, 16\lambda, 32\lambda$ for $\kappa = 25, 50, 100$ respectively. In (c) the error in the solution of the linear system for the different cases, and in (d) the corresponding conditioning number (in norm 2) for the linear systems.

compressed one (Sparse Assembly), and observe that they do not differ much as the most expensive part for this relative small problems is the computation of the self-interaction matrices.

TABLE 2.1. Compression performance $\epsilon = 1e - 10$, $\kappa = 100$

Order	% NNZ	Rel. Error	GMRES Full	GMRES Sparse	Full Assembly	Sparse Assembly
$L_{max} = 1$						
250	24	1e-10	25	12	109	96
300	24	1e-10	37	15	163	148
350	24	1e-10	48	19	215	198
400	24	1e-10	62	23	309	294
$L_{max} = 2$						
250	6	1e-10	25	8	109	95
300	6	1e-10	37	10	163	147
350	6	1e-10	48	12	215	198
400	6	1e-10	62	13	309	285
$L_{max} = 3$						
250	5	1e-10	25	7	109	95
300	3	1e-10	37	9	163	147
350	2	1e-10	48	9	215	196
400	1.7	1e-10	62	11	309	286

2.8. Concluding remarks

The present work presents a high-order discretization method for the wave scattering by multiple disjoint arcs based on weighted polynomials bases with proven convergence rates similar to the classical interpolation theory of smooth functions. As an efficient solver for the forward problem, our method could be easily used for solving optimization or inverse problems, tasks which are currently under development. Still, for increasing frequencies and numbers of arcs, we remark that the solution of the resulting linear system can become a bottleneck, thus requiring further improvements.

TABLE 2.2. Compression performance $\epsilon = 1e - 14$, $\kappa = 100$

Order	% NNZ	Rel. Error	GMRES Full	GMRES Sparse	Full Assembly	Sparse Assembly
$L_{max} = 1$						
250	24	1e-14	25	12	109	96
300	24	1e-14	37	16	163	149
350	25	1e-14	48	20	215	199
400	25	1e-14	62	24	309	294
$L_{max} = 2$						
250	6	1e-14	25	8	109	96
300	6	1e-14	37	10	163	147
350	7	1e-14	48	12	215	199
400	7	1e-14	62	14	309	284
$L_{max} = 3$						
250	5	1e-14	25	8	109	96
300	4	1e-14	37	10	163	148
350	5	1e-14	48	11	215	196
400	4	1e-14	62	12	309	283

Chapter 3. FAST SOLVER FOR QUASI-PERIODIC 2D-HELMHOLTZ SCATTERING IN LAYERED MEDIA

3.1. Introduction

A vast number of scientific and engineering applications rely on harnessing acoustic and electromagnetic wave diffraction by periodic and/or multilayered domains. Current highly demanding operation conditions for such devices require solving thousands of specific settings for design optimization or the quantification of shape or parameter uncertainties in the relevant quantities of interest, challenging the scientific computing community to continuously develop ever more efficient, fast and robust solvers (cf. (Bao, 2004; Y.-B. Chen & Zhang, 2007; E. G. Loewen & Popov, 2018; Silva-Oelker, Aylwin, Jerez-Hanckes, & Fay, 2018; Silva, Jerez-Hanckes, & Fay, 2019) and references therein). Assuming impinging time-harmonic plane waves, scattered and transmitted fields have been solved by a myriad of mathematical formulations and associated solution schemes. These range from volume variational formulations to various boundary integral representations and equations (cf. (Ammari, 1998; Ammari & Nédélec, 2001; Bao & Dobson, 2000; Barnett & Greengard, 2011; Dobson & Friedman, 1992; Nakata & Koshiba, 1990)), pure or coupled implementations of finite and boundary element methods (cf. (Ammari & Bao, 2008; Ammari & Nédélec, 2001; Elschner & Schmidt, 1998; Nédélec & Starling, 1991; Silva-Oelker, Aylwin, et al., 2018) or (Popov, 2012, Chapter 5)) and Nyström methods (Bruno & Haslam, 2009; Bruno, Shipman, Turc, & Venakides, 2016; Cho & Barnett, 2015; Greengard, Ho, & Lee, 2014; Liu & Barnett, 2016).

In this work, we build upon our theoretical review given in (Aylwin, Jerez-Hanckes, & Pinto, 2020) and present a spectral Galerkin method for solving second-kind direct boundary integral equations (BIEs) for the Helmholtz transmission problem for two-dimensional, periodic multi-layered gratings with smooth interfaces. Contrary to the low-order local basis functions used in the standard boundary element method, spectral bases are composed of high-order polynomials whose support lie on the whole scatterer boundary or on large portions of it. Successfully employed on two- and three-dimensional scattering problems

(Jerez-Hanckes & Pinto, 2018; Hu, 1995; Graham & Sloan, 2002), the main advantage of a spectral discretization is the ability to converge at a super-algebraic rate whenever solutions are smooth enough. Hence, our proposed method can in practice compete with Nyström methods while simultaneously inheriting all of the theoretical aspects of classical Galerkin methods.

In two dimensions, spectral methods are closely related to the theory of periodic pseudo-differential operators (Saranen & Vainikko, 2013), since the discretization through spectral elements can be interpreted as a truncation of the associated Fourier series where the action of the operators is well understood. We show that wave scattering by periodic domains is closely connected to the bounded domain case, making it possible to reuse almost all the pseudo-differential operator theory for our analysis. Key to our analysis are the results in (Nédélec & Starling, 1991; Starling & Bonnet-Bendhia, 1994; Elschner & Schmidt, 1998) regarding the unique solvability and eigenvalues of the associated volume problem. From here, we deduce that our BIE is uniquely solvable except at a countable set of wavenumbers composed of Rayleigh-Wood frequencies—wavenumbers for which the sum defining the quasi-periodic Green’s function is not convergent—and of eigenvalues of the Helmholtz transmission problem. Mindless of the several remedies developed to tackle Rayleigh-Wood anomalies through BIEs (Cho & Barnett, 2015; Bruno & Delourme, 2014; Bruno, Shipman, Turc, & Stephanos, 2017; Bruno & Fernandez-Lado, 2017), we choose to avoid them as they are not captured by our previous analysis in (Aylwin, Jerez-Hanckes, & Pinto, 2020).

Our discretization method employs a quasi-periodic basis so that techniques forcing the quasi-periodicity of the discrete solutions are not necessary (cf. (Greengard et al., 2014; Y. Zhang & Gillman, 2019)). Instead, an accurate approximation of the quasi-periodic Green’s function is required in order to extract its Fourier coefficients through the fast Fourier transform (FFT). Moreover, we prove that the chosen discretization basis enjoys a super-algebraic convergence rate on the degrees of freedom, which we then confirm through numerical experiments. In (Nguyen, 2012), a similar quasi-periodic exponential basis was employed to approximate solutions of a volume integral formulation.

The article is structured as follows. Section 3.2 presents the notation used throughout as well as the required quasi-periodic Sobolev spaces setting following (Aylwin, Jerez-Hanckes, & Pinto, 2020). In Section 3.3 we state the Helmholtz transmission problem for a multi-layered grating and study its solvability. Section 3.4 is concerned with the properties of quasi-periodic boundary integral operators (BIOs) along with an existence and uniqueness result for our BIEs. Section 3.5 provides rigorous error convergence rates of the spectral method and briefly describes the numerical algorithm used to compute the matrix entries associated with each integral operator. Numerical results are discussed in Section 3.6, followed by concluding remarks on Section B.5.

3.2. Notation and Functional Space Setting

3.2.1. General Notation

We denote the imaginary unit \imath . Boldface symbols will denote vectorial quantities and will use greek and roman letters for data over boundaries and volume, respectively. Canonical vectors in \mathbb{R}^2 are denoted $\mathbf{e}_1, \mathbf{e}_2$ respectively. Also, we make use of the symbols \lesssim, \gtrsim and \cong to avoid specifying constants irrelevant for the corresponding analysis.

Let H be a given Banach space. We shall denote its norm as $\|\cdot\|_H$ and its dual space by H' (set of antilinear functionals over H) with dual product denoted by $\langle \cdot, \cdot \rangle$. If H is a Hilbert space, the inner product between two of its elements, x and y , is denoted as $(x, y)_H$. Moreover, if H is a Hilbert space over the complex field, the inner product will be understood in the anti-linear sense.

For an open domain $\Omega \subset \mathbb{R}^2$, its boundary shall be denoted as $\partial\Omega$. Moreover, for any $\mathcal{O} \subset \mathbb{R}^2$ such that $\Omega \subseteq \mathcal{O}$, we introduce the closure of Ω relative to \mathcal{O} as $\overline{\Omega}^{\mathcal{O}} := \overline{\Omega} \cap \mathcal{O}$ and the boundary of Ω relative to \mathcal{O} as $\partial^{\mathcal{O}}\Omega := \overline{\Omega}^{\mathcal{O}} \setminus \Omega$.

For $n \in \mathbb{N}_0 := \mathbb{N} \cup \{0\}$, we denote by $\mathcal{C}^n(\Omega)$ the set of scalar functions over Ω with complex values and continuous derivatives up to order n . $\mathcal{C}^\infty(\Omega)$ refers to the space of functions with infinite continuous derivatives over Ω . We shall also make use of the

following subset of $\mathcal{C}^\infty(\Omega)$:

$$\mathcal{D}(\Omega) := \{u \in \mathcal{C}^\infty(\Omega) : \text{supp } u \subset\subset \Omega\}.$$

The space of p -integrable functions (for $p \geq 1$) with complex values over Ω is denoted as $L^p(\Omega)$.

We say that a one-dimensional Jordan curve Γ is of class $\mathcal{C}^{r,1}$, for $r \in \mathbb{N}_0$, if it may be parametrized by a function $z : (0, 2\pi) \rightarrow \Gamma$ which has r Lipschitz-continuous derivatives and a non-vanishing tangential vector. The first derivative of the parametrization is denoted as \dot{z} . Moreover, we say Γ is of class \mathcal{C}^∞ if it is of class $C^{r,1}$ for every $r \in \mathbb{N}_0$ (we will also use the notation $\mathcal{C}^{\infty,1}$ to refer to the same class).

Throughout the following sections, we will consider periodic geometries along e_1 with a fixed period of 2π . Moreover, we say that a continuous function f is a θ -quasi-periodic function if,

$$f(\mathbf{x} + 2\pi e_1) = e^{i2\pi\theta} f(\mathbf{x}) \quad \forall \mathbf{x} \in \mathbb{R}^2,$$

where the quasi-periodic shift θ is always assumed to be in $[0, 1)$. Finally, we define the canonic periodic cell on \mathbb{R}^2 as $\mathcal{G} := (0, 2\pi) \times \mathbb{R}$.

3.2.2. Quasi-periodic Sobolev Spaces

We denote by $\mathcal{D}_\theta(\mathbb{R}^2)$ the space of θ -quasi-periodic functions in $\mathcal{C}^\infty(\mathbb{R}^2)$ that vanish for large $|x_2|$, and denote by $\mathcal{D}'_\theta(\mathbb{R}^2)$ the space of θ -quasi-periodic distributions, which can be seen as the dual space of $\mathcal{D}_\theta(\mathbb{R}^2)$ (cf. (Aylwin, Jerez-Hanckes, & Pinto, 2020, Proposition 2.4)). For \mathcal{G} as before, we introduce $\mathcal{D}_\theta(\mathcal{G})$ the space of restrictions to \mathcal{G} of elements in $\mathcal{D}_\theta(\mathbb{R}^2)$. Moreover, for any open domain $\Omega \subset \mathcal{G}$ we define $\mathcal{D}_\theta(\Omega)$ as the set of elements of $\mathcal{D}_\theta(\mathcal{G})$ with compact support on Ω and $\mathcal{D}'_\theta(\Omega)$ as the space of elements of $\mathcal{D}'_\theta(\mathcal{G})$ restricted to $\mathcal{D}_\theta(\Omega)$. In what follows, for all $j \in \mathbb{Z}$ we define $j_\theta := j + \theta$.

PROPOSITION 3.2.1 (Proposition 2.6 in (Aylwin, Jerez-Hanckes, & Pinto, 2020)). *Every $u \in \mathcal{D}_\theta(\mathbb{R}^2)$ can be represented as a Fourier series, i.e.*

$$u(\mathbf{x}) = \sum_{j \in \mathbb{Z}} u_j(x_2) e^{ij_\theta x_1} \quad \text{with} \quad u_j(x_2) := \frac{1}{2\pi} \int_0^{2\pi} e^{-ij_\theta x_1} u(\mathbf{x}) dx_1,$$

so that $u_j \in \mathcal{D}(\mathbb{R})$. On the other hand, every element $F \in \mathcal{D}'_\theta(\mathbb{R}^2)$ can be identified with a formal Fourier series given by

$$\sum_{j \in \mathbb{Z}} F_j e^{ij_\theta x_1}, \quad \text{with} \quad F_j := \begin{cases} \mathcal{D}(\mathbb{R}) & \rightarrow \mathbb{C} \\ v & \mapsto F(v(x_2) e^{ij_\theta x_1}) \end{cases},$$

where $F_j \in \mathcal{D}'(\mathbb{R})$ for all $j \in \mathbb{Z}$ and $F(u) = \sum_{j \in \mathbb{Z}} F_j(u_j)$.

Let $s \in \mathbb{R}$. We define the θ -quasi-periodic Sobolev space of order s on \mathcal{G} as follows,

$$H_\theta^s(\mathcal{G}) := \left\{ F \in \mathcal{D}'_\theta(\mathbb{R}^2) \mid \sum_{j \in \mathbb{Z}} \int_{\mathbb{R}} (1 + j_\theta^2 + |\xi|^2)^s \left| \widehat{F}_j(\xi) \right|^2 d\xi < \infty \right\},$$

wherein \widehat{F}_j is the Fourier transform (in distributional sense (Steinbach, 2007, Section 2.4)) of F_j , defined as in Proposition 3.2.1. Additionally, we introduce the common notation $L_\theta^2(\mathcal{G}) := H_\theta^0(\mathcal{G})$ and note that, as in the standard case, $H_\theta^s(\mathcal{G})$ is a Hilbert space (Aylwin, Jerez-Hanckes, & Pinto, 2020, Proposition 2.8). Furthermore, for an open proper subset Ω of \mathcal{G} , we define $H_\theta^s(\Omega)$ as the Hilbert space of restrictions to Ω of elements of $H_\theta^s(\mathcal{G})$ (see (Aylwin, Jerez-Hanckes, & Pinto, 2020, Section 2) and (McLean, 2000, Chapter 3.6)). Finally, local Sobolev spaces on Ω are defined as

$$H_{\theta, \text{loc}}^s(\Omega) := \{ u \in \mathcal{D}'_\theta(\Omega) : u \in H_\theta^s(\Omega \cap \{ \mathbf{x} \in \mathcal{G} : |x_2| < R \}) \quad \forall R > 0 \}.$$

3.2.3. Quasi-periodic Sobolev Spaces on Boundaries and Traces

We begin by considering spaces of periodic functions over \mathbb{R} . As in (Kress, 2014, Definition 8.1), (Saranen & Vainikko, 2013, Section 5.3), we define Sobolev spaces on

$[0, 2\pi]$ of order $s \geq 0$ as follows,

$$H^s[0, 2\pi] := \left\{ \phi \in L^2((0, 2\pi)) : \sum_{j \in \mathbb{Z}} (1 + j^2)^s |\phi_j|^2 < \infty \right\},$$

where $\{\phi_j\}_{j \in \mathbb{Z}}$ are the Fourier coefficients of ϕ . Quasi-periodic spaces of order $s \geq 0$ over $(0, 2\pi)$ are defined from $H^s[0, 2\pi]$ straightforwardly, i.e.,

$$H_\theta^s[0, 2\pi] := \left\{ \phi \in L^2((0, 2\pi)) : e^{-i\theta t} \phi(t) \in H^s[0, 2\pi] \right\}.$$

Both $H^s[0, 2\pi]$ and $H_\theta^s[0, 2\pi]$ are Hilbert spaces, as are their respective dual spaces, denoted respectively $H^{-s}[0, 2\pi]$ and $H_\theta^{-s}[0, 2\pi]$ (see (Kress, 2014, Theorem 8.10) and (Aylwin, Jerez-Hanckes, & Pinto, 2020, Theorem 2.20)). Moreover, for $s \in \mathbb{R}$, the inner product and norm of $H_\theta^s[0, 2\pi]$ are given by:

$$(u, v)_{H_\theta^s[0, 2\pi]} := \sum_{j \in \mathbb{Z}} (1 + j_\theta^2)^s u_{j, \theta} \overline{v_{j, \theta}} \quad \text{and} \quad \|u\|_{H_\theta^s[0, 2\pi]} := (u, u)_{H_\theta^s[0, 2\pi]}^{\frac{1}{2}},$$

wherein, for positive s , we define

$$u_{j, \theta} := \frac{1}{2\pi} (u(t), e^{ij_\theta t})_{L^2((0, 2\pi))},$$

and the product is extended through duality to negative s (cf. (Aylwin, Jerez-Hanckes, & Pinto, 2020, Theorems 2.16 and 2.20)).

We continue by considering boundaries which are constructed as the single period of a $x1$ -periodic Jordan curve of class C^∞ . Let Γ be one of such curves and let $\mathbf{z} : (0, 2\pi) \rightarrow \Gamma$ be a parametrization of Γ . Then, for any $s \geq 0$, we define the θ -quasi-periodic Sobolev space of order s on Γ as

$$H_\theta^s(\Gamma) := \left\{ u \in L_\theta^2(\Gamma) \mid (u \circ \mathbf{z})(t) \in H_\theta^s[0, 2\pi] \right\}.$$

We define $H_\theta^{-s}(\Gamma)$ as the completion of $L_\theta^2(\Gamma)$ under the norm given by

$$\|u\|_{H_\theta^{-s}(\Gamma)} := \left\| (u \circ \mathbf{z}) \right\|_{H_\theta^{-s}[0, 2\pi]} \|\dot{\mathbf{z}}\|_{\mathbb{R}^2}.$$

Norms and inner products for these spaces are given through their respective pullbacks to $H_\theta^s[0, 2\pi]$ and $H_\theta^{-s}[0, 2\pi]$. Moreover, $H_\theta^{-s}(\Gamma)$ is identified with the dual space of $H_\theta^s(\Gamma)$ (Aylwin, Jerez-Hanckes, & Pinto, 2020, Theorem 2.26) where the duality is given by the extension of the following anti-linear form:

$$\langle \lambda, \vartheta \rangle_\Gamma := (\lambda, \vartheta)_{L_\theta^2(\Gamma)}, \quad \lambda, \vartheta \in L_\theta^2(\Gamma). \quad (3.1)$$

We also define the following space of smooth functions over Γ ,

$$\mathcal{D}_\theta(\Gamma) := \left\{ \phi : \Gamma \rightarrow \mathbb{C} \mid (\phi \circ z)(t) = \sum_{j=-n}^n \phi_j e^{ij\theta t}, \text{ for some } n \in \mathbb{N} \right\},$$

which is dense in $H_\theta^s(\Gamma)$ for any $s \in \mathbb{R}$. Finally, we introduce trace operators acting on quasi-periodic Sobolev spaces. Let Ω be a proper open subset of \mathcal{G} such that $\partial^\mathcal{G}\Omega = \Gamma$, we define the following operators for $s > \frac{1}{2}$:

$$\gamma_D : H_\theta^s(\Omega) \rightarrow H_\theta^{s-\frac{1}{2}}(\Gamma), \quad \gamma_D^e : H_\theta^s(\mathcal{G} \setminus \overline{\Omega}^\mathcal{G}) \rightarrow H_\theta^{s-\frac{1}{2}}(\Gamma),$$

that extend the notion of the restriction operator $u \mapsto u|_\Gamma$ to quasi-periodic Sobolev spaces (Aylwin, Jerez-Hanckes, & Pinto, 2020, Theorem 2.29). In this context, γ_D and γ_D^e are, respectively, the interior and exterior Dirichlet traces. Analogously, for $s > \frac{3}{2}$, we denote the interior and exterior Neumann traces on Ω as

$$\gamma_N : H_\theta^s(\Omega) \rightarrow H_\theta^{s-\frac{3}{2}}(\Gamma), \quad \gamma_N^e : H_\theta^s(\mathcal{G} \setminus \overline{\Omega}^\mathcal{G}) \rightarrow H_\theta^{s-\frac{3}{2}}(\Gamma),$$

extending the normal derivative $u \mapsto \nabla u|_\Gamma \cdot \mathbf{n}$, where \mathbf{n} is—for both traces—the unitary normal exterior to Ω . Moreover, introducing the subspace of elements of $H_\theta^1(\Omega)$ with integrable Laplacian,

$$H_{\theta,\Delta}^s(\Omega) := \{u \in H_\theta^1(\Omega) : \Delta u \in L_\theta^2(\Omega)\},$$

the Neumann trace may be extended as

$$\gamma_N : H_{\theta,\Delta}^1(\Omega) \rightarrow H_\theta^{-\frac{1}{2}}(\Gamma), \quad \gamma_N^e : H_{\theta,\Delta}^1(\mathcal{G} \setminus \overline{\Omega}^\mathcal{G}) \rightarrow H_\theta^{-\frac{1}{2}}(\Gamma),$$

through integration by parts (cf. (Aylwin, Jerez-Hanckes, & Pinto, 2020, Section 2)). All the previous results concerning trace operators follow analogously (with obvious modifications) for both local spaces—in the case that Ω is unbounded—and if Ω is the bounded space between two non-intersecting periodic curves Γ_1 and Γ_2 . Finally, we denote the following vector operators

$$\gamma u := (\gamma_D u, \gamma_N u)^t, \quad \gamma^e u := (\gamma_D^e u, \gamma_N^e u)^t \quad \text{and} \quad [\gamma u]_\Gamma := \gamma^e u - \gamma u,$$

as the interior, exterior and jump trace vectors on Γ , respectively.

3.3. Helmholtz problem in periodic layered media

3.3.1. Geometric Setting

We seek to establish a boundary integral representation for scattered and transmitted acoustic or electromagnetic fields resulting from plane waves impinging a multi-layered grating. The domain is described by $M \in \mathbb{N}$ finite non-intersecting periodic surfaces $\{\tilde{\Gamma}_i\}_{i=1}^M$ —ordered downwards—separating $M + 1$ periodic domains $\{\tilde{\Omega}_i\}_{i=0}^M$ such that for $0 < i < M$ it holds $\partial \tilde{\Omega}_i = \tilde{\Gamma}_i \cup \tilde{\Gamma}_{i+1}$, $\partial \tilde{\Omega}_0 = \tilde{\Gamma}_1$ and $\partial \tilde{\Omega}_M = \tilde{\Gamma}_M$ (see Figure 3.1). Moreover, while all domains $\{\tilde{\Omega}_i\}_{i=0}^M$ are unbounded along e_1 —due to their periodicity—only two of them, namely $\tilde{\Omega}_0$ and $\tilde{\Omega}_M$, are unbounded in the second spatial dimension (along e_2). The restrictions of the aforementioned domains and surfaces to the periodic cell \mathcal{G} are denoted by:

$$\Omega_i := \tilde{\Omega}_i \cap \mathcal{G} \quad \forall i \in \{0, \dots, M\}, \quad \Gamma_j := \tilde{\Gamma}_j \cap \mathcal{G} \quad \forall j \in \{1, \dots, M\}.$$

Additionally, we fix $H > 0$ so that

$$\bigcup_{i=1}^{M-1} \overline{\Omega}_i^{\mathcal{G}} \subset \{\mathbf{x} \in \mathcal{G} : |x_2| < H\}$$

holds. We will assume that the interfaces Γ_i , $i \in \{1, \dots, M\}$ are all Jordan curves of class \mathcal{C}^∞ . Furthermore, for each $i \in \{1, \dots, M\}$, the exterior and interior trace operators on Γ_i

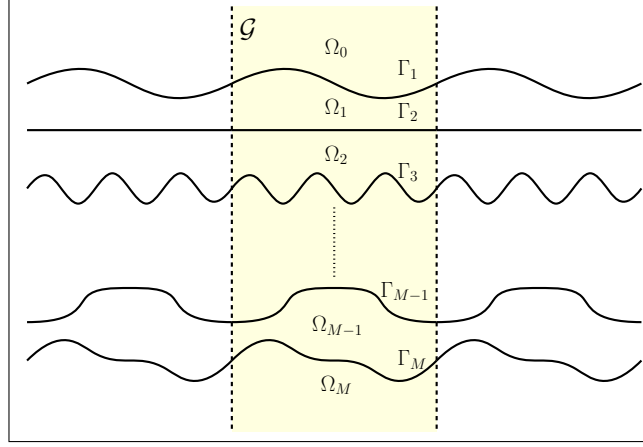


FIGURE 3.1. Example of a multi-layered grating. \mathcal{G} is highlighted and the dotted lines represent its boundaries at 0 and 2π .

are understood as

$$\begin{aligned} \gamma_D^e : H_\theta^1(\Omega_{i-1}) &\rightarrow H_\theta^{\frac{1}{2}}(\Gamma_i), & \gamma_D : H_\theta^1(\Omega_i) &\rightarrow H_\theta^{\frac{1}{2}}(\Gamma_i), \\ \gamma_N^e : H_{\theta,\Delta}^1(\Omega_{i-1}) &\rightarrow H_\theta^{-\frac{1}{2}}(\Gamma_i) & \text{and} & \quad \gamma_N : H_{\theta,\Delta}^1(\Omega_i) \rightarrow H_\theta^{-\frac{1}{2}}(\Gamma_i), \end{aligned}$$

and the normal vector on Γ_i is chosen to point towards Ω_{i-1} .

3.3.2. Helmholtz transmission problem on periodic media

For a time-dependence $e^{-i\omega t}$ for some frequency $\omega > 0$, let the grating described in the previous subsection be illuminated by an incident plane wave,

$$u^{(\text{inc})}(\mathbf{x}) := e^{i\mathbf{k}_0 \cdot \mathbf{x}} = e^{i(k_{0,1}x_1 + k_{0,2}x_2)},$$

where $\mathbf{k}_0 = (k_{0,1}, k_{0,2}) \in \mathbb{R}^2$. Furthermore, we denote $k_0 := |\mathbf{k}_0|$.

For $i = 0, \dots, M$, the material filling each domain Ω_i is assumed to be homogeneous and isotropic with refraction index η_i —we assume $\eta_0 \equiv 1$ —and wavenumber $k_i := \omega c_i^{-1} = \eta_i k_0$, where c_i is the wave speed in Ω_i . Throughout this section, we fix θ as the unique real

in $[0, 1)$ such that $\theta = k_{0,1} + n$ for some integer n and, for all $j \in \mathbb{Z}$, we define

$$\beta_j^{(0)} := \begin{cases} \sqrt{k_0^2 - j_\theta^2} & \text{if } k_0^2 - j_\theta^2 \geq 0 \\ \imath \sqrt{j_\theta^2 - k_0^2} & \text{if } k_0^2 - j_\theta^2 < 0 \end{cases}, \quad \beta_j^{(M)} := \begin{cases} \sqrt{k_M^2 - j_\theta^2} & \text{if } k_M^2 - j_\theta^2 \geq 0 \\ \imath \sqrt{j_\theta^2 - k_M^2} & \text{if } k_M^2 - j_\theta^2 < 0 \end{cases}, \quad (3.2)$$

where as before $j_\theta = j + \theta$. With these definitions, we can state our volume problem as follows.

PROBLEM 3.3.1 (Helmholtz transmission problem). We seek $u^{(\text{tot})}$ defined as

$$u^{(\text{tot})} := \begin{cases} u^{(\text{inc})} + u_0 & \text{in } \Omega_0, \\ u_i & \text{in } \Omega_i \text{ for } i \in \{1, \dots, M\}, \end{cases}$$

where $u_0 \in H_{\theta, \text{loc}}^1(\Omega_0)$, $u_M \in H_{\theta, \text{loc}}^1(\Omega_M)$ and $u_i \in H_\theta^1(\Omega_i)$ for all $1 \leq i \leq M - 1$, such that

$$-(\Delta + k_i^2)u^{(\text{tot})} = 0 \quad \text{in } \Omega_i \cap \{\mathbf{x} \in \mathcal{T} : |x_2| \leq H\}, \quad \forall i \in \{0, \dots, M\}, \quad (3.3a)$$

$$[\gamma u^{(\text{tot})}]_{\Gamma_i} = 0 \quad \text{on } \Gamma_i, \quad \forall i \in \{1, \dots, M\}, \quad (3.3b)$$

$$u_0(\mathbf{x}) = \sum_{j \in \mathbb{Z}} u_j^{(0)} e^{\imath(\beta_j^{(0)}(x_2 - H) + j_\theta x_1)} \quad \text{for } x_2 \geq H, \quad (3.3c)$$

$$u_m(\mathbf{x}) = \sum_{j \in \mathbb{Z}} u_j^{(M)} e^{\imath(\beta_j^{(M)}(x_2 + H) + j_\theta x_1)} \quad \text{for } x_2 \leq -H. \quad (3.3d)$$

Equation (3.3b) represents the continuity of Dirichlet and Neumann traces across each interface. This condition can be generalized to include different transmission coefficients without much effort. The last two conditions, namely (3.3c) and (3.3d), correspond to radiation conditions for u_0 and u_m , also known as the Rayleigh-Bloch expansions (cf. (Nédélec & Starling, 1991) for a detailed discussion), where $\{u_j^{(0)}\}_{j \in \mathbb{Z}}$ and $\{u_j^{(M)}\}_{j \in \mathbb{Z}}$ are the corresponding Rayleigh coefficients.

Through an analogous analysis to that presented in (Elschner & Schmidt, 1998, Section 3), one finds that—for a fixed choice of geometries $\{\Gamma_i\}_{i=1}^M$ and refraction indices $\{\eta_i\}_{i=1}^M$ —Problem 3.3.1 has a unique solution for all but a countable number of wavenumbers k_0 as all wavenumbers k_i for $i \in \{1, \dots, M\}$ depend on k_0 .

ASSUMPTION 3.1. *The wavenumber k_0 is such that Problem 3.3.1 has a unique solution.*

We shall make no further analysis of the volume problem as stated above, and limit ourselves to (Bao, 1997; Bao, Dobson, & Cox, 1995; Kirsch, 1993; Nédélec & Starling, 1991; Starling & Bonnet-Bendhia, 1994; B. Zhang & Chandler-Wilde, 1998; Elschner & Schmidt, 1998) and references therein for more detailed analyses of the radiation condition of similar problems.

3.4. Boundary integral equations

Following our previous work (Aylwin, Jerez-Hanckes, & Pinto, 2020), we introduce the quasi-periodic Green's function and recall some relevant properties. We then define the quasi-periodic single and double layer potentials and BIOs spanning from taking their respective traces on the periodic boundaries $\{\Gamma_i\}_{i=1}^M$. To conclude this section, we present an integral representation for the fields $\{u_i\}_{i=0}^M$ and a proof of unisolvency for the corresponding BIE. As before, θ will denote the quasi-periodic shift, which is assumed to be in $[0, 1)$.

3.4.1. Quasi-Periodic Fundamental Solution

Consider a positive wavenumber $k \in \mathbb{R}$, we recall the definition of the Rayleigh-Wood frequencies.

DEFINITION 3.4.1. We say $k > 0$ is a Rayleigh-Wood frequency, if there is $j \in \mathbb{Z}$, such that

$$|j + \theta| = k, \tag{3.4}$$

where θ is the previously fixed quasi-periodic shift.

These frequencies correspond to values where the quasi-periodic Green's function can not be represented in a traditional manner. While a number of alternatives have been developed to circumvent this issue (e.g., (Bruno & Fernandez-Lado, 2017; Bruno et al., 2017; Cho & Barnett, 2015)) their analysis is out of the scope of our current work. Hence, in what follows, we will work under the following assumption over the wavenumber k .

ASSUMPTION 3.2. *The wavenumber $k > 0$ is not a Rayleigh-Wood frequency for the given $\theta \in [0, 1)$.*

Under Assumption 3.2 we can define the θ -quasi-periodic Green's function as (cf. (Nédélec & Starling, 1991; Linton, 1998) and references therein)

$$G_\theta^k(\mathbf{x}, \mathbf{y}) := \lim_{m \rightarrow \infty} \sum_{n=-m}^m e^{-i2\pi n\theta} G^k(\mathbf{x} + 2\pi n\mathbf{e}_1, \mathbf{y}), \quad (3.5)$$

for all \mathbf{x}, \mathbf{y} in \mathbb{R}^2 such that $\mathbf{x} - \mathbf{y} \neq 2\pi n\mathbf{e}_1$ for all $n \in \mathbb{Z}$, wherein $G^k(\mathbf{x}, \mathbf{y})$ is the fundamental solution for the Helmholtz equation with wavenumber k , namely,

$$G^k(\mathbf{x}, \mathbf{y}) = \frac{i}{4} H_0^{(1)}(k \|\mathbf{x} - \mathbf{y}\|_{\mathbb{R}^2}),$$

where $H_0^{(1)}(\cdot)$ denotes the zeroth-order first kind Hankel function. Moreover, the quasi-periodic Green's function is a fundamental solution of the Helmholtz equation in the following sense:

$$-(\Delta_{\mathbf{y}} + k^2)G_\theta^k(\mathbf{x}, \mathbf{y}) = \sum_{n \in \mathbb{Z}} \delta(\mathbf{x} + 2\pi n\mathbf{e}_1) e^{i2\pi n\theta}$$

for all $\mathbf{x} \in \mathbb{R}^2$ and satisfies the radiation condition specified in the preceding section (cf. (Nédélec & Starling, 1991, Proposition 3.1)).

REMARK 3.4.2. If Assumption 3.2 is not met, the sum in (3.5) fails to converge for any pair of $\mathbf{x}, \mathbf{y} \in \mathbb{R}^2$.

3.4.2. Layer Potentials and Boundary Integral Operators

In this section, we will assume a given boundary Γ satisfying the following assumption.

ASSUMPTION 3.3. *Given $r \in [0, \infty]$, the interface Γ is a Jordan curve of class $\mathcal{C}^{r,1}$.*

Moreover, given Γ as before, we denote by Ω the part of \mathcal{G} below Γ (see Figure 3.1). For $\phi \in \mathcal{D}_\theta(\Gamma)$ we define the single and double layer potentials as

$$\text{SL}_{\theta,\Gamma}^k \phi(\mathbf{x}) := \int_{\Gamma} G_{\theta}^k(\mathbf{x}, \mathbf{y}) \phi(\mathbf{y}) \, d\mathbf{y}, \quad \text{DL}_{\theta,\Gamma}^k \phi(\mathbf{x}) := \int_{\Gamma} \gamma_{n,\mathbf{y}} G_{\theta}^k(\mathbf{x}, \mathbf{y}) \phi(\mathbf{y}) \, d\mathbf{y}, \quad (3.6)$$

where $\gamma_{n,\mathbf{y}}$ denotes the interior (with respect to Ω) Neumann trace operator acting on functions with argument \mathbf{y} .

LEMMA 3.4.3 (Theorems 4.7 and 4.10 in (Aylwin, Jerez-Hanckes, & Pinto, 2020)). *Let k and Γ be as in Assumptions 3.2 and 3.3 with $r \geq 0$, respectively. Then, the single and double layer potentials can be extended as continuous operators acting on Sobolev spaces as follows,*

$$\text{SL}_{\theta,\Gamma}^k : H_{\theta}^{s-\frac{1}{2}}(\Gamma) \rightarrow H_{\theta,loc}^{s+1}(\mathcal{G}) \quad \text{and} \quad \text{DL}_{\theta,\Gamma}^k : H_{\theta}^{s+\frac{1}{2}}(\Gamma) \rightarrow H_{\theta,loc}^{s+1}(\mathcal{G} \setminus \Gamma), \quad \text{for } |s| < \frac{1}{2}.$$

We then define BIOs by taking traces of the layer potentials as follows

$$\begin{aligned} \mathbf{V}_{\theta,\Gamma}^k &:= \gamma_D \text{SL}_{\theta,\Gamma}^k & \mathbf{K}_{\theta,\Gamma}^k &:= \gamma_N \text{SL}_{\theta,\Gamma}^k + \frac{1}{2} \mathbf{I}, \\ \mathbf{W}_{\theta,\Gamma}^k &:= -\gamma_N \text{DL}_{\theta,\Gamma}^k & \mathbf{K}_{\theta,\Gamma}^k &:= \gamma_D \text{DL}_{\theta,\Gamma}^k - \frac{1}{2} \mathbf{I}. \end{aligned} \quad (3.7)$$

Moreover, due to the jump properties of the layer potentials (Aylwin, Jerez-Hanckes, & Pinto, 2020, Lemma 4.11), the following relations hold:

$$\begin{aligned} \mathbf{V}_{\theta,\Gamma}^k &= \gamma_D^e \text{SL}_{\theta,\Gamma}^k, & \mathbf{K}_{\theta,\Gamma}^k &= \gamma_N^e \text{SL}_{\theta,\Gamma}^k - \frac{1}{2} \mathbf{I}, \\ \mathbf{W}_{\theta,\Gamma}^k &= -\gamma_N^e \text{DL}_{\theta,\Gamma}^k, & \mathbf{K}_{\theta,\Gamma}^k &= \gamma_D^e \text{DL}_{\theta,\Gamma}^k + \frac{1}{2} \mathbf{I}. \end{aligned} \quad (3.8)$$

REMARK 3.4.4. When considering interior and exterior traces acting on layer potentials, note that the normal vector on Γ is to be *fixed* so that the only difference between exterior and interior traces is the direction from which we approach Γ . Additionally, note

that, having fixed the normal vector to Γ , the choice of trace taken in the definition of $W_{\theta,\Gamma}^k$ is arbitrary and makes no difference.

LEMMA 3.4.5 (Theorem 4.10 in (Aylwin, Jerez-Hanckes, & Pinto, 2020)). *Let k and Γ be as in Assumptions 3.2 and 3.3 with $r \geq 0$, respectively, and let $|s| < \frac{1}{2}$. Then, the BIOs satisfy the following continuity conditions*

$$\begin{aligned} V_{\theta,\Gamma}^k : H_{\theta}^{s-\frac{1}{2}}(\Gamma) &\rightarrow H_{\theta}^{s+\frac{1}{2}}(\Gamma), & W_{\theta,\Gamma}^k : H_{\theta}^{s+\frac{1}{2}}(\Gamma) &\rightarrow H_{\theta}^{s-\frac{1}{2}}(\Gamma), \\ K_{\theta,\Gamma}^k : H_{\theta}^{s-\frac{1}{2}}(\Gamma) &\rightarrow H_{\theta}^{s-\frac{1}{2}}(\Gamma), & K_{\theta,\Gamma}^k : H_{\theta}^{s+\frac{1}{2}}(\Gamma) &\rightarrow H_{\theta}^{s+\frac{1}{2}}(\Gamma). \end{aligned}$$

3.4.2.1. Compactness Properties

Until this point, we have established continuity properties of the four BIOs defined in (3.7). However, the BIEs we consider in the coming section require the subtraction of two instances of the same BIO with different wavenumbers. This will require a number of results from pseudo-differential operator theory (Saranen & Vainikko, 2013) as well as a version of the Rellich theorem on quasi-periodic Sobolev spaces on boundaries. After our analysis, we will see that the difference between any two of the operators in (3.7)—with different wavenumbers—will result in a compact operator.

THEOREM 3.4.6 (Rellich Theorem for quasi-periodic Sobolev spaces). *Let s_1, s_2 be real numbers such that $s_1 < s_2$ and $\theta \in [0, 1)$. Then, $H_{\theta}^{s_2}(\Gamma)$ is compactly embedded in $H_{\theta}^{s_1}(\Gamma)$.*

PROOF. Follows directly from the definition of the quasi-periodic spaces and the result for standard Sobolev spaces (see (Kress, 2014, Theorem 8.3)). \square

REMARK 3.4.7. No smoothness assumptions are needed for the proof of the previous theorem. Thus, it can be extended to Lipschitz boundaries for any pair of real numbers $s_1, s_2 < 1$, and potentially less regular cases if we restrict s_1, s_2 to be non-negative.

THEOREM 3.4.8 (Theorem 6.1.1 in (Saranen & Vainikko, 2013)). *Let $a : \mathbb{R} \times \mathbb{R} \rightarrow \mathbb{C}$ be a bi-periodic function of class \mathcal{C}^∞ and S be a 2π -periodic distribution in \mathbb{R} . Consider*

the following formal operator acting on a periodic smooth function $u \in \mathcal{C}^\infty(\mathbb{R})$:

$$Au(s) = \int_0^{2\pi} S(s-t)a(s,t)u(t)dt \quad \forall s \in \mathbb{R}, \quad (3.9)$$

where integration is to be understood as a duality pairing. Furthermore, let us assume the Fourier coefficients of S to behave as

$$|S_n| \lesssim |n|^p,$$

for some $p \in \mathbb{R}$. Then, for any $s \in \mathbb{R}$, A in (3.9) may be continuously extended as an operator mapping from $H^s[0, 2\pi]$ to $H^{s-p}[0, 2\pi]$, i.e.,

$$A : H^s[0, 2\pi] \rightarrow H^{s-p}[0, 2\pi].$$

We also recall a classical result from Fourier analysis (c.f. (Taibleson, 1967)).

LEMMA 3.4.9. *Let $m \in \mathbb{N}$, $f : \mathbb{R} \rightarrow \mathbb{C}$ be a periodic \mathcal{C}^m -class function such that its distributional derivative of order $m+1$ belongs to $L^1((0, 2\pi))$. Then, its Fourier coefficients $\{f_n\}_{n \in \mathbb{Z}}$ are such that*

$$|f_n| \lesssim |n|^{-m-1}.$$

In order to employ Theorem 3.4.8 we will need to express the quasi-periodic BIOs in a convenient way: with periodic functions as kernels. Let k and Γ be as in Assumptions 3.2 and 3.3, respectively. We begin by considering a periodic version of the fundamental solution in (B.26) and its derivatives on Γ as

$$\widehat{G}_\theta^k(s, t) := e^{-i\theta(s-t)} G_\theta^k(\mathbf{z}(s), \mathbf{z}(t)), \quad (3.10)$$

which may be expressed as

$$\widehat{G}_\theta^k(s, t) = S(t-s)J_\theta^k(s, t) + R_\theta^k(s, t), \quad (3.11)$$

with

$$S(t) := -\frac{1}{2\pi} \log \left| 2 \sin \frac{|t|}{2} \right|, \quad (3.12)$$

$$J_\theta^k(s, t) := e^{-i\theta(s-t)} \sum_{j=-\infty}^{\infty} J_0(k\|\mathbf{z}(s) + 2\pi j\mathbf{e}_1 - \mathbf{z}(t)\|) e^{-i2\pi j\theta} \chi_\epsilon(s - t + 2\pi j),$$

where $J_0(\cdot)$ is the zeroth-first kind Bessel function, $\epsilon \in (0, 2\pi)$ and $\chi_\epsilon(\cdot)$ is a smooth function satisfying

$$\chi_\epsilon(s) = 0 \quad \text{if} \quad |s| > \epsilon \quad \text{and} \quad \chi_\epsilon(s) = 1 \quad \text{if} \quad |s| < \frac{1}{2}\epsilon,$$

and

$$R_\theta^k(s, t) = \widehat{G}_\theta^k(s, t) - S(t - s)J_\theta^k(s, t).$$

Using known expansions of the Hankel functions (see (Abramowitz & Stegun, 1965, 9.1.12-9.1.13)) one can check that R_θ^k belongs to $\mathcal{C}^\infty(\mathbb{R} \times \mathbb{R})$.

Before we proceed any further, it is necessary to introduce a second wavenumber. We will denote $\widetilde{k} > 0$ a wavenumber (not necessarily different from k) that also satisfies Assumption 3.2.

PROPOSITION 3.4.10. *Let k and \widetilde{k} satisfy Assumption 3.2, and let Γ satisfy Assumption 3.3 with $r = \infty$. Consider \mathbf{V}_θ^k and $\widetilde{\mathbf{V}}_\theta^{\widetilde{k}}$ the weakly singular BIOs on Γ defined in (3.7) and where we have dropped the Γ subscript for brevity. Both operators may be considered as pseudo-differential operators of order -1 , whence*

$$\mathbf{V}_\theta^k : H_\theta^s(\Gamma) \rightarrow H_\theta^{s+1}(\Gamma), \quad \widetilde{\mathbf{V}}_\theta^{\widetilde{k}} : H_\theta^s(\Gamma) \rightarrow H_\theta^{s+1}(\Gamma).$$

Moreover, the operator $\mathbf{V}_\theta^{k, \widetilde{k}} := \mathbf{V}_\theta^k - \widetilde{\mathbf{V}}_\theta^{\widetilde{k}}$ can be extended to

$$\mathbf{V}_\theta^{k, \widetilde{k}} : H_\theta^s(\Gamma) \rightarrow H_\theta^{s+3}(\Gamma),$$

as a bounded linear operator for every $s \in \mathbb{R}$.

PROOF. That V_θ^k (and $V_\theta^{\tilde{k}}$) may be extended as claimed follows directly from Theorem 3.4.8, the kernel representation (3.11) and the decay of the Fourier coefficients of $S(t)$ in (3.12) (cf. (Saranen & Vainikko, 2013, Example 5.6.1)). Take $\mu \in D_\theta(\Gamma)$, we have that

$$\left(V_\theta^{k,\tilde{k}}(\mu) \circ \mathbf{z}\right)(s) = e^{i\theta s} \int_0^{2\pi} \left(\widehat{G}_\theta^k(s, t) - \widehat{G}_\theta^{\tilde{k}}(s, t)\right) e^{-i\theta t} (\mu \circ \mathbf{z})(t) \|\mathbf{z}'(t)\| dt$$

as a Lebesgue integral. Moreover,

$$\widehat{G}_\theta^k(s, t) - \widehat{G}_\theta^{\tilde{k}}(s, t) = S(t - s) \left(J_\theta^k(s, t) - J_\theta^{\tilde{k}}(s, t)\right) + \left(R_\theta^k(s, t) - R_\theta^{\tilde{k}}(s, t)\right). \quad (3.13)$$

Employing Lemma 3.4.9, Theorem 3.4.8 and (Abramowitz & Stegun, 1965, Equation 9.1.13) we see that the second term of the right-hand side of (3.13) gives rise to a bounded operator from $H^s[0, 2\pi]$ to $H^{s+p}[0, 2\pi]$ for any $p > 0$. On the other hand, the first term in the right-hand side of (3.13) may be decomposed as

$$S(t - s) \left(J_\theta^k(s, t) - J_\theta^{\tilde{k}}(s, t)\right) = (|\sin(t - s)|^2 S(t - s)) \left(\frac{J_\theta^k(s, t) - J_\theta^{\tilde{k}}(s, t)}{|\sin(t - s)|^2}\right).$$

One can see (cf. (Abramowitz & Stegun, 1965, Equation 9.1.12)) that the term

$$(J_\theta^k(s, t) - J_\theta^{\tilde{k}}(s, t)) |\sin(t - s)|^{-2},$$

belongs to $\mathcal{C}^\infty(\mathbb{R} \times \mathbb{R})$, whereas the term $|\sin(t - s)|^2 S(t - s)$ give rise to an operator of order -3 . In fact, its Fourier transform is

$$\begin{aligned} & -\frac{1}{2\pi} \int_0^{2\pi} \sin(t)^2 \log \left| 2 \sin \frac{t}{2} \right| e^{int} dt = \\ & -\frac{1}{2\pi} \int_0^{2\pi} \log \left| 2 \sin \frac{t}{2} \right| (e^{i(n+2)t} + e^{i(n-2)t} - 2e^{i(n)t}) dt = O(n^{-3}), \end{aligned}$$

where the last equality follows from (Saranen & Vainikko, 2013, Example 5.6.1). Finally, define

$$\widehat{V}_\theta^{k,\tilde{k}}(\mu)(s) := e^{-i\theta s} V_\theta^{k,\tilde{k}}(\mu) \circ \mathbf{z}(s).$$

Then,

$$\|\mathbf{V}_\theta^{k,\tilde{k}}(\mu)\|_{H_\theta^s(\Gamma)} \cong \|\mathbf{V}_\theta^{k,\tilde{k}}(\mu) \circ \mathbf{z}\|_{H_\theta^s[0,2\pi]} = \|\widehat{\mathbf{V}}_\theta^{k,\tilde{k}}(\mu)(s)\|_{H^s[0,2\pi]}. \quad (3.14)$$

We may now bound the last term in (3.14) by Theorem 3.4.8:

$$\|\widehat{\mathbf{V}}_\theta^{k,\tilde{k}}(\mu)\|_{H^{s+3}[0,2\pi]} \lesssim \|\mu\|_{H_\theta^s(\Gamma)}.$$

The proof is completed by the density of $\mathcal{D}_\theta(\Gamma)$ in the corresponding Sobolev space. \square

For the hyper-singular BIO, a similar result requires a technical lemma. To this end, let us define the tangential curl operator:

$$\operatorname{curl}_\Gamma \varphi := \frac{1}{\|\dot{\mathbf{z}}(t)\|_{\mathbb{R}^2}} \frac{\mathbf{d}}{\mathbf{d}t}(\varphi \circ \mathbf{z})(t).$$

for any $\varphi \in \mathcal{D}_\theta(\Gamma)$ and where \mathbf{z} is a suitable (arbitrary) parametrization of Γ .

LEMMA 3.4.11. *Let k and Γ satisfy Assumptions 3.2 and 3.3 for $r = 0$, respectively, and let λ and φ belong to $\mathcal{D}_\theta(\Gamma)$. Then,*

$$\langle \mathbf{W}_\theta^k(\lambda), \varphi \rangle_\Gamma = \langle \mathbf{V}_\theta^k(\operatorname{curl}_\Gamma \lambda), \operatorname{curl}_\Gamma \varphi \rangle_\Gamma + \langle \check{\mathbf{V}}_\theta^k(\lambda), \varphi \rangle_\Gamma,$$

where $\langle \cdot, \cdot \rangle_\Gamma$ represents the duality product between $H_\theta^s(\Gamma)$ and $H_\theta^{-s}(\Gamma)$ for any $s > 0$ and $\check{\mathbf{V}}_\theta^k$ is the extension by density of the operator given by

$$\langle \check{\mathbf{V}}_\theta^k(\lambda), \varphi \rangle_\Gamma := -k^2 \int_\Gamma \int_\Gamma \mathbf{n}(\mathbf{x}) \cdot \mathbf{n}(\mathbf{y}) G_\theta^k(\mathbf{x}, \mathbf{y}) \lambda(\mathbf{y}) \overline{\varphi}(\mathbf{x}) \, d\mathbf{y} \, d\mathbf{x}.$$

PROOF. Notice that for λ, φ in $\mathcal{D}_\theta(\Gamma)$, it holds that

$$\langle \operatorname{curl}_\Gamma \lambda, \varphi \rangle_\Gamma = \int_0^{2\pi} \frac{\mathbf{d}(\lambda \circ \mathbf{z})(t)}{\mathbf{d}t} \overline{(\varphi \circ \mathbf{z})(t)} \, \mathbf{d}t = - \int_0^{2\pi} \frac{\mathbf{d}(\overline{\varphi \circ \mathbf{z}})(t)}{\mathbf{d}t} (\lambda \circ \mathbf{z})(t) \, \mathbf{d}t,$$

where the border terms cancel each other out due to the quasi-periodicity of λ and φ . Hence, the result for quasi-periodic functions follows *verbatim* from the standard case (see, for instance, (Steinbach, 2007, Theorem 6.15)). \square

COROLLARY 3.4.12. *Under the assumptions of Proposition 3.4.10, consider W_θ^k , and \tilde{W}_θ^k , the hyper-singular operators defined as in (3.7) and where we drop the Γ subscript. The operator $W_\theta^{k,\tilde{k}} := W_\theta^k - \tilde{W}_\theta^k$ can be extended to*

$$W_\theta^{k,\tilde{k}} : H_\theta^s(\Gamma) \rightarrow H_\theta^{s+1}(\Gamma),$$

as a bounded linear operator for every $s \in \mathbb{R}$.

PROOF. Let λ, φ in $\mathcal{D}_\theta(\Gamma)$. By Lemma 3.4.11, we have that

$$\langle W_\theta^{k,\tilde{k}}(\lambda), \varphi \rangle_\Gamma = \langle V_\theta^{k,\tilde{k}}(\text{curl}_\Gamma \lambda), \text{curl}_\Gamma \varphi \rangle_\Gamma + \langle (\tilde{V}_\theta^k - \tilde{V}_\theta^{\tilde{k}})(\lambda), \varphi \rangle_\Gamma.$$

Using Proposition 3.4.10, one obtains

$$\left| \langle W_\theta^{k,\tilde{k}}(\lambda), \varphi \rangle_\Gamma \right| \lesssim \|\text{curl}_\Gamma \lambda\|_{H_\theta^{s-1}(\Gamma)} \|\text{curl}_\Gamma \varphi\|_{H_\theta^{-s-2}(\Gamma)} + \|\lambda\|_{H_\theta^s(\Gamma)} \|\varphi\|_{H_\theta^{-s-1}(\Gamma)}.$$

Where the inequality for the second term of the right-hand side is obtained using that both $(\tilde{V}_\theta^k, \tilde{V}_\theta^{\tilde{k}})$ are operators of order -1 (this follow from Theorem 3.4.8 and (Saranen & Vainikko, 2013, Example 5.6.1)). Then, since the curl_Γ operator is a first-order differential operator, it holds that

$$|\langle W_\theta^{k,\tilde{k}}(\lambda), \varphi \rangle_\Gamma| \lesssim \|\lambda\|_{H_\theta^s(\Gamma)} \|\varphi\|_{H_\theta^{-s-1}(\Gamma)},$$

and the result follows by a duality argument and recalling the density of $\mathcal{D}_\theta(\Gamma)$ in our quasi-periodic Sobolev spaces. \square

We now consider the Dirichlet traces of the double layer potential and its adjoint, defined in Section B.4 as the principal value integrals,

$$\begin{aligned} (K_\theta^k(\mu) \circ \mathbf{r})(s) &= \oint_0^{2\pi} \mathcal{K}_\theta^k(s, t) (\mu \circ \mathbf{z})(t) \|\dot{\mathbf{z}}(t)\| \, d\mathbf{t}, \\ (K_\theta^k(\lambda) \circ \mathbf{r})(s) &= \oint_0^{2\pi} \mathcal{K}_\theta^k(s, t) (\lambda \circ \mathbf{z})(t) \|\dot{\mathbf{z}}(t)\| \, d\mathbf{t}, \end{aligned}$$

for which we have dropped the Γ index momentarily, and where the kernels are given by (Bruno & Delourme, 2014, Section 3):

$$\begin{aligned}\mathcal{K}'_{\theta}(s, t) &:= -\frac{\imath k}{4} \sum_{j=-\infty}^{\infty} \left(\frac{H_1^{(1)}(k\|\mathbf{z}(s) + 2\pi j\mathbf{e}_1 - \mathbf{z}(t)\|)}{\|\mathbf{z}(s) + 2\pi j\mathbf{e}_1 - \mathbf{z}(t)\|} e^{-\imath 2\pi j\theta} \times \right. \\ &\quad \left. (\mathbf{z}(s) + 2\pi j\mathbf{e}_1 - \mathbf{z}(t)) \cdot \mathbf{n}(\mathbf{z}(s)) \right), \\ \mathcal{K}_{\theta}^k(s, t) &:= \frac{\imath k}{4} \sum_{j=-\infty}^{\infty} \left(\frac{H_1^{(1)}(k\|\mathbf{z}(s) + 2\pi j\mathbf{e}_1 - \mathbf{z}(t)\|)}{\|\mathbf{z}(s) + 2\pi j\mathbf{e}_1 - \mathbf{z}(t)\|} e^{-\imath 2\pi j\theta} \times \right. \\ &\quad \left. (\mathbf{z}(s) + 2\pi j\mathbf{e}_1 - \mathbf{z}(t)) \cdot \mathbf{n}(\mathbf{z}(t)) \right).\end{aligned}$$

where \mathbf{n} denotes the unitary normal vector exterior to Ω (recall $\Gamma := \partial^{\mathcal{G}}\Omega$). These can be written as (Abramowitz & Stegun, 1965, Equation 9.1.11)

$$\begin{aligned}\mathcal{K}'_{\theta}(s, t) &= S_1(t - s)J_{1,\theta}^k(s, t) + R_{1,\theta}^k(s, t) \\ \mathcal{K}_{\theta}^k(s, t) &= S_1(t - s)J_{2,\theta}^k(s, t) + R_{2,\theta}^k(s, t),\end{aligned}\tag{3.15}$$

wherein

$$\begin{aligned}S_1(t - s) &:= -\frac{1}{2\pi} \log \left(2 \sin \left(\frac{1}{2}|t - s| \right) \right) |\sin(t - s)|^2, \\ J_{1,\theta}^k(s, t) &:= -k \sum_{j=-\infty}^{\infty} \left(\frac{J_1(k\|\mathbf{z}(s) + 2\pi j\mathbf{e}_1 - \mathbf{z}(t)\|)}{\|\mathbf{z}(s) + 2\pi j\mathbf{e}_1 - \mathbf{z}(t)\|} e^{-\imath 2\pi j\theta} \times \right. \\ &\quad \left. \frac{(\mathbf{z}(s) + 2\pi j\mathbf{e}_1 - \mathbf{z}(t)) \cdot \mathbf{n}(\mathbf{z}(s))}{|\sin(t - s)|^2} \chi_{\epsilon}(t - 2\pi j - s) \right), \\ J_{2,\theta}^k(s, t) &:= k \sum_{j=-\infty}^{\infty} \left(\frac{J_1(k\|\mathbf{z}(s) + 2\pi j\mathbf{e}_1 - \mathbf{z}(t)\|)}{\|\mathbf{z}(s) + 2\pi j\mathbf{e}_1 - \mathbf{z}(t)\|} e^{-\imath 2\pi j\theta} \times \right. \\ &\quad \left. \frac{(\mathbf{z}(s) + 2\pi j\mathbf{e}_1 - \mathbf{z}(t)) \cdot \mathbf{n}(\mathbf{z}(t))}{|\sin(t - s)|^2} \chi_{\epsilon}(t - 2\pi j - s) \right),\end{aligned}$$

and

$$\begin{aligned} R_{1,\theta}^k(s,t) &:= \mathcal{K}'_{\theta}{}^k(s,t) - S_1(t-s)J_{1,\theta}^k(s,t), \\ R_{2,\theta}^k(s,t) &:= \mathcal{K}_{\theta}^k(s,t) - S_1(t-s)J_{2,\theta}^k(s,t). \end{aligned}$$

As in the proof of Proposition 3.4.10, we have that $|S_{1,n}| \lesssim n^{-3}$, whence, arguing as in Proposition 3.4.10, we have the following result.

PROPOSITION 3.4.13. *For k and Γ as in Assumptions 3.2 and 3.3 with $r = \infty$, respectively, and for any $s \in \mathbb{R}$, it holds that*

$$\mathcal{K}_{\theta}'{}^k : H_{\theta}^s(\Gamma) \rightarrow H_{\theta}^{s+3}(\Gamma), \quad \mathcal{K}_{\theta}^k : H_{\theta}^s(\Gamma) \rightarrow H_{\theta}^{s+3}(\Gamma),$$

are bounded and linear operators.

As in the case of the weakly and hyper-singular operator, we define:

$$\mathcal{K}_{\theta}'{}^{k,\tilde{k}} := \mathcal{K}_{\theta}'{}^k - \mathcal{K}_{\theta}'{}^{\tilde{k}}, \quad \mathcal{K}_{\theta}^{k,\tilde{k}} := \mathcal{K}_{\theta}^k - \mathcal{K}_{\theta}^{\tilde{k}}.$$

Finally, we obtain our compactness result.

PROPOSITION 3.4.14. *Let k and \tilde{k} satisfy Assumption 3.2, let Γ be as in Assumption 3.3 with $r = \infty$. Then, for $s \in \mathbb{R}$, the following operators*

$$\begin{aligned} \mathcal{V}_{\theta}^{k,\tilde{k}} : H_{\theta}^s(\Gamma) &\rightarrow H_{\theta}^{s+3-\epsilon}(\Gamma), & \mathcal{W}_{\theta}^{k,\tilde{k}} : H_{\theta}^s(\Gamma) &\rightarrow H_{\theta}^{s+1-\epsilon}(\Gamma), \\ \mathcal{K}_{\theta}^{k,\tilde{k}} : H_{\theta}^s(\Gamma) &\rightarrow H_{\theta}^{s+3-\epsilon}(\Gamma), & \mathcal{K}_{\theta}'{}^{k,\tilde{k}} : H_{\theta}^s(\Gamma) &\rightarrow H_{\theta}^{s+3-\epsilon}(\Gamma), \end{aligned}$$

are compact for every $\epsilon > 0$.

PROOF. The result is direct from the mapping properties shown and Theorem 3.4.6. □

Lastly, we require the compactness of the operator resulting from taking traces of the single and double layer operators acting on densities lying on a boundary Γ_1 over another

x_1 -periodic curve, say Γ_2 , that does not intersect with Γ_1 . Let us denote by γ_d^2, γ_n^2 Dirichlet and Neumann traces over Γ_2 , respectively. Then, by an application of Lemma 3.4.9, Theorem 3.4.6 and Theorem 3.4.8, we obtain the following result.

PROPOSITION 3.4.15. *Let k satisfy Assumption 3.2. If Γ_1 and Γ_2 are x_1 -periodic \mathcal{C}^∞ -Jordan curves then the application of the following traces to the layer potentials:*

$$\begin{aligned} \gamma_D^2 \text{SL}_{\theta, \Gamma_1}^k : H_\theta^{s_1}(\Gamma_1) &\rightarrow H_\theta^{s_2}(\Gamma_2), & \gamma_N^2 \text{SL}_{\theta, \Gamma_1}^k : H_\theta^{s_1}(\Gamma_1) &\rightarrow H_\theta^{s_2}(\Gamma_2), \\ \gamma_D^2 \text{DL}_{\theta, \Gamma_1}^k : H_\theta^{s_1}(\Gamma_1) &\rightarrow H_\theta^{s_2}(\Gamma_2), & \gamma_N^2 \text{DL}_{\theta, \Gamma_1}^k : H_\theta^{s_1}(\Gamma_1) &\rightarrow H_\theta^{s_2}(\Gamma_2), \end{aligned}$$

are compact operators for any choice of $s_1, s_2 \in \mathbb{R}$. The result holds regardless of the direction from which the traces are taken.

REMARK 3.4.16. For the main results in this section, we have assumed the interfaces to be of class \mathcal{C}^∞ . While this simplifies the analysis, we could obtain similar results with less stringent regularity requirements. Consider k and \tilde{k} satisfying Assumption 3.2 and Γ as in Assumption 3.3 with $r \in [1, \infty)$, and the weakly-singular operator V_θ^k (where we have omitted the Γ sub-index momentarily). The expression in (3.11) still holds for the kernel of V_θ^k , but R_θ^k and J_θ^k would be only of class $\mathcal{C}^{r,1}$, instead of arbitrarily smooth. Corollary 6.1.1 and Lemma 6.1.3 in (Saranen & Vainikko, 2013) imply the same results of Propositions 3.4.10 and 3.4.14 for s in a range limited by r .

REMARK 3.4.17. As previously mentioned, we have limited ourselves to extend the classical mapping results of the boundary integral operators to the context of quasi-periodic spaces. For the classical result see, for example, (Boubendir, Dominguez, & Turc, 2014, Theorem 2.1).

3.4.3. Boundary Integral Formulation

We recall the notation and geometry configuration introduced in Section 3.3, that is:

- (i) $u^{(\text{inc})}$ denotes a plane incident wave with wavenumber k_0 , which is assumed to be quasi-periodic with shift $\theta \in [0, 1)$.

- (ii) $\{\Gamma_i\}_{i=1}^M$ denotes a set of $M \in \mathbb{N}$ non-intersecting $\mathcal{C}^{r,1}$ -Jordan curves, with $r \in [1, \infty]$, ordered downwards.
- (iii) $\{\Omega_i\}_{i=0}^M$ denotes a set of $M + 1$ open domains, ordered downwards with boundaries

$$\partial^{\mathcal{G}}\Omega_0 = \Gamma_1, \quad \partial^{\mathcal{G}}\Omega_i = \Gamma_i \cup \Gamma_{i+1} \quad \forall i \in \{1, \dots, M-1\}, \quad \partial^{\mathcal{G}}\Omega_M = \Gamma_M.$$

- (iv) $\{\eta_i\}_{i=1}^M$ denotes a parameter set such that the wavenumber in Ω_i is given by $k_i = \eta_i k_0$ for $i \in \{1, \dots, M\}$.

ASSUMPTION 3.4. *For the given shift, θ , the wavenumber k_0 and the parameters $\{\eta_i\}_{i=1}^M$ are such that neither k_0 nor the wavenumbers $k_i = \eta_i k_0$ are Rayleigh-Wood frequencies.*

Following the notation of Problem 3.3.1, the scattered field—defined as the total field $u^{(\text{tot})}$ minus the incident field $u^{(\text{inc})}$ —is written as

$$u^{(\text{sc})} := u_i \quad \text{in } \Omega_i, \quad \text{for } i \in \{0, \dots, M\}.$$

Under Assumption 3.4, we make the following representation *Ansatz* for the scattered field:

$$u^{(\text{sc})} = \begin{cases} \text{SL}_{\theta, \Gamma_1}^{k_0}(\mu_1) - \text{DL}_{\theta, \Gamma_1}^{k_0}(\lambda_1) & \text{in } \Omega_0, \\ \text{SL}_{\theta, \Gamma_i}^{k_i}(\mu_i) - \text{DL}_{\theta, \Gamma_i}^{k_i}(\lambda_i) + \\ \text{SL}_{\theta, \Gamma_{i+1}}^{k_i}(\mu_{i+1}) - \text{DL}_{\theta, \Gamma_{i+1}}^{k_i}(\lambda_{i+1}) & \text{in } \Omega_i, \text{ for } i \in \{1, \dots, M-1\}, \\ \text{SL}_{\theta, \Gamma_M}^{k_M}(\mu_m) - \text{DL}_{\theta, \Gamma_M}^{k_M}(\lambda_m) & \text{in } \Omega_m, \end{cases}$$

where, for each $i \in \{1, \dots, M\}$, the boundary data λ_i and μ_i are assumed to belong to $H_{\theta}^s(\Gamma_i)$ for some possibly different values of $s \in \mathbb{R}$, i.e., s may be different for each boundary datum. $\text{SL}_{\theta, \Gamma_i}^{k_j}$ and $\text{DL}_{\theta, \Gamma_i}^{k_j}$ are, respectively, the single and double layer potentials of wavenumber k_j on Γ_i .

As shorthand, in what follows, we denote, for each $i \in \{1, \dots, M\}$,

$$\Lambda_i := (\lambda_i, \mu_i)^t, \quad \mathbf{L}_{\theta, \Gamma_i}^k \Lambda_i := \text{SL}_{\theta, \Gamma_i}^k(\mu_i) - \text{DL}_{\theta, \Gamma_i}^k(\lambda_i), \quad (3.16)$$

where λ_i and μ_i are defined over Γ_i . For $s_1, s_2 \in \mathbb{R}$, we define the Cartesian product spaces:

$$\mathcal{V}_{\theta, \Gamma_i}^{s_1, s_2} := H_{\theta}^{s_1}(\Gamma_i) \times H_{\theta}^{s_2}(\Gamma_i) \quad \text{for } i = 0, \dots, M \quad \text{and} \quad \mathcal{V}_{\theta}^{s_1, s_2} := \prod_{i=1}^M \mathcal{V}_{\theta, \Gamma_i}^{s_1, s_2},$$

where all of these spaces are equipped with their natural graph inner products. For each $i \in \{1, \dots, M\}$ let us define the following operators:

$$A_i \Lambda_i := \begin{pmatrix} -K_{\theta, \Gamma_i}^{k_{i-1}, k_i}(\lambda_i) + V_{\theta, \Gamma_i}^{k_{i-1}, k_i}(\mu_i) \\ W_{\theta, \Gamma_i}^{k_{i-1}, k_i}(\lambda_i) + K'_{\theta, \Gamma_i}^{k_{i-1}, k_i}(\mu_i) \end{pmatrix}, \quad (3.17)$$

corresponding to self-interactions between the potentials defined over each Γ_i with themselves. Analogously, for $i, j \in \{1, \dots, M\}$, we define the following operators:

$$B_{i,j} \Lambda_j := \begin{cases} \begin{pmatrix} -\gamma_D^i \text{DL}_{\theta, \Gamma_j}^{k_{\min\{i,j\}}}(\lambda_j) + \gamma_D^i \text{SL}_{\theta, \Gamma_j}^{k_{\min\{i,j\}}}(\mu_j) \\ -\gamma_N^i \text{DL}_{\theta, \Gamma_j}^{k_{\min\{i,j\}}}(\lambda_j) + \gamma_N^i \text{SL}_{\theta, \Gamma_j}^{k_{\min\{i,j\}}}(\mu_j) \end{pmatrix} & \text{if } |i - j| = 1 \\ \mathbf{0} & \text{a.o.c.} \end{cases} \quad (3.18)$$

corresponding to interactions between potentials defined over Γ_i with those defined over Γ_j .

PROPOSITION 3.4.18. *Let Assumption 3.4 hold and let interfaces $\{\Gamma_i\}_{i=1}^M$ be of class \mathcal{C}^∞ . Then, the self-interaction operators defined in (3.17)*

$$A_i : \mathcal{V}_{\theta, \Gamma_i}^{s_1, s_2} \rightarrow \mathcal{V}_{\theta, \Gamma_i}^{s_1, s_2}$$

are compact operators for any $s_1, s_2 \in \mathbb{R}$ with $s_2 < s_1 < s_2 + 2$. Furthermore, the cross-interaction operators (3.18)

$$B_{i,j} : \mathcal{V}_{\theta, \Gamma_j}^{s_1, s_2} \rightarrow \mathcal{V}_{\theta, \Gamma_i}^{s_1, s_2},$$

are compact for any choice of $s_1, s_2 \in \mathbb{R}$.

PROOF. The first result is directly found using Proposition 3.4.14, whereas the second one follows from Proposition 3.4.15. \square

With the above definitions and using the jump properties of the BIOs, it holds that

$$[\gamma u^{(\text{sc})}]_{\Gamma_i} = \mathbf{B}_{i,i-1}\Lambda_{i-1} + (\mathbf{A}_i - \mathbf{I}_i)\Lambda_i - \mathbf{B}_{i,i+1}\Lambda_{i+1}, \quad (3.19)$$

for each $i \in \{1, \dots, M\}$, where \mathbf{I}_i corresponds to the identity map over $\mathcal{V}_{\theta, \Gamma_j}^{s_1, s_2}$, with $s_1, s_2 \in \mathbb{R}$. We now introduce the following operator matrix over $\mathcal{V}_{\theta}^{s_1, s_2}$,

$$\mathcal{M} := \begin{pmatrix} \mathbf{A}_1 - \mathbf{I}_1 & -\mathbf{B}_{1,2} & 0 & 0 & 0 & \dots & 0 \\ \mathbf{B}_{2,1} & \mathbf{A}_2 - \mathbf{I}_2 & -\mathbf{B}_{2,3} & 0 & 0 & \dots & 0 \\ \vdots & \vdots & \vdots & \vdots & \vdots & \vdots & \vdots \\ 0 & 0 & \dots & 0 & \mathbf{B}_{M-1, M-2} & \mathbf{A}_{M-1} - \mathbf{I}_{M-1} & \mathbf{B}_{M-1, M} \\ 0 & 0 & \dots & 0 & 0 & \mathbf{B}_{M, M-1} & \mathbf{A}_M - \mathbf{I}_M \end{pmatrix}. \quad (3.20)$$

Imposing the boundary conditions of Problem 3.3.1 to $u^{(\text{sc})}$ leads to the following system of BIEs.

PROBLEM 3.4.19. Let Assumption 3.4 hold and let $s \in \mathbb{R}$. Define $s_1 := s + \frac{1}{2}$ and $s_2 := s - \frac{1}{2}$. We seek $\Lambda \in \mathcal{V}_{\theta}^{s_1, s_2}$ such that

$$\mathcal{M}\Lambda = \begin{pmatrix} -\gamma^{e,1}u^{(\text{inc})} \\ 0 \\ \vdots \\ 0 \end{pmatrix}$$

where \mathcal{M} corresponds to the operator matrix in (3.20) and $\gamma^{e,1}$ corresponds to the exterior trace vector on Γ_1 .

In order to ensure the well-posedness of Problem 3.4.19, we introduce the following set of auxiliary problems.

PROBLEM 3.4.20 (Auxiliary problems). We seek $\{v_i\}_{i=1}^M$ such that $v_i \in H_{\theta, \text{loc}}^1(\mathcal{G} \setminus \Gamma_i)$

$$\begin{aligned} -(\Delta + k_i^2)v_i(\mathbf{x}) &= 0 \quad \text{in } \left(\Omega_{i-1} \cup \bigcup_{j=0}^{i-2} \overline{\Omega_j}^\mathcal{G} \right) \cap \{\mathbf{x} \in \mathcal{G} : |x_2| < H\}, \\ -(\Delta + k_{i-1}^2)v_i(\mathbf{x}) &= 0 \quad \text{in } \Omega_i \cup \left(\bigcup_{j=i+1}^M \overline{\Omega_j}^\mathcal{G} \right) \cap \{\mathbf{x} \in \mathcal{G} : |x_2| < H\}, \\ [\gamma v_i]_{\Gamma_i} &= 0 \quad \text{on } \Gamma_i, \end{aligned} \tag{3.21}$$

$$v_i(\mathbf{x}) = \sum_{j \in \mathbb{Z}} v_j^{(i)} e^{i(\beta_j^{(0)}(x_2 - H) + j_\theta x_1)} \quad \text{for all } x_2 \geq H,$$

$$v_i(\mathbf{x}) = \sum_{j \in \mathbb{Z}} v_j^{(i)} e^{i(\beta_j^{(M)}(x_2 + H) + j_\theta x_1)} \quad \text{for all } x_2 \leq -H,$$

for each $i \in \{1, \dots, M\}$, where $H > 0$ is as in Section 3.3.1, and $\{k_i\}_{i=0}^M$ are the wavenumbers in each $\{\Omega_i\}_{i=0}^M$, as introduced in Section 3.3.

By the same analysis as that presented in (Starling & Bonnet-Bendhia, 1994, Section 3.4), each interface Γ_i , $i \in \{1, \dots, M\}$, potentially adds a countable set of wavenumbers, k_0 , such that Problem 3.4.20 is unsolvable. This justifies the following Assumption (recall $k_i = \eta_i k_0$ for all $i \in \{1, \dots, M\}$).

ASSUMPTION 3.5. *Given $\{\eta_i\}_{i=1}^M$, the wavenumber k_0 is such that the auxiliary Problem 3.4.20 has only one solution $\{v_i\}_{i=1}^M$ given by $v_i := 0$ for all $i \in \{1, \dots, M\}$.*

Assumption 3.5 will force us to discard yet more wavenumbers, but the set of wavenumbers neglected by Assumptions 3.1 and 3.5 is still countable.

THEOREM 3.4.21. *Let the parameters k_0 and $\{\eta_i\}_{i=1}^M$ satisfy Assumption 3.4 and let the interfaces $\{\Gamma_i\}_{i=1}^M$ be \mathcal{C}^∞ periodic Jordan arcs. Further assume Assumptions 3.1 and 3.5 to be satisfied. Then, Problem 3.4.19 is well posed for any $s \in \mathbb{R}$.*

PROOF. Note that the operator matrix \mathcal{M} may be written as

$$\mathcal{M} = \begin{pmatrix} A_1 & -B_{1,2} & 0 & 0 & \dots & 0 \\ B_{2,1} & A_2 & -B_{2,3} & 0 & \dots & 0 \\ \vdots & \vdots & \vdots & \vdots & \vdots & \vdots \\ 0 & 0 & \dots & 0 & A_{M-1} & B_{M-1,M} \\ 0 & 0 & \dots & 0 & 0 & B_{M,M-1} & A_M \end{pmatrix} - \begin{pmatrix} I_1 & 0 & 0 & 0 & \dots & 0 \\ 0 & I_2 & 0 & 0 & \dots & 0 \\ \vdots & \vdots & \vdots & \vdots & \vdots & \vdots \\ 0 & 0 & \dots & 0 & I_{M-1} & 0 \\ 0 & 0 & \dots & 0 & 0 & I_M \end{pmatrix}.$$

Then, by the Fredholm alternative, we need only show uniqueness of Problem 3.4.19, as the above tridiagonal block is compact by Proposition 3.4.18. The proof is very similar to that for the classical scattering problem of a bounded object in free space (cf. (Colton & Kress, 2013, Theorem 3.41)).

Let $\Lambda \in \mathcal{V}_{\theta}^{s_1, s_2}$, with $s_1 = s + \frac{1}{2}$ and $s_2 = s - \frac{1}{2}$, be such that $\mathcal{M}\Lambda = 0$. We define

$$\begin{aligned} \tilde{u}_0(\mathbf{x}) &:= (\mathbf{L}_{\theta, \Gamma_1}^{k_0}(\Lambda_1))(\mathbf{x}) & \forall \mathbf{x} \in \mathcal{G} \setminus \Gamma_1, \\ \tilde{u}_i(\mathbf{x}) &:= (\mathbf{L}_{\theta, \Gamma_i}^{k_i}(\Lambda_i))(\mathbf{x}) + (\mathbf{L}_{\theta, \Gamma_i}^{k_i}(\Lambda_{i+1}))(\mathbf{x}) & \forall \mathbf{x} \in \mathcal{G} \setminus (\Gamma_i \cup \Gamma_{i+1}), \forall i \in \{1, \dots, M-1\}, \\ \tilde{u}_m(\mathbf{x}) &:= (\mathbf{L}_{\theta, \Gamma_m}^{k_M}(\Lambda_m))(\mathbf{x}) & \forall \mathbf{x} \in \mathcal{G} \setminus \Gamma_m, \end{aligned}$$

where the representation \mathbf{L} is defined as in (3.16). We further define

$$\tilde{u}(\mathbf{x}) := \tilde{u}_i(\mathbf{x}) \quad \forall \mathbf{x} \in \Omega_i, \quad \forall i \in \{0, \dots, M\},$$

which is well defined in each Ω_i , but could potentially have non-zero jumps across each interface Γ_i . Moreover, \tilde{u} solves the Helmholtz equation with wavenumber k_i in each Ω_i and satisfies the appropriate radiation conditions at infinity (Aylwin, Jerez-Hanckes, & Pinto, 2020, Section 4). Hence, \tilde{u} solves Problem 3.3.1, and Assumption 3.1 implies $\tilde{u} \equiv 0$.

We continue by defining the following auxiliary functions

$$v_i(\mathbf{x}) := \begin{cases} \tilde{u}_i(\mathbf{x}) & \forall \mathbf{x} \in \Omega_{i-1} \cup \left(\bigcup_{j=0}^{i-2} \overline{\Omega_j}^{\mathcal{G}} \right) \\ -\tilde{u}_{i-1}(\mathbf{x}) & \forall \mathbf{x} \in \Omega_i \cup \left(\bigcup_{j=i+1}^M \overline{\Omega_j}^{\mathcal{G}} \right) \end{cases}, \quad \forall i \in \{1, \dots, M\}.$$

It is clear from this definition that

$$\begin{aligned} (-\Delta - k_i^2)v_i(\mathbf{x}) &= 0, \quad \text{in } \Omega_{i-1} \cup \left(\bigcup_{j=0}^{i-2} \overline{\Omega_j^{\mathcal{G}}} \right), \\ (-\Delta - k_{i-1}^2)v_i(\mathbf{x}) &= 0, \quad \text{in } \Omega_i \cup \left(\bigcup_{j=i+1}^M \overline{\Omega_j^{\mathcal{G}}} \right). \end{aligned}$$

Furthermore, each v_i satisfies the appropriate radiation conditions at infinity. Using the jump relationships of BIOs (see (Aylwin, Jerez-Hanckes, & Pinto, 2020, Lemma 4.11)), we have that

$$\gamma^{i,e}v_i - \gamma^i\tilde{u} = \Lambda_i, \quad \gamma^{i,e}\tilde{u} + \gamma^iv_i = \Lambda_i. \quad (3.22)$$

Since $\tilde{u} \equiv 0$, we have that

$$[\gamma v_i]_{\Gamma_i} = \gamma^{i,e}v_i - \gamma^iv_i = \gamma^{i,e}v_i - \gamma^i\tilde{u} - (\gamma^{i,e}\tilde{u} + \gamma^iv_i) = 0,$$

from where it follows that $\{v_i\}_{i=1}^M$ solves Problem 3.4.20. Assumption 3.5 implies that $v_i \equiv 0$, for all i in $\{1, \dots, M\}$. Finally, (3.22) implies $\Lambda \equiv 0$ as stated. \square

REMARK 3.4.22. Theorem 3.4.21 states that if all the interfaces are of arbitrary smoothness, the solution Λ is also arbitrarily smooth. This result can be generalized to geometries of limited regularity by following the ideas presented in Remark 3.4.16, obtaining a solution which is also of limited regularity.

3.5. Spectral Galerkin Method

We now provide a numerical method to approximate solutions of Problem 3.4.19, along with its corresponding error estimates. We restrict ourselves to cases where the interfaces $\{\Gamma_i\}_{i=1}^M$ are \mathcal{C}^∞ -Jordan curves. By Theorem 3.4.21, the solution is of arbitrary smoothness, and a spectral method should converge at a super-algebraic rate (cf. (Saranen & Vainikko, 2013, Chapter 9) and (Hu, 1995; Jerez-Hanckes & Pinto, 2018)).

3.5.1. Discrete Spaces

Let us define a suitable family of finite dimensional subspaces of $\mathcal{V}_\theta^{s_1, s_2}$. From the definition of quasi-periodic Sobolev spaces, it is natural to consider the following finite dimensional functional spaces over $(0, 2\pi)$

$$\widehat{\mathcal{E}}_\theta^N := \text{span}\{\widehat{e}_\theta^n(t) := e^{i(n+\theta)t} : n \in \{-N, \dots, N\}\}.$$

It is clear that $\widehat{\mathcal{E}}^N \subset \widehat{\mathcal{E}}^{N+1}$ for all $N \in \mathbb{N}$ and that $\bigcup_{N \in \mathbb{N}} \widehat{\mathcal{E}}^N$ is dense in $H_\theta^s[0, 2\pi]$ for any $s \in \mathbb{R}$. Denoting $\mathbf{z}_i : (0, 2\pi) \rightarrow \Gamma_i$ a parametrization of Γ_i , we define

$$\widetilde{\mathcal{E}}_{\theta, \Gamma_i}^N := \text{span}\{\widetilde{e}_{\theta, i}^n := \widehat{e}_\theta^n \circ \mathbf{z}_i^{-1}, : n \in \{-N, \dots, N\}\}, \quad (3.23)$$

$$\mathcal{E}_{\theta, \Gamma_i}^N := \text{span}\{e_{\theta, i}^n := \|\dot{\mathbf{z}}_i \circ \mathbf{z}_i^{-1}\|_{\mathbb{R}^2}^{-1} \widetilde{e}_{\theta, i}^n : n \in \{-N, \dots, N\}\}. \quad (3.24)$$

We can see that $\widetilde{\mathcal{E}}_{\theta, \Gamma_i}^N$ is the space spanned by finite Fourier basis parametrized on Γ_i and that $\mathcal{E}_{\theta, \Gamma_i}^N$ is constructed from the previous space by dividing the basis by the norm of the tangential vector of the corresponding interface. As before, it is clear that both $\bigcup_{N \in \mathbb{N}} \mathcal{E}_{\theta, \Gamma_i}^N$ and $\bigcup_{N \in \mathbb{N}} \widetilde{\mathcal{E}}_{\theta, \Gamma_i}^N$ are dense subspaces of $H_\theta^s(\Gamma_i)$ for $s \in \mathbb{R}$. Finally, we define the Cartesian product of discrete spaces

$$\mathcal{E}_{\theta, \Gamma_i}^N := \widetilde{\mathcal{E}}_{\theta, \Gamma_i}^N \times \mathcal{E}_{\theta, \Gamma_i}^N,$$

whose infinite union on N forms a dense subspace of $\mathcal{V}_{\theta, \Gamma_i}^{s_1, s_2}$ for any pair $s_1, s_2 \in \mathbb{R}$.

3.5.2. Discrete Problem

We now consider the Galerkin discretization of Problem 3.4.19 on the finite dimensional product space

$$\mathbb{E}_\theta^N := \prod_{i=1}^M \mathcal{E}_{\theta, \Gamma_i}^{N_i} \subset \mathcal{V}_\theta^{s_1, s_2} \quad \text{for } \mathbf{N} = \{N_i\}_{i=1}^M \subset \mathbb{N}, \quad s_1, s_2 \in \mathbb{R}.$$

PROBLEM 3.5.1 (Discrete BIEs). Let the parameters k_0 and $\{\eta_i\}_{i=1}^M$ satisfy Assumption 3.4 and let the interfaces $\{\Gamma_i\}_{i=1}^M$ be of class \mathcal{C}^∞ . For some $\mathbf{N} = \{N_i\}_{i=1}^M \subset \mathbb{N}$, we

seek $\Lambda^N \in \mathbb{E}_\theta^N$ such that

$$\langle \mathcal{M}\Lambda^N, \Xi^N \rangle_\Gamma = \langle \varrho, \Xi^N \rangle_\Gamma, \quad \forall \Xi^N \in \mathbb{E}_\theta^N, \quad (3.25)$$

where the duality product

$$\langle \Psi, \Xi \rangle_\Gamma := \sum_{i=1}^M \langle \Psi_i, \Xi_i \rangle_{\Gamma_i} \quad \forall \Psi, \Xi \in \mathcal{V}_\theta^{s_1, s_2},$$

denotes the sum of two standard duality pairings in $H_\theta^{\frac{1}{2}}(\Gamma_i)$ and $H_\theta^{-\frac{1}{2}}(\Gamma_i)$, and ϱ accounts for the right-hand side of Problem 3.4.19.

Since this is a second-kind BIE, we can deduce a quasi-optimality approximation result for the Galerkin discretization (cf. (Sauter & Schwab, 2011, Theorem 4.2.9)), i.e. there exists $N^\star = \{N_i^\star\}_{i=1}^M$ such that for all $N = \{N_i\}_{i=1}^M$ such that $N_i > N_i^\star$ for all $i \in \{1, \dots, M\}$, it holds that

$$\|\Lambda - \Lambda^N\|_{\mathcal{V}_\theta^{s_1, s_2}} \lesssim \inf_{\Xi^N \in \mathbb{E}_\theta^N} \|\Lambda - \Xi^N\|_{\mathcal{V}_\theta^{s_1, s_2}}. \quad (3.26)$$

From (3.26) we see that, in order to establish error convergence rates for the discrete solution, we need to bound those of the best approximation. From the definition of our discrete and continuous spaces, the problem of bounding the best approximation on $\mathcal{V}_\theta^{s_1, s_2}$ is equivalent to that of establishing bounds for the best approximation of an element of $H^s[0, 2\pi]$ when approximated by elements of $\widehat{\mathcal{E}}_\theta^N$ with $\tilde{\theta} = 0$. This issue was already addressed, for example, in (Saranen & Vainikko, 2013, Theorem 8.2.1). Specifically, for any pair $r_1, r_2 \in \mathbb{R}$ with $r_2 > r_1$ and $f \in H^{r_2}[0, 2\pi]$, there holds

$$\inf_{q \in \widehat{\mathcal{E}}_\theta^N} \|f - q\|_{H^{r_1}[0, 2\pi]} \lesssim N^{r_1 - r_2} \|f\|_{H^{r_2}[0, 2\pi]}. \quad (3.27)$$

THEOREM 3.5.2. *Let the parameters k_0 and $\{\eta_i\}_{i=1}^M$ satisfy Assumption 3.4 and let the interfaces $\{\Gamma_i\}_{i=1}^M$ be of class \mathcal{C}^∞ . Further assume Assumptions 3.1 and 3.5 to be satisfied and let $s \geq 0$, $s_1 = s + \frac{1}{2}$ and $s_2 = s - \frac{1}{2}$. Then, there exists $N^\star = \{N_i^\star\}_{i=1}^M \subset \mathbb{N}$ such that*

for any $\mathbf{N} = \{N_i\}_{i=1}^M \subset \mathbb{N}$ with $N_i > N_i^*$ for all $i \in \{1, \dots, M\}$, it holds

$$\|\Lambda - \Lambda^{\mathbf{N}}\|_{\mathcal{V}_\theta^{\frac{1}{2}, -\frac{1}{2}}} \lesssim \left(\max_{i \in \{1, \dots, M\}} N_i^{-s} \right) \|\varrho\|_{\mathcal{V}_\theta^{s_1, s_2}},$$

where Λ and $\Lambda^{\mathbf{N}}$ are the solutions to Problems 3.4.19 and 3.5.1, respectively.

PROOF. For any $\Xi^{\mathbf{N}} \in \mathbb{E}_\theta^{\mathbf{N}}$, we denote $\Xi_i^{N_i} = (\xi_i^{N_i}, \zeta_i^{N_i})^t$ for all $i \in \{1, \dots, M\}$, so that

$$\|\Lambda - \Xi^{\mathbf{N}}\|_{\mathcal{V}_\theta^{\frac{1}{2}, -\frac{1}{2}}}^2 = \sum_{i=1}^M \|\lambda_i - \xi_i^{N_i}\|_{H_\theta^{\frac{1}{2}}(\Gamma_i)}^2 + \|\mu_i - \zeta_i^{N_i}\|_{H_\theta^{-\frac{1}{2}}(\Gamma_i)}^2.$$

By definition of our continuous and discrete spaces together with (3.27), we see that for all $i \in \{1, \dots, M\}$, one deduces

$$\|\lambda_i - \xi_i^{N_i}\|_{H_\theta^{\frac{1}{2}}(\Gamma_i)}^2 \lesssim N_i^{-2s} \|\lambda_i\|_{H_\theta^{s+\frac{1}{2}}(\Gamma_i)}^2, \quad \|\mu_i - \zeta_i^{N_i}\|_{H_\theta^{-\frac{1}{2}}(\Gamma_i)}^2 \lesssim N_i^{-2s} \|\mu_i\|_{H_\theta^{s-\frac{1}{2}}(\Gamma_i)}^2,$$

where the unspecified constant depends only on Γ_i . Hence,

$$\|\Lambda - \Xi^{\mathbf{N}}\|_{\mathcal{V}_\theta^{\frac{1}{2}, -\frac{1}{2}}}^2 \lesssim \left(\max_{i \in \{1, \dots, M\}} N_i^{-2s} \right) \|\Lambda\|_{\mathcal{V}_\theta^{s_1, s_2}}^2.$$

Since the problem is well posed, we obtain

$$\|\Lambda - \Xi^{\mathbf{N}}\|_{\mathcal{V}_\theta^{\frac{1}{2}, -\frac{1}{2}}}^2 \lesssim \left(\max_{i \in \{1, \dots, M\}} N_i^{-2s} \right) \|\varrho\|_{\mathcal{V}_\theta^{s_1, s_2}}^2,$$

where the unspecified constant now also depends on the wavenumbers $\{k_i\}_{i=0}^M$. \square

REMARK 3.5.3. Theorem 3.5.2 states that the proposed spectral Galerkin method has a similar performance to the Nyström method, since if interfaces belong to \mathcal{C}^∞ then one obtains super-algebraic convergence (commonly observed with the Nyström method (Y. Zhang & Gillman, 2019)). The super-algebraic convergence rate of the Nyström method for the transmission problem on a bounded object in two dimension was rigorously proved in (Boubendir et al., 2014). Similar convergence results for quasi-periodic problems using the Nyström scheme are, to the best of our knowledge, not available.

REMARK 3.5.4. It follows from Remark 3.4.22 that we can obtain convergence of limited order if the interfaces are of class $\mathcal{C}^{r,1}$ with $r \in [1, \infty)$.

3.5.3. Implementation

We continue with an overview of the procedure employed to compute the approximation Λ^N . For a given $N \in \mathbb{N}$ and $l, m \in \mathbb{Z}$ such that $-N \leq |l|, |m| \leq N$, integrals

$$I_l^1 := \int_0^{2\pi} f(t) e^{-ult} \, dt \quad \text{and} \quad I_{l,m}^2 := \int_0^{2\pi} \int_0^{2\pi} F(s, t) e^{-uls} e^{vmt} \, dt \, ds, \quad (3.28)$$

where f and F are smooth periodic and bi-periodic functions, respectively, can be computed to exponential accuracy through the FFT to construct trigonometric interpolations of the corresponding functions (cf. (Saranen & Vainikko, 2013, Theorem 8.4.1)). Since the associated kernels correspond to smooth bi-periodic functions, the computation of the block matrices $B_{i,j}$ on (3.20) is performed in this way.

In terms of computational cost, the set of integrals $\{I_l^1\}_{l=-N}^N$ involves $2N + 1$ evaluations of the function f and one FFT application to a vector of length $2N + 1$, whence the total computational cost is $O((2N + 1) \log(2N + 1))^1$ arithmetic operations—plus $2N + 1$ function evaluations—to compute the $2N + 1$ integrals. For the set of integrals $\{I_{l,m}^2\}_{l,m=-N}^N$, we require $(2N + 1)^2$ evaluations of the function F , and $2(2N + 1)$ FFTs for vectors of length $2N + 1$, yielding a cost of $O(2(2N + 1) \log(2N + 1))$ arithmetic operations (plus $(2N + 1)^2$ function evaluations).

On the other hand, the block matrices A_i in (3.20) consist of differences of the self-interaction operators on Γ_i for the four BIOs. While the difference of two operators is compact—the resulting kernel is smoother than that associated to a single evaluation of the same operator—the kernel is not arbitrarily smooth, even if the geometry is. Consequently, a deeper analysis is required before applying classical algorithms for the computation of Fourier transforms.

¹This is the classical estimation of the computational cost for the FFT.

Let us consider, as an illustrative example, the weakly singular operator. We are required to compute integrals such as

$$\int_0^{2\pi} \int_0^{2\pi} \widehat{G}_\theta^k(s, t) e^{-\imath ls} e^{\imath mt} \, \mathbf{d}t \, \mathbf{d}s,$$

where \widehat{G}_θ^k is as in (3.10). Decomposing \widehat{G}_θ^k as shown in (3.11), we obtain two integrals,

$$I_{l,m}^S := \int_0^{2\pi} \int_0^{2\pi} S(t-s) J_\theta^k(s, t) e^{-\imath ls} e^{\imath mt} \, \mathbf{d}t \, \mathbf{d}s, \quad I_{l,m}^R := \int_0^{2\pi} \int_0^{2\pi} R_\theta^k(s, t) e^{-\imath ls} e^{\imath mt} \, \mathbf{d}t \, \mathbf{d}s.$$

Since $R_\theta^k(s, t)$ is smooth and periodic (see Section 3.4.2.1), $I_{l,m}^R$ may be computed via the FFT. To compute $I_{l,m}^S$, we use the expansion (c.f. (Hu, 1995, Equation 12)):

$$S(t-s) = \sum_{\substack{n=-\infty \\ n \neq 0}}^{\infty} \frac{1}{4\pi n} e^{\imath n(t-s)}.$$

Thus,

$$I_{l,m}^S = \sum_{\substack{n=-\infty \\ n \neq 0}}^{\infty} \frac{1}{4\pi n} \int_0^{2\pi} \int_0^{2\pi} J_\theta^k(s, t) e^{-\imath(l+n)s} e^{\imath(m+n)t} \, \mathbf{d}t \, \mathbf{d}s. \quad (3.29)$$

Since $J_\theta^k(s, t)$ is smooth and periodic, each of the integrals of the right-hand side is easy to compute. Moreover, the terms in the series in (3.29) decay exponentially and the series may be truncated at the cost of a small approximation error. Furthermore, the sum in (3.29) may be understood as a discrete convolution, allowing it to be computed by multiplying the corresponding Fourier transforms (see (Hu, 1995) for details).

The computational cost of computing $\{I_{l,m}^S\}_{l,m=-N}^N$ and $\{I_{l,m}^R\}_{l,m=-N}^N$ is dominated by the latter set of integrals, since it involves $2(N+1)^2$ evaluations of the quasi-periodic Green's function, which is done following (Bruno & Delourme, 2014). The evaluation cost of the quasi-periodic Green's function corresponds to $(2N+1)^2(2N'+1)$ evaluations of the Hankel function, with $N' > N$ is a truncation parameter for the series in (B.26)². Meanwhile, the total cost for $I_{l,m}^S$ is proportional to $(2N+1) \log(2N+1)$.

²The value of N' has to be chosen depending of k_0 , but typically one can assume that it need not be greater than $2N$, for N large enough to ensure convergence.

For the operators K_θ^k and K_θ^{lk} , a similar technique can be applied using (3.15). The integrals corresponding to the hyper-singular BIO are approximated by first using the integration-by-parts formula in Lemma 3.4.11, reducing it to two different integrals which are then approximated as those corresponding to the weakly-singular BIO.

Considering $M > 1$ interfaces, $2N + 1$ degrees of freedom on each interface and N' proportional to N the total cost of the matrix assembly process can be estimated as $O(N^3 M)$ Hankel function evaluations and $O(MN^2 \log N)$ arithmetic operations. We point out that the cost could be reduced drastically by constructing an accurate algorithm to approximate the Hankel functions by pre-computing some values.

REMARK 3.5.5. We have restricted ourselves to the analysis of the semi-discrete case, that is, we do not take into consideration the error coming from the approximation of the integrals for the error bound in Theorem 3.5.2. However, it is not difficult to incorporate it. Assuming that the parametrizations $\{z_i\}_{i=1}^M$ correspond to Jordan curves of class C^∞ and using the aliasing properties of the Fourier basis (L. N. Trefethen, 2000, Chapter 4) and Lemma 3.4.9 we have that the approximation error for the computation of the required integrals is $O(N^{-\ell-1})$, with $2N + 1$ being the number of degrees of freedom per interface and ℓ an arbitrarily large integer. Then, the fully discrete error can be obtained by an application of Strang's lemma (Sauter & Schwab, 2011, Section 4.2.4), from where it follows that the behaviour of the fully discrete error, with respect to N , is the same as in Theorem 3.5.2.

3.6. Numerical Examples

We now showcase computational experiments verifying the convergence estimates found in Theorem 3.5.2. The implementation of the aforementioned algorithms was carried through a C++ cpu-only library. All the experiments ran on a Intel I7-4770@3.4GHZ processor with 8 threads. The code was compiled with gcc 4.9.4, openmp and O2 flags on.

3.6.1. Code Validation

We begin by considering the simple case of a grating with two media separated by a single horizontal line segment acting as its layer. Hence, using the following expansion of the Green's function (Aylwin, Jerez-Hanckes, & Pinto, 2020, Proposition 4.2):

$$G_{\theta}^k(\mathbf{x}, \mathbf{y}) = \frac{i}{4\pi} \sum_{j \in \mathbb{Z}} \frac{1}{\beta_j} e^{i\beta_j |x_2 - y_2| - i j_{\theta} (y_1 - x_1)} \text{ for all } \mathbf{x}, \mathbf{y} \in \mathbb{R}^2,$$

$$\beta_j := \begin{cases} \sqrt{k^2 - j_{\theta}^2} & \text{if } k^2 - j_{\theta}^2 \geq 0 \\ i\sqrt{j_{\theta}^2 - k^2} & \text{if } k^2 - j_{\theta}^2 < 0 \end{cases},$$

it is possible to assemble the matrix analytically. The matrix \mathcal{M} is then composed of only block diagonal terms. Since the right-hand side only has two non-null components³, only the corresponding components for the solution are non-zero, yielding a closed form for the solution.

In order to test the implementation, we consider an artificial (harder) problem by including ghost domains, i.e., we add extra smooth (ghost) layers that separate domains with the same refraction index. Hence, the solution is the same as if these additional domains did not exist and has a closed form, as before. The results for different ghost layers are reported in Figure 3.2.

We also display the convergence behaviour of the method for interfaces with limited regularity by repeating the previous experiment (same incident field) with one ghost domain and an interface given by

$$z_3(t) = (t, a|\sin(t)|^p + b),$$

where a, b are real numbers that scale the interface, and p is an odd integer that determines the smoothness degree of the interface. In particular, z_3 is in $\mathcal{C}^{p-2,1}$ or, more precisely, \mathcal{C}^{p-1} with an integrable p -th derivative. Results are reported in Figure 3.3.

³One for the Dirichlet trace of the incident wave and another for the Neumann trace.

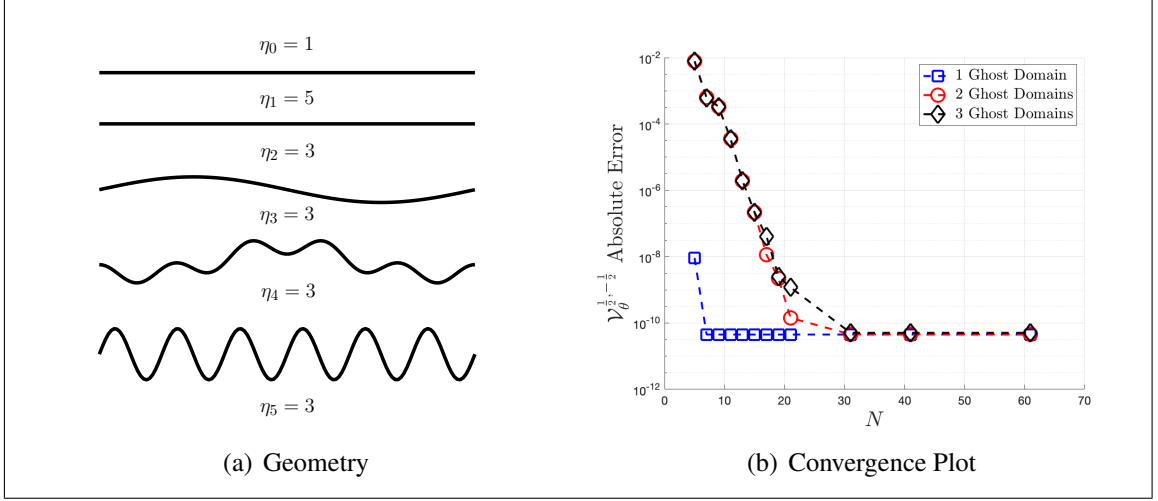


FIGURE 3.2. Subfigure (a) shows the problem geometry. Subfigure (b) shows the error in the $\mathcal{V}_\theta^{\frac{1}{2}, -\frac{1}{2}}$ norm with respect to the analytic solution. We have included results for different numbers ghost layers (1,2 and 3, respectively), i.e., the first experiment considers only the first 3 layers (counting downwards), the second one considers the first 4 layers and the third considers all 5 layers.

For all experiments in this section, the frequency is chosen as $k_0 = 1$ and the incidence angle is 0.47 radians.

3.6.2. Convergence results

We now consider a smooth geometry composed of the 12 layers and varying refraction indices. Two different scenarios for the choice of indices are employed, reported in Table 3.1 (η_i^1 and η_i^2 for the first and second cases, respectively). We also consider three different wavenumbers for the incident wave, $k_0 = 2.8, 14$ and 28 . Convergence results in the energy norm for the solution of Problem 3.5.1 for the different cases of parameters and wavenumbers are reported in Figure 3.4, where exponential convergence is observed for all considered scenarios, as expected. All errors were computed with respect to an overkill solution, with approximately 50 more bases per interface than the last plotted point for each curve. The incidence angle is, again, 0.47 radians. While is not an easy task to establish the number of basis needed, for a desire accuracy, in terms of the frequency k_0 and the refraction indices η_i , it seems from the presented experiments that they should be chosed proportional to the maximum value $k_i = \eta_i k_0$.

	1	2	3	4	5	6	7	8	9	10	11	12
η_i^1	4.7	4.2	4.8	3.6	1.1	4.4	4.7	3.7	4.0	3.9	2.6	3.6
η_i^2	4.7	8.4	4.8	7.2	1.1	8.8	4.7	7.4	4.0	7.8	2.6	7.2

TABLE 3.1. Value of the refraction indices $\{\eta_i^1\}_{i=1}^{12}$ and $\{\eta_i^2\}_{i=1}^{12}$ (corresponding to the two considered cases) for the grating in Figure 3.5 (counting downwards).

Finally, in Figure 3.5 we present an illustration of the total field corresponding to the refraction indices given in Table 3.1.

3.7. Conclusions

We have proposed a fast spectral method for the efficient representation, through surface potentials based on the quasi-periodic Green's function, for the solution of the Helmholtz equation with transmission boundary conditions on a periodic domain. In Theorem 3.5.2, we obtained convergence estimates for the discrete approximation of the corresponding boundary data, and found that discrete solutions converge at a super-algebraic rate to continuous solutions of the considered boundary integral equation. Though, we focused on the

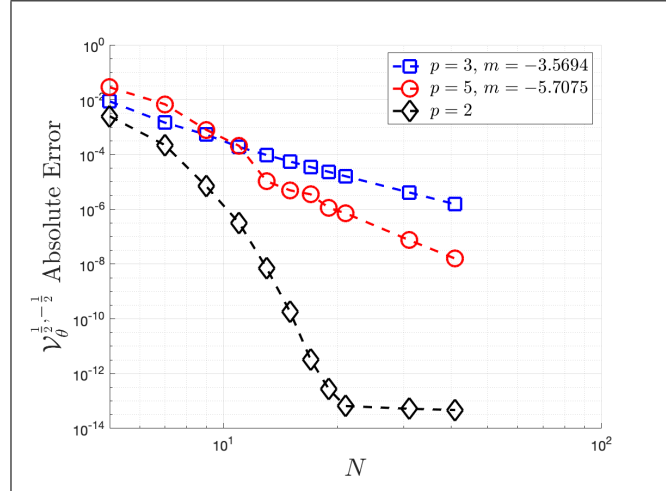


FIGURE 3.3. Error in the $\mathcal{V}_\theta^{\frac{1}{2}, -\frac{1}{2}}$ norm with respect to the analytic solution. The legend indicates an estimate of the slope of the error convergence curves for different values of p (degrees of smoothness). Classically, error convergence estimates for spectral methods indicate the slope to be at least equal to p . We also consider the case $p = 2$, where the extra layer is \mathcal{C}^∞ and the super-algebraic convergence rate is observed.

Helmholtz transmission problem, our approximation results and convergence estimates can be easily extended to other boundary integral equations on quasi-periodic Sobolev spaces whenever the formulation is well posed. We avoided Rayleigh-Wood anomalies from our analysis since the series in (B.26) fails to converge for said frequencies and, for the same

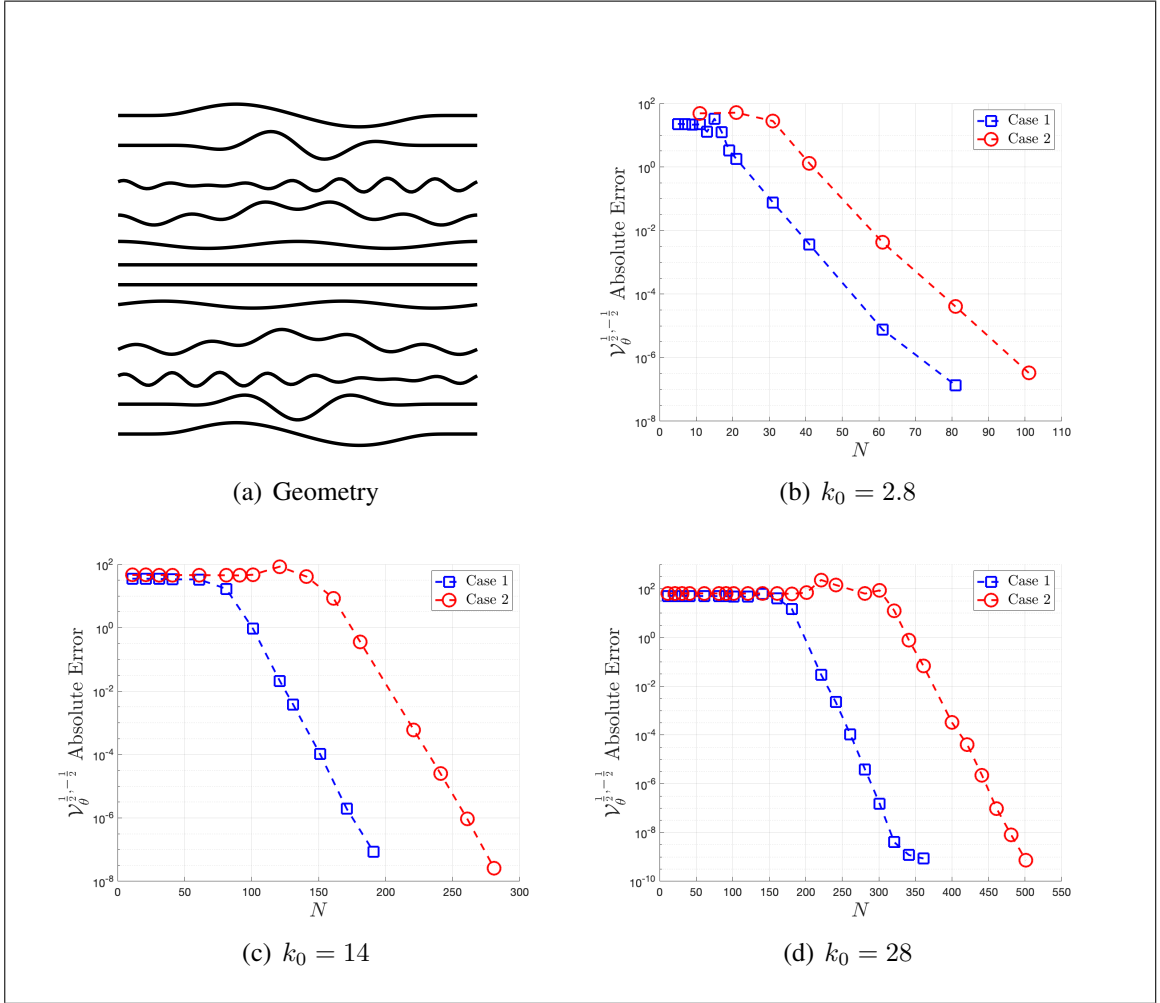


FIGURE 3.4. Subfigure (a) shows the problem geometry (with 12 layers). Subfigures (b), (c) and (d) display the errors (in the corresponding energy norm) for the different values of k_0 , i.e., 2.8, 14 and 28, respectively. Each of these subfigures present error convergence curves for the two scenarios of refraction indices considered and specified in Table 3.1. Notice that the curves in red—corresponding to parameters η_i^2 in Table 3.1, with higher discrepancy between layers—display a longer preasymptotic regime before convergence is observed for all considered values of k_0 .

reason, our previous results from (Aylwin, Jerez-Hanckes, & Pinto, 2020) exclude them as well.

Though similar numerical results are known for the Nyström Method, theoretical results confirming the observed convergence rates are scarce (Boubendir et al., 2014), which is an advantage of Galerkin discretizations such as that presented in this article. Moreover, the convergence rate for the proposed discretization is equal to that expected of Nyström methods, so that it is numerically competitive with them while inheriting the theoretical benefits of a Galerkin discretization.

Future work considers: (i) including Rayleigh-Wood anomalies to our analysis, (ii) extending our results to three dimensional Helmholtz equations and Maxwell's equations on periodic domains and (iii) applications in uncertainty quantification (Silva-Oelker, Aylwin, et al., 2018) and shape optimization (Aylwin, Silva-Oelker, Jerez-Hanckes, & Fay, 2020).

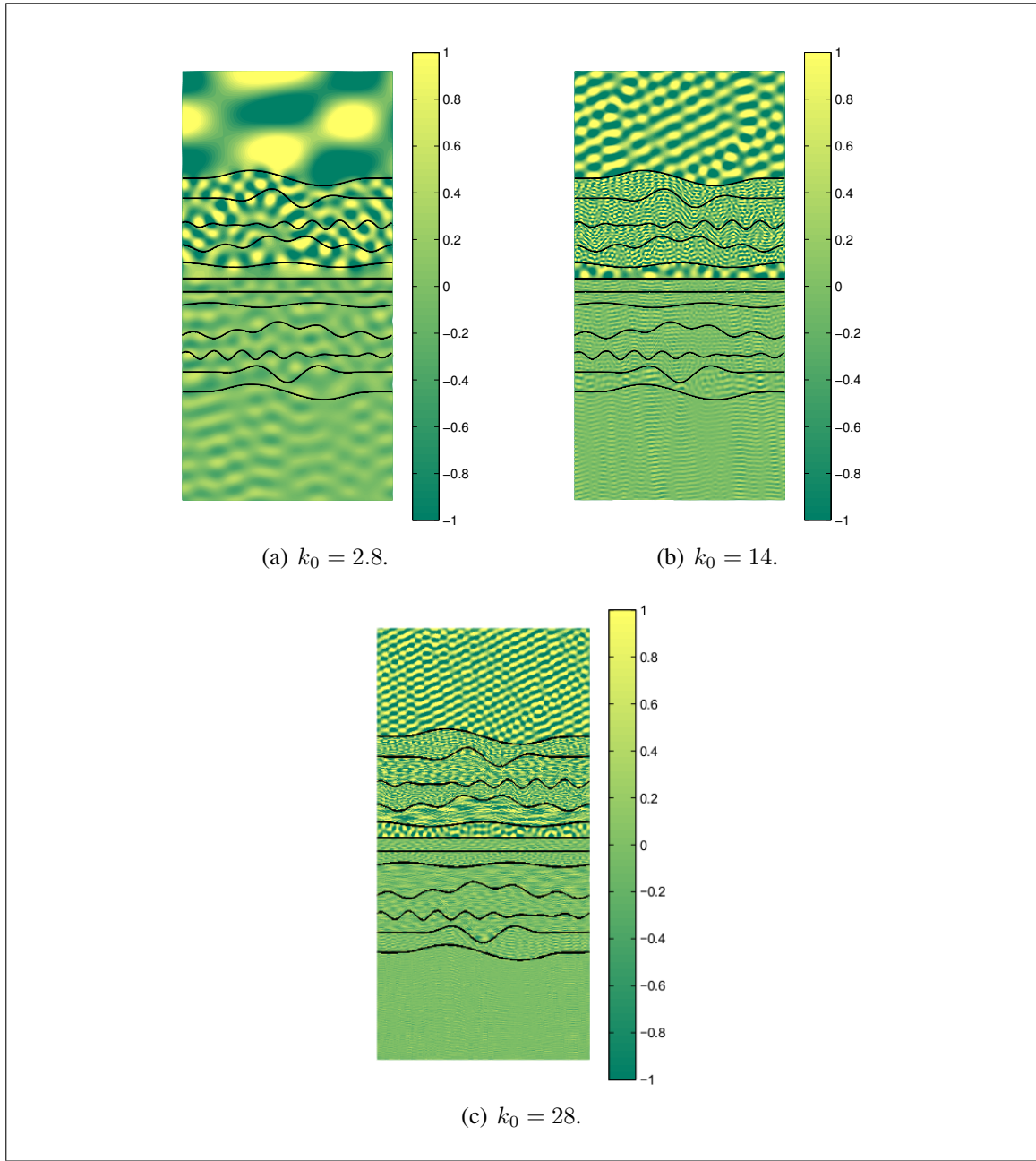


FIGURE 3.5. Real part of the total wave ($u^{(\text{tot})} = u^{(\text{sc})} + u^{(\text{inc})}$) for each different value of k_0 , namely 2.8, 14 and 28. The refraction indices on each layer are those indicated on Table 3.1. The incidence angle is again 0.47.

Chapter 4. FAST GALERKIN METHOD FOR SOLVING HELMHOLTZ BOUNDARY INTEGRAL EQUATIONS ON SCREENS

4.1. Introduction

We study the solution of the Helmholtz and Laplace problems with Dirichlet or Neumann conditions posed on an open orientable bounded surface $\Gamma \subset \mathbb{R}^3$. These can be summarized as follows:

PROBLEM 4.1. *Let $k \geq 0$, find u defined in \mathbb{R}^3 , such that*

$$\begin{aligned} -\Delta u - k^2 u &= 0, \quad \text{on } \mathbb{R}^3 \setminus \bar{\Gamma}, \\ u &= g_d \quad \text{or} \quad \partial_n u = g_n \quad \text{in } \Gamma, \\ &\text{condition at infinity}(k), \end{aligned}$$

where $\partial_n u$ is the normal derivative of u with the normal defined via the parametrization used¹, g_d and g_n are suitable Dirichlet and Neumann data, respectively, and the condition at infinity reads

$$\begin{cases} \lim_{\|\mathbf{x}\| \rightarrow \infty} \|\mathbf{x}\| (\partial_{\|\mathbf{x}\|} u - iku) = 0, & k > 0, \\ u(\mathbf{x}) = O(\|\mathbf{x}\|^{-1}), \text{ as } \|\mathbf{x}\| \rightarrow \infty, & k = 0, \end{cases}$$

For a detailed discussion of these conditions see (McLean, 2000, Chap. 8 and 9). The Laplace case occurs when $k = 0$.

Problem 4.1 and associated boundary integral equations (BIEs) have been extensively studied (E. P. Stephan, 1987, 1986; Costabel & Dauge, 2002; Ha-Duong, 1990; Hiptmair, Jerez-Hanckes, & Urzúa-Torres, 2018; S. K. Lintner & Bruno, 2015; Ramaciotti & Nédélec, 2017; Hiptmair, Jerez-Hanckes, & Urzúa-Torres, 2020). Indeed, BIEs rigorously recast the volume problem onto the screen while taking into account the corresponding

¹A fixed orientation for the normal vector is required, and one can choose either of the two orientations that yield continuous normal vectors without loss of generality.

condition at infinity. By meshing the open surface Γ , standard local low-order approximations can be built and solved by today's compression algorithms (Bebendorf, 2008; Yijun, 2009) to accelerate computations. However, solving Problem 4.1 remains far from trivial as standard boundary element implementations converge at the worst rate possible due to the solution's singular behavior near the screen boundary. Thus, one has to resort to special meshing techniques (von Petersdorff & Stephan, 1990; Heuer et al., 1999) or to increase the polynomial degree of the underlying discretization in a suitable manner (Heuer, Melado, & Stephan, 2002; Bepalov & Heuer, 2007) so as to recover better error convergence rates. This however is a tedious procedure when solving for multiple configurations as in uncertainty quantification or inverse problems.

In two-dimensional space, i.e. when Γ is an open arc, an alternative discretization of BIEs can be performed by means of weighted Chebyshev polynomials (spectral discretization), which explicitly capture the edge singularity and allow for super-algebraic convergence whenever g_d and g_n are smooth functions (Saranen & Vainikko, 2013; Jerez-Hanckes & Nédélec, 2012; Jerez-Hanckes & Pinto, 2020). Opposingly, for screens in \mathbb{R}^3 , to the best of our knowledge, no such equivalent discretization exists. Moreover, though for closed surfaces a spectral BIE method was presented by Sloan *et al.* (Graham & Sloan, 2002), the presence of extra singularities around the surface edges and the structure of the underlying fundamental solution renders impossible the extension of this method to the context of open surfaces directly.

Our main contribution is the derivation and analysis of spectral Galerkin-Bubnov methods to tackle Laplace and Helmholtz BIEs on open surfaces in three-dimensional space. In contrast to the Nyström approach (Bruno & Lintner, 2013), our spectral Galerkin method preserves all the theoretical properties of a Galerkin method and its implementation relies on suitable quadrature rules and change of variables without the need of special window functions, while maintaining the convergence rate for smooth geometries. On the other hand, while special p - and hp -discretizations (see (Heuer et al., 1999, 2002; Bepalov & Heuer, 2007)) could also achieve super-algebraic convergence rates, and being more flexible for non-smooth geometries, they need a mesh which in practice could slowdown the

implementation when solutions for different geometries are needed as in uncertainty quantification or inverse problem (Kress, 1995).

Our work is structured as follows. In Section 4.2.3 we define a family of finite-dimensional functional spaces by projecting the spherical harmonics into the unitary disk and consider their linear span. We then define the trial and test spaces for the Galerkin method by mapping the functions to the screen in consideration. From the definition of our trial space, we construct adequate auxiliary functional spaces which allow for the associated error analysis, and we describe how these spaces are related to the standard Sobolev one. This fact, in conjunction with standard Galerkin properties for the variational versions of the BIEs (Section 4.3.1), lead to a semi-discrete a priori error bound in Theorem 4.3. Then, in Section 4.5.1, we detail the quadrature procedure used to approximate the action of the weakly- and hyper-singular boundary integral operators (BIOs) on the trial space, and provide a full error analysis which incorporate the quadrature error. Finally, in Section 4.6 we show some numerical examples that exhibit the super-algebraic convergence method.

4.2. Mathematical Tools

This section introduces general definitions needed for the analysis of Problem 4.1 and of the proposed Galerkin spectral method.

Given $\mathbf{x}, \mathbf{x}' \in \mathbb{C}^d$, $d \in \mathbb{N}$, the standard dot product is denoted by $\mathbf{x} \cdot \mathbf{x}' = \sum_{j=1}^d x_j \overline{x'_j}$, and the Euclidean norm satisfies $\|\mathbf{x}\|^2 = \mathbf{x} \cdot \mathbf{x}$. For $d = 3$ and real vectors, we denote $\mathbf{x} \times \mathbf{x}'$ the cross-product –vectorial product. For $a, b \in \mathbb{R}$ we will make use of the notation $a \lesssim b$ whenever there is a positive number C such that $a \leq Cb$, typically C is a constant not relevant for the underlying analysis. Also, we will denote by $L^2(A)$ the classical Lebesgue space of square-integrable functions over a measurable set $A \subset \mathbb{R}^d$, $d = 2, 3$.

4.2.1. Geometry

Throughout, we denote $\Gamma \subset \mathbb{R}^3$ a smooth orientable connected surface with boundary, also called smooth screen or simply screen. We assume that the screen is contained on a smooth orientable closed surface which will be denoted $\tilde{\Gamma}$. The canonical disk and spheres are given, respectively, by

$$\mathbb{D} := \{\mathbf{x} \in \mathbb{R}^2 : \|\mathbf{x}\| \leq 1\}, \quad \mathbb{S} := \{\mathbf{x} \in \mathbb{R}^3 : \|\mathbf{x}\| = 1\}.$$

On \mathbb{S} , we will often consider spherical coordinates characterized by two angles $(\theta, \varphi) \in [0, 2\pi] \times [0, \pi]$. We will always assume that θ corresponds to the polar angle of a given point when projected to the $x_3 = 0$ plane, and φ denotes the angle measured from the x_3 -axis. Similarly, in \mathbb{D} we use polar coordinates $(r, \theta) \in [0, 1] \times [-\frac{\pi}{2}, \frac{3\pi}{2}]$.

For any given screen, we assume that there is a parametrization $\mathbf{r} : \mathbb{D} \rightarrow \Gamma$, being a smooth injective function such that in every argument and coordinate can be extended to an analytic function on a Bernstein ellipse in the complex plane of parameter² $\rho > 1$. The class of functions portraying the regularity previously described are referred to as ρ -analytic. Furthermore, we impose that the gradients of \mathbf{r} (as a matrix) have full rank for any point, and the Jacobian, $J_{\mathbf{r}}(\mathbf{x}) = \|\partial_r \mathbf{r} \times \partial_\theta \mathbf{r}\|$ is such that $J_{\mathbf{r}}(\mathbf{x})/\|\mathbf{x}\|$ is bounded and nowhere null.

The direction of the unitary normal vector of Γ is selected to be equal to $\partial_r \mathbf{r} \times \partial_\theta \mathbf{r}$. This imply that, rigorously speaking, a screen is characterized by the particular parametrization \mathbf{r} and no by the set of points that represent the physical domain Γ .

4.2.2. Classical Functional Spaces

Given a set $\mathcal{O} \subset \mathbb{R}^d$, $d \in \{2, 3\}$, we denote by $\mathcal{D}(\mathcal{O})$ the space of smooth functions with compact support in \mathcal{O} with topological dual $\mathcal{D}(\mathcal{O})'$. If \mathcal{O} is open then $\mathcal{D}(\mathcal{O})$ are smooth functions whose extension by zero is also smooth. If \mathcal{O} is compact then $\mathcal{D}(\mathcal{O})$ are the set of infinity differentiable functions. We will require Sobolev spaces defined on open and

²Given an interval $[a, b] \subset \mathbb{R}$, the Bernstein ellipse of parameter ρ , corresponds to an ellipse on the complex plane with foci at a, b , semi-major axis $\frac{(b-a)(\rho+\rho^{-1})}{4}$, and semi-minor axis $\frac{(b-a)(\rho-\rho^{-1})}{4}$.

closed surfaces. For Γ an open surface, the Sobolev spaces $H^s(\tilde{\Gamma})$, $s \in \mathbb{R}$, are defined by using local parametrizations and a partition of unity (McLean, 2000, Chap. 2). Spaces $H^s(\Gamma)$, and $\tilde{H}^s(\Gamma)$, with $s \in \mathbb{R}$, are also standard and can be defined as

$$\begin{aligned} H^s(\Gamma) &:= \{u \in \mathcal{D}'(\Gamma) : \exists U \in H^s(\tilde{\Gamma}), u = U|_{\Gamma}\}, \\ \tilde{H}^s(\Gamma) &:= \{u \in H^s(\tilde{\Gamma}) : \text{supp}(u) \subset \bar{\Gamma}\}, \end{aligned}$$

where the support and restriction have to be understood in the context of distributions. One can identify the dual space of $H^s(\Gamma)$ with $\tilde{H}^{-s}(\Gamma)$, the corresponding duality product is denoted $\langle \cdot, \cdot \rangle_{\Gamma}$. The duality product is an extension of the $L^2(\Gamma)$ inner product as we work under the identification, $H^0(\Gamma) = \tilde{H}^0(\Gamma) = L^2(\Gamma)$. The following Lemma is useful to retain control over the norms of functions defined on an arbitrary screen.

Lemma 4.1 (Theorem 3.23 in (McLean, 2000)). *Let $s \in \mathbb{R}$, if $u \in H^s(\Gamma)$, we can define an equivalent norm as*

$$\|u \circ \mathbf{r}\|_{H^s(\mathbb{D})} \cong \|u\|_{H^s(\Gamma)},$$

where the unspecified constant depends on Γ only. The same result holds true when we change $H^s(\Gamma)$ for $\tilde{H}^s(\Gamma)$ and $H^s(\mathbb{D})$ for $\tilde{H}^s(\mathbb{D})$, accordingly.

REMARK 4.1. *Lemma 4.1 can be generalized to screens of restricted regularity by limiting the range of s depending on the regularity (cf. (McLean, 2000, Theorem 3.2.3) for details).*

Customarily, we extend the definitions of restrictions and normal derivatives over Γ to linear bounded maps in appropriate Sobolev spaces. In particular, following (McLean, 2000, Chapter 2), we define the Dirichlet traces as the maps $\gamma_d^{\pm} : H^s(\mathbb{R}^3 \setminus \bar{\Gamma}) \rightarrow H^{s-\frac{1}{2}}(\Gamma)$ that extend the following operator:

$$\gamma_d^{\pm} u(\mathbf{x}) = \lim_{\epsilon \downarrow 0} u(\mathbf{x} \pm \epsilon \hat{\mathbf{n}}(\mathbf{x})), \quad \mathbf{x} \in \Gamma,$$

for $s > \frac{1}{2}$, and where $\hat{\mathbf{n}}$ denotes the unitary normal vector whose direction depends on the parametrization \mathbf{r} of Γ . The Neumann trace γ_n is defined as the extension of the normal derivative:

$$\gamma_n^\pm u(\mathbf{x}) = \lim_{\epsilon \downarrow 0} \nabla u(\mathbf{x} \pm \epsilon \hat{\mathbf{n}}(\mathbf{x})) \cdot \hat{\mathbf{n}}(\mathbf{x}), \quad \mathbf{x} \in \Gamma,$$

where the extension can be done from $H^s(\mathbb{R}^3 \setminus \bar{\Gamma}) \rightarrow H^{s-\frac{1}{2}}(\Gamma)$ for $s > \frac{3}{2}$, or from $H^1(\mathbb{R}^3 \setminus \bar{\Gamma}) \rightarrow H^{-\frac{1}{2}}(\Gamma)$ for functions such that Δu is locally in $L^2(\mathbb{R}^3 \setminus \Gamma)$ (McLean, 2000, Chapter 4). Whenever $\gamma_d^+ = \gamma_d^-$ (resp. $\gamma_n^+ = \gamma_n^-$) we denote $\gamma_d = \gamma_d^\pm$ (resp. $\gamma_n = \gamma_n^\pm$).

4.2.3. Spherical Harmonics and Projected Basis

The standard spherical harmonics functions consist of a family of smooth functions defined in \mathbb{S} given by

$$Y_m^l(\theta, \varphi) := c_m \sqrt{\frac{(2l+1)(l-|m|)!}{4\pi(l+|m|)!}} P_{|m|}^l(\cos \varphi) e^{im\theta},$$

where $c_m = (-1)^m$ if $m < 0$ or $c_m = 1$ otherwise, with $(\theta, \varphi) \in [0, 2\pi] \times [0, \pi]$ are the spherical coordinates on \mathbb{S} , P_m^l denotes the associated Legendre function, and the indices $l \in \mathbb{N}$, $m \in \mathbb{Z} : |m| \leq l$. We will write $Y_m^l(\mathbf{x})$ to denote the corresponding spherical harmonic evaluated at a point $\mathbf{x} \in \mathbb{S}$. The spherical harmonics form an orthonormal basis of $L^2(\mathbb{S})$ (cf. (MacRobert, 1948) for more details).

Functions Y_m^l can be projected onto \mathbb{D} , this fact being key ingredient of our approximation basis. Let us start by defining two lifting operators on $\mathcal{D}(\mathbb{D})$, the first is the *even lifting*

$$L_e : \mathcal{D}(\mathbb{D}) \rightarrow \mathcal{D}(\mathbb{S}),$$

$$L_e(f)(\mathbf{x}) = f(x_1, x_2), \quad \mathbf{x} \in \mathbb{S} \subset \mathbb{R}^3,$$

using polar-spherical coordinates we see that $L_e(g)(\theta, \varphi) = g(\sin \varphi, \theta)$, where the arguments of g are the distance to the origin and the polar angle on the plane $x_3 = 0$. The odd lifting has to be defined on $\mathcal{D}_0(\mathbb{D})$ the space of smooth functions on \mathbb{D} which vanish on the

unitary circle in the plane $x_3 = 0$.

$$L_o : \mathcal{D}_0(\mathbb{D}) \rightarrow \mathcal{D}(\mathbb{S}),$$

$$L_o(f)(\mathbf{x}) = \begin{cases} f(x_1, x_2) & x_3 \geq 0 \\ -f(x_1, x_2) & x_3 \leq 0 \end{cases}, \quad \mathbf{x} \in \mathbb{S} \subset \mathbb{R}^3,$$

Notice that every function in the image of L_e (resp. L_o) is a even (resp. odd) function on the x_3 variable. In particular, the spherical harmonic Y_m^l is even (resp. odd) when $m + l$ is even (resp. odd). The definition of the lifting operators can be extended to distributions by duality. In parallel, one can define a projection operator as

$$\Pi_{\mathbb{S}} : \mathcal{D}(\mathbb{S}) \rightarrow \mathcal{D}(\mathbb{D}),$$

$$\Pi_{\mathbb{S}}(f)(\mathbf{x}) := f\left(\mathbf{x}, \sqrt{1 - x_1^2 - x_2^2}\right) \quad \mathbf{x} \in \mathbb{D} \subset \mathbb{R}^2,$$

which is the inverse L_e (resp. L_o) when restricted to the functions with the corresponding symmetries on \mathbb{S} . Finally, following (Wolfe, 1971; Ramaciotti Morales, 2016), the projected basis are defined as

$$p_m^l(\mathbf{x}) := \sqrt{2}\Pi_{\mathbb{S}}(Y_m^l)(\mathbf{x}), \quad q_m^l(\mathbf{x}) := \frac{p_m^l(\mathbf{x})}{\sqrt{1 - \|\mathbf{x}\|^2}},$$

where $\mathbf{x} \in \mathbb{D}$. From the orthogonality property of spherical harmonics, it holds that

$$\int_{\mathbb{D}} p_m^l(\mathbf{x}) \overline{q_{m'}^{l'}(\mathbf{x})} d\mathbf{x} = \delta_{m,m'} \delta_{l,l'}. \quad (4.1)$$

From the recurrence relations of the associated Legendre functions it can be shown that if $m + l$ is even, then p_m^l is a smooth function, while, if $m + l$ is odd, then q_m^l is smooth, we refer to (Arfken, Weber, & Harris, 2013, Chapter 15), for details.

An explicit formula for the projected basis is given by:

$$p_m^l(r, \theta) = C_m^l P_{|m|}^l(\sqrt{1 - r^2}) e^{im\theta}, \quad (4.2)$$

where $C_m^l = \sqrt{\frac{(2l+1)(l-|m|)!}{2\pi(l+|m|)!}}$ if $m \geq 0$ and $C_m^l = (-1)^m C_{-m}^l$ if $m < 0$.

To simplify notations, we sporadically use only one sub-index for the projected basis. For $m + l$ even, we can reorder the basis with a one-dimensional index defined as

$$I_e(l, m) := \frac{l(l+1) + (l+m)}{2}.$$

The even function indexed in this way will be denoted $p_{I_e(l, m)}^e$ (resp. $q_{I_e(l, m)}^e$) whereas for $m + l$ odd, we set

$$I_o(l, m) = \frac{(l-1)l + m + l - 1}{2},$$

with functions denoted $p_{I_o(l, m)}^o$ (resp. $q_{I_o(l, m)}^o$). For example, this leads to

$$\begin{array}{cccc} p_0^e = p_0^0, & p_1^e = p_{-1}^1, & p_2^e = p_1^1, & p_3^e = p_{-2}^2, \\ q_0^o = q_0^1 & q_1^o = q_{-1}^2 & q_2^o = q_1^2 & q_3^o = q_{-2}^3. \end{array}$$

Lemma 4.2 (Proposition 2.1.20 in (Urzúa-Torres, 2018)). *The following inclusions are dense in the corresponding Sobolev spaces:*

$$\begin{aligned} \text{span}\{p_l^e\}_{l \in \mathbb{N}} &\subset H^{\frac{1}{2}}(\mathbb{D}), & \text{span}\{p_l^o\}_{l \in \mathbb{N}} &\subset \tilde{H}^{\frac{1}{2}}(\mathbb{D}), \\ \text{span}\{q_l^e\}_{l \in \mathbb{N}} &\subset \tilde{H}^{-\frac{1}{2}}(\mathbb{D}), & \text{span}\{q_l^o\}_{l \in \mathbb{N}} &\subset H^{-\frac{1}{2}}(\mathbb{D}). \end{aligned}$$

4.2.4. Auxiliary Functional Spaces

Classically, Sobolev spaces on \mathbb{S} can be defined in terms of functions expressed as an expansion of spherical harmonics in the following way (*cf.* (Pham, Tran, & Chernov, 2011) or (K. Atkinson & Han, 2001, Chapter 7)):

$$H^s(\mathbb{S}) := \left\{ u \in \mathcal{D}'(\mathbb{S}) : \|u\|_{H^s(\mathbb{S})}^2 := \sum_{l=0}^{\infty} (l+1)^{2s} \sum_{m=-l}^l |\langle u, Y_m^l \rangle|^2 < \infty \right\}, \quad s \in \mathbb{R},$$

where $\langle u, Y_m^l \rangle$ is the extension by duality of the $L^2(\mathbb{S})$ -inner product. From this definition, given $u \in H^s(\mathbb{S})$ and $N \in \mathbb{N}$, we can define a finite-dimensional projection of u as

$$\Pi_N u = \sum_{l=0}^N \sum_{m=-l}^l \langle u, Y_m^l \rangle Y_m^l.$$

and using elementary properties we can bound the error of this projection as:

$$\|u - u_N\|_{H^s(\mathbb{S})} \leq (N + 1)^{s-r} \|u\|_{H^r(\mathbb{S})},$$

for any reals s, r such that $s < r$. The space $H_e^s(\mathbb{S})$ (resp. $H_o^s(\mathbb{S})$) is defined as the completion of the even (resp. odd) functions in the x_3 variable in $\mathcal{D}(\mathbb{S})$, with the same norm. For these cases, the norms can be written as

$$\begin{aligned} \|u\|_{H_e^s(\mathbb{S})}^2 &= \sum_{l=0}^{\infty} (l+1)^{2s} \sum_{\substack{m=-l \\ m+l \text{ even}}}^l |\langle u, Y_m^l \rangle|^2, \\ \|u\|_{H_o^s(\mathbb{S})}^2 &= \sum_{l=0}^{\infty} (l+1)^{2s} \sum_{\substack{m=-l \\ m+l \text{ odd}}}^l |\langle u, Y_m^l \rangle|^2. \end{aligned}$$

We will also consider the special function $w_{\mathbb{S}} := \sqrt{1 - x_1^2 - x_2^2}$ defined in \mathbb{S} . In spherical coordinates can be written as $w_{\mathbb{S}} = |\cos \varphi|$.

REMARK 4.2. *As the function $w_{\mathbb{S}}$ do not depend on the x_3 coordinate, it holds that*

$$w_{\mathbb{S}} L_e(u) = L_e(w_{\mathbb{D}} u), \quad w_{\mathbb{S}} L_o(u) = L_o(w_{\mathbb{D}} u),$$

where $w_{\mathbb{D}}(\mathbf{x}) = \sqrt{1 - \|\mathbf{x}\|^2}$, for $\mathbf{x} \in \mathbb{D}$.

Let us introduce two families of auxiliary spaces on \mathbb{D} associated with even functions:

$$\begin{aligned} P_e^s(\mathbb{D}) &:= \{u \in \mathcal{D}'(\mathbb{D}) : L_e(u) \in H_e^s(\mathbb{S})\} \\ Q_e^s(\mathbb{D}) &:= \{u \in \mathcal{D}'(\mathbb{D}) : w_{\mathbb{S}} L_e(u) \in H_e^s(\mathbb{S})\}, \end{aligned}$$

with norms given by:

$$\|u\|_{P_e^s(\mathbb{D})} := \|L_e(u)\|_{H_e^s(\mathbb{S})} = \left(\sum_{l=0}^{\infty} (l+1)^{2s} \sum_{\substack{m=-l \\ m+l \text{ even}}}^l |\langle u, q_m^l \rangle_{\mathbb{D}}|^2 \right)^{\frac{1}{2}},$$

$$\|u\|_{Q_e^s(\mathbb{D})} := \|w_{\mathbb{S}} L_e(u)\|_{H_e^s(\mathbb{S})} = \left(\sum_{l=0}^{\infty} (l+1)^{2s} \sum_{\substack{m=-l \\ m+l \text{ even}}}^l |\langle u, p_m^l \rangle_{\mathbb{D}}|^2 \right)^{\frac{1}{2}}.$$

Odd function spaces $P_o^s(\mathbb{D})$, $Q_o^s(\mathbb{D})$ are defined in a similar fashion. While the connection with standard spaces is not as direct as the definition suggests, the next Lemma will be useful.³

Lemma 4.3. *The following relations between auxiliary and classical spaces on \mathbb{D} holds:*

$$P_e^0(\mathbb{D}) = L_{1/w_{\mathbb{D}}}^2(\mathbb{D}) := \left\{ u : \int_{\mathbb{D}} \frac{u\bar{u}}{w_{\mathbb{D}}} d\mathbf{x} < \infty \right\} \quad (4.3)$$

$$Q_e^{-\frac{1}{4}}(\mathbb{D}) \subset \tilde{H}^{-\frac{1}{2}}(\mathbb{D}) \subset Q_e^{-\frac{1}{2}}(\mathbb{D}) \quad (4.4)$$

$$P_o^{\frac{1}{2}}(\mathbb{D}) \subset \tilde{H}^{\frac{1}{2}}(\mathbb{D}) \subset P_o^{\frac{1}{4}}(\mathbb{D}). \quad (4.5)$$

with continuous inclusions.

Corollary 4.1. *The following inclusions are continuous:*

$$Q_o^{-\frac{1}{4}}(\mathbb{D}) \subset H^{-\frac{1}{2}}(\mathbb{D}) \subset Q_o^{-\frac{1}{2}}(\mathbb{D}) \quad (4.6)$$

$$P_e^{\frac{1}{2}}(\mathbb{D}) \subset H^{\frac{1}{2}}(\mathbb{D}) \subset P_e^{\frac{1}{4}}(\mathbb{D}). \quad (4.7)$$

PROOF. Both results are immediate consequences of the duality relation between classical Sobolev spaces and Lemma 4.3. \square

³The proof is given in Appendix C.1.

By definition of the auxiliary spaces as well the projector Π_N , we can introduce four projectors onto the disk. Namely,

$$\begin{aligned}\Pi_N^{e,p} : \sum_{l=0}^{\infty} u_l p_l^e &\mapsto \sum_{l=0}^{I(N)} u_l p_l^e, & \Pi_N^{o,p} : \sum_{l=0}^{\infty} u_l p_l^o &\mapsto \sum_{l=0}^{I(N)} u_l p_l^o, \\ \Pi_N^{e,q} : \sum_{l=0}^{\infty} u_l q_l^e &\mapsto \sum_{l=0}^{I(N)} u_l q_l^e, & \Pi_N^{o,q} : \sum_{l=0}^{\infty} u_l q_l^o &\mapsto \sum_{l=0}^{I(N)} u_l q_l^o,\end{aligned}$$

where $I(N) = I_e(N, N) = \frac{N(N+1)}{2} + N$. Using the norm definitions on the corresponding spaces, it holds that

$$\|\Pi_N^{e,p} u - u\|_{P_e^s(\mathbb{D})} \leq (N+1)^{s-r} \|u\|_{P_e^r(\mathbb{D})}, \quad (4.8)$$

$$\|\Pi_N^{o,p} u - u\|_{P_o^s(\mathbb{D})} \leq (N+1)^{s-r} \|u\|_{P_o^r(\mathbb{D})}, \quad (4.9)$$

$$\|\Pi_N^{e,q} u - u\|_{Q_e^s(\mathbb{D})} \leq (N+1)^{s-r} \|u\|_{Q_e^r(\mathbb{D})}, \quad (4.10)$$

$$\|\Pi_N^{o,q} u - u\|_{Q_o^s(\mathbb{D})} \leq (N+1)^{s-r} \|u\|_{Q_o^r(\mathbb{D})}, \quad (4.11)$$

for any reals s, r such that $s < r$.

4.3. Boundary Integral Formulation

We now reduce the original problem to the screen.

4.3.1. Boundary Integral Operators

Let us recall the definitions of the single and double layer potentials:

$$(\mathcal{S}_\Gamma[k]\lambda)(\mathbf{x}) := \int_\Gamma G_k(\mathbf{x}, \mathbf{x}') \lambda(\mathbf{x}') d\mathbf{x}', \quad \mathbf{x} \in \mathbb{R}^3 \setminus \bar{\Gamma},$$

$$(\mathcal{D}_\Gamma[k]\nu)(\mathbf{x}) := \int_\Gamma \gamma_{n, \mathbf{x}'} G_k(\mathbf{x}, \mathbf{x}') \nu(\mathbf{x}') d\mathbf{x}', \quad \mathbf{x} \in \mathbb{R}^3 \setminus \bar{\Gamma},$$

respectively, where

$$G_k(\mathbf{x}, \mathbf{x}') = \frac{e^{ik\|\mathbf{x}-\mathbf{x}'\|}}{4\pi\|\mathbf{x}-\mathbf{x}'\|}$$

denotes the Helmholtz fundamental solution and $\gamma_{n,\mathbf{x}'}$ corresponds to the Neumann trace in the specified variable.

Following the classical formulation of Dirichlet (resp. Neumann) problems, we seek for solutions of the form $u(\mathbf{x}) = (\mathcal{S}_\Gamma[k]\lambda)(\mathbf{x})$ (resp. $u(\mathbf{x}) = (\mathcal{D}_\Gamma[k]\nu)(\mathbf{x})$), where λ (resp. ν) is an unknown density defined on Γ . By taking traces, one naturally defines the weakly- and hyper-singular boundary integral operators (BIOs),

$$(V_\Gamma[k]\lambda)(\mathbf{x}) := \gamma_d(\mathcal{S}_\Gamma[k]\lambda)(\mathbf{x}) = \int_\Gamma G_k(\mathbf{x}, \mathbf{x}')\lambda(\mathbf{x}')d\mathbf{x}', \quad x \in \Gamma,$$

$$(W_\Gamma[k]\nu)(\mathbf{x}) := -\gamma_n(\mathcal{D}_\Gamma[k]\nu)(\mathbf{x}) = -\gamma_n \int_\Gamma \gamma_{n,\mathbf{x}'} G_k(\mathbf{x}, \mathbf{x}')\nu(\mathbf{x}')d\mathbf{x}', \quad x \in \Gamma,$$

where first BIO is defined as a Lebesgue integral, while the second one is understood as a principal value (McLean, 2000, Chapter 5).

4.3.2. Boundary Integral Equations

With the above definitions, Problem 4.1 can be reduced to

PROBLEM 4.2 (BIEs). *For $k \geq 0$, find $\lambda, \nu \in \tilde{H}^{-1/2}(\Gamma) \times \tilde{H}^{1/2}(\Gamma)$ such that*

$$V_\Gamma[k]\lambda = g_d, \quad (\text{Dirichlet BIE}), \quad (4.12)$$

$$W_\Gamma[k]\nu = g_n, \quad (\text{Neumann BIE}). \quad (4.13)$$

The equivalence between these BIEs and their corresponding original problems is established in (E. P. Stephan, 1987).

Theorem 4.1 (Theorem 2.7, Lemma 2.8, in (E. P. Stephan, 1987), Theorem 2.1.60 in (Sauter & Schwab, 2011)). *For any $k \geq 0$, $g_d \in H^{\frac{1}{2}}(\Gamma)$ (resp. $g_n \in H^{-\frac{1}{2}}(\Gamma)$), there exists one solution $\lambda \in \tilde{H}^{-\frac{1}{2}}(\Gamma)$ (resp. $\nu \in \tilde{H}^{\frac{1}{2}}(\Gamma)$) for Problem 4.2. Moreover, the solution operators are bounded:*

$$\|\lambda\|_{\tilde{H}^{-\frac{1}{2}}(\Gamma)} \lesssim \|g_d\|_{H^{\frac{1}{2}}(\Gamma)}, \quad \|\nu\|_{\tilde{H}^{\frac{1}{2}}(\Gamma)} \lesssim \|g_n\|_{H^{-\frac{1}{2}}(\Gamma)},$$

with unspecified constants depending on Γ and k .

Theorem 4.2 (Corollary A.4 in (Costabel, Dauge, & Duduchava, 2003)). *Given g_d, g_n smooth functions on Γ , the pulled-back solutions multiplied by the corresponding weight functions, $(\lambda \circ \mathbf{r})w_{\mathbb{D}}$ and $(\nu \circ \mathbf{r})(w_{\mathbb{D}})^{-1}$, are as smooth as $g_d \circ \mathbf{r}$, and $g_n \circ \mathbf{r}$, respectively.*

REMARK 4.3. *The last theorem is far from trivial. In the two-dimensional case –open arcs– solutions are also singular at the arc endpoints, which is proven straightforwardly for any k and arc as a perturbation of the simpler case $k = 0$, $\Gamma = (-1, 1) \times \{0\}$. On the other hand, for screens in three-dimensional space a careful analysis of the BIO symbols is needed (cf. (Costabel et al., 2003) and references therein).*

4.4. Spectral Discretizations

From the definition of auxiliary spaces Lemma 4.2, it is natural to consider a collection of finite-dimensional spaces spanned by elements q_l^e (resp. p_l^o) for the discretization of the Dirichlet (resp. Neumann) BIEs.

For $N \in \mathbb{N}$, we set the following spaces defined over the disk:

$$\mathbb{Q}_e^N(\mathbb{D}) := \text{span}\{q_l^e\}_{l=0}^{I(N)} = \left\{ u : u = \sum_{l=0}^N \sum_{\substack{m=-l \\ m+l \text{ even}}}^l u_m^l q_m^l, u_m^l \in \mathbb{C} \right\} \subset \tilde{H}^{-\frac{1}{2}}(\mathbb{D}),$$

$$\mathbb{P}_o^N(\mathbb{D}) := \text{span}\{p_l^o\}_{l=0}^{I(N)} = \left\{ u : u = \sum_{l=0}^{N+1} \sum_{\substack{m=-l \\ m+l \text{ odd}}}^l u_m^l p_m^l, u_m^l \in \mathbb{C} \right\} \subset \tilde{H}^{\frac{1}{2}}(\mathbb{D}),$$

where again $I(N) = \frac{N(N+1)}{2} + N$. For an arbitrary smooth screen, we define corresponding spaces through pullbacks as follows

$$\mathbb{Q}_e^N(\Gamma) := \left\{ u : u = \frac{(v \circ \mathbf{r}^{-1})\|\mathbf{r}^{-1}\|}{J_{\mathbf{r}} \circ \mathbf{r}^{-1}}, v \in \mathbb{Q}_e^N(\mathbb{D}) \right\} \subset \tilde{H}^{-\frac{1}{2}}(\Gamma),$$

$$\mathbb{P}_o^N(\Gamma) := \left\{ u : u = v \circ \mathbf{r}^{-1}, v \in \mathbb{P}_o^N(\mathbb{D}) \right\} \subset \tilde{H}^{\frac{1}{2}}(\Gamma).$$

where the inclusions can be easily shown. These spaces are spanned by the basis functions:

$$q_n^{e,r} := \frac{(q_n^e \circ \mathbf{r}^{-1})\|\mathbf{r}^{-1}\|}{J_{\mathbf{r}} \circ \mathbf{r}^{-1}}, \quad p_n^{o,r} := p_n^o \circ \mathbf{r}^{-1},$$

respectively, and where $n = 0, \dots, I(N)$.

4.4.1. Discrete Problem

Before we introduce discrete versions of Problem 4.2, we set forth the following notation. Given $N \in \mathbb{N}$, vectors on $\mathbb{C}^{I(N)+1}$ are written in bold symbols and superindex N . Associated to every vector, there are two functions which are denoted with the same symbol (not in bold) and superindex N , and an extra sub-index e if the function is to be understood in $\mathbb{Q}_e^N(\Gamma)$, and o if in $\mathbb{P}_o^N(\Gamma)$. For example, given $\boldsymbol{\lambda}^N \in \mathbb{C}^{I(N)+1}$, one can write

$$\lambda_e^N = \sum_{m=0}^{I(N)} \lambda_m^N q_m^{e,r}, \quad \lambda_o^N = \sum_{m=0}^{I(N)} \lambda_m^N p_m^{o,r}.$$

Given $N \in \mathbb{N}$, the Galerkin discretization of the BIE formulation (4.12) reads as

PROBLEM 4.3. *Seek $\boldsymbol{\lambda}^N \in \mathbb{C}^{I(N)+1}$ (resp. $\boldsymbol{\nu}^N \in \mathbb{C}^{I(N)+1}$) such that*

$$V_\Gamma^N[k] \boldsymbol{\lambda}^N = \mathbf{g}_d^N, \quad (\text{discrete Dirichlet BIE}).$$

$$W_\Gamma^N[k] \boldsymbol{\nu}^N = \mathbf{g}_n^N, \quad (\text{discrete Neumann BIE}),$$

where the respective discretization matrices elements are defined as

$$(V_\Gamma^N[k])_{l,m} = \langle V_\Gamma[k] q_m^{e,r}, q_l^{e,r} \rangle_\Gamma, \quad (W_\Gamma^N[k])_{l,n} = \langle W_\Gamma[k] p_m^{o,r}, p_l^{o,r} \rangle_\Gamma,$$

and the corresponding discrete right-hand sides are, for $l, m = 0, \dots, I(N)$,

$$(g_d^N)_l = \langle g_d, q_l^{e,r} \rangle_\Gamma, \quad (g_n^N)_l = \langle g_n, p_l^{o,r} \rangle_\Gamma.$$

The discrete approximations for λ, ν (solutions of Problem 4.2) are λ_e^N, ν_o^N respectively. From standard Galerkin properties we have the following result:

Lemma 4.4 (Theorem 4.29 in (Sauter & Schwab, 2011)). *There exists $N_0 \in \mathbb{N}_0$ – potentially different for the weakly- and hyper-singular BIEs– such that, for any $N \in \mathbb{N}$ with $N > N_0$, the solutions $\boldsymbol{\lambda}^N$, and $\boldsymbol{\nu}^N$ of Problem 4.3 exist, are unique and also we*

obtain quasi-optimality:

$$\|\lambda - \lambda_e^N\|_{\tilde{H}^{-\frac{1}{2}}(\Gamma)} \lesssim \inf_{v \in \mathbb{Q}_N^e(\Gamma)} \|\lambda - v\|_{\tilde{H}^{-\frac{1}{2}}(\Gamma)}, \quad \|\nu - \nu_o^N\|_{\tilde{H}^{\frac{1}{2}}(\Gamma)} \lesssim \inf_{v \in \mathbb{P}_N^o(\Gamma)} \|\nu - v\|_{\tilde{H}^{\frac{1}{2}}(\Gamma)}.$$

From these last estimates we obtain the rate of convergence.

Theorem 4.3. *Given $g_d, g_n \in \mathcal{D}(\Gamma)$, then for any regularity indices $s_d > -\frac{1}{4}$, $s_n > \frac{1}{2}$, it holds that*

$$\|\lambda - \lambda_e^N\|_{\tilde{H}^{-\frac{1}{2}}(\Gamma)} \lesssim N^{-\frac{1}{4}-s_d} \|\lambda \circ \mathbf{r}\|_{Q_e^{s_d}(\mathbb{D})}, \quad (4.14)$$

$$\|\nu - \nu_o^N\|_{\tilde{H}^{\frac{1}{2}}(\Gamma)} \lesssim N^{\frac{1}{2}-s_n} \|\nu \circ \mathbf{r}\|_{P_o^{s_n}(\mathbb{D})}. \quad (4.15)$$

PROOF. We prove only the Dirichlet case as the Neumann follows similar arguments. Denote by R a smooth non-zero function $R(\mathbf{x}) := \frac{\|\mathbf{x}\|}{J_{\mathbf{r}}(\mathbf{x})}$. By using Lemmas 4.1 and 4.4 one finds that

$$\|\lambda - \lambda_e^N\|_{\tilde{H}^{-\frac{1}{2}}(\Gamma)} \lesssim \inf_{v \in \mathbb{Q}_N^e(\Gamma)} \|\lambda - v\|_{\tilde{H}^{-\frac{1}{2}}(\Gamma)} \lesssim \inf_{v \in \mathbb{Q}_N^e(\mathbb{D})} \|\lambda \circ \mathbf{r} - Rv\|_{\tilde{H}^{-\frac{1}{2}}(\mathbb{D})}.$$

We can use the relation between Sobolev and auxiliary spaces (Lemma 4.3) to obtain

$$\|\lambda - \lambda_e^N\|_{\tilde{H}^{-\frac{1}{2}}(\Gamma)} \lesssim \inf_{v \in \mathbb{Q}_N^e(\mathbb{D})} \|\lambda \circ \mathbf{r} - Rv\|_{Q_e^{-\frac{1}{4}}(\mathbb{D})} \lesssim \inf_{v \in \mathbb{Q}_N^e(\mathbb{D})} \left\| \frac{\lambda}{R} - v \right\|_{Q_e^{-\frac{1}{4}}(\mathbb{D})}.$$

Since R^{-1} is smooth, the results follow by selecting $v = \Pi_N^{e,q} \frac{\lambda}{R}$ and estimation (4.10) with $s = -1/4, r = s_d$. \square

REMARK 4.4. *Notice that the right-hand side in (4.14) is indeed finite for any $s_d > -\frac{1}{4}$, $s_n > \frac{1}{2}$. This follows from the norm definitions as*

$$\|\lambda \circ \mathbf{r}\|_{Q_e^{s_d}(\mathbb{D})} = \|L_e(w_{\mathbb{D}}\lambda \circ \mathbf{r})\|_{H^{s_d}(\mathbb{S})},$$

and by Theorem 4.2, which ensures that $w_{\mathbb{D}}\lambda \circ \mathbf{r}$ is smooth. Thus, implying a smooth lifting to the sphere. Using definitions of the Sobolev spaces (McLean, 2000, Chapter 2), any Sobolev norm is finite. The same is true for the Neumann case.

One concludes from Theorem 4.3 that the spectral method converges *super algebraically*, i.e. faster than any fixed negative power of N .

4.4.2. Matrix Computation

We now describe how matrix entries are computed. We start by detailing the approximation of weakly-singular integrals that appear in the corresponding matrix, namely

$$V_{l,m}[k] = \langle V_\Gamma[k] q_m^{e,r}, q_l^{e,r} \rangle_\Gamma.$$

Then, we briefly discuss how integrals for the hyper-singular BIO are obtained using the same techniques, and also how regular entries are computed. Before we proceed, we recall some notions of numerical quadrature and convergence.

4.4.2.1. Numerical Quadrature

Let $a < b$ two real numbers, and $f : (a, b) \rightarrow \mathbb{C}$. The Gauss-Legendre quadrature rule approximate the integral of f as a weighted sum of point evaluations of f , the approximation is constructed as

$$\int_a^b f(x) dx \approx \sum_{i=1}^{N_q} w_i^L f(x_i^L),$$

where N_q is the order of the quadrature, and $(\{w_i^L\}_{i=1}^{N_q}, \{x_i^L\}_{i=1}^{N_q})$ are the weights and points⁴ of the quadrature respectively. When f is smooth, the quadrature converges with a rate bounded as a function of N_q . In particular, by using the fact that the quadrature rule is constructed to be exact for every polynomial up to some degree and classical bounds for polynomial interpolation (L. Trefethen, 2013, Chap. 7 and 8), one can establish that for f with $(m + 1)$ continuous derivatives⁵:

$$\left| \int_a^b f(x) dx - \sum_{i=1}^{N_q} w_i^L f(x_i^L) \right| \lesssim N_q^{-m}.$$

⁴Notice that the points and weights depend on a, b , but once given for a fixed interval they can be translated using a linear change of variable. Consequently, we omit this dependence in notation.

⁵Better convergence rates can be achieved for Gaussian quadrature rules (Stoer & Bulirsch, 1980, Theorem 3.6.24).

Moreover, if f admits an analytic extension to a Bernstein ellipse of parameter ρ in the complex plane, one can show⁶ that

$$\left| \int_a^b f(x) dx - \sum_{i=1}^{N_q} w_i^L f(x_i^L) \right| \lesssim \rho^{-N_q}.$$

Whenever an integral of a function can be approximated with the same rates as the last two, we say that the approximation is optimal. In particular, Gauss-Legendre quadrature rules are optimal for any smooth function integral. Jacobi quadrature rules are built as an approximation of the following family of integrals:

$$\int_a^b f(x)(x-a)^\alpha(b-x)^\beta dx \approx \sum_{i=1}^{N_q} w_i^{\alpha,\beta} f(x_i^{\alpha,\beta}),$$

where, again, N_q is the quadrature order, $(\{w_i^{\alpha,\beta}\}_{i=1}^{N_q}, \{x_i^{\alpha,\beta}\}_{i=1}^{N_q})$ are the pair of weights and points, and $\alpha, \beta > -1$. This rule is also optimal, i.e. that the rate of convergence is again N_q^{-m} when f has $(m+1)$ continuous derivative and ρ^{-N_q} when f is ρ -analytic.

4.4.2.2. Approximation of weakly-singular integrals

Given a screen Γ para-metrized by a function \mathbf{r} , we consider the computation of integrals of the form:

$$I_{m,l}[k] = \int_{\Gamma} \int_{\Gamma} \frac{\cos(k\|\mathbf{x} - \mathbf{x}'\|)}{4\pi\|\mathbf{x} - \mathbf{x}'\|} q_m^{e,r}(\mathbf{x}') \overline{q_l^{e,r}(\mathbf{x})} d\mathbf{x} d\mathbf{x}'.$$

These integrals are associated with the real part of the weakly-singular BIO. Its imaginary part is regular since the function $\sin(k\|\mathbf{x} - \mathbf{x}'\|)/\|\mathbf{x} - \mathbf{x}'\|$ is smooth. Moreover, the cosine factor is smooth so from here onwards, we assume that $k = 0$ and denote $I_{m,l}[0]$, as $I_{m,l}$. By performing a change of variable, this integral becomes

$$I_{m,l} = \int_{\mathbb{D}} \int_{\mathbb{D}} \frac{1}{4\pi\|\mathbf{r}(\mathbf{x}) - \mathbf{r}(\mathbf{x}')\|} q_m^e(\mathbf{x}') \overline{q_l^e(\mathbf{x})} d\mathbf{x} d\mathbf{x}'.$$

⁶see (L. Trefethen, 2013, Chapter 8)

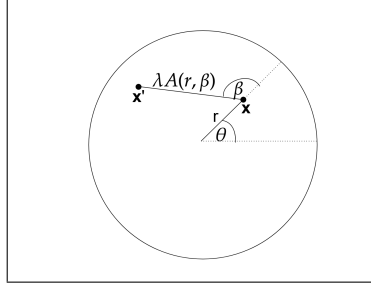


FIGURE 4.1. Polar change of variables performed in (4.16).

The first step is to take care of the kernel singularity, i.e. when $\mathbf{x} = \mathbf{x}'$. To this end, we make the following parametrization:

$$\mathbf{x} = r\mathbf{e}_\theta, \quad \mathbf{x}' = \mathbf{x} + \lambda A(r, \beta)\mathbf{e}_{\theta+\beta}, \quad (4.16)$$

where

$$\mathbf{e}_\theta = (\cos \theta, \sin \theta), \quad A(r, \beta) := \sqrt{1 - r^2 \sin^2 \beta} - r \cos \beta, \quad (4.17)$$

the latter represents the length of the segment whose direction is $\theta + \beta$, and goes from point \mathbf{x} to the boundary of the disk (see Figure 4.4.2.2). The integral can be expressed as

$$I_{m,l} = \int_{-\frac{\pi}{2}}^{\frac{3\pi}{2}} \int_0^1 \int_{-\frac{\pi}{2}}^{\frac{3\pi}{2}} \int_0^1 G_{m,l}(\theta, r, \lambda, \beta) d\lambda d\beta dr d\theta,$$

$$G_{m,l}(\theta, r, \lambda, \beta) := \frac{\lambda A^2(r, \beta)}{4\pi \|\mathbf{r}(\mathbf{x}) - \mathbf{r}(\mathbf{x} + \lambda A(r, \beta)\mathbf{e}_{\theta+\beta})\|} \frac{rp_m^e(\mathbf{x})\overline{p_l^e(\mathbf{x}')}}{\sqrt{1 - r^2} \sqrt{1 - \|\mathbf{x} + \lambda A(r, \beta)\mathbf{e}_{\theta+\beta}\|^2}}.$$

Since \mathbf{r} is smooth, injective and its gradient has full rank, the factor

$$\frac{\lambda A^2(r, \beta)}{4\pi \|\mathbf{r}(\mathbf{x}) - \mathbf{r}(\mathbf{x} + \lambda A(r, \beta)\mathbf{e}_{\theta+\beta})\|},$$

is at least bounded. The term $(1 - r^2)^{-\frac{1}{2}}$ while singular can be tackled with the Jacobi rule. However, this is not enough since $A(r, \beta)$ and $\sqrt{1 - \|\mathbf{x} + \lambda A(r, \beta)\mathbf{e}_{\theta+\beta}\|^2}$ also have singularities that prevent an optimal rate of convergence. The following results characterize the behavior of these functions.

Lemma 4.5. *The function $A : [0, 1] \times [\frac{-\pi}{2}, \frac{3\pi}{2}] \rightarrow [0, 2]$ has the following properties:*

- (i) $A(r, \beta) \geq 0$.
- (ii) *Partial derivatives discontinuities of $A(r, \beta)$ are located at $\{r = 1, \beta = \frac{-\pi}{2}, \frac{\pi}{2}, \frac{3\pi}{2}\}$.*
- (iii) *For $|\beta| \leq \frac{\pi}{2}$, $A(r, \beta) \cos \beta \leq 1 - r$.*

PROOF. The first item is immediate by definition. For the second one, notice that the discontinuities occur when the square-root parts vanish, i.e.

$$(1 - r^2) + r^2 \cos^2 \beta = 0.$$

As a sum of two non negative terms, the singularities occurs when both terms vanish, thus leading to our result directly. The last item is obtained by direct evaluation at extreme points $\beta = \pm \frac{\pi}{2}$ and critical values of β such that $\frac{\partial A(r, \beta) \cos \beta}{\partial \beta} = 0$, or by directly using elementary geometrical proprieties. \square

Lemma 4.6. *Discontinuities of any partial derivative of the term*

$$\sqrt{1 - \|\mathbf{x} + \lambda A(r, \beta) \mathbf{e}_{\theta+\beta}\|^2},$$

occur at $\{\lambda = 1\} \cup \{r = 1, \lambda = 0\} \cup \{r = 1, \beta = \pm \frac{\pi}{2}, \frac{3\pi}{2}\}$.

PROOF. Again, critical points occur only when the term inside the square-root vanishes. This term can be expressed as

$$1 - \|\mathbf{x} + \lambda A(r, \beta) \mathbf{e}_{\theta+\beta}\|^2 = (1 - \lambda) [(1 + \lambda)(1 - r^2) - 2\lambda r \cos(\beta) A(r, \beta)] , \quad (4.18)$$

for which all previously listed points are critical. Hence, we are left to check that no other critical points exist.

First, let us consider the case $\frac{\pi}{2} \leq \beta \leq \frac{3\pi}{2}$ so that $-2\lambda r \cos \beta A(r, \beta) \geq 0$. Thus, the singularities are characterized by $\lambda = 1$ –because of the first factor–, and also the points where

$$(1 + \lambda)(1 - r^2) = 0,$$

$$2\lambda r \cos \beta A(r, \beta) = 0.$$

From this condition and Lemma 4.5 it is easy to see that no further critical points take place. Now, if $|\beta| \leq \frac{\pi}{2}$, by the third item of Lemma 4.5 we have that

$$((1 + \lambda)(1 - r^2) - 2\lambda r \cos \beta A(r, \beta)) \geq (1 + \lambda)(1 - r^2) - 2\lambda r(1 - r),$$

which implies that the singularities can only occur if $\lambda = 1$ –because of the first term–, or $r = 1$, and the result follows. \square

Based on the above considerations, we split the integrals $I_{m,l}$ according to the singularities and critical points as follows. The detailed analysis for the last three types is given in the Appendix C.2.

(a) The first type is

$$I_{m,l}^a := \int_{-\frac{\pi}{2}}^{\frac{3\pi}{2}} \int_0^{\frac{\sqrt{3}}{2}} \int_{-\frac{\pi}{2}}^{\frac{3\pi}{2}} \int_0^1 G_{m,l}(\theta, r, \lambda, \beta) d\lambda d\beta dr d\theta,$$

for which only a singularity of the form $(1 - \lambda)^{-\frac{1}{2}}$ occurs. This can numerically be treated using the corresponding Jacobi rule when integrating in λ and Gauss-Legendre for the integrals in θ, r, β , resulting in an optimal approximation.

(b) The second type is

$$I_{m,l}^b := \int_{-\frac{\pi}{2}}^{\frac{3\pi}{2}} \int_{\frac{\sqrt{3}}{2}}^1 \int_{(-\frac{\pi}{3}, \frac{\pi}{3}) \cup (\frac{2\pi}{3}, \frac{4\pi}{3})} \int_{\frac{1}{2}}^1 G_{m,l}(\theta, r, \lambda, \beta) d\lambda d\beta dr d\theta,$$

which has singularities of the form $(1 - r)^{-\frac{1}{2}}$, and $(1 - \lambda)^{-\frac{1}{2}}$, so we use a Jacobi rule in these two variables and Gauss-Legendre for θ and β .

(c) The third one has critical points occurring as a combination of variables:

$$I_{m,l}^c := \int_{-\frac{\pi}{2}}^{\frac{3\pi}{2}} \int_{\frac{\sqrt{3}}{2}}^1 \int_{(-\frac{\pi}{2}, -\frac{\pi}{3}) \cup (\frac{\pi}{3}, \frac{\pi}{2}) \cup (\frac{\pi}{2}, \frac{2\pi}{3}) \cup (\frac{4\pi}{3}, \frac{3\pi}{2})} \int_0^{\frac{1}{2}} G_{m,l}(\theta, r, \lambda, \beta) d\lambda d\beta dr d\theta, \quad (4.19)$$

Here, critical points lie in $(\lambda, r, \beta) = (0, 1, \beta)$, and $(\lambda, r, \beta) = (\lambda, 1, \beta_0)$, $\beta_0 \in \{\pm \frac{\pi}{2}, \frac{3\pi}{2}\}$. To tackle this, we will use two polar change of variables (see C.2.2).

(d) The fourth one is of the form

$$I_{m,l}^d := \int_{-\frac{\pi}{2}}^{\frac{3\pi}{2}} \int_{\frac{\sqrt{3}}{2}}^1 \int_{(-\frac{\pi}{3}, \frac{\pi}{3}) \cup (\frac{2\pi}{3}, \frac{4\pi}{3})} \int_0^{\frac{1}{2}} G_{m,l}(\theta, r, \lambda, \beta) d\lambda d\beta dr d\theta, \quad (4.20)$$

being slightly simpler than the previous case and only requiring one polar change of variable in λ and r variables.

(e) Finally, the last integral type is given by

$$I_{m,l}^e := \int_{-\frac{\pi}{2}}^{\frac{3\pi}{2}} \int_{\frac{\sqrt{3}}{2}}^1 \int_{(-\frac{\pi}{2}, -\frac{\pi}{3}) \cup (\frac{\pi}{3}, \frac{\pi}{2}) \cup (\frac{\pi}{2}, \frac{2\pi}{3}) \cup (\frac{4\pi}{3}, \frac{3\pi}{2})} \int_{\frac{1}{2}}^1 G_{m,l}(\theta, r, \lambda, \beta) d\lambda d\beta dr d\theta, \quad (4.21)$$

which needs one polar change of variable in $(r, \cos \beta)$ and application of a Jacobi rule for the integral in the λ variable.

4.4.2.3. Approximation of smooth integrals

Smooth integrals can be of two forms:

$$I_{m,l}^f := \int_{\Gamma} \int_{\Gamma} G_{reg}(\mathbf{x}, \mathbf{x}') q_m^{e,r}(\mathbf{x}') \overline{q_l^{e,r}(\mathbf{x})} d\mathbf{x} d\mathbf{x}', \quad I_{m,l}^g := \int_{\Gamma} g(\mathbf{x}) \overline{q_l^{e,r}(\mathbf{x})} d\mathbf{x},$$

where G_{reg} , and g are smooth functions. The former comes from the imaginary part of the fundamental solution, whereas the latter from testing the right-hand side. We focus only in the second case, as the first one is just a tensorisation. By using the screen parametrization, we obtain

$$I_{m,l}^g = \int_{-\frac{\pi}{2}}^{\frac{3\pi}{2}} \int_0^1 g(\mathbf{r}(\mathbf{x})) \frac{\overline{p_l^e(\mathbf{x})}}{\sqrt{1-r^2}} r dr d\theta,$$

where $\mathbf{x} = r\mathbf{e}_\theta$. Using the Gauss-Legendre rule when integrating in θ and Jacobi for r we obtain optimal rates of convergence.

4.4.2.4. Approximation of hyper-singular Integrals

As it was pointed out, the discretization basis for the hyper-singular operator BIO ($p_m^{o,r}$) vanishes on the boundary $\partial\Gamma$, and consequently, the entries of the corresponding matrix can be computed using the integration-by-parts formula (Sauter & Schwab, 2011, Corollary

3.3.24):

$$\begin{aligned} \langle W_\Gamma[k]p_m^{o,r}, p_l^{o,r} \rangle &= \int_\Gamma \int_\Gamma \frac{e^{ik\|\mathbf{x}-\mathbf{x}'\|}}{4\pi\|\mathbf{x}-\mathbf{x}'\|} \text{curl}_\Gamma p_m^{o,r}(\mathbf{x}') \cdot \overline{\text{curl}_\Gamma p_l^{o,r}(\mathbf{x})} d\mathbf{x}' d\mathbf{x} \\ &\quad - k^2 \int_\Gamma \int_\Gamma \frac{e^{ik\|\mathbf{x}-\mathbf{x}'\|}}{4\pi\|\mathbf{x}-\mathbf{x}'\|} \hat{\mathbf{n}}(\mathbf{x}) \cdot \hat{\mathbf{n}}(\mathbf{x}') p_m^{o,r}(\mathbf{x}') \overline{p_l^{o,r}(\mathbf{x})} d\mathbf{x}' d\mathbf{x}, \end{aligned} \quad (4.22)$$

where $\hat{\mathbf{n}}$ denote the unitary normal vector to Γ (with a fixed orientation) and $\text{curl}_\Gamma f = \hat{\mathbf{n}} \times \nabla f$, whenever f can be extended to a neighborhood of Γ . We start by considering the second integral on the right-hand side, we reduce the computations to \mathbb{D} and obtain

$$k^2 \int_{\mathbb{D}} \int_{\mathbb{D}} \frac{e^{ik\|\mathbf{r}(\mathbf{x})-\mathbf{r}(\mathbf{x}')\|}}{4\pi\|\mathbf{r}(\mathbf{x})-\mathbf{r}(\mathbf{x}')\|} \hat{\mathbf{n}}(\mathbf{r}(\mathbf{x})) \cdot \hat{\mathbf{n}}(\mathbf{r}(\mathbf{x}')) p_m^o(\mathbf{x}') \overline{p_l^o(\mathbf{x})} \frac{J_{\mathbf{r}}(\mathbf{x})}{\|\mathbf{x}\|} \frac{J_{\mathbf{r}}(\mathbf{x}')}{\|\mathbf{x}'\|} d\mathbf{x}' d\mathbf{x},$$

Since functions p_l^o can be characterized as the product between a smooth function and the weight function $w_{\mathbb{D}}$ the same change of variables used for the weakly-singular case works for this integral⁷. For the first integral in the right-hand side in (4.22), we compute the surface curl operators. Using the parametrization of Γ , the explicit expression

$$(\text{curl}_\Gamma f)(\mathbf{r}) = \frac{1}{J_{\mathbf{r}}} (\partial_{x_2} \mathbf{r} \partial_{x_1} (f \circ \mathbf{r}) - \partial_{x_1} \mathbf{r} \partial_{x_2} (f \circ \mathbf{r}))$$

arises, where $\partial_{x_1}, \partial_{x_2}$ denote the partial derivatives with respect to the arguments of the parametrization \mathbf{r} . In our implementation, \mathbf{r} is given in polar coordinates and so x_1 and x_2 are the radial and angular variables, respectively. The function $f \circ \mathbf{r}$ corresponds to p_m^o for some m , and thus, we require their partial derivatives. Moreover, using the two-indices representation we can write $p_m^o = p_m^\ell$, for a pair of integers ℓ, m such that $m + \ell$ is odd. The angular derivative is given by

$$\partial_\theta p_m^\ell = \partial_\theta \left(C_m^\ell P_{|m|}^\ell(\sqrt{1-r^2}) e^{im\theta} \right) = im C_m^\ell P_{|m|}^\ell(\sqrt{1-r^2}) e^{im\theta} = im p_m^\ell,$$

where the first equality is the explicit definition of the projected basis (4.2). We can express this in terms of the basis used for the discretization of the weakly-singular BIO as we have

⁷It is necessary to change the parameters of the Jacobi quadrature rule, as now the singularity is of the form $\sqrt{1-x^2}$, instead of $1/\sqrt{1-x^2}$.

the following recursive relation (see (Arfken et al., 2013, 15.87)):

$$P_m^\ell(x) = \frac{-\sqrt{1-x^2}}{2mx} (P_{m+1}^\ell(x) + (\ell+m)(\ell-m+1)P_{m-1}^\ell(x)), \quad m \neq 0$$

so we conclude that

$$\partial_\theta p_m^\ell = \frac{-ir}{2} (a_m^\ell q_{m+1}^\ell + b_m^\ell q_{m-1}^\ell), \quad (4.23)$$

where

$$a_m^\ell := e^{-i\theta} \begin{cases} \sqrt{(\ell-|m|)(\ell+|m|+1)}, & m \geq 0 \\ -\sqrt{(\ell+|m|)(\ell-|m|+1)}, & m < 0 \end{cases} \quad (4.24)$$

$$b_m^\ell := e^{i\theta} \begin{cases} \sqrt{(\ell+|m|)(\ell-|m|+1)}, & m \geq 0 \\ -\sqrt{(\ell-|m|)(\ell+|m|+1)}, & m < 0 \end{cases} \quad (4.25)$$

Notice that, for $m = 0$, the derivative is zero and this is also true for expression (4.23). Since $m + \ell$ is odd, we have that q_{m+1}^ℓ and q_{m-1}^ℓ are even functions. For the derivative with respect to r , we need the derivative of the associated Legendre functions, given by the following recursion (see (Arfken et al., 2013, 15.91)):

$$\frac{dP_m^\ell(x)}{dx} = \frac{1}{2\sqrt{1-x^2}} (-P_{m+1}^\ell(x) + (\ell+m)(\ell-m+1)P_{m-1}^\ell(x)),$$

Hence, we obtain

$$\partial_r p_m^\ell = \frac{1}{2} (a_m^\ell q_{m+1}^\ell - b_m^\ell q_{m-1}^\ell),$$

where a_m^ℓ, b_m^ℓ are defined as in (4.24). Again, we have expressed the derivative in terms of the basis of the weakly-singular case. We conclude that for the computation of the hyper-singular BIO only minor modifications respect to the weakly-singular one are needed. These modifications are the change of the parameter of the respective Jacobi rule, the inclusion of the product of the normal vectors, and the extra smooth factors $e^{\pm i\theta}, \partial_{x_j} \mathbf{r} \cdot \partial_{x'_j} \mathbf{r}$ ($j, j' = 1, 2$) that have to be included in the kernel function. We have omitted the details of smooth integrals associated with the hyper-singular BIO as they do not present any extra challenge.

4.4.3. Numerical Implementation

Throughout this section we denote by $\widehat{N} = I(N) + 1 = N + \frac{N(N+1)}{2} + 1$, the number of degrees of freedom when using the spaces $\mathbb{Q}_e^N(\Gamma)$, $\mathbb{P}_o^N(\Gamma)$ for the discretization of the underlying integral equations. Every integral needed to assembly the matrix discretization of the weakly-singular BIO $(I^a, I^b, I^c, I^d, I^e, I^f)$ is a four-dimensional integral. The total number of these integral computations can be reduced using the matrix symmetries⁸. Consequently, only $\frac{\widehat{N}(\widehat{N}+1)}{2}$ combinations are needed instead of \widehat{N}^2 . Furthermore, since $p_{-m}^l = (-1)^m \overline{p_m^l}$ the actual number of interactions needed to compute the weakly-singular BIO is $\frac{1}{4} \left(\widehat{N} + \frac{N+2}{2} \right) \left(\frac{3}{2} \widehat{N} - \frac{N-2}{4} \right)$, assuming N even⁹.

A four-dimensional integral computed by tensorized 1D-quadrature rules, with parameters $N_q^1, N_q^2, N_q^3, N_q^4$, has a computational cost of $\mathcal{O}(\prod_{j=1}^4 N_q^j)$ operations and evaluations. To compute integrals arising from the weakly singular BIO $I^\alpha, \alpha \in \{b, c, d, e\}$, we denote by N_q^θ the number of points for the θ variable, and N_q^α the number of points for the other three variables depending on α . For $\alpha = a$, we use N_q^θ for variables θ and β , and N_q^a for the rest. For the hyper-singular case, same rules apply.

For the smooth integrals $\alpha \in \{f, g\}$ we could use N_q^θ for the θ and θ' variables, and $N_q^\alpha, \alpha \in \{f, g\}$ for \mathbf{r} , and \mathbf{r}' . However, in practice it is better to reformulate the integrals onto the sphere, where the basis correspond to spherical harmonics, and approximate the integrals using the spherical harmonics transforms. In particular we use the implementation detailed in (Schaeffer, 2013).

4.5. Full Discretization Error Analysis

The rate of convergence of the spectral Galerkin discretization method was already established in Theorem 4.3. Yet, this does not illustrate the performance of the fully discrete method as extra error terms appears as consequence of the quadrature approximation of

⁸The matrix associated with the real part of the fundamental solution $(I^\alpha, \alpha \in \{a, b, c, d, e\})$ is Hermitian, while the imaginary one (I^f) is anti-Hermitian.

⁹If N is odd, the computational cost is $\frac{1}{4} \left(\widehat{N} + \frac{N+1}{2} \right) \left(\frac{3}{2} \widehat{N} - \frac{N-3}{4} \right)$.

integral terms. Thus, we first measure the perturbation in error convergence rates due to quadrature error.

4.5.1. Quadrature Error

For the sake of brevity, we denote Q^α the quadrature approximation of I^α , $\alpha \in \{a, b, c, d, e, f, g\}$, defined in Section 4.4.2.2. Since we assume that the screen is parametrized by a ρ -analytic function, and the approximation is optimal, we have that

$$|I^\alpha - Q^\alpha| \lesssim \rho^{-N_q^\theta} + \rho^{-N_q^\alpha}. \quad (4.26)$$

While this bound is precise in terms of how the quadrature error decreases with increasing number of quadrature points, the unspecified constant depends on the trial and test basis indices. Hence, since the rate of convergence depends on the number of trial functions, we need a more detailed quadrature error analysis considering the exact index of the trial and test basis. For this, let us consider the canonical integral

$$I_m^l = \int_0^1 \int_{-\frac{\pi}{2}}^{\frac{3\pi}{2}} g(\mathbf{x}) p_m^l(\mathbf{x}) r d\theta dr,$$

where $\mathbf{x} = r\mathbf{e}_\theta$, g is ρ -analytic in (r, θ) and $l + m$ is even. It is enough to consider this case, as all integrals discussed in Section 4.4.2.2 can be reduced to this form by means of analytic change of variables to tensorization of integral. Denote by Q_m^l the quadrature approximation of I_m^l obtained by a Gauss-Legendre rule in both variables, with N_q^θ points in the θ variable, and N_q points in the r variable.

We denote by $\mathcal{E}_\rho[a, b]$ the region enclosed by the Bernstein ellipse in the complex plane with foci in a, b and parameter ρ . Now, we recall the classical error bound for analytic integrands.

Theorem 4.4 (Theorem 5.3.13 in (Sauter & Schwab, 2011)). *If $m + l$ is even, for g ρ -analytic in $[0, 1]$ in the radial variable and ρ -analytic in $[-\frac{\pi}{2}, \frac{3\pi}{2}]$ for the angular one, it*

holds that

$$\begin{aligned} |I_m^l - Q_m^l| &\lesssim (2\rho)^{-2N_q^\theta} \max_{r \in [0,1]} \max_{z \in \partial \mathcal{E}_\rho[\frac{-\pi}{2}, \frac{3\pi}{2}]} |g(r, z) p_m^l(r, z)| \\ &\quad + (2\rho)^{-2N_q} \max_{\theta \in [\frac{-\pi}{2}, \frac{3\pi}{2}]} \max_{z \in \partial \mathcal{E}_\rho[0,1]} |g(z, \theta) p_m^l(z, \theta)| \end{aligned}$$

where the unspecified constant does not depend on the integrand of I_m^l .

Since g is assumed to be known, we can further simplify the error bound as

$$\begin{aligned} |I_m^l - Q_m^l| &\lesssim (2\rho)^{-2N_q^\theta} \max_{r \in [0,1]} \max_{z \in \partial \mathcal{E}_\rho[\frac{-\pi}{2}, \frac{3\pi}{2}]} |p_m^l(r, z)| \\ &\quad + (2\rho)^{-2N_q} \max_{\theta \in [\frac{-\pi}{2}, \frac{3\pi}{2}]} \max_{z \in \partial \mathcal{E}_\rho[0,1]} |p_m^l(z, \theta)|, \end{aligned}$$

with a constant that now depends on g .

Corollary 4.2. *Under hypothesis of Theorem 4.4, for the integral*

$$\tilde{I}_m^l := \int_0^1 \int_{-\frac{\pi}{2}}^{\frac{3\pi}{2}} g(\mathbf{x}) q_m^l(\mathbf{x}) r d\theta dr,$$

it holds that

$$\begin{aligned} |\tilde{I}_m^l - \tilde{Q}_m^l| &\lesssim (2\rho)^{-2N_q^\theta} \max_{r \in [0,1]} \max_{z \in \partial \mathcal{E}_\rho[\frac{-\pi}{2}, \frac{3\pi}{2}]} |p_m^l(r, z)| \\ &\quad + (2\rho)^{-2N_q} \max_{\theta \in [\frac{-\pi}{2}, \frac{3\pi}{2}]} \max_{z \in \partial \mathcal{E}_\rho[0,1]} |p_m^l(z, \theta)|, \end{aligned}$$

where \tilde{Q}_m^l denotes the quadrature approximation using a Gauss-Legendre rule with N_q^θ points in θ , and a Jacobi rule with N_q points in the r variable.

We now proceed to estimate maxima of analytic extensions for the functions p_m^l . Remember that the explicit definition (4.2) (see Section 4.2.3):

$$p_m^l(r, \theta) = C_m^l P_{|m|}^l(\sqrt{1-r^2}) e^{im\theta},$$

where $|C_m^l| = \sqrt{\frac{(2l+1)(l-|m|)!}{2\pi(l+|m|)!}}$, with $P_{|m|}^l(\sqrt{1-r^2})$ smooth in the r variable. By using (Lohöfer, 1991, Theorem 3), one deduces that

$$\max_{r \in [0,1]} \max_{z \in \partial \mathcal{E}_\rho \left[\frac{-\pi}{2}, \frac{3\pi}{2} \right]} |p_m^l(r, z)| \lesssim \sqrt{2l+1} e^{|m|\frac{\pi}{2}(\rho-\rho^{-1})} \lesssim \sqrt{2l+1} e^{l\pi\rho},$$

where the last inequality follows for $|m| \leq l$ and $\rho > 1$. On the other hand, the second term can be bounded as

$$\max_{\theta \in \left[\frac{-\pi}{2}, \frac{3\pi}{2} \right]} \max_{z \in \partial \mathcal{E}_\rho [0,1]} |p_m^l(z, \theta)| \leq |C_m^l| \max_{z \in \partial \mathcal{E}_\rho [0,1]} |P_{|m|}^l(\sqrt{1-z^2})|.$$

We can use the Rodríguez formula to express the associated Legendre function in terms of Legendre polynomials:

$$|P_{|m|}^l(\sqrt{1-z^2})| = |z^m| \left| \left(\frac{d^m}{dx^m} P^l(x) \right) \Big|_{x=\sqrt{1-z^2}} \right|,$$

where P^l denotes the l th Legendre polynomial. Obviously, $|z| < \frac{\rho+\rho^{-1}}{2}$, for every $z \in \partial \mathcal{E}_\rho [0, 1]$. Moreover,

$$\max_{z \in \partial \mathcal{E}_\rho [0,1]} \left| \left(\frac{d^m}{dx^m} P^l(x) \right) \Big|_{x=\sqrt{1-z^2}} \right| = \max_{z \in A_\rho} \left| \left(\frac{d^m}{dx^m} P^l(x) \right) \Big|_{x=z} \right|,$$

where A_ρ is the image of $\partial \mathcal{E}_\rho [0, 1]$ under the transformation $(1-x^2)^{\frac{1}{2}}$, where the square root has to be understood as the pre-image of the square function. Since P^l are polynomials and using the maximum modulus principle, there exists $\hat{\rho} > 1$ such that

$$\max_{z \in A_\rho} \left| \left(\frac{d^m}{dx^m} P^l(x) \right) \Big|_{x=z} \right| \leq \max_{z \in \partial \mathcal{E}_{\hat{\rho}} [-1,1]} \left| \left(\frac{d^m}{dx^m} P^l(x) \right) \Big|_{x=z} \right|.$$

Furthermore, using the Cauchy integral formula we have that

$$\frac{d^m}{dz^m} P^l(z) = \frac{m!}{2i\pi} \int_{\partial \mathcal{E}_{\hat{\rho}} [-1,1]} \frac{P^l(x)}{(z-x)^{m+1}} dx, \quad \forall z \in \partial \mathcal{E}_{\hat{\rho}} [-1,1], c > 1.$$

Hence, by using (Wang & Zhang, 2018)[Theorem 4.1] we have

$$\max_{z \in \partial \mathcal{E}_{\hat{\rho}}[-1, 1]} \left| \left(\frac{d^m}{dx^m} P^l(x) \right) \Big|_{x=z} \right| \leq \frac{m!}{2\pi} L(\partial \mathcal{E}_{c\hat{\rho}}[-1, 1]) P^l \left(\frac{c\hat{\rho} + (c\hat{\rho})^{-1}}{2} \right) \max_{x \in \partial \mathcal{E}_{c\hat{\rho}}[-1, 1]} \frac{1}{|z - x|^{m+1}}, \quad c > 1$$

where $L(\partial \mathcal{E}_{c\hat{\rho}}[-1, 1])$ is the length of the corresponding ellipse, and as such, it can be estimated as $L(\partial \mathcal{E}_{c\hat{\rho}}[-1, 1]) \lesssim (c\hat{\rho} + (c\hat{\rho})^{-1})$. Also, notice that the minimum distance between $\partial \mathcal{E}_{c\hat{\rho}}[-1, 1]$ and $\partial \mathcal{E}_{\hat{\rho}}[-1, 1]$ is larger¹⁰ than $\frac{1}{2}(c-1) \left(\rho - \frac{1}{c\rho} \right)$. Thus, one has

$$\begin{aligned} \max_{z \in \partial \mathcal{E}_{\hat{\rho}}[-1, 1]} \left| \left(\frac{d^m}{dx^m} P^l(x) \right) \Big|_{x=z} \right| &\lesssim \\ m!(c\hat{\rho} + (c\hat{\rho})^{-1}) \left(\frac{2}{(c-1)(\hat{\rho} - (c\hat{\rho})^{-1})} \right)^{m+1} P^l \left(\frac{c\hat{\rho} + (c\hat{\rho})^{-1}}{2} \right) &\lesssim \\ m! \left(\frac{2}{(c-1)(\hat{\rho} - (c\hat{\rho})^{-1})} \right)^{m+1} (c\hat{\rho} + (c\hat{\rho})^{-1})^{l+1}, \end{aligned}$$

wherein the last inequality follows for l is large as the polynomial is dominated by the monomial of greatest degree. Using some basic bound, selecting $c < \rho$ and also that l is large enough we can write the previous equation as

$$\max_{z \in \partial \mathcal{E}_{\hat{\rho}}[-1, 1]} \left| \left(\frac{d^m}{dx^m} P^l(x) \right) \Big|_{x=z} \right| \lesssim m! c^l \left(\frac{2}{c-1} \right)^{m+1} \hat{\rho}^{l-m},$$

Finally we redefine $\hat{\rho}$, (based in the last expression) such that,

$$\max_{\theta \in [-\frac{\pi}{2}, \frac{3\pi}{2}]} \max_{z \in \partial \mathcal{E}_{\rho}[0, 1]} |p_m^l(z, \theta)| \lesssim |C_{|m|}^l| m! \hat{\rho}^l \lesssim \sqrt{2l+1} \hat{\rho}^l,$$

and the quadrature error is then bounded as

$$|I_m^l - Q_m^l| \lesssim \sqrt{2l+1} \left[(2\rho)^{-2N_q^\theta} e^{\pi l \rho} + (2\rho)^{-2N_q} \hat{\rho}^l \right].$$

This bound be further simplified to

$$|I_m^l - Q_m^l| \lesssim \sqrt{2l+1} \left[(2\rho)^{-2N_q^\theta} + (2\rho)^{-2N_q} \right] \hat{\rho}^l$$

¹⁰This can be shown using elementary geometrical computations.

where $\tilde{\rho} > 1$. We can summarize quadrature error bound in the following result:

Lemma 4.7. *There is $N_0 \in \mathbb{N}$ such that given integers m, l , $|m| < l$ and $l > N_0$, and $g : [0, 1] \times [-\frac{\pi}{2}, \frac{3\pi}{2}] \rightarrow \mathbb{C}$ ρ -analytic in both variables. For the integral*

$$I_m^l := \int_0^1 \int_{-\frac{\pi}{2}}^{\frac{3\pi}{2}} g(\mathbf{x}) p_m^l(\mathbf{x}) r d\theta dr,$$

we have the error bound

$$|I_m^l - Q_m^l| \lesssim \sqrt{2l+1} \left((2\rho)^{-2N_q^\theta} + (2\rho)^{-2N_q} \right) \tilde{\rho}^l$$

where Q_m^l denotes the approximation by Gauss-Legendre of order N_q, N_q^θ , for both variables accordingly, $\tilde{\rho} > 1$, and the unspecified constant does not depend on l, m .

Corollary 4.3. *Under the hypothesis and notations of Lemma 4.7, given another pair of integers l', m' such that $|m'| < l'$ and $l' > N_0$, and $G(\mathbf{x}, \mathbf{x}') : ([0, 1] \times [-\frac{\pi}{2}, \frac{3\pi}{2}])^2 \rightarrow \mathbb{C}$, for the integral*

$$I_{m,m'}^{l,l'} := \int_0^1 \int_{-\frac{\pi}{2}}^{\frac{3\pi}{2}} \int_0^1 \int_{-\frac{\pi}{2}}^{\frac{3\pi}{2}} G(\mathbf{x}, \mathbf{x}') p_m^l(\mathbf{x}) p_{m'}^{l'}(\mathbf{x}') r r' d\theta dr d\theta' dr',$$

it holds that

$$|I_{m,m'}^{l,l'} - Q_{m,m'}^{l,l'}| \lesssim \sqrt{(2l+1)(2l'+1)} \left((2\rho)^{-2N_q^\theta} + (2\rho)^{-2N_q} \right) \tilde{\rho}^l \tilde{\rho}^{l'}$$

where $Q_{m,m'}^{l,l'}$ denotes the Gauss-Legendre quadrature of orders N_q in r, r' and N_q^θ for θ, θ' , $\tilde{\rho} > 1$ and $\tilde{\rho}' > 1$, and the unspecified constant does not depend of l, m, l', m' .

4.5.2. Fully Discrete Error Analysis:

Recall Problem 4.3, where the unknowns are vectors of dimension $I(N) = \frac{N(N+1)}{2} + N$. Let us now consider the same problem where the corresponding matrices and right-hand sides are approximated with the quadrature method detailed in Section 4.4.2.

PROBLEM 4.4. Find $\lambda^{N,q}, \nu^{N,q} \in \mathbb{C}^{I(N)+1}$ such that

$$V^{N,q}[k] \lambda^{N,q} = \mathbf{g}_d^{N,q}, \quad (\text{Fully discrete Dirichlet BIE}), \quad (4.27)$$

$$W^{N,q}[k] \nu^{N,q} = \mathbf{g}_n^{N,q}, \quad (\text{Fully discrete Neumann BIE}), \quad (4.28)$$

where $V^{N,q}[k]$ (resp. $W^{N,q}[k]$, $\mathbf{g}_d^{N,q}$, $\mathbf{g}_n^{N,q}$) is the quadrature approximation to $V^N[k]$ (resp. $W^N[k]$, \mathbf{g}_d^N , \mathbf{g}_n^N) constructed as described in Section 4.4.2.

The approximations obtained from the fully discrete problems are written

$$\lambda_e^{N,q} = \sum_{m=0}^{I(N)} \lambda_m^{N,q} q_m^{e,r}, \quad \nu_o^{N,q} = \sum_{m=0}^{I(N)} \nu_m^{N,q} p_m^{o,r}.$$

We refer to Problem 4.4 as fully discrete problems. For their analysis, we detail the Dirichlet case as the Neumann case follows similar ideas. Results for both cases are reported at the end of the section.

We first estimate the quadrature error between matrices $V^N[k] - V^{N,q}[k]$. Recall the notation introduced at beginning of Section 4.4.1. For simplicity, the number of quadrature points is determined by only two variables N_q^θ and N_q . Following the notation in Section 4.4.3, this corresponds to the simpler case $N_q^\alpha = N_q$ for every $\alpha \in \{a, b, c, d, e, f\}$. For different values of N_q^α , the results are essentially the similar but we forgo this analysis for the sake of brevity.

Lemma 4.8. *There is $N_0 \in \mathbb{N}$, such that for $N > N_0$, given vectors $\mu^N, \psi^N \in \mathbb{C}^{I(N)+1}$, we have that*

$$\begin{aligned} |\psi^N \cdot (V^N[k] - V^{N,q}[k]) \mu^N| &\lesssim \tilde{\rho}^{2N} N^4 \left[(2\rho)^{-2N_q} + (2\rho)^{-2N_q^\theta} \right] \\ &\quad \times \|\mu_e^N\|_{\tilde{H}^{-\frac{1}{2}}(\Gamma)} \|\psi_e^N\|_{\tilde{H}^{-\frac{1}{2}}(\Gamma)}, \end{aligned}$$

where, as before, $\rho > 1, \tilde{\rho} > 1$.

PROOF. Expanding matrix products yields

$$\left| \boldsymbol{\psi}^N \cdot (V^N[k] - V^{N,q}[k]) \boldsymbol{\mu}^N \right| = \left| \sum_{l'=0}^N \sum_{\substack{m'=-l' \\ m'+l' \text{ even}}}^{l'} \overline{\psi_{I_e(l',m')}^N} \sum_{l=0}^N \sum_{\substack{m=-l \\ m+l \text{ even}}}^l (V^N[k] - V^{N,q}[k])_{I_e(l',m'), I_e(l,m)} \mu_{I_e(l,m)}^N \right|,$$

where the index $I_e(l, m) = \frac{l(l+1)+(l+m)}{2}$ was defined in Section 4.2.3. Now, $V^N[k]$ (see Section 4.4.1) is a matrix whose entries can be written as the sum of integrals $I^a, I^b, I^c, I^d, I^e, I^f$, and $V^{N,q}[k]$ is the sum corresponding to quadratures approximations $Q^a, Q^b, Q^c, Q^d, Q^e, Q^f$ as described in Section 4.4.2.2. By construction, we can use¹¹ Corollary 4.3 and obtain

$$\left| \boldsymbol{\psi}^N \cdot (V^N[k] - V^{N,q}[k]) \boldsymbol{\mu}^N \right| \lesssim \left[(2\rho)^{-2N_q^\theta} + (2\rho)^{-2N_q} \right] \times \left| \sum_{l'=0}^N \sum_{\substack{m'=-l' \\ m'+l' \text{ even}}}^{l'} \sum_{l=0}^N \sum_{\substack{m=-l \\ m+l \text{ even}}}^l \sqrt{(2l+1)(2l'+1)} \left(\tilde{\rho}^{l'} \tilde{\rho}^l \right) \overline{\psi_{I_e(l',m')}^N} \mu_{I_e(l,m)}^N \right|.$$

Redefining $\tilde{\rho} := \max\{\tilde{\rho}', \tilde{\rho}\}$ leads to

$$\left| \boldsymbol{\psi}^N \cdot (V^N[k] - V^{N,q}[k]) \boldsymbol{\mu}^N \right| \lesssim \tilde{\rho}^{2N} \left[(2\rho)^{-2N_q^\theta} + (2\rho)^{-2N_q} \right] \times \left| \sum_{l'=0}^N \sum_{\substack{m'=-l' \\ m'+l' \text{ even}}}^{l'} \sum_{l=0}^N \sum_{\substack{m=-l \\ m+l \text{ even}}}^l \sqrt{(2l+1)(2l'+1)} \psi_{I_e(l',m')}^N \mu_{I_e(l,m)}^N \right|.$$

Applying the Cauchy-Schwartz inequality one obtains

$$\left| \boldsymbol{\psi}^N \cdot (V^N[k] - V^{N,q}[k]) \boldsymbol{\mu}^N \right| \lesssim \tilde{\rho}^{2N} \left[(2\rho)^{-2N_q^\theta} + (2\rho)^{-2N_q} \right] \times N^4 \left(\sum_{l'=0}^N \sum_{\substack{m'=-l' \\ m'+l' \text{ even}}}^{l'} \frac{(\psi_{I_e(l',m')}^N)^2}{l'+1} \right)^{\frac{1}{2}} \left(\sum_{l=0}^N \sum_{\substack{m=-l \\ m+l \text{ even}}}^l \frac{(\mu_{I_e(l,m)}^N)^2}{l+1} \right)^{\frac{1}{2}},$$

¹¹Each of the integrals $I^\alpha, \alpha \in \{a, b, c, d, e, f\}$ have different integration domain but they could be fixed using smooth window functions that extend the integrands to the required domain to apply the Corollary directly.

and by the auxiliary spaces norms definitions, it holds that

$$|\boldsymbol{\psi}^N \cdot (V^N[k] - V^{N,q}[k]) \boldsymbol{\mu}^N| \lesssim \tilde{\rho}^{2N} \left[(2\rho)^{-2N_q^\theta} + (2\rho)^{-2N_q} \right] \\ \times N^4 \|\boldsymbol{\psi}^N \circ \mathbf{r}\|_{Q_e^{-\frac{1}{2}}(\mathbb{D})} \|\boldsymbol{\mu}^N \circ \mathbf{r}\|_{Q_e^{-\frac{1}{2}}(\mathbb{D})}.$$

The results follows directly from Lemmas 4.3 and 4.1. \square

We notice that for any fixed value of N the error term

$$\tilde{\rho}^{2N} \left[(2\rho)^{-2N_q^\theta} + (2\rho)^{-2N_q} \right] N^4$$

goes to zero as the quadrature order increases. Thus, we can use the standard Strang's Lemma to bound the fully discrete error.

Theorem 4.5 (Theorem 4.2.11 in (Sauter & Schwab, 2011)). *There exists $N_0 > 0$ such that for every $N > N_0$, there is a $N_{q,0}$ that depends on N such that, if N_q^θ, N_q are both greater than $N_{q,0}$, the fully discrete Dirichlet problem 4.4 has a unique solution, and the following error estimate follows for $s > -\frac{1}{4}$:*

$$\|\lambda - \lambda_e^{N,q}\|_{\tilde{H}^{-\frac{1}{2}}(\Gamma)} \lesssim N^{-\frac{1}{4}-s} \|\lambda \circ \mathbf{r}\|_{Q_e^s(\mathbb{D})} \\ + \tilde{\rho}^{2N} \left[(2\rho)^{-2N_q^\theta} + (2\rho)^{-2N_q} \right] N^4 \|\lambda\|_{\tilde{H}^{-\frac{1}{2}}(\Gamma)} \quad (4.29) \\ + \tilde{\rho}^N \left[(2\rho)^{-2N_q^\theta} + (2\rho)^{-2N_q} \right] N^2,$$

where λ denotes the continuous solution of the Dirichlet BIE (4.12).

PROOF. Existence and uniqueness are obtained following (Sauter & Schwab, 2011, Theorem 4.2.11). Moreover from the same reference, it holds that

$$\|\lambda - \lambda_e^{N,q}\|_{\tilde{H}^{-\frac{1}{2}}(\Gamma)} \lesssim \inf_{v^N \in \mathbb{Q}_N^e(\Gamma)} \left(\|\lambda - v^N\|_{\tilde{H}^{-\frac{1}{2}}(\Gamma)} + c(N_q, N) \|v^N\|_{\tilde{H}^{-\frac{1}{2}}(\Gamma)} \right) \\ + \sup_{v^N \in \mathbb{Q}_N^e(\Gamma)} \frac{\boldsymbol{v}^N \cdot (\mathbf{g}_d^N - \mathbf{g}_d^{N,q})}{\|v^N\|_{\tilde{H}^{-\frac{1}{2}}(\Gamma)}},$$

where $c(N_q, N) := \tilde{\rho}^{2N} \left[(2\rho)^{-2N_q^\theta} + (2\rho)^{-2N_q} \right] N^4$. The second term on the right-hand side can be estimated following the same ideas of Lemma 4.8, and we obtain:

$$\sup_{v^N \in \mathbb{Q}_N^e(\Gamma)} \frac{\mathbf{v}^N \cdot (\mathbf{g}_d^N - \mathbf{g}_d^{N,q})}{\|v^N\|_{\tilde{H}^{-\frac{1}{2}}(\Gamma)}} \lesssim \tilde{\rho}^N \left[(2\rho)^{-2N_q^\theta} + (2\rho)^{-2N_q} \right] N^2.$$

With this, the result is obtained following Theorem 4.3. \square

REMARK 4.5. *In the right-hand side of (4.29), the last term grows as $\tilde{\rho}^N N^2$ due to a single numeric quadrature whereas the second term does at rate of $\tilde{\rho}^{2N} N^4$ as it arises from the tensorization of two quadrature rules.*

In a similar fashion, we obtain the equivalent result for the Neumann problem.

Theorem 4.6. *There exists $N_0 > 0$ such that for every $N > N_0$, there is a $N_{q,0}$ that depends on N such that, if N_q^θ, N_q are both greater than $N_{q,0}$, the fully discrete Neumann Problem 4.4 has a unique solution, and the following error estimate follows for $s > \frac{1}{2}$:*

$$\begin{aligned} \|\nu - \nu_o^{N,q}\|_{\tilde{H}^{\frac{1}{2}}(\Gamma)} &\lesssim N^{\frac{1}{2}-s} \|\nu \circ \mathbf{r}\|_{P_o^s(\mathbb{D})} + \tilde{\rho}^{2N} \left[(2\rho)^{-2N_q^\theta} + (2\rho)^{-2N_q} \right] N^2 \|\nu\|_{\tilde{H}^{\frac{1}{2}}(\Gamma)} \\ &\quad + \tilde{\rho}^N \left[(2\rho)^{-2N_q^\theta} + (2\rho)^{-2N_q} \right] N. \end{aligned} \tag{4.30}$$

REMARK 4.6. *The differences between the second (resp. third) terms in the right hand-sides of (4.29) and (4.30) are caused by the norm used to measure the error in each case.*

REMARK 4.7. *From the fully discrete error analysis, one concludes that the number of quadrature points should be a linear function of the parameter N so as to obtain good approximations of the BIOs.*

4.6. Numerical Results

In what follows, we conduct a series of numerical experiments to verify our claims, showcase insights and show limitations of the provided results. These computational results were carried out on a desktop PC I7-4790k with 8Gb of RAM.

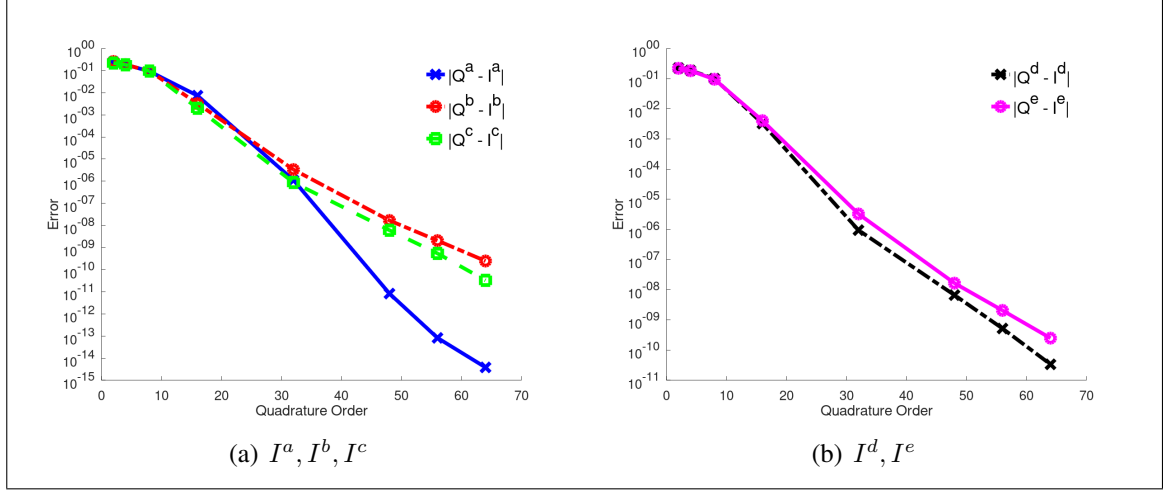


FIGURE 4.2. Quadrature errors for $k = 2.8$, computed against an overkill with $N_q = 76$. The error is computed by taking the 2-norm ($\|A\|_2 = \sup_{\mathbf{v} \neq 0} \frac{\mathbf{v} \cdot A \mathbf{v}}{\|\mathbf{v}\|}$) we fix $N = 8$, (45 degrees of freedom).

4.6.1. Quadrature Results

Before studying the accuracy of the full spectral Galerkin method, we consider the performance of the quadrature procedure detailed in Section 4.4.2.2. To this end, we consider the screen Γ given by the following parametrization:

$$\mathbf{r}(r, \theta) = r(\cos \theta, 2.8 \sin \theta, -0.56r).$$

We compute the integrals I^α , $\alpha \in \{a, b, c, d, e\}$ for an increasing number of quadrature points. In particular, we only select the variable N_q^α and fix $N_q^\theta = N_q^\alpha + 12$. Results reported in Figure 4.2 show that quadrature errors decay linearly in the log-linear scale—exponential decay—as described in (4.26).

As a second test, we consider the same screen and wavenumber for an increasing number of functions and quadrature points. As before, we only modify the variable N_q^α , $\alpha \in a, b, c, d, e, f$ and fix $N_q^\theta = N_q^\alpha + 12$. The results are presented in Table 4.1. In contrast to the previous experiment, we show the error for the consolidated variable $V^N[k] - V^{N,q}[k]$ and observe that the quadrature error is almost constant when the quadrature points increase linearly with N as stated in Remark 4.7.

TABLE 4.1. Quadrature error for the weakly-singular operator with $k = 2.8$ computed against an overkill with $N_q = 92, N = 24$. The rule for increasing the quadrature points with N is $N_q(N) = 1.75N + 50$. The error again is computed as the 2-norm of the approximation of the weakly-singular operator matrix.

N	2	6	14	16	18	20
N_q	18	25	39	42	46	49
Error	6.20e-15	4.89e-15	8.88e-15	9.60e-15	7.14e-15	8.39e-15

4.6.2. Code Validation

We now show that our method is correctly implemented for the case of the Laplace Dirichlet and Neumann problem for the disk \mathbb{D} . Recall the closed form of the matrix entries in (C.2). We consider g_d (resp. g_n) as the Dirichlet (resp. Neumann) traces of a plane wave:

$$\exp(\imath k_0 \mathbf{x} \cdot \mathbf{d})$$

where \mathbf{d} is an unitary vector which can be characterized in terms of two angles:

$$\mathbf{d} = (\cos \theta_0 \cos \varphi_0, \sin \theta_0 \cos \varphi_0, \sin \varphi_0),$$

and k_0 is the wavenumber of the plane wave. In Figure 4.3 we show the error of the approximated solution with respect to the semi-analytic solution –the one obtained using (C.2) for the matrix computations and a fixed value of N . Notice that the super-algebraic convergence rate is achieved, i.e. linear behavior in log-linear scale.

As in the two-dimensional case (Jerez-Hanckes & Pinto, 2020), Figure 4.3 suggests that one could deduce the decaying behavior of solution coefficients from the right-hand side coefficients. For the Laplace case on a disk, this comes directly from (C.2) but for more general cases, to the best of our knowledge, this has not been done. One could prove results in this context by establishing a complete theory of pseudo-differential operators on screens acting in the auxiliary spaces, in a similar fashion to (Alouges & Averseng, 2019) presented for the two-dimensional case.

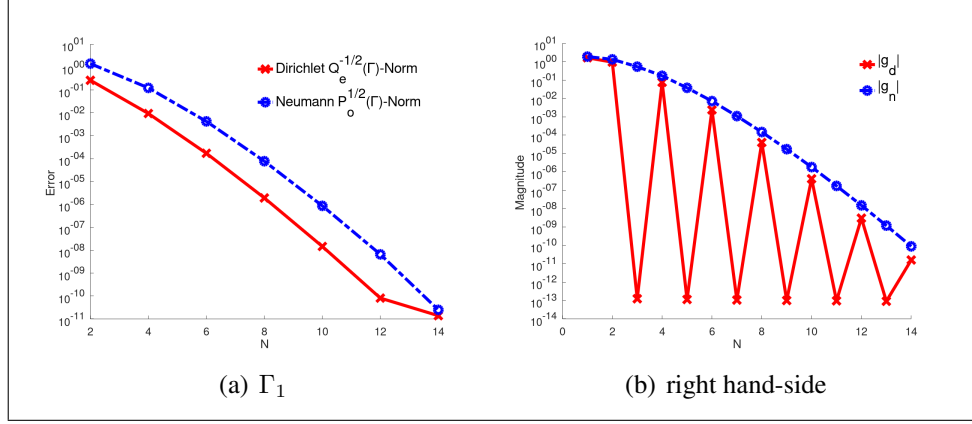


FIGURE 4.3. (a) Convergence curves for the Laplace problems on the disk. Parameters for the plane wave are $k_0 = 2.8$, $\theta_0 = \pi/3$, $\varphi_0 = \pi/4$. Running times for $N = 14$ are 181s, 730s for Dirichlet and Neumann cases, respectively. (b) Maximum of the absolute values in the right-hand side for each of the corresponding levels N , i.e. for $N = 4$ are the maximum value between the terms $m = -4, -2, 0, 2, 4$.

4.6.3. More complex screens

We fix the wave-numbers $k = 2.8$, and for right-hand side we use a plane wave with $k_0 = k$, $\theta_0 = \pi/3$, $\varphi_0 = \pi/4$. Let us first consider two distinct geometries: Γ_1 an elliptic screen given by

$$\mathbf{r}_1(r, \theta) = r(\cos \theta, 2.8 \sin \theta, 0)$$

and Γ_2 a truncated paraboloid,

$$\mathbf{r}_2(r, \theta) = r(\cos \theta, 2.8 \sin \theta, -0.56r).$$

Results for Γ_1, Γ_2 are presented in Figure 4.4, wherein we obtain super-algebraic convergence –linear convergence in log-linear scale– as stated in Theorems 4.5, 4.6.

Next, we show the impact of critical points through the following screens. Γ_3 , described by

$$\mathbf{r}_3(r, \theta) = r(1 - 0.2r^3 \cos(3\theta))(\cos \theta, \sin \theta, 0),$$

and Γ_4 , with parametrization

$$\mathbf{r}_4(r, \theta) = r(1 - 0.3r^3 \cos(3\theta))(\cos \theta, \sin \theta, 0).$$

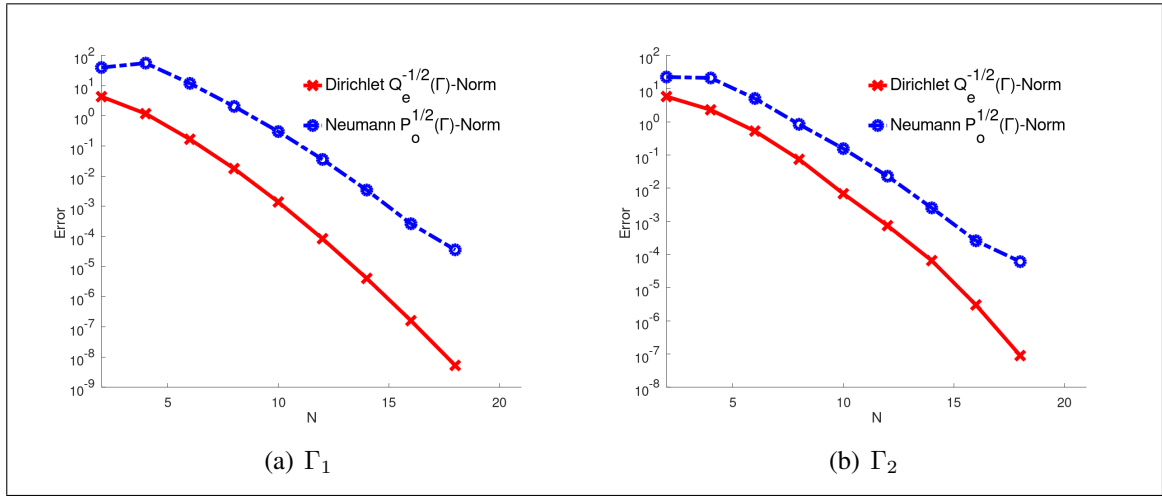


FIGURE 4.4. Error in the $Q_e^{-\frac{1}{2}}$ -Norm for the Dirichlet problems, and $P_o^{\frac{1}{2}}$ for the Neumann problems. Overkill solutions are computed using $N = 20$. Run times for Dirichlet and Neumann problems (with $N = 20$) are 749s, 2087s respectively.

graphical presentations of these two screens are presented in Figure 4.5. The case $k = 2.8$ is depicted in Figure 4.6. While these last two screens are similar, one can see that the error convergence for Γ_4 is worse than for the other cases. This is explained by the Jacobians' behavior: for Γ_3 , one has

$$|r(1 - 0.2r^3 \cos(3\theta))(1 - 0.8r^3 \cos \theta)|,$$

which is no-where null, whereas for Γ_4

$$|r(1 - 0.3r^3 \cos(3\theta))(1 - 1.2r^3 \cos \theta)|,$$

is zero on the curve $1 - 1.2r^3 \cos \theta = 0$.

Finally, and for illustration purposes, we consider a highly complex screen, Γ_5 , along with error convergence and volume solution plots (see Figures 4.7(a)–(d)). The screen is given by the parametrization:

$$\mathbf{r}_5(r, \theta) = (x_5(r, \theta), y_5(r, \theta), z_5(r, \theta)),$$

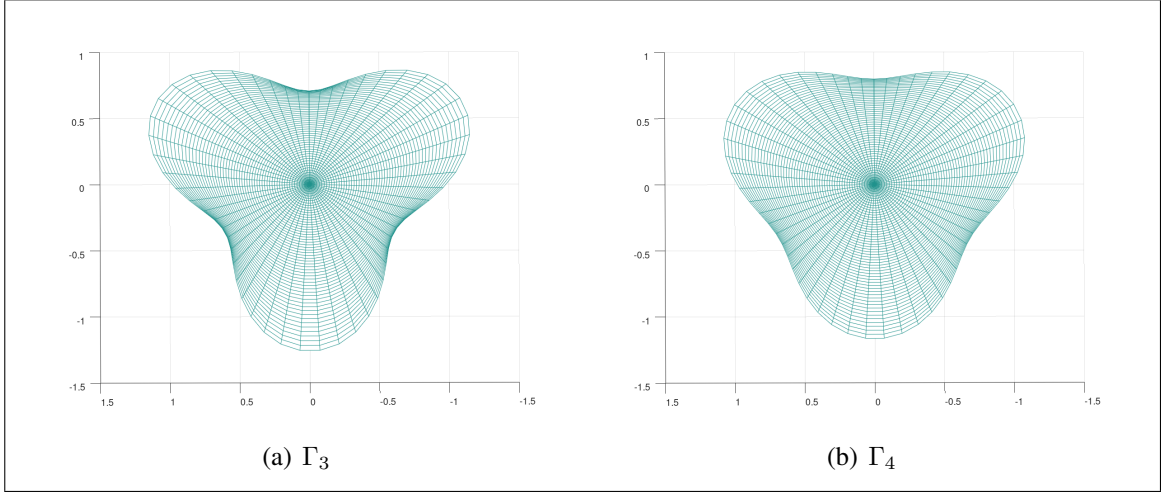
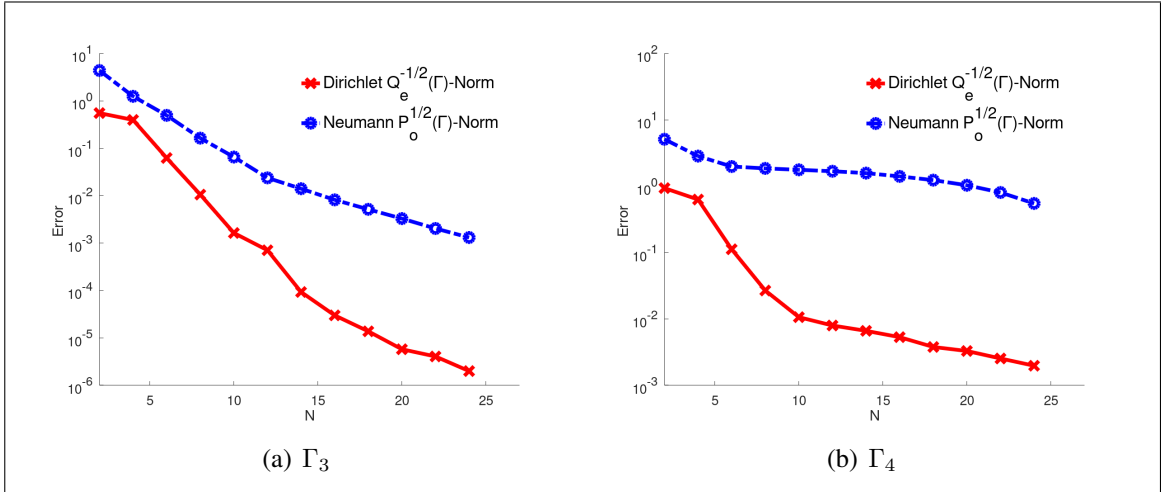
FIGURE 4.5. Geometry of Γ_3 , and Γ_4 .

FIGURE 4.6. Error in the $Q_e^{-\frac{1}{2}}$ -Norm for the Dirichlet problems, and $P_o^{\frac{1}{2}}$ for the Neumann. Overkill solutions are computed using $N = 28$. Run times for Dirichlet and Neumann problem (with $N = 28$) are 2800s, 6198s respectively.

where $(x_5(r, \theta), y_5(r, \theta)) := r(1 - 0.2r^3 \cos(3\theta))(\cos \theta, \sin \theta)$ and $z_5(r, \theta) := 0.2r \cos(7y_5(r, \theta))$.

4.7. Concluding Remarks

The present work presents a high-order discretization method for open screens based on weighted projections of the spherical harmonics functions. We have proved that the

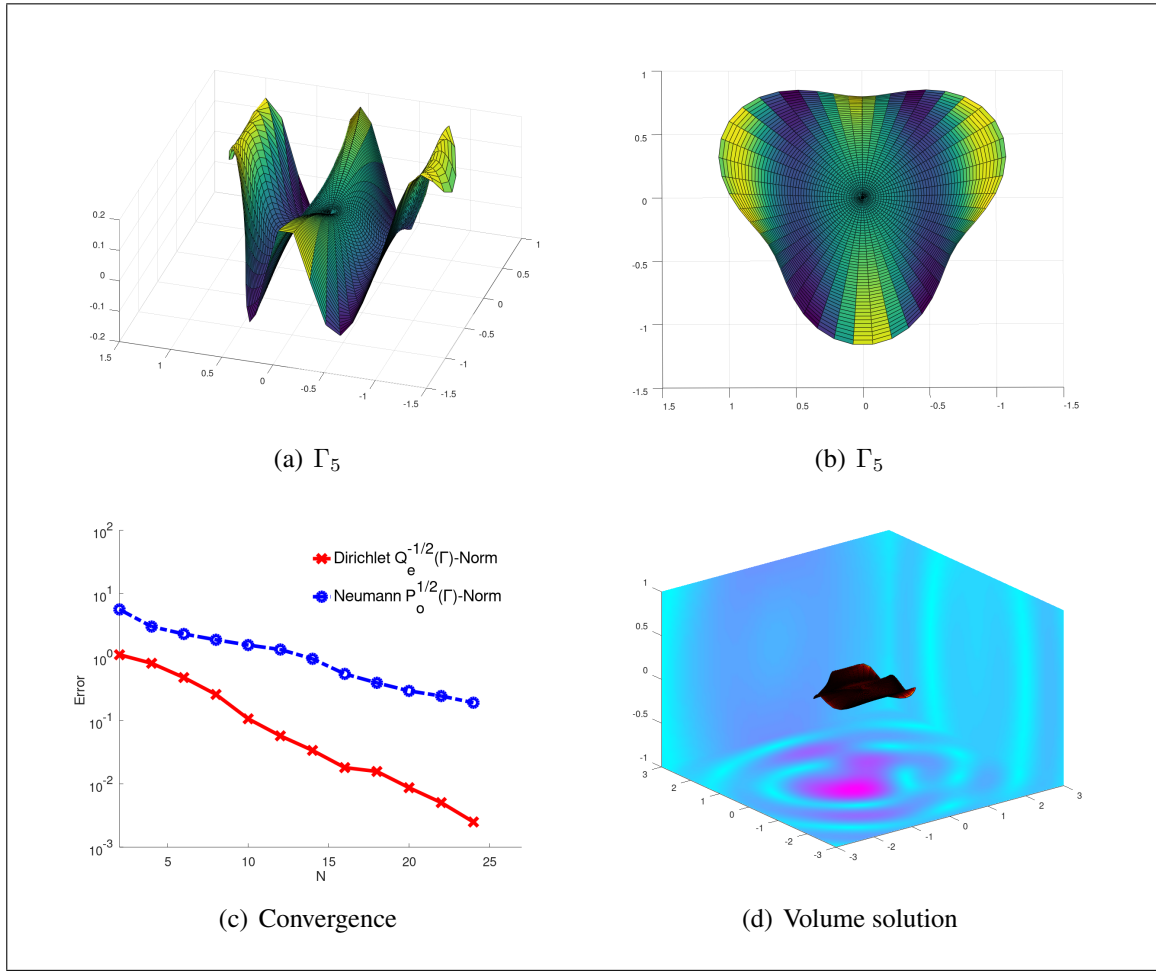


FIGURE 4.7. (a)-(b) Screen Γ_5 profiles. (c) Convergence plots for Dirichlet and Neumann problems computed against an overkill solution computed with $N = 28$, for $k = 2.8$, $k_0 = k$, $\theta_0 = \frac{\pi}{2}$, and $\phi_0 = 0$. (d) Plot of the volume solution for the Dirichlet problem.

method converges super-algebraically and also described implementation details. As an efficient solver for the forward problem, future efforts are directed towards using our method to solve shape optimization or inverse problems.

While the analysis presented here describes how approximation errors behave as a function of the number of degrees of freedom, it does not provide any insight on how to choose this number in terms of the problem parameters, in particular, the wavenumber k . We refer to (Chandler-Wilde et al., 2012) for a general review on this topic and (Chandler-Wilde & Hewett, 2015) for results related to screens.

Chapter 5. FINAL CONCLUSIONS

Throughout this thesis, we have presented and analyzed Galerkin-Spectral methods for three different boundary-integral formulations. For each of these situations, adequate spectral bases have been selected. These bases reflect any special characteristic of the underlying solution, hence they are well suited to approximate the aforementioned solutions. In particular, the special features for the different problems are,

- (i) For problems presented in Chapters 2, 4 the solution exhibit singular behavior near the edges of the geometry.
- (ii) For Chapter 3 the solution is quasi-periodic.

In all the presented cases we have rigorously proved that in terms of rate of convergence the corresponding methods are at least super-algebraically convergent whenever the data is smooth enough. In contrast, commonly used low-order discretization methods converge as a low power of the characteristic size of the underlying mesh.

We notice that for two-dimensional problems the convergence is super-algebraic in terms of the number of functions used (or low power when low-order local bases are used). However, for three-dimensional problems, the convergence is with respect to the maximum levels of functions used, which is a quadratic function of the number of functions used. While this could suggest that for higher dimension spectral method perform comparatively worse than low-order alternatives, in fact low order methods suffer from the same phenomena as the characteristic size of the associated mesh, in three-dimensions, is a quadratic function of the number of functions used, in three dimensions (boundaries of two dimensions).

We have detailed efficient implementations for all of the three cases. We put special care in the handling of the kernel singularity reducing the integration of singular functions to the integration of analytic functions that converge exponentially respect to the corresponding quadrature parameters.

An important conclusion that arises when we compare the integration procedure, is that while for two-dimensional problems (Chapter 2, 3) the kernel singularity can be completely subtracted by using a singular function (which are independent of the geometry that is then integrated using analytic expressions). For the three-dimensional problem presented in Chapter 4 the kernel singularity could not be subtracted and an adequate change of variables had to be used.

It is not clear for us at the moment if this would hold true for other problems in three dimensions. For example for problems arising from smooth deformation of the sphere, as are presented in (Graham & Sloan, 2002), a procedure that resembles the two-dimensional singularity extraction is possible.

Finally, we want to remark once again that spectral methods are specialty attractive for situations in which many direct problems defined on different but smooth geometries have to be solved. This situation is fairly common in optimization procedures where each iteration of the optimization method implies the solution of a direct problem, inverse problems where a non-linear equation has to be solved and again these are done using an iterative method, in which each iteration implies a solution of the direct problem, or in uncertainty-quantification problems where a realization also implies the solution of a direct problem.

References

- Abda, A. B., Ameur, H. B., & Jaoua, M. (1999). Identification of 2D cracks by elastic boundary measurements. *Inverse Problems*, 15(1), 67. Retrieved from <http://stacks.iop.org/0266-5611/15/i=1/a=011>
- Abramowitz, M., & Stegun, I. (1965). *Handbook of mathematical functions: with formulas, graphs, and mathematical tables*. Dover Publications. Retrieved from <https://books.google.cl/books?id=MtU8uP7XMvoC>
- Alber, H. D. (1979). A quasi-periodic boundary value problem for the Laplacian and the continuation of its resolvent. *Proceedings of the Royal Society of Edinburgh*, 82(3-4), 251-272.
- Alouges, F., & Averseng, M. (2019). New preconditioners for Laplace and Helmholtz integral equations on open curves: Analytical framework and numerical results.
- Ammari, H. (1998). Scattering of waves by thin periodic layers at high frequencies using the on-surface radiation condition method. *IMA journal of Applied Mathematics*, 60(2), 199–214.
- Ammari, H., & Bao, G. (2008, March). Coupling of finite element and boundary element methods for the scattering by periodic chiral structures. *Journal of Computational Mathematics*, 26(3), 261-283.
- Ammari, H., & He, S. (1997). Homogenization and scattering for gratings. *Journal of electromagnetic waves and applications*, 11(12), 1669–1683.

Ammari, H., & Nédélec, J.-C. (2001). 6. analysis of the diffraction from chiral gratings. In *Mathematical modeling in optical science* (p. 179-206). Retrieved from <https://epubs.siam.org/doi/abs/10.1137/1.9780898717594.ch6>

Andrieux, S., & Abda, A. B. (1996). Identification of planar cracks by complete overdetermined data: inversion formulae. *Inverse Problems*, 12(5), 553. Retrieved from <http://stacks.iop.org/0266-5611/12/i=5/a=002>

Arfken, G. B., Weber, H. J., & Harris, F. E. (2013). Chapter 15 - Legendre functions. In G. B. Arfken, H. J. Weber, & F. E. Harris (Eds.), *Mathematical methods for physicists (seventh edition)* (Seventh Edition ed., p. 715 - 772). Boston: Academic Press. Retrieved from <http://www.sciencedirect.com/science/article/pii/B9780123846549000153> doi: <https://doi.org/10.1016/B978-0-12-384654-9.00015-3>

Atkinson, K., & Han, W. (2001). *Theoretical numerical analysis: A functional analysis framework*. Springer New York. Retrieved from <https://books.google.cl/books?id=C8izGCKXJyMC>

Atkinson, K. E., & Sloan, I. H. (1991). The numerical solution of first-kind logarithmic-kernel integral equations on smooth open arcs. *Mathematics of Computation*, 56(193), 119–139. Retrieved from <http://www.jstor.org/stable/2008533>

Aylwin, R., Jerez-Hanckes, C., & Pinto, J. (2020). On the properties of quasi-periodic boundary integral operators for the Helmholtz equation. *Integral Equations and Operator Theory*, 92(2), 17. Retrieved from <https://doi.org/10.1007/s00020-020-2572-9> doi: 10.1007/s00020-020-2572-9

- Aylwin, R., Silva-Oelker, G., Jerez-Hanckes, C., & Fay, P. (2020, Aug). Optimization methods for achieving high diffraction efficiency with perfect electric conducting gratings. *J. Opt. Soc. Am. A*, 37(8), 1316–1326. doi: 10.1364/JOSAA.394204
- Bao, G. (1995, August). Finite element approximation of time harmonic waves in periodic structures. *SIAM Journal on Numerical Analysis*, 32(4), 1155-1169.
- Bao, G. (1997). Variational approximation of Maxwell's equations in bi-periodic structures. *SIAM Journal on Applied Mathematics*, 57(2), 364–381.
- Bao, G. (2004). Recent mathematical studies in the modeling of optics and electromagnetics. *Journal of Computational Mathematics*, 22(2), 148-155.
- Bao, G., & Dobson, D. C. (2000, April). On the scattering by a bi-periodic structure. *Proceedings of the American Mathematical Society*, 128(9), 2715-2723.
- Bao, G., Dobson, D. C., & Cox, J. A. (1995). Mathematical studies in rigorous grating theory. *Journal of the Optical Society of America A*, 12(5), 1029-1042.
- Barnett, A., & Greengard, L. (2011). A new integral representation for quasi-periodic scattering problems in two dimensions. *BIT Numerical mathematics*, 51(1), 67–90.
- Bebendorf, M. (2008). *Hierarchical matrices: A means to efficiently solve elliptic boundary value problems*. Springer Science & Business Media.
- Bespalov, A., & Heuer, N. (2005, 09). The p -version of the boundary element method for a three-dimensional crack problem. *J. Integral Equations Applications*, 17(3), 243–258. Retrieved from <https://doi.org/10.1216/jiea/1181075334> doi: 10.1216/jiea/1181075334
- Bespalov, A., & Heuer, N. (2007, 03). The p -version of the boundary element method for weakly singular operators on piecewise plane open surfaces. *Numerische Mathematik*, 106, 69-97. doi: 10.1007/s00211-006-0058-6

Bisciotti, G., & Eirale, C. (2013). *Muscle injuries in sport medicine*. IntechOpen. Retrieved from <https://books.google.cl/books?id=4PyPDwAAQBAJ>

Bittencourt, T., Wawrzynek, P., Ingraffea, A., & Sousa, J. (1996). Quasi-automatic simulation of crack propagation for 2D LEFM problems. *Engineering Fracture Mechanics*, 55(2), 321 - 334. Retrieved from <http://www.sciencedirect.com/science/article/pii/0013794495002472> doi: [https://doi.org/10.1016/0013-7944\(95\)00247-2](https://doi.org/10.1016/0013-7944(95)00247-2)

Boubendir, Y., Dominguez, V., & Turc, C. (2014, 04). High-order Nyström discretizations for the solution of integral equation formulations of two-dimensional Helmholtz transmission problems. *IMA Journal of Numerical Analysis*, 36. doi: [10.1093/imanum/drv010](https://doi.org/10.1093/imanum/drv010)

Bruno, O. P., & Delourme, B. (2014). Rapidly convergent two-dimensional quasi-periodic Green function throughout the spectrum—including Wood anomalies. *Journal of Computational Physics*, 262, 262–290.

Bruno, O. P., & Fernandez-Lado, A. G. (2017). Rapidly convergent quasi-periodic Green functions for scattering by arrays of cylinders—including Wood anomalies. *Proc. R. Soc. A*, 473(2199), 20160802.

Bruno, O. P., & Haslam, M. C. (2009). Efficient high-order evaluation of scattering by periodic surfaces: deep gratings, high frequencies, and glancing incidences. *JOSA A*, 26(3), 658–668.

Bruno, O. P., & Lintner, S. K. (2012). Second-kind integral solvers for TE and TM problems of diffraction by open arcs. *Radio Science*, 47(6). Retrieved from <https://agupubs.onlinelibrary.wiley.com/doi/abs/10.1029/2012RS005035> doi: [10.1029/2012RS005035](https://doi.org/10.1029/2012RS005035)

Bruno, O. P., & Lintner, S. K. (2013). A high-order integral solver for scalar problems of diffraction by screens and apertures in three-dimensional

space. *Journal of Computational Physics*, 252, 250 - 274. Retrieved from <http://www.sciencedirect.com/science/article/pii/S0021999113004464> doi: <https://doi.org/10.1016/j.jcp.2013.06.022>

Bruno, O. P., Shipman, S. P., Turc, C., & Stephanos, V. (2017). Three-dimensional quasi-periodic shifted Green function throughout the spectrum, including Wood anomalies. *Proc. R. Soc. A*, 473(2207), 20170242.

Bruno, O. P., Shipman, S. P., Turc, C., & Venakides, S. (2016). Superalgebraically convergent smoothly windowed lattice sums for doubly periodic green functions in three-dimensional space. *Proc. R. Soc. A*, 472(2191), 20160255.

Burkardt, J. (2010). *Gauss-Jacobi Quadrature Rules*. (https://people.sc.fsu.edu/~jburkardt/cpp_src/jacobi_rule/jacobi_rule)

Chandler-Wilde, S., Graham, I., Langdon, S., & Spence, E. (2012, 04). Numerical-asymptotic boundary integral methods in high-frequency acoustic scattering. *Acta Numerica*, 21, 89 - 305. doi: 10.1017/S0962492912000037

Chandler-Wilde, S., & Hewett, D. (2015, 07). Wavenumber-explicit continuity and coercivity estimates in acoustic scattering by planar screens. *Integral Equations and Operator Theory*, 82, 423-449. doi: 10.1007/s00020-015-2233-6

Chen, X., & Friedman, A. (1991). Maxwell's equations in a periodic structure. *Transactions of the American Mathematical Society*, 323(2), 465–507. Retrieved from <http://www.jstor.org/stable/2001542>

Chen, Y.-B., & Zhang, Z. (2007). Design of tungsten complex gratings for thermophotovoltaic radiators. *Optics communications*, 269(2), 411–417.

Cho, M. H., & Barnett, A. H. (2015). Robust fast direct integral equation solver for quasi-periodic scattering problems with a large number of layers. *Optics Express*, 23(2), 1775-1799.

Colton, D., & Kress, R. (2013). *Integral equation methods in scattering theory*. Philadelphia, PA: Society for Industrial and Applied Mathematics. Retrieved from <https://epubs.siam.org/doi/abs/10.1137/1.9781611973167> doi: 10.1137/1.9781611973167

Costabel, M. (1988, June). Boundary integral operators on Lipschitz domains: Elementary results. *SIAM Journal on Mathematical Analysis*, 19(3), 613-626.

Costabel, M., & Dauge, M. (2002). Crack singularities for general elliptic systems. *Mathematische Nachrichten*, 235(1), 29-49.

Costabel, M., Dauge, M., & Duduchava, R. (2003). Asymptotics without logarithmic terms for crack problems. *Communications in Partial Differential Equations*, 28(5-6), 869-926. Retrieved from <https://doi.org/10.1081/PDE-120021180> doi: 10.1081/PDE-120021180

Dobson, D. C. (1994). A variational method for electromagnetic diffraction in biperiodic structures. *ESAIM: Mathematical Modelling and Numerical Analysis*, 28(4), 419-439.

Dobson, D. C., & Cox, J. A. (1991). An integral equation method for biperiodic diffraction structures. *International Conference on the Application and Theory of Periodic Structures*, 1545, 106-114.

Dobson, D. C., & Friedman, A. (1992). The time-harmonic Maxwell equations in a doubly periodic structure. *Journal of Mathematical Analysis and Applications*, 166(2), 507-528.

Domínguez, V. (2003). High-order collocation and quadrature methods for some logarithmic kernel integral equations on open arcs. *Journal of Computational and Applied Mathematics*, 161(1), 145 - 159. Retrieved from <http://www.sciencedirect.com/science/article/pii/S0377042703005831> doi: [https://doi.org/10.1016/S0377-0427\(03\)00583-1](https://doi.org/10.1016/S0377-0427(03)00583-1)

- Elschner, J., & Schmidt, G. (1998). Diffraction in periodic structures and optimal design of binary gratings. Part i: direct problems and gradient formulas. *Mathematical Methods in the Applied Sciences*, 21(14), 1297-1342.
- Epstein, M. (2017). *Partial differential equations: Mathematical techniques for engineers*. Springer.
- Evans, L. C. (2010). *Partial differential equations*. Providence, R.I.: American Mathematical Society.
- Fang, Q. (1995). *A spectral boundary integral equation method for the 2-d helmholtz equation*. Computational Physics.
- Feischl, M., Führer, T., Heuer, N., Karkulik, M., & Praetorius, D. (2015, Jul 01). Adaptive boundary element methods. *Archives of Computational Methods in Engineering*, 22(3), 309–389. Retrieved from <https://doi.org/10.1007/s11831-014-9114-z> doi: 10.1007/s11831-014-9114-z
- Frenkel, A. (1983). A chebyshev expansion of singular integral equations with a logarithmic kernel. *Journal of Computational Physics*, 51(2), 326 - 334. Retrieved from <http://www.sciencedirect.com/science/article/pii/0021999183900967> doi: [https://doi.org/10.1016/0021-9991\(83\)90096-7](https://doi.org/10.1016/0021-9991(83)90096-7)
- Galkowski, J., Müller, E., & Spence, E. (2016, 08). Wavenumber-explicit analysis for the Helmholtz h -BEM: error estimates and iteration counts for the Dirichlet problem. *Numerische Mathematik*, 142. doi: 10.1007/s00211-019-01032-y
- Ganesh, M., & Hawkins, S. C. (2011, May). An efficient algorithm for simulating scattering by a large number of two dimensional particles. In W. McLean & A. J. Roberts (Eds.), *Proceedings of the 15th biennial computational techniques and applications conference, ctac-2010* (Vol. 52, pp. C139–C155).

Gautschi, W. (1959). Some elementary inequalities relating to the gamma and incomplete gamma function. *Journal of Mathematics and Physics*, 38(1-4), 77-81. Retrieved from <https://onlinelibrary.wiley.com/doi/abs/10.1002/sapm195938177> doi: 10.1002/sapm195938177

Graham, I., Löhndorf, M., Melenk, J., & Spence, E. (2014, 03). When is the error in the h-BEM for solving the Helmholtz equation bounded independently of k ? *BIT Numerical Mathematics*, 55, 171-214. doi: 10.1007/s10543-014-0501-5

Graham, I., & Sloan, I. (2002, 01). Fully discrete spectral boundary integral methods for helmholtz problems on smooth closed surfaces in \mathbb{R}^3 . *Numerische Mathematik*, 92, 289-323. doi: 10.1007/s002110100343

Greengard, L., Ho, K. L., & Lee, J.-Y. (2014). A fast direct solver for scattering from periodic structures with multiple material interfaces in two dimensions. *Journal of Computational Physics*, 258, 738–751.

Grisvard, P. (2011). *Elliptic problems in nonsmooth domains* (Vol. 69). SIAM.

Guo, B., & Heuer, N. (2004, 01). The optimal rate of convergence of the p-version of the boundary element method in two dimensions. *Numerische Mathematik*, 98, 499-538. doi: 10.1007/s00211-004-0535-8

Ha-Duong, T. (1990, 10). On the transient acoustic scattering by a flat object. *Japan Journal of Applied Mathematics*, 7.

Henríquez, F., & Jerez-Hanckes, C. (2018). Multiple traces formulation and semi-implicit scheme for modelling biological cells under electrical stimulation. *ESAIM: M2AN*, 52(2), 659-703. Retrieved from <https://doi.org/10.1051/m2an/2018019> doi: 10.1051/m2an/2018019

Heuer, N., Maischak, M., & Stephan, E. (1999, 02). Exponential convergence of the hp-version for the boundary element method on open surfaces. *Numerische Mathematik*, 83. doi: 10.1007/s002119900082

Heuer, N., Mellado, M. E., & Stephan, E. P. (2002). A p-adaptive algorithm for the BEM with the hypersingular operator on the plane screen. *International Journal for Numerical Methods in Engineering*, 53(1), 85-104. Retrieved from <https://onlinelibrary.wiley.com/doi/abs/10.1002/nme.393> doi: 10.1002/nme.393

Hewett, D. P., Langdon, S., & Chandler-Wilde, S. N. (2014). A frequency-independent boundary element method for scattering by two-dimensional screens and apertures. *IMA Journal of Numerical Analysis*, 35(4), 1698–1728.

Hiptmair, R., Jerez-Hanckes, C., & Urzua-Torres, C. (2014). Mesh-independent operator preconditioning for boundary elements on open curves. *SIAM Journal on Numerical Analysis*, 52(5), 2295–2314.

Hiptmair, R., Jerez-Hanckes, C., & Urzúa-Torres, C. (2018). Closed-form inverses of the weakly singular and hypersingular operators on disks. *Integral Equations Operator Theory*, 90(1), Art. 4, 14. Retrieved from <https://doi.org/10.1007/s00020-018-2425-y> doi: 10.1007/s00020-018-2425-y

Hiptmair, R., Jerez-Hanckes, C., & Urzúa-Torres, C. (2020). Optimal operator preconditioning for Galerkin boundary element methods on 3-dimensional screens. *SIAM Journal on Numerical Analysis*, 58(1), 834–857.

Hu, F. Q. (1994). *A spectral boundary integral equation method for the 2-D Helmholtz equation* (Tech. Rep.). Institute for Computer Applications in Science and Engineering Hampton Va.

Hu, F. Q. (1995). A spectral boundary integral equation method for the 2d Helmholtz equation. *Journal of Computational Physics*, 120(2), 340 - 347.

Retrieved from <http://www.sciencedirect.com/science/article/pii/S0021999185711692> doi: <https://doi.org/10.1006/jcph.1995.1169>

Ikeno, H. (2016). *C++ templated library for Wigner 3j, 6j, 9j symbols and Gaunt coefficients*. (<https://github.com/hydeik/wigner-cpp>)

Jerez-Hanckes, C. (2008). *Modeling elastic and electromagnetic surface waves in piezoelectric transducers and optical waveguides* (Unpublished doctoral dissertation). École Polytechnique.

Jerez-Hanckes, C., & Nédélec, J.-C. (2011). Variational forms for the inverses of integral logarithmic operators over an interval. *Comptes Rendus Mathématique*, 349(9), 547 - 552. Retrieved from <http://www.sciencedirect.com/science/article/pii/S1631073X11000252> doi: <https://doi.org/10.1016/j.crma.2011.01.016>

Jerez-Hanckes, C., & Nédélec, J.-C. (2012, jan). Explicit variational forms for the inverses of integral logarithmic operators over an interval. *SIAM Journal on Mathematical Analysis*, 44(4), 2666–2694. doi: 10.1137/100806771

Jerez-Hanckes, C., Nicaise, S., & Urzúa-Torres, C. (2018, oct). Fast spectral Galerkin method for logarithmic singular equations on a segment. *Journal of Computational Mathematics*, 36(1), 128–158. doi: 10.4208/jcm.1612-m2016-0495

Jerez-Hanckes, C., & Pinto, J. (2018). *High-order Galerkin method for Helmholtz and Laplace problems on multiple open arcs* (Tech. Rep. No. 2018-49). Switzerland: Seminar for Applied Mathematics, ETH Zürich.

Jerez-Hanckes, C., & Pinto, J. (2020). High-order Galerkin method for Helmholtz and Laplace problems on multiple open arcs. *ESAIM: M2AN*, 54(6), 1975-2009. Retrieved from <https://doi.org/10.1051/m2an/2020017> doi: 10.1051/m2an/2020017

Jerez-Hanckes, C., Pinto, J., & Tournier, S. (2015). Local multiple traces formulation for high-frequency scattering problems. *Journal of Computational and Applied Mathematics*, 289(Supplement C), 306 - 321. Retrieved from <http://www.sciencedirect.com/science/article/pii/S0377042715000102> (Sixth International Conference on Advanced Computational Methods in Engineering (ACOMEN 2014)) doi: <https://doi.org/10.1016/j.cam.2014.12.045>

Jiang, Y., & Xu, Y. (2010). Fast Fourier Galerkin methods for solving singular boundary integral equations: Numerical integration and precondition. *Journal of Computational and Applied Mathematics*, 234(9), 2792 - 2807. Retrieved from <http://www.sciencedirect.com/science/article/pii/S0377042710000269> (Third International Workshop on Analysis and Numerical Approximation of Singular Problems [IWANASP08]) doi: <https://doi.org/10.1016/j.cam.2010.01.022>

Kirsch, A. (1993). Diffraction by periodic structures. In *Inverse problems in mathematical physics* (pp. 87–102). Springer.

Kirsch, A. (1994). Uniqueness theorems in inverse scattering theory for periodic structures,. *Inverse Problems*, 10, 145-152.

Kress, R. (1995). Inverse scattering from an open arc. *Mathematical Methods in the Applied Sciences*, 18(4), 267-293. Retrieved from <https://onlinelibrary.wiley.com/doi/abs/10.1002/mma.1670180403> doi: 10.1002/mma.1670180403

Kress, R. (2014). *Linear integral equations* (Third Edition ed., Vol. 82). Applied Mathematical Sciences.

Krutitskii, P. A. (2000). The Dirichlet problem for the two-dimensional Laplace equation in a multiply connected domain with cuts. *Proc. Edinburgh Math.*

Soc. (2), 43(2), 325–341. Retrieved from <https://doi.org/10.1017/S0013091500020952> doi: 10.1017/S0013091500020952

Lai, J., Kobayashi, M., & Barnett, A. (2015). A fast and robust solver for the scattering from a layered periodic structure containing multi-particle inclusions. *Journal of Computational Physics*, 298, 194–208.

Lechleiter, A., & Nguyen, D.-L. (2013, 02). Volume integral equations for scattering from anisotropic diffraction gratings. *Mathematical Methods in the Applied Sciences*, 36. doi: 10.1002/mma.2585

Lechleiter, A., & Zhang, R. (2016, 11). A floquet–bloch transform based numerical method for scattering from locally perturbed periodic surfaces. *SIAM Journal on Scientific Computing*, 39. doi: 10.1137/16M1104111

Liew, K., Cheng, Y., & Kitipornchai, S. (2007). Analyzing the 2d fracture problems via the enriched boundary element-free method. *International Journal of Solids and Structures*, 44(11), 4220 - 4233. Retrieved from <http://www.sciencedirect.com/science/article/pii/S0020768306004860> doi: <https://doi.org/10.1016/j.ijsolstr.2006.11.018>

Lintner, S. (2012). *High-order integral equation methods for diffraction problems involving screens and apertures* (Doctoral dissertation, California Institute of Technology). Retrieved from <http://resolver.caltech.edu/CaltechTHESIS:06072012-004925615>

Lintner, S. K., & Bruno, O. P. (2015). A generalized Calderón formula for open-arc diffraction problems: theoretical considerations. *Proceedings of the Royal Society of Edinburgh: Section A Mathematics*, 145(2), 331–364. doi: 10.1017/S0308210512000807

Linton, C. M. (1998, May). The green’s function for the two-dimensional Helmholtz equation in periodic domains. *Journal of Engineering Mathematics*, 33(4), 377–401.

Liu, Y., & Barnett, A. (2016). Efficient numerical solution of acoustic scattering from doubly-periodic arrays of axisymmetric objects. *Journal of Computational Physics*, 324, 226–245.

Loewen, E., & Popov, E. (1997). *Diffraction gratings and applications*. Taylor & Francis. Retrieved from <https://books.google.cl/books?id=I1MBiFGO4pMC>

Loewen, E. G., & Popov, E. (2018). *Diffraction gratings and applications*. CRC Press.

Lohöfer, G. (1991). Inequalities for Legendre functions and Gegenbauer functions. *Journal of Approximation Theory*, 64(2), 226 - 234. Retrieved from <http://www.sciencedirect.com/science/article/pii/002190459190077N> doi: [https://doi.org/10.1016/0021-9045\(91\)90077-N](https://doi.org/10.1016/0021-9045(91)90077-N)

MacRobert, T. (1948). *Spherical harmonics: An elementary treatise on harmonic functions, with applications*. Dover Publications. Retrieved from <https://books.google.cl/books?id=HRQJAQAAIAAJ>

McLean, W. (2000). *Strongly elliptic systems and boundary integral equations*. Cambridge University Press. Retrieved from <https://books.google.cl/books?id=RILqjEeMfK0C>

McLean, W., & Steinbach, O. (1999). Boundary element preconditioners for a hypersingular integral equation on an interval. *Advances in Computational Mathematics*, 11(4), 271–286.

Melenk, J., & Sauter, S. (2011). Wavenumber explicit convergence analysis for galerkin discretizations of the helmholtz equation. *SIAM Journal on Numerical Analysis*, 49(3), 1210-1243. Retrieved from <https://doi.org/10.1137/090776202> doi: 10.1137/090776202

- Nakata, Y., & Koshiba, M. (1990). Boundary-element analysis of plane-wave diffraction from groove-type dielectric and metallic gratings. *JOSA A*, 7(8), 1494–1502.
- Necas, J. (2011). *Direct methods in the theory of elliptic equations*. Springer Science & Business Media.
- Nédélec, J. C., & Starling, F. (1991, November). Integral equation methods in a quasi-periodic diffraction problem for the time-harmonic Maxwell's equations. *SIAM Journal on Mathematical Analysis*, 22(6), 1679–1701.
- Nguyen, D. (2012, 12). Spectral methods for direct and inverse scattering from periodic structures.
- Oughstun, K. (1982, 07). Electromagnetic theory of gratings. *Proceedings of the IEEE*, 70, 687 - 687. doi: 10.1109/PROC.1982.12371
- Pestourie, R., Pérez-Arancibia, C., Lin, Z., Shin, W., Capasso, F., & Johnson, S. (2018, 08). Inverse design of large-area metasurfaces.
- Pham, D., Tran, T., & Chernov, A. (2011, 09). Pseudodifferential equations on the sphere with spherical splines. *Mathematical Models and Methods in Applied Sciences*, 21, 1933-1959. doi: 10.1142/S021820251100560X
- Popov, E. (2012). *Gratings: theory and numeric applications*. Popov, Institut Fresnel.
- Ramaciotti, P., & Nédélec, J.-C. (2017). About some boundary integral operators on the unit disk related to the Laplace equation. *SIAM J. Numer. Anal.*, 55(4), 1892–1914. Retrieved from <https://doi.org/10.1137/15M1033721> doi: 10.1137/15M1033721

Ramaciotti Morales, P. (2016). *Theoretical and numerical aspects of wave propagation phenomena in complex domains and applications to remote sensing* (Unpublished doctoral dissertation).

Reade, J. B. (1979). Asymptotic behaviour of eigen-values of certain integral equations. *Proceedings of the Edinburgh Mathematical Society*, 22(2), 137–144. doi: 10.1017/S0013091500016254

Saad, Y. (1996). *Iterative methods for sparse linear systems*. PWS Publishing Company. Retrieved from <https://books.google.cl/books?id=jLtiQgAACAAJ>

Saad, Y. (2003). *Iterative Methods for Sparse Linear Systems* (Second ed.). SIAM. Retrieved from http://www-users.cs.umn.edu/~{ }saad/IterMethBook_2ndEd.pdf doi: 10.1137/1.9780898718003

Saranen, J., & Vainikko, G. (2013). *Periodic integral and pseudodifferential equations with numerical approximation*. Springer Berlin Heidelberg. Retrieved from <https://books.google.cl/books?id=5qPyCAAAQBAJ>

Sauter, S. A., & Schwab, C. (2011). *Boundary element methods* (Vol. 39). Springer Series in Computational Mathematics.

Schaeffer, N. (2013). Efficient spherical harmonic transforms aimed at pseudospectral numerical simulations. *Geochemistry, Geophysics, Geosystems*, 14(3), 751–758. Retrieved from <https://agupubs.onlinelibrary.wiley.com/doi/abs/10.1002/ggge.20071> doi: 10.1002/ggge.20071

Schmidt, G. (2009, 12). Boundary integral methods for periodic scattering problems. In (p. 337–363). doi: 10.1007/978-1-4419-1343-2_16

- Schmidt, G. (2011, 03). Integral equations for conical diffraction by coated grating. *Journal of Integral Equations and Applications - J INTEGRAL EQU APPL*, 23. doi: 10.1216/JIE-2011-23-1-71
- Shiraishi, K., Higuchi, S., Muraki, K., & Yoda, H. (2016). Silver-film subwavelength gratings for polarizers in the terahertz and mid-infrared regions. *Optics express*, 24(18), 20177–20186.
- Silva, G., Jerez-Hanckes, C., & Fay, P. (2019). High-temperature tungsten-hafnia optimized selective thermal emitters for thermophotovoltaic applications. *Journal of Quantitative Spectroscopy & Radiative Transfer*, 231, 61–68.
- Silva-Oelker, G., Aylwin, R., Jerez-Hanckes, C., & Fay, P. (2018). Quantifying the impact of random surface perturbations on reflective gratings. *IEEE Transactions on Antennas and Propagation*, 66(2), 838–847.
- Silva-Oelker, G., Jerez-Hanckes, C., & Fay, P. (2018). Study of W/HfO₂ grating selective thermal emitters for thermophotovoltaic applications. *Optics express*, 26(22), A929–A936.
- Slevinsky, R. M., & Olver, S. (2017). A fast and well-conditioned spectral method for singular integral equations. *Journal of Computational Physics*, 332, 290 - 315. Retrieved from <http://www.sciencedirect.com/science/article/pii/S0021999116306507> doi: <https://doi.org/10.1016/j.jcp.2016.12.009>
- Starling, F., & Bonnet-Bendhia, A.-S. (1994, April). Guided waves by electromagnetic gratings and non-uniqueness examples for the diffraction problem. *Mathematical Methods in the Applied Sciences*, 17, 305-338.
- Steinbach, O. (2007). *Numerical approximation methods for elliptic boundary value problems*. Springer Science & Business Media.

Stephan, E., & Suri, M. (1989, 01). On the convergence of the p-version of the boundary element Galerkin method. *Mathematics of Computation*, 52. doi: 10.2307/2008651

Stephan, E. P. (1986). A boundary integral equation method for three-dimensional crack problems in elasticity. *Math. Methods Appl. Sci.*, 8(4), 609–623. Retrieved from <https://doi.org/10.1002/mma.1670080140> doi: 10.1002/mma.1670080140

Stephan, E. P. (1987, Mar 01). Boundary integral equations for screen problems in \mathbb{R}^3 . *Integral Equations and Operator Theory*, 10(2), 236–257. Retrieved from <https://doi.org/10.1007/BF01199079> doi: 10.1007/BF01199079

Stephan, E. P., & Wendland, W. L. (1984). An augmented Galerkin procedure for the boundary integral method applied to two-dimensional screen and crack problems. *Applicable Analysis*, 18(3), 183–219.

Stoer, J., & Bulirsch, R. (1980). *Introduction to numerical analysis*. Springer-Verlag. Retrieved from <https://books.google.cl/books?id=zDPvAAAAMAAJ>

Sukharevsky, O. I., Vasilets, V. A., Nechitailo, S. V., & Khlopov, G. I. (2016). High-frequency methods for applied problems of electromagnetic wave scattering. In *9th international kharkiv symposium on physics and engineering of microwaves, millimeter and submillimeter waves (msmw)*. doi: 10.1109/MSMW.2016.7538212

Taibleson, M. (1967). Fourier coefficients of functions of bounded variation. In *Proc. Amer. Math. Soc.* (Vol. 18).

Tanaka, S., Okada, H., Okazawa, S., & Fujikubo, M. (2013). Fracture mechanics analysis using the wavelet Galerkin method and extended finite element method. *International Journal for Numerical Methods in Engineering*, 93(10), 1082–1108.

Retrieved from <http://dx.doi.org/10.1002/nme.4433> doi: 10.1002/nme.4433

Tanaka, S., Suzuki, H., Ueda, S., & Sannomaru, S. (2015, Jul 01). An extended wavelet Galerkin method with a high-order B-spline for 2D crack problems. *Acta Mechanica*, 226(7), 2159–2175. Retrieved from <https://doi.org/10.1007/s00707-015-1306-6> doi: 10.1007/s00707-015-1306-6

Tartar, L. (2007). *An introduction to sobolev spaces and interpolation spaces* (Vol. 3). Springer Science & Business Media.

Thierry, B., Antoine, X., Chniti, C., & Alzubaidi, H. (2015). *μ -diff: an open-source matlab toolbox for computing multiple scattering problems by disks*. Computer Physics Communications.

Trefethen, L. (2013). *Approximation theory and approximation practice*. SIAM. Retrieved from <https://books.google.cl/books?id=h80N5JHm-u4C>

Trefethen, L. N. (2000). *Spectral methods in matlab*. USA: Society for Industrial and Applied Mathematics.

Urzúa-Torres, C. (2018). *Operator preconditioning for Galerkin boundary element methods on screens* (Unpublished doctoral dissertation).

Verrall, G., Slavotinek, J., Barnes, P., Fon, G., & Spriggins, A. (2001). Clinical risk factors for hamstring muscle strain injury: a prospective study with correlation of injury by magnetic resonance imaging. *British Journal of Sports Medicine*, 35(6), 435–439. Retrieved from <http://bjsm.bmj.com/content/35/6/435> doi: 10.1136/bjsm.35.6.435

von Petersdorff, T., & Stephan, E. P. (1990). On the convergence of the multigrid method for a hypersingular integral equation of the first kind. *Numerische Mathematik*, 57(1), 379–391.

- Von Petersdorff, T., & Stephan, E. P. (1990). Regularity of mixed boundary value problems in \mathbb{R}^3 and boundary element methods on graded meshes. *Mathematical Methods in the Applied Sciences*, 12(3), 229-249. Retrieved from <https://onlinelibrary.wiley.com/doi/abs/10.1002/mma.1670120306>
doi: 10.1002/mma.1670120306
- Walsh, J., & Gill, E. (2000). An analysis of the scattering of high-frequency electromagnetic radiation from rough surfaces with application to pulse radar operating in backscatter mode. *Radio Science*, 35, 1337-1359.
- Wang, H., & Zhang, L. (2018, April). Jacobi polynomials on the Bernstein ellipse. *J. Sci. Comput.*, 75(1), 457–477. Retrieved from <https://doi.org/10.1007/s10915-017-0542-4> doi: 10.1007/s10915-017-0542-4
- Wolfe, P. (1971, July). Eigenfunctions of the Integral Equation for the Potential of the Charged Disk. *Journal of Mathematical Physics*, 12, 1215-1218. doi: 10.1063/1.1665723
- Yijun, L. (2009). *Fast multipole boundary element method: Theory and applications in engineering*. Cambridge University.
- Zhang, B., & Chandler-Wilde, S. N. (1998). A uniqueness result for scattering by infinite rough surfaces. *SIAM Journal on Applied Mathematics*, 58(6), 1774–1790.
- Zhang, Y., & Gillman, A. (2019). A fast direct solver for two dimensional quasi-periodic multilayered medium scattering problems. *arXiv preprint arXiv:1907.06223*.

APPENDIX A. TECHNICAL RESULTS FOR MULTIPLE OPEN ARCS PROBLEMS.

A.1. Laplace Uniqueness Result

We define the energy space of homogeneous boundary condition as

$$W_0(\Omega) := \{U \in W(\Omega) : \gamma_i^\pm U = 0, \quad \text{for } i = 1, \dots, M\}.$$

We also will need the traces over the complementary arcs $\Gamma_i^c := \partial\Omega_i \setminus \bar{\Gamma}_i$ that we denote them as γ_{ic}^\pm and $\gamma_{N,ic}^\pm$ respectively. The following technical results will be needed, we omit the proofs as they can be found in the given references.

LEMMA A.1.1 (Lemma 2.2, (Jerez-Hanckes & Nédélec, 2012)). *The semi-norm $|U|_{W(\Omega)} := \|\nabla U\|_{L^2(\Omega)}$ bounds the $W(\Omega)$ -norm for functions in $W_0(\Omega)$, i.e. there exists a constant $c > 0$ such that*

$$\|U\|_{W(\Omega)} \leq c |U|_{W(\Omega)}, \quad \forall U \in W_0(\Omega).$$

LEMMA A.1.2 (Proposition 2.6, (Jerez-Hanckes & Nédélec, 2012)). *Let U belong to $W(\Omega)$ such that $-\Delta U \in L_{loc}^2(\Omega)$. For $R > 0$, denote the ball of radius R centered at the origin by $B_R := \{\mathbf{x} \in \mathbb{R}^2 : \|\mathbf{x}\|_2 < R\}$. Then,*

$$\lim_{R \rightarrow \infty} \langle \gamma_{N,R}^- U, \gamma_R^- V \rangle_{\partial B_R} = 0, \quad \forall V \in W(\Omega),$$

where γ_R^- and $\gamma_{N,R}^-$ denote interior Dirichlet and Neumann traces on ∂B_R , respectively, the latter being equivalent to the radial derivative on the boundary.

LEMMA A.1.3 (Theorem 1.7.1, (Grisvard, 2011)). *Let $V \in W_0(\Omega)$. Then it holds*

$$\gamma_{ic}^+ V = \gamma_{ic}^- V \quad i \in \{1, \dots, M\}.$$

Hence, we can denote indistinctly by γ_{ic} the trace defined over Γ_i^c on $W_0(\Omega)$.

LEMMA A.1.4 (Section 2.6.1, (Jerez-Hanckes & Nédélec, 2012)). *Let a function $U \in W_0(\Omega)$ such that $-\Delta U = 0$ in Ω . Then, the normal jump on Γ_i^c is null, i.e. $\gamma_{N,ic}^+ U - \gamma_{N,ic}^- U = 0$.*

LEMMA A.1.5. *If $U \in W_0(\Omega)$, is such that $\Delta U = 0$, then $U = 0$.*

PROOF. Let $\Omega_* := \bigcup_{j=1}^M \Omega_j$, where the collection is disjoint by Assumption 2.2, and choose $R > 0$ such that $\Omega_* \subset B_R$. Set $\Omega_0(R) := B_R \cap \overline{\Omega_*}^c$. We have that $\nabla U, \nabla V \in L^2(B_R)$ (as they are in $L^2(\Omega)$), hence

$$\langle \nabla U, \nabla V \rangle_{B_R} = \sum_{i=1}^M \langle \nabla U, \nabla V \rangle_{\Omega_i} + \langle \nabla U, \nabla V \rangle_{\Omega_0(R)}.$$

Using the Green formulas, and the null condition of V in Γ we obtain that

$$\langle \nabla U, \nabla V \rangle_{\Omega_i} = \langle -\Delta U, V \rangle_{\Omega_i} + \langle \gamma_{N,i^c}^+ U, \gamma_{i^c} V \rangle_{\Gamma_i^c}$$

$$\langle \nabla U, \nabla V \rangle_{\Omega_0(R)} = \langle -\Delta U, V \rangle_{\Omega_0(R)} + \langle \gamma_{N,R} U, \gamma_R V \rangle_{\partial B_R} - \sum_{i=1}^M \langle \gamma_{N,i^c}^- U, \gamma_{i^c} V \rangle_{\Gamma_i^c}$$

Finally adding the two terms and using Lemma A.1.4, and the condition $-\Delta U = 0$ in Ω we have that

$$\langle \nabla U, \nabla V \rangle_{B_R} = \langle \gamma_{N,R} U, \gamma_R V \rangle_{\partial B_R}$$

The results follows directly from this last equation, and Lemmas A.1.1 and A.1.2. \square

A.2. Technical Lemmas

A.2.1. Proof of Lemma 2.2.1

We only prove for $H^{1/2}$ as the $\tilde{H}^{-1/2}$ case is obtained by duality arguments. By definition, it holds

$$\|\zeta \circ \mathbf{r}_i\|_{H^{\frac{1}{2}}(\hat{\Gamma})}^2 = \int_{-1}^1 |\zeta \circ \mathbf{r}_i(t)|^2 dt + \int_{-1}^1 \int_{-1}^1 \frac{|\zeta \circ \mathbf{r}_i(t) - \zeta \circ \mathbf{r}_i(s)|^2}{|t - s|^2} dt ds. \quad (\text{A.1})$$

For the first integral on the right-hand side, we deduce

$$\begin{aligned} \int_{-1}^1 |\zeta \circ \mathbf{r}_i(t)|^2 dt &= \int_{-1}^1 |\zeta \circ \mathbf{r}_i|^2 \frac{\|\mathbf{r}'_i(t)\|_2}{\|\mathbf{r}'_i(t)\|_2} dt = \int_{\Gamma_i} \frac{|\zeta|^2}{\|\mathbf{r}'_i \circ \mathbf{r}_i^{-1}\|_2} d\Gamma_i \\ &\leq \left\| \|\mathbf{r}'_i \circ \mathbf{r}_i^{-1}\|_2^{-1} \right\|_{L^\infty(\Gamma_i)} \int_{\Gamma_i} |\zeta|^2 d\Gamma_i. \end{aligned} \quad (\text{A.2})$$

Similarly, by changing variables, the second term in (A.1) becomes

$$\int_{\Gamma_i} \int_{\Gamma_i} \frac{|\zeta(\mathbf{x}) - \zeta(\mathbf{y})|^2}{\|\mathbf{x} - \mathbf{y}\|_2^2} \left(\frac{\|\mathbf{x} - \mathbf{y}\|_2^2}{\|\mathbf{r}_i^{-1}(\mathbf{x}) - \mathbf{r}_i^{-1}(\mathbf{y})\|_2^2} \right) \frac{d\Gamma_i(\mathbf{x})d\Gamma_i(\mathbf{y})}{\|\mathbf{r}'_i \circ \mathbf{r}_i^{-1}(\mathbf{x})\|_2 \|\mathbf{r}'_i \circ \mathbf{r}_i^{-1}(\mathbf{y})\|_2}.$$

Using the mean value theorem for \mathbf{r}_i^{-1} , we arrive at

$$\int_{-1}^1 \int_{-1}^1 \frac{|\zeta \circ \mathbf{r}_i(t) - \zeta \circ \mathbf{r}_i(s)|^2}{|t - s|^2} dt ds \leq C_i \int_{\Gamma_i} \int_{\Gamma_i} \frac{|\zeta(\mathbf{x}) - \zeta(\mathbf{y})|^2}{\|\mathbf{x} - \mathbf{y}\|_2^2} d\Gamma_i(\mathbf{x})d\Gamma_i(\mathbf{y}), \quad (\text{A.3})$$

where

$$C_i = \left\| \|\mathbf{r}'_i \circ \mathbf{r}_i^{-1}\|_2^{-1} \right\|_{L^\infty(\Gamma_i)}^4$$

Using (A.2), and (A.3) to define C we obtain the following inequality

$$\|\zeta \circ \mathbf{r}_i\|_{H^{\frac{1}{2}}(\hat{\Gamma})} \leq C \|\zeta\|_{H^{\frac{1}{2}}(\hat{\Gamma}_i)}.$$

The second equivalence inequality is obtained using the same arguments.

A.2.2. Proof of Lemma 2.4.6

For any $s \in [-1, 1]$, we can write the univariate Fourier-Chebyshev expansion in t :

$$h(t, s) = \sum_{n=0}^{\infty} a_n(s) T_n(t), \quad \forall t \in [-1, 1].$$

In fact, the regularity of $h(t, \cdot)$ implies that the functions $a_n(s)$ belong to $\mathcal{C}^m(-1, 1)$, and consequently, one can write down expansions:

$$a_n(s) = \sum_{k=0}^{\infty} b_{nk} T_k(s), \quad \forall s \in [-1, 1], \quad \forall n \in \mathbb{N}_0.$$

If $m < \infty$, by (L. Trefethen, 2013, Theorem 7.1), we have that $b_{nk} \lesssim k^{-m}$, where the constant depends on the m -th derivative of $a_n(s)$, which is bounded by the m -th derivative of h in s .

For the ρ -analytic case we have by (L. Trefethen, 2013, Theorem 8.1) that $b_{nk} \lesssim \rho_n^{-k}$, with $\rho_n > 1$. However, the coefficients $a_n(s)$ are given by

$$a_n(s) = c_n \int_{-1}^1 h(t, s) w^{-1}(t) T_n(t) dt,$$

where $c_0 = \pi^{-1}$, and $c_n = 2\pi^{-1}$, for $n \in \mathbb{N}$. Hence, since $h(t, \cdot)$ is ρ -analytic, we have that, for every z in the corresponding ellipse we can write

$$a_n(z) = \sum_{p \geq 0} z^p \int_{-1}^1 A_p(t) w^{-1}(t) T_n(t) dt,$$

where $A_p(t)$ are the coefficients of the power series of $h(t, \cdot)$. From this last expression, we have that a_n is analytic in the ellipse of parameter ρ for every n , and thus, we can take $\rho_n = \rho$ for every $n \in \mathbb{N} \cup \{0\}$.

The final result is obtained by repeating the above arguments inverting the roles of n and k .

A.2.3. Proof of Lemma 2.4.7

Consider $f = \sum_{n \geq 0} a_n w^{-1} T_n(t)$, by Lemma 2.4.6, we expand $h(t, s)$ as the series $\sum_{n=0}^{\infty} \sum_{k=0}^{\infty} b_{nk} T_n(t) T_k(s)$. Hence, by the Chebyshev polynomials' orthogonality property, we can write

$$v_l = \frac{\pi^2}{4} \sum_{n=1}^{\infty} b_{nl} a_n + \frac{\pi^2}{2} b_{0l} a_0, \quad \forall l > 0.$$

Thus, by definition of constants d_n (2.9) and the series expression for $\tilde{H}^{-1/2}(\hat{\Gamma})$ -norm, we obtain the following bound:

$$|v_l|^2 \lesssim \|f\|_{\tilde{H}^{-1/2}(\hat{\Gamma})}^2 \sum_{n=0}^{\infty} |b_{nl}|^2 d_n^{-1}.$$

From here the result is direct if h is bivariate ρ -analytic function. For $m \in \mathbb{N}$, using Lemma 2.4.6, it holds

$$|b_{nl}|^2 \lesssim l^{-2(m+1)\mu} n^{-2(m+1)(1-\mu)}, \quad \forall \mu \in (0, 1).$$

With the above bound and the estimate $d_n \sim n^{-1}$, we arrive to

$$|v_l|^2 \lesssim \|f\|_{\tilde{H}^{-1/2}(\hat{\Gamma})}^2 l^{-2(m+1)\mu} \sum_{n=1}^{\infty} n^{-2(m+1)(1-\mu)+1},$$

by choosing $\mu = 1 - \frac{1}{m+1} - \epsilon$, the series in the right-hand side converges and we get the stated result.

A.3. Basic Approximation properties

LEMMA A.3.1. *The discretization is conforming, i.e. $\mathbb{Q}_N(\Gamma_i) \subset \tilde{H}^{-\frac{1}{2}}(\Gamma_i)$ (resp. $\mathbb{Q}_{N,\langle 0 \rangle}(\Gamma_i) \subset \tilde{H}_{\langle 0 \rangle}^{-\frac{1}{2}}(\Gamma_i)$).*

PROOF. For any $\zeta^i \in \mathbb{Q}_N(\Gamma_i)$ the representation:

$$\zeta^i = \frac{\hat{p} \circ \mathbf{r}_i^{-1}}{w_i \|\mathbf{r}_i' \circ \mathbf{r}_i^{-1}\|_2},$$

holds, where \hat{p} is a polynomial in $(-1, 1)$. By definition of dual norms, one can write

$$\|\zeta^i\|_{\tilde{H}^{-\frac{1}{2}}(\Gamma_i)} = \sup_{\vartheta \in H^{\frac{1}{2}}(\Gamma_i)} \frac{\langle \zeta^i, \vartheta \rangle_{H^{\frac{1}{2}}(\Gamma_i)}}{\|\vartheta\|_{H^{\frac{1}{2}}(\Gamma_i)}}.$$

At the same time, it holds

$$\begin{aligned} \langle \zeta^i, \vartheta \rangle_{\Gamma_i} &= \int_{-1}^1 \frac{\hat{p}(t)}{\sqrt{1-t^2}} (\vartheta \circ \mathbf{r}_i)(t) dt \leq \|\hat{p}\|_{L^\infty(-1,1)} \int_{-1}^1 \frac{(\vartheta \circ \mathbf{r}_i)(t)}{w(t)} dt \\ &\leq \|\hat{p}\|_{L^\infty(-1,1)} \|w^{-1}\|_{\tilde{H}^{-\frac{1}{2}}(\hat{\Gamma})} \|\vartheta \circ \mathbf{r}_i\|_{H^{\frac{1}{2}}(\hat{\Gamma})}, \end{aligned}$$

where $w(t) := \sqrt{1-t^2}$. Applying Lemma 2.2.1, we only need to check that the $\tilde{H}^{-\frac{1}{2}}(\hat{\Gamma})$ -norm of w^{-1} is finite, which was already proved in (Jerez-Hanckes, 2008, Lemma 6.1.19). The inclusion for the mean-zero spaces is immediate from the Chebyshev polynomials' orthogonality property. \square

LEMMA A.3.2. *The family $\{\mathbb{Q}_N(\Gamma_i)\}_{N \in \mathbb{N}}$ is dense in $\tilde{H}^{-\frac{1}{2}}(\Gamma_i)$, while the family $\{\mathbb{Q}_{N,\langle 0 \rangle}(\Gamma_i)\}_{N \in \mathbb{N}}$ is dense in $\tilde{H}_{\langle 0 \rangle}^{-\frac{1}{2}}(\Gamma_i)$.*

PROOF. We only need to prove that there is a fixed constant C such that, for a given $\epsilon > 0$ and $\phi \in \mathcal{D}(\Gamma_i)$, there exists $\zeta^i \in \mathbb{Q}_N(\Gamma_i)$ satisfying

$$\|\zeta^i - \phi\|_{\tilde{H}^{-\frac{1}{2}}(\Gamma_i)} \leq C\epsilon.$$

By (Jerez-Hanckes, 2008, Lemma 6.1.20), there exists a polynomial $\hat{p} \in \mathbb{P}_N(-1, 1)$ satisfying

$$\|w^{-1}\hat{p} - \|\mathbf{r}'_i\|_2(\phi \circ \mathbf{r}_i)\|_{\tilde{H}^{-\frac{1}{2}}(\hat{\Gamma})} < \epsilon.$$

Let $\zeta^i = \frac{\hat{p} \circ \mathbf{r}_i}{w_i \|\mathbf{r}'_i \circ \mathbf{r}_i^{-1}\|_2}$. Again, we take the dual norm

$$\|\zeta^i - \phi\|_{\tilde{H}^{-\frac{1}{2}}(\Gamma_i)} = \sup_{\vartheta \in H^{\frac{1}{2}}(\Gamma_i)} \frac{\langle \zeta^i - \phi, \vartheta \rangle_{\Gamma_i}}{\|\vartheta\|_{H^{\frac{1}{2}}(\Gamma_i)}}.$$

We can write

$$\begin{aligned} \langle \zeta^i - \phi, \vartheta \rangle_{\Gamma_i} &= \int_{\Gamma_i} (\zeta^i - \phi)(\mathbf{x}) \vartheta(\mathbf{x}) d\Gamma_i(\mathbf{x}) \\ &= \int_{-1}^1 (w^{-1}(t)\hat{p}(t) - \|\mathbf{r}'_i\|_2(t)(\phi \circ \mathbf{r}_i)(t)) (\vartheta \circ \mathbf{r}_i)(t) dt. \end{aligned}$$

By Lemma 2.2.1, there exists a constant C independent of ϵ such that

$$\langle \zeta^i - \phi, \vartheta \rangle_{\Gamma_i} \leq C \|\vartheta\|_{H^{\frac{1}{2}}(\Gamma_i)} \|w^{-1}\hat{p} - \|\mathbf{r}'_i\|_2(\phi \circ \mathbf{r}_i)\|_{\tilde{H}^{-\frac{1}{2}}(\hat{\Gamma})} \leq C\epsilon \|\vartheta\|_{H^{\frac{1}{2}}(\Gamma_i)},$$

and thus $\|\zeta^i - \phi\|_{\mathcal{H}^i} \leq C\epsilon$ as stated.

For the family $\{\mathbb{Q}_{N, \langle 0 \rangle}(\Gamma_i)\}_{N \in \mathbb{N}}$, by the previous result, we observe that, given $\phi \in \tilde{H}_{\langle 0 \rangle}^{-\frac{1}{2}}(\Gamma_i)$ and $\epsilon > 0$, there exists $N \in \mathbb{N}$ and $\zeta^i \in \mathbb{Q}_N(\Gamma_i)$, such that

$$\|\zeta^i - \phi\|_{\tilde{H}^{-\frac{1}{2}}(\Gamma_i)} \leq \epsilon.$$

Thus, by the definition of the norm in $\tilde{H}^{-\frac{1}{2}}(\Gamma_i)$, it holds

$$\langle \zeta^i, 1 \rangle_{\Gamma_i} = \langle \zeta^i - \phi, 1 \rangle_{\Gamma_i} \leq \|\zeta^i - \phi\|_{\tilde{H}^{-\frac{1}{2}}(\Gamma_i)},$$

Hence, we can define $\zeta_0^i := \zeta^i - |\Gamma_i|^{-1} \langle \zeta^i, 1 \rangle_{\Gamma_i}$, where $|\Gamma_i|$ is the length of the arc Γ_i . Now, it is direct that $\zeta_0^i \in \mathbb{Q}_{N, \langle 0 \rangle}(\Gamma_i)$ and

$$\|\zeta_0^i - \phi\|_{\tilde{H}^{-\frac{1}{2}}(\Gamma_i)} \leq 2\epsilon,$$

which gives the desired density. \square

A.3.1. Proof of Lemma 2.4.14

We proceed as in the one-dimensional case and assume, for simplicity, that the Chebyshev polynomials are normalized, thus omitting constants c_n . The coefficients C_{ij}^p are given by

$$\begin{aligned} C_{ij}^p &= \int_{-1}^1 \int_{-1}^1 R_p(t, s) |t - s|^{2p} \log |t - s| \frac{T_i(t)}{w(t)} \frac{T_j(s)}{w(s)} dt ds \\ &= \sum_{n=0}^{\infty} \sum_{l=0}^{\infty} b_{nl}^p \int_{-1}^1 \int_{-1}^1 R_p(t, s) \frac{1}{4} \frac{T_{n+i}(t) + T_{|n-i|}(t)}{w(t)} \frac{T_{l+j}(s) + T_{|l-j|}(s)}{w(s)} dt ds \\ &= \sum_{n=0}^{\infty} \sum_{l=0}^{\infty} \frac{b_{nl}^p}{4} (r_{n+i, l+j} + r_{n+i, |l-j|} + r_{|n-i|, l+j} + r_{|n-i|, |l-j|}). \end{aligned}$$

Now, we have to find the decay order for the different terms. Define the index set $I_p(l) := \{l, l \pm 2, l \pm 4, \dots, l \pm 2p\}$. By Lemma 2.4.11, we have the estimate:

$$C_{ij}^p \sim \sum_{l=1}^{\infty} \sum_{n \in I_p(l)} l^{-2p-1} (r_{n+i, l+j} + r_{n+i, |l-j|} + r_{|n-i|, l+j} + r_{|n-i|, |l-j|}). \quad (\text{A.4})$$

By Lemma 2.4.6, it holds

$$r_{\nu, \mu} = \mathcal{O}(\min\{\nu^{-m-1}, \mu^{-m-1}\}), \quad \text{for } \nu, \mu \in \mathbb{N},$$

and we can estimate each term in C_{ij}^p as follows, we provide details for the first two.

Define $K_1 := \sum_{l=1}^{\infty} \sum_{n \in I_p(l)} l^{-2p-1} r_{n+i, l+j}$. Assume that $r_{n+i, l+j} = \mathcal{O}((l+j)^{-m-1})$, then

$$K_1 \lesssim 2p \sum_{l=1}^{\infty} l^{-2p-1} (l+j)^{-m-1} = \mathcal{O}(j^{-m-1}).$$

Alternatively, we can use that $r_{n+i,l+j} = \mathcal{O}((n+i)^{-m-1})$ so that

$$K_1 \lesssim \sum_{l=1}^{\infty} \sum_{n \in I_p(l)} l^{-2p-1} (n+i)^{-m-1} = \mathcal{O}(i^{-m-1}).$$

Thus, we then conclude that

$$K_1 = \mathcal{O}(\min\{i^{-m-1}, j^{-m-1}\})$$

Now set $K_2 := \sum_{l=1}^{\infty} \sum_{n \in I_p(l)} l^{-2p-1} r_{n+i,|l-j|}$. Let $r_{n+i,|l-j|} = \mathcal{O}((|l-j|+1)^{-m-1})$, we obtain

$$K_2 \lesssim \sum_{l=1}^{\infty} l^{-2p-1} (|l-j|+1)^{-m-1},$$

where we added one to avoid infinity. Thus, we can split this last sum into two terms

$$K_2 \lesssim \sum_{l=1}^{j/2} l^{-2p-1} (j-l)^{-m-1} + \sum_{l>j/2} l^{-2p-1} (|l-j|+1)^{-m-1}.$$

The first one is bounded as

$$\sum_{l=0}^{j/2} l^{-2p-1} (j-l)^{-m-1} \lesssim j^{-m-1} \sum_{l=0}^{j/2} l^{-2p-1} \lesssim j^{-m-1},$$

whereas the second one

$$\sum_{l>j/2} l^{-2p-1} (|l-j|+1)^{-m-1} \lesssim j^{-2p-1}.$$

Hence, we have

$$K_2 = \mathcal{O}(j^{-m-1}) + \mathcal{O}(j^{-2p-1}) = \mathcal{O}(j^{-\min\{m, 2p+1\}}).$$

If alternatively we use $r_{n+i,|l-j|} = \mathcal{O}((n+i)^{-m-1})$, then

$$K_2 \lesssim \sum_{l=0}^{\infty} l^{-2p-1} (n+i)^{-m-1} = \mathcal{O}(i^{-m-1}).$$

Combining both results yields

$$K_2 = \mathcal{O}(\min\{i^{-m-1}, j^{-\min\{m+1, 2p+1\}}\}).$$

TABLE A.1. Coefficients used in Lemma A.4.1.

	$\beta_n^{(-1)}$	$\beta_n^{(0)}$
$n = 0$	$\frac{1}{4}a_0$	$a_0 - \frac{1}{2}a_1$
$n = 1$	$-a_0 + \frac{1}{4}a_1$	$-a_0 + \frac{5}{4}a_1 - \frac{1}{2}a_2$
$n = 2$	$\frac{1}{2}a_0 - \frac{1}{2}a_1 + \frac{1}{4}a_2$	$-\frac{1}{2}a_1 + a_2 - \frac{1}{2}a_3$
$n \geq 3$	$\frac{1}{4}a_{n-2} - \frac{1}{2}a_{n-1} + \frac{1}{4}a_n$	$-\frac{1}{2}a_{n-1} + a_n - \frac{1}{2}a_{n+1}$

The remaining two terms in (A.4) are bounded in a similar manner so that

$$K_3 := \sum_{l=0}^{\infty} \sum_{n \in I_p(l)} l^{-2p-1} r_{|n-i|, l+j} = \mathcal{O} \left(\min\{j^{-m-1}, i^{-\min\{m+1, 2p+1\}}\} \right)$$

$$K_4 := \sum_{l=0}^{\infty} \sum_{n \in I_p(l)} l^{-2p-1} r_{|n-i|, |l-j|} = \mathcal{O} \left(\min\{j^{-\min\{m+1, 2p+1\}}, i^{-\min\{m+1, 2p+1\}}\} \right)$$

Finally, considering all the bounds yields the stated result. The ρ -analytic case follows from the same arguments.

A.4. Some properties of Chebyshev polynomials

The next two identities follow directly from the explicit definition of Chebyshev polynomials as $T_n(t) = \cos(n \arccos(t))$.

LEMMA A.4.1. *For $n, k \in \mathbb{N}_0$, let T_n and T_k denote two Chebyshev polynomials of first kind. Then,*

$$T_n T_k = \frac{1}{2} (T_{n+k} + T_{|n-k|}).$$

Moreover, for $(t, s) \in [-1, 1]^2$, it holds

$$|t - s|^2 = 1 + \frac{1}{2} (T_2(t) + T_2(s)) - 2T_1(t)T_1(s).$$

LEMMA A.4.2. *Consider a function of the form:*

$$U(t, s) = \sum_{n=0}^{\infty} a_n T_n(t) T_{|n-k|}(s).$$

Then,

$$|t - s|^2 U(t, s) = \sum_{j \in \{-1, 0, 1\}} \sum_{n=0}^{\infty} \beta_n^{(j)} T_n(t) T_{|n-k+2j|}(s),$$

wherein

$$\beta_n^{(1)} := \frac{1}{4}a_n - \frac{1}{2}a_{n+1} + \frac{1}{4}a_{n+2},$$

and coefficients $\beta_n^{(-1)}$ and $\beta_n^{(0)}$ are given in Table A.1 for $n \in \mathbb{N}_0$.

PROOF. Using Lemma A.4.1, we have that

$$\begin{aligned} |t - s|^2 U(t, s) &= \sum_{n=0}^{\infty} a_n (T_n(t) T_{|n-k|}(s) + \frac{1}{4} T_{n+2}(t) T_{|n-k|}(s) + \frac{1}{4} T_{|n-2|}(t) T_{|n-k|}(s) \\ &\quad + \frac{1}{4} T_n(t) T_{||n-k|+2|} + \frac{1}{4} T_n(t) T_{|n-k-2|} \\ &\quad - \frac{1}{2} [T_{|n-k|+1}(s) + T_{|n-k|-1}(s)] [T_{|n-1|}(t) + T_{n+1}]) \end{aligned}$$

Observe that, for $i \in \{1, 2\}$, the index sums

$$|n - k| + i = \begin{cases} |n - k + i| & n \geq k, \\ |n - k - i| & n < k, \end{cases} \quad ||n - k| - i| = \begin{cases} |n - k - i| & n \geq k, \\ |n - k + i| & n < k. \end{cases}$$

Employing this in writing $|t - s|^2 U(t, s)$ as a series expansion, we find expressions for different $u_n(s)$:

$$\begin{aligned} u_0 &= \frac{a_0}{4} T_{|k+2|}(s) + \left(a_0 - \frac{a_1}{2}\right) T_{|k|}(s) + \left(\frac{a_0}{4} - \frac{a_1}{2} + \frac{a_2}{4}\right) T_{|k-2|}(s) \\ u_1 &= \left(-a_0 + \frac{a_1}{4}\right) T_{|k+1|}(s) - \left(a_0 + \frac{5a_1}{4} + \frac{a_2}{2}\right) T_{|1-k|}(s) + \left(\frac{a_1}{4} - \frac{a_2}{2} + \frac{a_3}{4}\right) T_{|k-3|}(s) \\ u_2 &= \left(\frac{a_0}{2} - \frac{a_1}{2} + \frac{a_2}{4}\right) T_{|k|}(s) - \left(\frac{a_1}{2} - a_2 + \frac{a_3}{2}\right) T_{|k-2|}(s) + \left(\frac{a_2}{4} - \frac{a_3}{2} + \frac{a_4}{4}\right) T_{|k-4|}(s) \\ u_n &= \left(\frac{a_{n-2}}{4} - \frac{a_{n-1}}{2} + \frac{a_n}{4}\right) T_{|n-k-2|}(s) + \left(-\frac{a_{n-1}}{2} + a_n - \frac{a_{n+1}}{2}\right) T_{|n-k|}(s) \\ &\quad + \left(\frac{a_n}{4} - \frac{a_{n+1}}{2} + \frac{a_{n+2}}{4}\right) T_{|n-k+2|}(s) \end{aligned}$$

for $n \geq 3$, yielding the stated result. \square

APPENDIX B. ON THE PROPERTIES OF QUASI-PERIODIC BOUNDARY INTEGRAL OPERATORS FOR THE HELMHOLTZ EQUATION

The following Annex is a transcription of a publication with the same title which is refereed in Chapter 3. It is not included in the body of the thesis as some policies of the school prevent a publication to appear in two different thesis.

B.1. Introduction

Due to its multiple applications in engineering and technology, considerable attention has been devoted to the mathematical modeling and computational simulation of acoustic and electromagnetic wave diffraction by periodic or bi-periodic structures in unbounded domains (*cf.* (Bao, 2004; Lechleiter & Zhang, 2016; Pestourie et al., 2018; Oughstun, 1982; Shiraishi, Higuchi, Muraki, & Yoda, 2016; Silva-Oelker, Aylwin, et al., 2018; Silva-Oelker, Jerez-Hanckes, & Fay, 2018) and references therein). Among the various numerical methods devised to tackle the forward problem of finding the scattered field, one finds (i) homogenization techniques for periodic gratings with periods much smaller than the incoming wave's wavelength (Ammari & He, 1997); (ii) volume formulations in truncated domains with Dirichlet-to-Neumann (DtN) maps imposing suitable radiation conditions at infinity (Bao & Dobson, 2000; Bao et al., 1995; Dobson, 1994; Starling & Bonnet-Bendhia, 1994); (iii) boundary integral methods based on the integral representation formula to condense the problem to the grating surface (Barnett & Greengard, 2011; Cho & Barnett, 2015; Dobson & Cox, 1991; Dobson & Friedman, 1992; Liu & Barnett, 2016; Nédélec & Starling, 1991); and, (iv) hybrid methods coupling finite and boundary element methods (Ammari & Bao, 2008; Ammari & Nédélec, 2001). In this note, we are primarily concerned with theoretical aspects linked to the last two techniques as these hinge on the properties of the boundary integral operators (BIOs) built upon the quasi-periodic Green's function (Bruno & Fernandez-Lado, 2017; X. Chen & Friedman, 1991; Cho & Barnett, 2015; Linton, 1998; Nédélec & Starling, 1991). We will not consider the case of Rayleigh-Wood frequencies –frequencies for which the sum defining the quasi-periodic Green's function

ceases to converge— since their analysis lies beyond the scope of this article and several of the aforementioned references address this case.

Classically, the unique solvability of boundary integral equations (BIEs) for the two-dimensional scattering of time-harmonic waves by periodic structures is commonly established via Fredholm operator theory. This is achieved by acknowledging that the quasi-periodic Green's function and the fundamental solution for the Helmholtz operator have the same singularity order. However, this approach requires the scatterer surface to be at least twice continuously differentiable, which makes the strategy inadequate for Lipschitz continuous scatterers (see, for example, the geometric restrictions enforced to derive existence and uniqueness results in (Bruno & Fernandez-Lado, 2017; Lai, Kobayashi, & Barnett, 2015; Nédélec & Starling, 1991; Schmidt, 2009, 2011)). In this work, we present an alternative strategy based on the mapping properties of BIOs, which relies on suitable definitions of quasi-periodic Sobolev spaces for arbitrary order $s \in \mathbb{R}$. This allows for an analysis similar to that presented by Costabel (Costabel, 1988) in the case of bounded obstacles. An equivalent space definition was already introduced in (Alber, 1979; Nédélec & Starling, 1991; Starling & Bonnet-Bendhia, 1994) for the particular case of $s = 1$. Moreover, we study properties of quasi-periodic BIOs that have, to our knowledge, not been presented before, such as the coercivity of the weakly-singular and hyper-singular quasi-periodic BIOs.

Existence and uniqueness results will play a critical role in our analysis, since the general definition of BIOs require the use of the so-called *solution operators* that map boundary conditions to the solution of the scattering problem. Dirichlet, Neumann and transmission problems are known to possess unique solutions for all but a countable set of wavenumbers (Elschner & Schmidt, 1998; Nédélec & Starling, 1991; Starling & Bonnet-Bendhia, 1994) and, under more stringent geometrical assumptions, uniqueness is ensured for all wavenumbers for the Dirichlet problem (Alber, 1979; Kirsch, 1993, 1994). We could not find similar results for the Neumann problem. Thus, our main contributions are the derivation of continuity and coercivity results for the relevant quasi-periodic BIOs (Theorems B.12 and B.13), as well as existence and uniqueness results for first-kind BIEs (Theorems

B.14 and B.15). In particular, we rigorously extend the Dirichlet trace to quasi-periodic Sobolev spaces of order $s > \frac{1}{2}$, thereby improving the proof in (Nédélec & Starling, 1991; Starling & Bonnet-Bendhia, 1994) holding only for $s = 1$.

This article is structured as follows. In Section B.2 we introduce conventions used throughout as well as the definition of quasi-periodic Sobolev spaces. Section B.3 is devoted to the analysis of the volume problem following (Bao, 1995; Elschner & Schmidt, 1998; Nédélec & Starling, 1991; Starling & Bonnet-Bendhia, 1994) in order to build appropriate radiation conditions to guarantee well-posedness. Novel properties of the arising quasi-periodic BIOs are provided in Section B.4 and are deduced after generalizing tools given in (Costabel, 1988; Kress, 2014) to the quasi-periodic setting. Finally, concluding remarks are found in Section B.5 along with appendices containing technical results.

B.2. Functional space framework

B.2.1. General notation

Let B be a Banach space. We denote its norm as $\|\cdot\|_B$ and its dual space by B' , where we consider elements of B' as antilinear rather than linear forms over B . If B is Hilbert, we shall denote the inner product between two elements $x, y \in B$ as $(x, y)_B$, unless stated otherwise. For the special case $B = \mathbb{R}^2$ or \mathbb{C}^2 , we write the inner product between $\mathbf{x}, \mathbf{y} \in B$ as $\mathbf{x} \cdot \overline{\mathbf{y}}$, where the bar represents complex conjugation.

For $d = 1, 2$, let $\Omega \subset \mathbb{R}^d$ be an open domain and denote its boundary $\partial\Omega$. For any $\Upsilon \subset \mathbb{R}^d$ such that $\Omega \subseteq \Upsilon$, we define $\overline{\Omega}^\Upsilon := \overline{\Omega} \cap \Upsilon$ and $\partial^\Upsilon\Omega := \overline{\Omega}^\Upsilon \setminus \Omega$. We denote the set of continuous scalar functions in Ω with complex values as $\mathcal{C}(\Omega)$ and define, for $n \in \mathbb{N}_0$,

the following spaces of continuous functions:

$$\begin{aligned}\mathcal{C}^n(\Omega) &:= \{u \in \mathcal{C}(\Omega) \mid \partial^\beta u \in \mathcal{C}(\Omega) \forall \beta \in \mathbb{N}^d, \text{ with } |\beta| \leq n\}, \\ \mathcal{C}_0^n(\Omega) &:= \{u \in \mathcal{C}^n(\Omega) \mid \text{supp } u \subset\subset \Omega\}, \\ \mathcal{C}^\infty(\Omega) &:= \{u \in \mathcal{C}(\Omega) \mid \partial^\beta u \in C(\Omega) \forall \beta \in \mathbb{N}^d\}, \\ \mathcal{D}(\Omega) &:= \{u \in \mathcal{C}^\infty(\Omega) \mid \text{supp } u \subset\subset \Omega\},\end{aligned}$$

where the multi-index $\beta = (\beta_1, \beta_2) \in \mathbb{N}^2$ with $|\beta| = \beta_1 + \beta_2$.

We say that a one-dimensional curve Γ is of class $\mathcal{C}^{r,1}$, for $r \in \mathbb{N}_0$, if it may be parametrized by a continuous function $\mathbf{z} : (0, 2\pi) \rightarrow \Gamma$ so that \mathbf{z} has continuous derivatives up to order r and its derivatives of order r are Lipschitz continuous.

The space of antilinear distributions on Ω is referred to as $\mathcal{D}'(\Omega)$, and its duality pairing with $\mathcal{D}(\Omega)$ is written as

$$f(u) = \langle f, u \rangle_\Omega,$$

for any $f \in \mathcal{D}'(\Omega)$ and $u \in \mathcal{D}(\Omega)$. As usual, we can identify $f \in L^1_{\text{loc}}(\mathbb{R}^d)$ with an element of $\mathcal{D}'(\mathbb{R}^d)$, denoted f , as:

$$\langle f, u \rangle_{\mathbb{R}^d} := \int_{\mathbb{R}^d} f(\mathbf{x}) \overline{u(\mathbf{x})} \, d\mathbf{x}, \quad u \in \mathcal{D}(\mathbb{R}^d).$$

For $s \geq 0$ and $p \geq 1$, $W^{s,p}(\Omega)$ denotes standard Sobolev spaces on Ω (McLean, 2000, Chapter 3.5). For $s \in \mathbb{R}$, we also introduce the spaces $H^s(\Omega)$, $H^s_0(\Omega)$ and $\tilde{H}^s(\Omega)$ as the second family of Sobolev spaces of order s defined in (McLean, 2000, Chapter 3.6). Recall the equivalence $W^{s,2}(\Omega) \equiv H^s(\Omega)$ (assuming Ω is a Lipschitz domain). We shall also make use of the Sobolev space $H^s[0, 2\pi]$ given in (Kress, 2014, Chapter 8).

Finally, we shall use the symbols \lesssim , \gtrsim , and \cong to avoid specifying constants, which do not depend on values relevant to the corresponding analysis.

B.2.2. Quasi-periodic functions and distributions

The definitions and results in the present subsection extend the notions presented in (Saranen & Vainikko, 2013, Chapter 5.2), dealing with periodic distributions, to the quasi-periodic setting. Set $\{\mathbf{e}_i\}_{i=1}^2$ as the canonical orthonormal basis of \mathbb{R}^2 . Let $\theta \geq 0$ and $\ell > 0$.

Definition B.1 (Quasi-periodic function). *A function $\psi : \mathbb{R}^2 \rightarrow \mathbb{C}$ is said to be quasi-periodic with shift θ and period ℓ if*

$$\psi(\mathbf{x} + \ell \mathbf{e}_1) = e^{i\ell\theta} \psi(\mathbf{x}) \quad \forall \mathbf{x} \in \mathbb{R}^2.$$

For any $n \in \mathbb{Z}$ and for all $\mathbf{x} \in \mathbb{R}^2$, it holds

$$\psi(\mathbf{x} + n\ell \mathbf{e}_1) = e^{i\ell\theta n} \psi(\mathbf{x}),$$

and $e^{-ix_2\theta} \psi(\mathbf{x})$ is x_2 -periodic with period ℓ . Following (Alber, 1979; Nédélec & Starling, 1991), we define $\mathcal{D}_{\theta,\ell}(\mathbb{R}^2)$ as the set of $\mathcal{C}^\infty(\mathbb{R}^2)$ -functions vanishing for large $|x_2|$ and that are quasi-periodic with shift θ and period ℓ in the direction of \mathbf{e}_1 . In order to properly define quasi-periodic distributions, we introduce the next operator.

Definition B.2 (Translation operator). *Let $s \in \mathbb{R}$, $j \in \mathbb{N}$. We define the translation operator:*

$$\tau_s := \begin{cases} \mathcal{D}(\mathbb{R}^2) & \rightarrow \mathcal{D}(\mathbb{R}^2) \\ \psi(\mathbf{x}) & \mapsto \psi(\mathbf{x} + s\mathbf{e}_1) \end{cases}.$$

It follows that $\tau_{s_1} \circ \tau_{s_2} = \tau_{s_1+s_2}$. Let now $n \in \mathbb{Z}$ and $\psi \in \mathcal{D}(\mathbb{R}^2)$. We say that $f \in L^1_{\text{loc}}(\mathbb{R}^2)$ is quasi-periodic with shift θ and period ℓ if, for all $n \in \mathbb{Z}$,

$$\int_{\mathbb{R}^2} f(\mathbf{x}) \overline{\tau_{n\ell} \psi(\mathbf{x})} \, d\mathbf{x} = \int_{\mathbb{R}^2} f(\mathbf{x} - n\ell \mathbf{e}_1) \overline{\psi(\mathbf{x})} \, d\mathbf{x} = e^{-in\ell\theta} \int_{\mathbb{R}^2} f(\mathbf{x}) \overline{\psi(\mathbf{x})} \, d\mathbf{x}.$$

Definition B.3 (Quasi-periodic distribution). *We say that a distribution $f \in \mathcal{D}'(\mathbb{R}^2)$ is quasi-periodic with shift θ and period ℓ if, for all $n \in \mathbb{Z}$ and $\psi \in \mathcal{D}(\mathbb{R}^2)$, there holds*

$$\langle f, \tau_{n\ell}\psi \rangle_{\mathbb{R}^2} = e^{-in\ell\theta} \langle f, \psi \rangle_{\mathbb{R}^2}.$$

We write $\mathcal{D}'_{\theta,\ell}(\mathbb{R}^2)$ for the space of quasi-periodic distributions with shift θ and period ℓ . Their action on elements of $\mathcal{D}_{\theta,\ell}(\mathbb{R}^2)$ is understood as

$$\langle u, v \rangle_{\theta,\ell} := \langle u, \Theta_\ell v \rangle_{\mathbb{R}^2}, \quad \forall u \in \mathcal{D}'_{\theta,\ell}(\mathbb{R}^2) \quad \forall v \in \mathcal{D}_{\theta,\ell}(\mathbb{R}^2),$$

where $\Theta_\ell \in \mathcal{D}(\mathbb{R})$ is a one-dimensional periodic function such that (cf. (Jerez-Hanckes, 2008, Section 3.2.1) or (Saranen & Vainikko, 2013, Equation 5.11))

$$\sum_{j \in \mathbb{Z}} \Theta_\ell(x_1 + j\ell) = 1, \quad \forall x_1 \in \mathbb{R}.$$

Furthermore, one can check that $\mathcal{D}'_{\theta,\ell}(\mathbb{R}^2)$ is indeed the dual space of $\mathcal{D}_{\theta,\ell}(\mathbb{R}^2)$.

PROPOSITION B.1. *Let T be an element of the dual space of $\mathcal{D}_{\theta,\ell}(\mathbb{R}^2)$, then the distribution F_T defined, for all ϕ in $\mathcal{D}(\mathbb{R}^2)$, as*

$$\langle F_T, \phi \rangle_{\mathbb{R}^2} = T \left(\sum_{j \in \mathbb{Z}} \exp(-i\theta j\ell) \tau_{j\ell} \phi \right),$$

is such that $F_T \in \mathcal{D}'_{\theta,\ell}(\mathbb{R}^2)$ and $\langle F_T, \varphi \rangle_{\theta,\ell} = T(\varphi)$ for all $\varphi \in \mathcal{D}_{\theta,\ell}(\mathbb{R}^2)$.

PROOF. Given $\varphi \in \mathcal{D}_{\theta,\ell}(\mathbb{R}^2)$, it is easy to see that

$$\sum_{j \in \mathbb{Z}} \exp(-i\theta j\ell) \tau_{j\ell} (\Theta_\ell(x_1) \varphi(\mathbf{x})) = \varphi(\mathbf{x}),$$

so that $\langle F_T, \varphi \rangle_{\theta,\ell} = T(\varphi)$. For any element $\phi \in \mathcal{D}(\mathbb{R}^2)$ and $m \in \mathbb{Z}$, we have

$$\begin{aligned} \langle F_T, \tau_{m\ell}\phi \rangle_{\mathbb{R}^2} &= T \left(\sum_{j \in \mathbb{Z}} \exp(-i\theta j\ell) \tau_{(j+m)\ell} \phi \right) \\ &= T \left(e^{i\theta m\ell} \sum_{j \in \mathbb{Z}} \exp(-i\theta j\ell) \tau_{j\ell} \phi \right) = e^{-i\theta m\ell} \langle F_T, \phi \rangle_{\mathbb{R}^2}. \end{aligned}$$

Thus, $F_T \in \mathcal{D}'_{\theta,\ell}(\mathbb{R}^2)$ by Definition B.3. \square

Equivalent results hold for spaces defined over open bounded and unbounded subsets of \mathbb{R}^d , $d = 1, 2$. We also introduce the quasi-periodic train of δ -distributions as it will be of later use.

Definition B.4 (Quasi-periodic train of δ -distributions). *We define the quasi-periodic train of δ -distributions, $\widehat{\delta}_{\theta,\ell}$ as:*

$$\widehat{\delta}_{\theta,\ell} := \sum_{j \in \mathbb{Z}} \delta(\mathbf{x} + j\ell \mathbf{e}_1) \exp(i\theta j\ell), \quad (\text{B.1})$$

which converges in $\mathcal{D}'(\mathbb{R}^2)$ and belongs to $\mathcal{D}'_{\theta,\ell}(\mathbb{R}^2)$.

For the remainder of this article, we restrict ourselves to quasi-periodic functions with period 2π in x_1 , which shall be henceforth referred to simply as *quasi-periodic with shift θ* , or θ -quasi-periodic. Thus, we employ the equivalences $\mathcal{D}_\theta(\mathbb{R}^2) \equiv \mathcal{D}_{\theta,2\pi}(\mathbb{R}^2)$ as well as $\langle \cdot, \cdot \rangle_\theta \equiv \langle \cdot, \cdot \rangle_{\theta,2\pi}$. Furthermore, it is clear that elements of both $\mathcal{D}_\theta(\mathbb{R}^2)$ and $\mathcal{D}'_\theta(\mathbb{R}^2)$ may formally be written as Fourier series.

PROPOSITION B.2 (Fourier expansion). *Let $j_\theta := j + \theta$ for all $j \in \mathbb{Z}$. Every $u \in \mathcal{D}_\theta(\mathbb{R}^2)$ and $F \in \mathcal{D}'_\theta(\mathbb{R}^2)$ may be represented as a Fourier series, i.e.*

$$u(x_1, x_2) = \sum_{j \in \mathbb{Z}} u_j(x_2) e^{ij_\theta x_1}, \quad F(x_1, x_2) = \sum_{j \in \mathbb{Z}} F_j(x_2) e^{ij_\theta x_1},$$

where the coefficients u_j and F_j belong to $\mathcal{D}(\mathbb{R})$ and $\mathcal{D}'(\mathbb{R})$, respectively.

PROOF. Let $u \in \mathcal{D}_\theta(\mathbb{R}^2)$, $F \in \mathcal{D}'_\theta(\mathbb{R}^2)$ and define, for $j \in \mathbb{Z}$,

$$u_j(x_2) := \frac{1}{2\pi} \langle e^{ij_\theta(\cdot)}, u(\cdot, x_2) \rangle_\theta = \frac{1}{2\pi} \int_0^{2\pi} e^{-ij_\theta x_1} u(x_1, x_2) \, dx_1.$$

Consequently, $u_j \in \mathcal{D}(\mathbb{R})$. Then, it holds

$$u(\mathbf{x}) = \sum_{j \in \mathbb{Z}} u_j(x_2) e^{ij_\theta x_1}, \quad \langle F, u \rangle_\theta = \sum_{j \in \mathbb{Z}} \langle F, u_j(x_2) e^{ij_\theta x_1} \rangle_\theta.$$

For each $j \in \mathbb{Z}$, let us introduce

$$F_j(x_2) := \begin{cases} \mathcal{D}(\mathbb{R}) & \rightarrow \mathbb{C} \\ v & \mapsto \langle F, v(x_2)e^{ij\theta x_1} \rangle_\theta \end{cases}.$$

Clearly, $F_j \in \mathcal{D}'(\mathbb{R})$ and $\langle F, u \rangle_\theta = \sum_{j \in \mathbb{Z}} \langle F_j, u_j \rangle_{\mathbb{R}}$, from where F may be represented as $F(x_1, x_2) = \sum_{j \in \mathbb{Z}} F_j(x_2)e^{ij\theta x_1}$. \square

To avoid redundancies, we limit the range of θ to $[0, 1)$. Indeed, notice that θ and $\theta + n$ define the same quasi-periodic spaces for any integer n .

B.2.3. Quasi-periodic Sobolev spaces

Let $\mathcal{G} := \{\mathbf{x} \in \mathbb{R}^2 \mid 0 < x_1 < 2\pi\}$ (see Figure B.3). We define $\mathcal{D}_\theta(\mathcal{G})$ as the set of restrictions to \mathcal{G} of elements of $\mathcal{D}_\theta(\mathbb{R}^2)$. For any open set $\mathcal{O} \subset \mathcal{G}$, we say that $u \in \mathcal{D}_\theta(\mathcal{O})$ if $u = U|_{\mathcal{O}}$ for some $U \in \mathcal{D}_\theta(\mathcal{G})$ such that $\overline{\text{supp } U}^{\mathcal{G}} \subset \mathcal{O}$. We define the restriction of $F \in \mathcal{D}'_\theta(\mathbb{R}^2)$ to \mathcal{O} , denoted $F|_{\mathcal{O}}$, as an antilinear map acting on $u \in \mathcal{D}_\theta(\mathcal{O})$ in the following manner

$$\langle F|_{\mathcal{O}}, u \rangle_{\mathcal{O}, \theta} := \langle F, U \rangle_\theta,$$

where U is an extension by zero of u to \mathcal{G} , which may then be easily extended to an element of $\mathcal{D}_\theta(\mathbb{R}^2)$. Furthermore, we introduce $\mathcal{D}'_\theta(\mathcal{O})$ as the space of these restrictions.

Definition B.5 (Quasi-periodic Sobolev spaces). *Set $s \in \mathbb{R}$ and let $j_\theta := j + \theta$ for all $j \in \mathbb{Z}$. Recall that u_j denotes the j -th Fourier coefficient of u (cf. Proposition B.2). Let us introduce the quasi-periodic Bessel potential*

$$\mathcal{J}_\theta^s(u)(\xi_1, \xi_2) := \sum_{j \in \mathbb{Z}} (1 + j_\theta^2 + |\xi_2|^2)^{\frac{s}{2}} \widehat{u}_j(\xi_2) e^{i\xi_1 j_\theta}, \quad \forall \xi_1, \xi_2 \in \mathcal{G},$$

wherein $\widehat{u}_j(\xi_2)$ are the Fourier transforms of $u_j(x_2)$ in distributional sense. We define the quasi-periodic Sobolev space $H_\theta^s(\mathcal{G})$ as

$$H_\theta^s(\mathcal{G}) := \left\{ u \in \mathcal{D}'_\theta(\mathbb{R}^2) : u = \sum_{j \in \mathbb{Z}} u_j e^{ij_\theta x_1}, u_j \in H^s(\mathbb{R}) \text{ and } \mathcal{J}_\theta^s(u) \in L_\theta^2(\mathcal{G}) \right\},$$

with

$$L_\theta^2(\mathcal{G}) \equiv H_\theta^0(\mathcal{G}) := \left\{ u \in \mathcal{D}'_\theta(\mathbb{R}^2) : \sum_{j \in \mathbb{Z}} \|u_j\|_{L^2(\mathbb{R})}^2 < \infty \right\}.$$

Furthermore, we shall identify elements of $H_\theta^s(\mathcal{G})$ with their restrictions to \mathcal{G} . Notice that $L_\theta^2(\mathcal{G})$ is a Hilbert space with inner product given by

$$(u, v)_{L_\theta^2(\mathcal{G})} := \sum_{j \in \mathbb{Z}} (u_j, v_j)_{L^2(\mathbb{R})}.$$

It is natural, then, to consider the following norm on $H_\theta^s(\mathcal{G})$:

$$\|u\|_{H_\theta^s(\mathcal{G})} := \|\mathcal{J}_\theta^s(u)\|_{L_\theta^2(\mathcal{G})}, \quad \forall u \in H_\theta^s(\mathcal{G}),$$

from where it follows directly that the quasi-periodic Bessel potential, as an operator $\mathcal{J}_\theta^s : H_\theta^s(\mathcal{G}) \rightarrow L_\theta^2(\mathcal{G})$ is an isometric isomorphism. This last statement can be verified by proceeding analogously to the construction of the usual Sobolev spaces $H^s(\mathbb{R}^n)$ for $n \in \mathbb{N}$ (McLean, 2000, Chapter 3.6). The same is true for the following proposition and we omit its proof.

PROPOSITION B.3. *Let $s \in \mathbb{R}$. Then, $\mathcal{D}_\theta(\mathcal{G})$ is dense in $H_\theta^s(\mathcal{G})$ and $H_\theta^s(\mathcal{G})$ is a Hilbert space with inner product and norm respectively defined as*

$$(u, v)_{H_\theta^s(\mathcal{G})} := (\mathcal{J}_\theta^s u, \mathcal{J}_\theta^s v)_{L_\theta^2(\mathcal{G})}, \quad \|u\|_{H_\theta^s(\mathcal{G})} := (u, u)_{H_\theta^s(\mathcal{G})}^{\frac{1}{2}}.$$

From the density of trigonometric polynomials in $L^2([0, 2\pi])$, it holds $L_\theta^2(\mathcal{G}) \equiv L^2(\mathcal{G})$, so that we can identify the dual space of $L_\theta^2(\mathcal{G})$ with itself. Then, we can characterize the dual of $H_\theta^s(\mathcal{G})$ by an isometric isomorphic space to $H_\theta^{-s}(\mathcal{G})$ and introduce the *Gelfand triple* $H_\theta^s(\mathcal{G}) \subseteq L_\theta^2(\mathcal{G}) \subseteq H_\theta^{-s}(\mathcal{G})$ for positive $s \in \mathbb{R}$. Proposition B.3 and its form for

$H_\theta^s(\mathcal{O})$ may be proved using analogous arguments as for the construction of usual Sobolev spaces of order $s \in \mathbb{R}$ (McLean, 2000, Chapter 3).

One can easily check that the spaces defined as the closure of $\mathcal{D}_\theta(\mathcal{G})$ for positive $s \in \mathbb{Z}$, i.e. $\overline{\mathcal{D}_\theta(\mathcal{G})}^{\|\cdot\|_{H^s(\mathcal{G})}}$, introduced in (Alber, 1979) and revisited in (Ammari & Bao, 2008; Nédélec & Starling, 1991; Starling & Bonnet-Bendhia, 1994), are equivalent to the spaces $H_\theta^s(\mathcal{G})$ in Definition B.5. For spaces of non-integer order, the result follows by direct application of interpolation theory.

Theorem B.1. *For any $0 \leq s < \infty$, the norms $\|\cdot\|_{H_\theta^s(\mathcal{G})}$ and $\|\cdot\|_{H^s(\mathcal{G})}$ are equivalent in $H_\theta^s(\mathcal{G})$. Hence, $H_\theta^s(\mathcal{G})$ may be equivalently defined as $\overline{\mathcal{D}_\theta(\mathcal{G})}^{\|\cdot\|_{H^s(\mathcal{G})}}$.*

PROOF. Take $s \in \mathbb{N}_0$, then $H^s(\mathcal{G}) = W^{s,2}(\mathcal{G})$. For $u \in \mathcal{D}_\theta(\mathcal{G})$ and for a multi-index $\alpha = (\alpha_1, \alpha_2) \in \mathbb{N}_0^2$, it holds

$$\begin{aligned}
\|u\|_{H^s(\mathcal{G})}^2 &= \sum_{|\alpha| \leq s} \|D^\alpha u\|_{L^2(\mathcal{G})}^2 = \sum_{|\alpha| \leq s} \left\| D^\alpha \sum_{j \in \mathbb{Z}} u_j(x_2) e^{ij_\theta x_1} \right\|_{L^2(\mathcal{G})}^2 \\
&= \sum_{\alpha_1 + \alpha_2 \leq s} \left\| \sum_{j \in \mathbb{Z}} D^{\alpha_2} u_j(x_2) (ij_\theta)^{\alpha_1} e^{ij_\theta x_1} \right\|_{L^2(\mathcal{G})}^2 \\
&= \sum_{\alpha_1 + \alpha_2 \leq s} \sum_{j \in \mathbb{Z}} j_\theta^{2\alpha_1} \|D^{\alpha_2} u_j(x_2)\|_{L^2(\mathbb{R})}^2 \\
&\cong \sum_{j \in \mathbb{Z}} \sum_{\alpha_1 + \alpha_2 \leq s} j_\theta^{2\alpha_1} \|\xi_2^{\alpha_2} \widehat{u}_j(\xi_2)\|_{L^2(\mathbb{R})}^2 \\
&= \sum_{j \in \mathbb{Z}} \sum_{\alpha_1 + \alpha_2 \leq s} \|j_\theta^{\alpha_1} \xi_2^{\alpha_2} \widehat{u}_j(\xi_2)\|_{L^2(\mathbb{R})}^2 \\
&\cong \sum_{j \in \mathbb{Z}} \left\| (1 + j_\theta^2 + \xi_2^2)^{\frac{s}{2}} \widehat{u}_j(\xi_2) \right\|_{L^2(\mathbb{R})}^2 = \|u\|_{H_\theta^s(\mathcal{G})}^2.
\end{aligned}$$

The extension to $u \in H_\theta^s(\mathcal{G})$ follows by a density argument. An interpolation argument via the K -method yields the same result for positive $s \in \mathbb{R}$ (see (McLean, 2000, Appendix B) or (Tartar, 2007)). \square

Definition B.6. Let $s \in \mathbb{R}$. For open subsets of \mathcal{G} , i.e. $\mathcal{O} \subset \mathcal{G}$, we define $H_\theta^s(\mathcal{O})$ as restrictions of elements of $H_\theta^s(\mathcal{G})$ to \mathcal{O} , i.e.

$$H_\theta^s(\mathcal{O}) := \{u \in \mathcal{D}'_\theta(\mathcal{O}) : u = U|_\Omega \text{ and } U \in H_\theta^s(\mathcal{G})\}.$$

As in the standard case, we may construct a unitary isomorphism $P_{s,\theta,\mathcal{O}}$ mapping a closed subspace of $H_\theta^s(\mathcal{G})$ onto $H_\theta^s(\mathcal{O})$, whereby an inner product may be defined on $H_\theta^s(\mathcal{O})$ as

$$(u, v)_{H_\theta^s(\mathcal{O})} := (P_{s,\theta,\mathcal{O}}^{-1}(u), P_{s,\theta,\mathcal{O}}^{-1}(v))_{H_\theta^s(\mathcal{G})}.$$

Moreover, the same isomorphism allows us to verify that $H_\theta^s(\mathcal{O})$ is a Hilbert space with the aforementioned inner product. The complete argument is the same than for classical Sobolev spaces (see (McLean, 2000, Chapter 3.6)).

Let $\mathcal{O} \subset \mathcal{G}$ be open and $s \in \mathbb{R}$. That $H_\theta^s(\mathcal{O})$ is a Hilbert space is easily verified through the same procedure as in (McLean, 2000, Chapter 3.6) for the usual Sobolev spaces of order $s \in \mathbb{R}$.

Corollary B.1. Let \mathcal{O} be an open set such that $\overline{\mathcal{O}} \subset \mathcal{G}$, then

$$H_\theta^s(\mathcal{O}) = H^s(\mathcal{O}) \quad \forall s \in \mathbb{R}.$$

PROOF. Notice that $\mathcal{D}(\overline{\mathcal{O}}) = \mathcal{D}_\theta(\mathcal{G})|_\mathcal{O}$. Then, the result follows from the equivalence of norms given in Theorem B.1 and corresponding densities of $\mathcal{D}(\overline{\mathcal{O}})$ in $H^s(\mathcal{O})$ (McLean, 2000, Chapter 3), and $\mathcal{D}_\theta(\mathcal{G})|_\mathcal{O}$ in $H_\theta^s(\mathcal{O})$. \square

Definition B.7. We introduce the Sobolev space of quasi-periodic functions

$$\tilde{H}_\theta^s(\mathcal{O}) := \overline{\mathcal{D}_\theta(\mathcal{O})}^{\|\cdot\|_{H_\theta^s(\mathcal{G})}}.$$

Just as with classical Sobolev spaces, it is possible to show that $(H_\theta^s(\mathcal{O}))'$ and $\tilde{H}_\theta^{-s}(\mathcal{O})$ are isometric and isomorphic under some assumptions on the regularity of \mathcal{O} . We shall also introduce local Sobolev spaces of quasi-periodic functions as they play a key role in the formulation of problems in unbounded domains. Let the θ -quasi-periodic local Sobolev

space of order $s \in \mathbb{R}$ be defined as follows

$$H_{\theta, \text{loc}}^s(\mathcal{O}) := \{u \in \mathcal{D}'_\theta(\mathcal{O}) \mid u \in H_\theta^s(\mathcal{O}^R) \forall R > 0\}, \quad (\text{B.2})$$

where $\mathcal{O}^R := \mathcal{O} \cap \{|x_2| < R\}$. An operator with range in $H_{\theta, \text{loc}}^s(\mathcal{O})$ is said to be bounded if it is bounded on $H_\theta^s(\mathcal{O}^R)$ for all $R > 0$.

We now characterize quasi-periodic Sobolev spaces on one-dimensional boundaries to be used when introducing trace spaces.

Definition B.8 (Definition 8.1 in (Kress, 2014)). *Let $0 \leq s < \infty$. We define $H^s[0, 2\pi]$ as*

$$H^s[0, 2\pi] := \left\{ \varphi \in L^2((0, 2\pi)) \mid \sum_{j \in \mathbb{Z}} (1 + j^2)^s |\varphi_j|^2 < \infty \right\},$$

where $\{\varphi_j\}_{j \in \mathbb{Z}}$ are the Fourier coefficients for $\varphi \in L^2((0, 2\pi))$.

Though we choose to follow the presentation in (Kress, 2014, Chapters 8.1 and 8.2) throughout this subsection, similar results for $H^s[0, 2\pi]$ may be found in (Saranen & Vainikko, 2013, Chapter 5.3), including a definition analogous to Definition B.8.

Theorem B.2 (Theorem 8.2 in (Kress, 2014)). *For $0 \leq s < \infty$, $H^s[0, 2\pi]$ is a Hilbert space with inner product and induced norm given by*

$$(u, v)_{H^s[0, 2\pi]} := \sum_{j \in \mathbb{Z}} (1 + j^2)^s u_j \overline{v_j}, \quad \|u\|_{H^s[0, 2\pi]} := (u, u)_{H^s[0, 2\pi]}^{\frac{1}{2}}.$$

Definition B.9. *Let $0 \leq s < \infty$. We define $H_\theta^s[0, 2\pi]$ as*

$$H_\theta^s[0, 2\pi] := \{\varphi \in L^2((0, 2\pi)) \mid e^{-i\theta x} \varphi(x) \in H^s[0, 2\pi]\}.$$

Theorem B.3. *For $0 \leq s < \infty$, $H_\theta^s[0, 2\pi]$ is a Hilbert space with inner product and induced norm given by*

$$(u, v)_{H_\theta^s[0, 2\pi]} := \sum_{j \in \mathbb{Z}} (1 + j_\theta^2)^s u_{j, \theta} \overline{v_{j, \theta}}, \quad \|u\|_{H_\theta^s[0, 2\pi]} := (u, u)_{H_\theta^s[0, 2\pi]}^{\frac{1}{2}},$$

respectively, wherein

$$u_{j,\theta} = \frac{1}{2\pi} \int_0^{2\pi} e^{-\imath jx} e^{-\imath \theta x} u(x) \, dx.$$

PROOF. Let

$$\mathbf{i} : \begin{cases} H_\theta^s[0, 2\pi] & \rightarrow H^s[0, 2\pi] \\ u & \mapsto e^{-\imath \theta x} u \end{cases}.$$

Then, $H_\theta^s[0, 2\pi]$ equipped with the product and norm

$$(u, v)_\mathbf{i} := (\mathbf{i}u, \mathbf{i}v)_{H^s[0, 2\pi]}, \quad \|u\|_\mathbf{i} := \|\mathbf{i}u\|_{H^s[0, 2\pi]},$$

is a Hilbert space. It is easy to see that $(\cdot, \cdot)_{H_\theta^s[0, 2\pi]}$ is an inner product on $H_\theta^s[0, 2\pi]$ and that, therefore, $\|\cdot\|_{H_\theta^s[0, 2\pi]}$ is a norm. Completeness follows from noticing that, since $\theta \in [0, 1)$,

$$(1 + j_\theta^2) = (1 + j^2 + 2j\theta + \theta^2) < (1 + 2\theta)(1 + j^2),$$

so that, for all $u \in H_\theta^s[0, 2\pi]$, it holds

$$\|u\|_{H_\theta^s[0, 2\pi]}^2 < (1 + 2\theta)^s \|u\|_\mathbf{i}^2.$$

Similarly,

$$\begin{aligned} (1 + j^2) &= (1 + j_\theta^2 + \theta^2 - 2\theta j_\theta) \leq (1 + j_\theta^2 + \theta + 2\theta |j_\theta|) \\ &\leq \left(1 + j_\theta^2 + \theta + 2\theta \frac{j_\theta^2}{1 - \theta}\right) \leq \left(1 + 2\frac{\theta}{1 - \theta}\right) (1 + j_\theta^2), \end{aligned}$$

so that

$$\|u\|_\mathbf{i}^2 \leq \left(1 + 2\frac{\theta}{1 - \theta}\right)^s \|u\|_{H_\theta^s[0, 2\pi]}^2.$$

Hence, both norms are equivalent and the statement holds. \square

Definition B.10 (Definition 8.9 in (Kress, 2014)). *For $0 \leq s < \infty$, we define $H^{-s}[0, 2\pi]$ as the dual space of $H^s[0, 2\pi]$.*

Theorem B.4 (Theorem 8.10 in (Kress, 2014)). *For $0 \leq s < \infty$, the norm and product for $F, L \in H^{-s}[0, 2\pi]$ are given by*

$$(F, L)_{H^{-s}[0, 2\pi]} := \sum_{j \in \mathbb{Z}} (1 + j^2)^s F_j \overline{L_j}, \quad \|F\|_{H^{-s}[0, 2\pi]} := (F, F)_{H^{-s}[0, 2\pi]}^{\frac{1}{2}},$$

where $F_j := \frac{1}{2\pi} F(e^{ijx})$ and analogously for L_j .

Definition B.11. *For $0 \leq s < \infty$, $H_\theta^{-s}[0, 2\pi]$ is the dual space of $H_\theta^s[0, 2\pi]$.*

Theorem B.5. *For $0 \leq s < \infty$, $H_\theta^{-s}[0, 2\pi]$ is isomorphic to $H^{-s}[0, 2\pi]$. Moreover, $F \in H_\theta^{-s}[0, 2\pi]$ may be represented as*

$$F = \sum_{j \in \mathbb{Z}} F_{j,\theta} e^{ij_\theta x},$$

with $F_{j,\theta} := \frac{1}{2\pi} F(e^{ij_\theta x})$, and its action on $u \in H_\theta^s[0, 2\pi]$ is given by

$$F(u) = \sum_{j \in \mathbb{Z}} F_{j,\theta} \overline{u_{j,\theta}}.$$

Also, $H_\theta^{-s}[0, 2\pi]$ is a Hilbert space when equipped with inner product and norm

$$(F, L)_{H_\theta^{-s}[0, 2\pi]} := \sum_{j \in \mathbb{Z}} (1 + j_\theta^2)^{-s} F_{j,\theta} \overline{L_{j,\theta}}, \quad \|F\|_{H_\theta^{-s}[0, 2\pi]} := (F, F)_{H_\theta^{-s}[0, 2\pi]}^{\frac{1}{2}},$$

with $L \in H_\theta^{-s}[0, 2\pi]$.

PROOF. Follows arguments similar to those of the proof of Theorem B.3. \square

ASSUMPTION B.1. *Henceforth, we assume $\Gamma \subset \mathcal{G}$ to be a single period of a periodic curve parametrized by a Lipschitz continuous function \mathbf{z} so that*

$$\Gamma := \{\mathbf{z}(t), t \in (0, 2\pi)\},$$

where \mathbf{z} may be continuously extended to all \mathbb{R} , with

$$\mathbf{z}(t) = (z_1(t), z_2(t)), \quad z_1(t + 2\pi n) = z_1(t) + 2\pi n, \quad z_2(t + 2\pi n) = z_2(t),$$

for all $n \in \mathbb{Z}$ and $t \in [0, 2\pi)$.

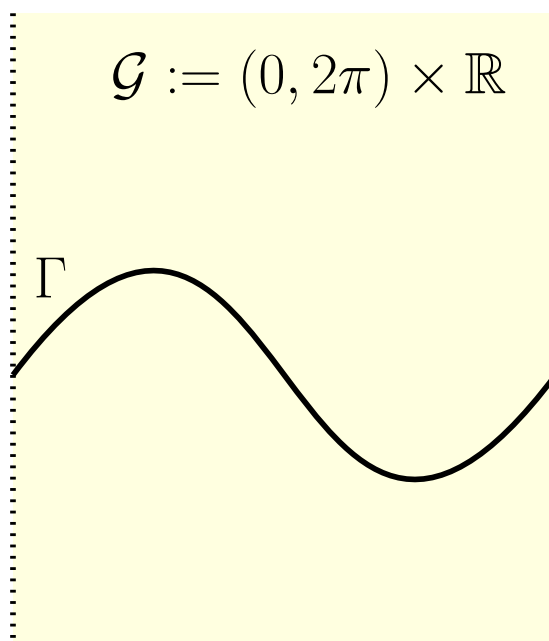


FIGURE B.1. Sinusoidal grating

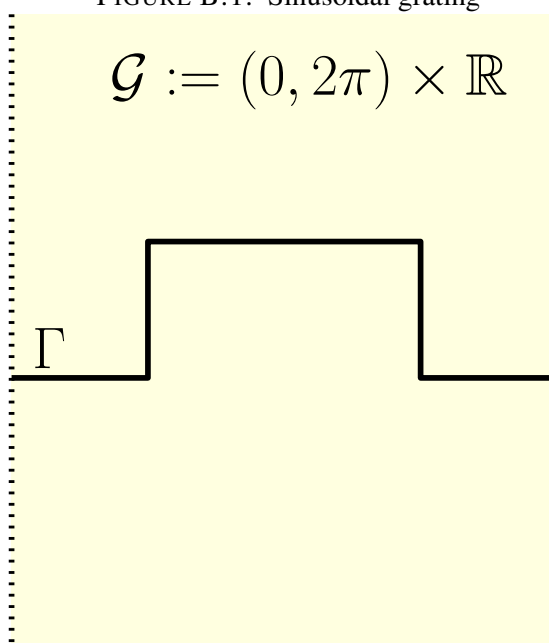


FIGURE B.2. Square grating

FIGURE B.3. Example of possible curves. Dotted lines represent periodic boundaries.

Definition B.12. For any periodic curve Γ , Consider an open neighborhood \mathcal{O} of Γ , we define $\mathcal{D}_\theta(\Gamma)$ as the restrictions to Γ of functions in $\mathcal{D}_\theta(\mathcal{O})$.

We introduce quasi-periodic Sobolev spaces on arbitrary curves as in (Kress, 2014, Chapter 8.2).

Definition B.13. Let $0 \leq s < r$, with $r \in \mathbb{N}$ such that Γ is a periodic curve of class $\mathcal{C}^{r-1,1}$. We define the quasi-periodic Sobolev space of order s over Γ as

$$H_\theta^s(\Gamma) := \{u \in L^2(\Gamma) \mid (u \circ \mathbf{z})(t) \in H_\theta^s[0, 2\pi]\},$$

and equip it with the inner product

$$(u, v)_{H_\theta^s(\Gamma)} := (u \circ \mathbf{z}, v \circ \mathbf{z})_{H_\theta^s[0, 2\pi]},$$

where $\mathbf{z} : (0, 2\pi) \rightarrow \Gamma$ is a parametrization of Γ .

The following result follows easily from (Kress, 2014, Chapter 8.2).

PROPOSITION B.4. Let $0 \leq s < \infty$. The space $H_\theta^s(\Gamma)$, along with the inner product $(\cdot, \cdot)_{H_\theta^s(\Gamma)}$ is a Hilbert space. Moreover, $\mathcal{D}_\theta(\Gamma)$ is dense in $H_\theta^s(\Gamma)$ and these spaces are independent of the chosen parametrization of Γ .

Definition B.14. For $0 \leq s < \infty$, we define $H_\theta^{-s}(\Gamma)$ as the completion of $H_\theta^0(\Gamma) \equiv L_\theta^2(\Gamma)$ with respect to the norm:

$$\|u\|_{H_\theta^{-s}(\Gamma)} := \left\| (u \circ \mathbf{z}) \|\dot{\mathbf{z}}\|_{\mathbb{R}^2} \right\|_{H_\theta^{-s}[0, 2\pi]},$$

with $\dot{\mathbf{z}}(t) := (\dot{z}_1(t), \dot{z}_2(t))$ and \mathbf{z} as in Assumption B.1.

Theorem B.6. For $0 \leq s < \infty$, $H_\theta^{-s}(\Gamma)$ is a realization of the dual space of $H_\theta^s(\Gamma)$. Furthermore, $\mathcal{D}_\theta(\Gamma)$ is dense in $H_\theta^{-s}(\Gamma)$.

PROOF. Follows directly from the definition of standard Sobolev spaces over closed curves (cf. (Kress, 2014, Chapter 8.2) and (McLean, 2000, Chapter 3.11)) and the duality

between $H_\theta^s[0, 2\pi]$ and $H_\theta^{-s}[0, 2\pi]$ (cf. Definition B.11) is understood as in Theorem B.5. \square

For all $h \in \mathbb{R}$, we set $\Gamma^h := \{\mathbf{x} \in \mathcal{G} \mid x_2 = h\}$. Quasi-periodic Sobolev spaces on boundaries have already been considered for straight segments such as Γ^h but only for $s = \pm \frac{1}{2}$ (cf. (Ammari, 1998; Ammari & Bao, 2008; Nédélec & Starling, 1991; Starling & Bonnet-Bendhia, 1994) and references therein).

Lemma B.1. *Let $h \in \mathbb{R}$ and $u \in \mathcal{D}_\theta(\mathcal{G})$. Then, the restriction operator*

$$u(\mathbf{x}) \mapsto u(x_1, h)$$

can be extended uniquely to a continuous functional (Dirichlet trace)

$$\gamma_0 : H_\theta^s(\mathcal{G}) \rightarrow H_\theta^{s-\frac{1}{2}}(\Gamma^h),$$

for all $\frac{1}{2} < s < \infty$, with continuous right-inverse

$$\eta_h : H_\theta^{s-\frac{1}{2}}(\Gamma^h) \rightarrow H_\theta^s(\mathcal{G}).$$

PROOF. The proof is very similar to that of (McLean, 2000, Lemma 3.35). We focus on the special case $h = 0$, since the generalization to $h \neq 0$ is trivial. Let $u \in \mathcal{D}_\theta(\mathcal{G})$, then

$$u(\mathbf{x}) = \sum_{j \in \mathbb{Z}} u_j(x_2) e^{-ij_\theta x_1},$$

and its restriction to $x_2 = 0$ is

$$u(x_1, 0) = \sum_{j \in \mathbb{Z}} u_j(0) e^{-ij_\theta x_1}.$$

For $j \in \mathbb{N}$, we bound each coefficient $u_j(0)$ as follows. If \widehat{u}_j denotes the Fourier transform of u_j , then

$$u_j(x_2) = \int_{\mathbb{R}} e^{i2\pi\xi x_2} \widehat{u}_j(\xi) \, \mathrm{d}\xi \quad \text{and} \quad u_j(0) = \int_{\mathbb{R}} \widehat{u}_j(\xi) \, \mathrm{d}\xi.$$

Then, it holds

$$\begin{aligned} u_j(0) &= \int_{\mathbb{R}} \frac{(1 + j_\theta^2 + |\xi|^2)^{\frac{s}{2}}}{(1 + j_\theta^2 + |\xi|^2)^{\frac{s}{2}}} \widehat{u}_j(\xi) \, d\xi \\ &\leq \left\| (1 + j_\theta^2 + |\xi|^2)^{\frac{s}{2}} \widehat{u}_j(\xi) \right\|_{L^2(\mathbb{R})} \left\| (1 + j_\theta^2 + |\xi|^2)^{-\frac{s}{2}} \right\|_{L^2(\mathbb{R})}. \end{aligned} \quad (\text{B.3})$$

The second term in (B.3) becomes

$$\begin{aligned} \int_{\mathbb{R}} \frac{1}{(1 + j_\theta^2 + |\xi|^2)^s} \, d\xi &= (1 + j_\theta^2)^{-s} \int_{\mathbb{R}} \frac{1}{\left(1 + \frac{|\xi|^2}{1 + j_\theta^2}\right)^s} \, d\xi \\ &= (1 + j_\theta^2)^{\frac{1}{2}-s} \int_{\mathbb{R}} \frac{1}{(1 + t^2)^s} \, dt, \end{aligned} \quad (\text{B.4})$$

where the integral in (B.4) is finite for $s > \frac{1}{2}$. Setting $C_s := \left\| (1 + t^2)^{-\frac{s}{2}} \right\|_{L^2(\mathbb{R})}$ and considering both (B.3) and (B.4), leads to

$$\begin{aligned} |u_j(0)|^2 &\leq C_s^2 (1 + j_\theta^2)^{\frac{1}{2}-s} \left\| (1 + j_\theta^2 + |\xi|^2)^{\frac{s}{2}} \widehat{u}_j(\xi) \right\|_{L^2(\mathbb{R})}^2 \\ (1 + j_\theta^2)^{s-\frac{1}{2}} |u_j(0)|^2 &\leq C_s^2 \left\| (1 + j_\theta^2 + |\xi|^2)^{\frac{s}{2}} \widehat{u}_j(\xi) \right\|_{L^2(\mathbb{R})}^2. \end{aligned}$$

Taking the sum over $j \in \mathbb{Z}$ yields

$$\|u(x_1, 0)\|_{H_\theta^{s-\frac{1}{2}}(\Gamma^0)} \leq C_s \|u(\mathbf{x})\|_{H_\theta^s(\mathcal{G})}.$$

With this, the proof follows from the density of $\mathcal{D}_\theta(\mathcal{G})$ in $H_\theta^s(\mathcal{G})$ (cf. Proposition B.3). For the inverse operator, we consider $\psi \in \mathcal{D}(\mathbb{R})$ such that $\psi(0) = 1$. Hence, for $w(x_1) = \sum_{j \in \mathbb{Z}} w_j e^{ij_\theta x_1}$, we define

$$\eta_0 w(\mathbf{x}) := \sum_{j \in \mathbb{Z}} w_j \psi(x_2) e^{ij_\theta x_1} \quad \forall \mathbf{x} \in \mathbb{R}^2.$$

It is clear that $\gamma_0^h \eta_0 w = w$. Moreover,

$$\begin{aligned}
& \|\eta_0 w\|_{H_\theta^s(\mathcal{G})}^2 \\
&= \sum_{j \in \mathbb{Z}} \int_{\mathbb{R}} (1 + j_\theta^2 + |\xi|^2)^s |w_j|^2 \left| \widehat{\psi}(\xi) \right|^2 d\xi \\
&= \sum_{j \in \mathbb{Z}} |w_j|^2 \int_{\mathbb{R}} (1 + j_\theta^2 + |\xi|^2)^s \left| \widehat{\psi}(\xi) \right|^2 d\xi \\
&= \sum_{j \in \mathbb{Z}} |w_j|^2 (1 + j_\theta^2)^{s-\frac{1}{2}} \int_{\mathbb{R}} (1 + |t|^2)^s (1 + j_\theta^2) \left| \widehat{\psi} \left(t (1 + j_\theta^2)^{\frac{1}{2}} \right) \right|^2 dt \\
&\leq C \sum_{j \in \mathbb{Z}} |w_j|^2 (1 + j_\theta^2)^{s-\frac{1}{2}} = C \|w\|_{H_\theta^{s-\frac{1}{2}}(\Gamma^h)}^2,
\end{aligned}$$

where C depends only on ψ and s (cf. (McLean, 2000, Lemma 3.36)). \square

REMARK B.1. A proof for the case $s = 1$ is given in (Nédélec & Starling, 1991, Section 2.2). However, the strategy does not admit a generalization to arbitrary $s > \frac{1}{2}$ since it relies on properties specific to $H_\theta^1(\mathcal{G})$.

Theorem B.7. For $\frac{1}{2} < s < r$, the restriction operator $u \mapsto u|_\Gamma$ can be extended uniquely to a continuous functional (Dirichlet trace):

$$\gamma_0 : H_\theta^s(\mathcal{G}) \rightarrow H_\theta^{s-\frac{1}{2}}(\Gamma),$$

which may also be extended to subsets \mathcal{O} of \mathcal{G} such that $\Gamma \subset \overline{\mathcal{O}}$. In both cases, the operator has a continuous right-inverse, denoted γ_0^{-1} .

PROOF. Take $u \in \mathcal{D}_\theta(\mathcal{G})$. Since by Assumption B.1 there is a real function $z \in [\mathcal{C}^{r-1,1}(0, 2\pi)]^2$ such that it holds $\Gamma = \{x \mid x = z(t), t \in (0, 2\pi)\}$, there exists a periodic isomorphism $R \in [\mathcal{C}^{r-1,1}(\mathcal{G})]^2$ satisfying

$$R : \mathcal{G} \rightarrow \mathcal{G}, \quad R((0, 2\pi) \times \{0\}) = \Gamma, \quad \text{supp}(R - I) \subset\subset \mathcal{G},$$

where I is the \mathbb{R}^2 identity operator, i.e. $I(x) = x$. Then, $u_R(x) = u \circ R(x)$ is at least $\mathcal{C}^{r-1,1}$ and remains quasi-periodic and compactly supported in \mathcal{G} . From Theorem B.1 and the invariance of regular Sobolev spaces of order $1 - r \leq s \leq r$ (McLean, 2000, Theorem

3.23), it follows that

$$\|u|_{\Gamma}\|_{H_{\theta}^{s-\frac{1}{2}}(\Gamma)} = \|u \circ R(\cdot, 0)\|_{H_{\theta}^{s-\frac{1}{2}}[0, 2\pi]} \leq C_s \|u_R\|_{H_{\theta}^s(\mathcal{G})} \cong C_s \|u\|_{H_{\theta}^s(\mathcal{G})},$$

for a positive constant C_s depending on s . The density of $\mathcal{D}_{\theta}(\mathcal{G})$ in $H_{\theta}^s(\mathcal{G})$ (cf. Proposition B.3) yields the first result. The case for \mathcal{O} follows directly from considering extensions in $H_{\theta}^s(\mathcal{G})$ of elements of $H_{\theta}^s(\mathcal{O})$. The inverse is constructed using the isomorphism R and Lemma B.1. \square

As in the non-periodic case, it is possible to extend the regularity range of the Dirichlet trace on Lipschitz domains to $\frac{1}{2} < s < \frac{3}{2}$. The result follows from modifying the proof of (Costabel, 1988, Lemma 3.6) –also available in (McLean, 2000, Theorem 3.38)– similarly to how the proof for Lemma B.1 was adapted from (McLean, 2000, Lemma 3.35).

Lemma B.2. *For $\frac{1}{2} < s < \frac{3}{2}$, the Dirichlet trace operator $\gamma_0 : H_{\theta}^s(\mathcal{G}) \rightarrow H_{\theta}^{s-\frac{1}{2}}(\Gamma)$ is bounded.*

Let $\mathcal{O} \subset \mathcal{G}$ be the open subset above Γ , so that $\partial^{\mathcal{G}}\mathcal{O} = \Gamma$. We define interior and exterior Dirichlet trace operators for $\frac{1}{2} < s < r$, and $\frac{1}{2} < s < \frac{3}{2}$ for $r = 1$, respectively denoted

$$\gamma_0^i : H_{\theta}^s(\mathcal{O}) \rightarrow H_{\theta}^{s-\frac{1}{2}}(\Gamma), \quad \gamma_0^e : H_{\theta}^s(\mathcal{G} \setminus \overline{\mathcal{O}^{\mathcal{G}}}) \rightarrow H_{\theta}^{s-\frac{1}{2}}(\Gamma).$$

Both operators can be built by observing that the elements of the corresponding Sobolev spaces are restrictions of elements of $H_{\theta}^s(\mathcal{G})$. Moreover, by construction, these operators also have right-inverses denoted $(\gamma_0^i)^{-1}$ and $(\gamma_0^e)^{-1}$, respectively.

We also require an operator that extends the notion of normal derivative on the boundary. This operator (Neumann trace) may be seen as an extension of the mapping $u \mapsto \nabla u|_{\Gamma} \cdot \mathbf{n}$, where \mathbf{n} denotes the unit normal exterior to \mathcal{O} –the open domain above or below Γ . Then, for $u \in H_{\theta}^s(\mathcal{O})$ with $s > \frac{3}{2}$, we define interior and exterior Neumann trace

operators:

$$\gamma_1^i := \gamma_0^i(\nabla u) \cdot \mathbf{n}, \quad \gamma_1^e := \gamma_0^e(\nabla u) \cdot \mathbf{n}.$$

From the mapping properties of the Dirichlet trace (Theorem B.7), we obtain continuity of the Neumann traces

$$\gamma_1^i : H_\theta^s(\mathcal{O}) \rightarrow H_\theta^{s-\frac{3}{2}}(\Gamma), \quad \gamma_1^e : H_\theta^s(\mathcal{G} \setminus \overline{\mathcal{O}}) \rightarrow H_\theta^{s-\frac{3}{2}}(\Gamma),$$

for $s > \frac{3}{2}$. By the use of integration-by-parts formulas, the Neumann trace may also be defined on a subspace of $H_\theta^1(\mathcal{O})$. With this, we state Green's formulas for quasi-periodic smooth functions, which we shall later extend to Sobolev spaces (*cf.* (Nédélec & Starling, 1991; Starling & Bonnet-Bendhia, 1994)).

Lemma B.3. *Consider $\mathcal{O} \subset \mathcal{G}$ an open subset whose boundary $\partial^\mathcal{G} \mathcal{O}$ is a finite number of periodic curves of class $\mathcal{C}^{0,1}$ and set \mathbf{n} its unit exterior normal. If $u, v \in \mathcal{D}_\theta(\mathcal{G})$, the following formulas hold:*

$$\int_{\mathcal{O}} \left(\Delta u(\mathbf{x}) \overline{v(\mathbf{x})} + \nabla u(\mathbf{x}) \cdot \overline{\nabla v(\mathbf{x})} \right) d\mathbf{x} = \int_{\partial^\mathcal{G} \mathcal{O}} (\nabla u(\mathbf{x}) \cdot \mathbf{n}(\mathbf{x})) \overline{v(\mathbf{x})} dS_{\mathbf{x}}, \quad (\text{B.5})$$

$$\begin{aligned} \int_{\mathcal{O}} \left(\Delta u(\mathbf{x}) \overline{v(\mathbf{x})} - u(\mathbf{x}) \overline{\Delta v(\mathbf{x})} \right) d\mathbf{x} = \\ \int_{\partial^\mathcal{G} \mathcal{O}} (\nabla u(\mathbf{x}) \cdot \mathbf{n}(\mathbf{x})) \overline{v(\mathbf{x})} dS_{\mathbf{x}} - \int_{\partial^\mathcal{G} \mathcal{O}} \overline{(\nabla v(\mathbf{x}) \cdot \mathbf{n}(\mathbf{x}))} u(\mathbf{x}) dS_{\mathbf{x}}. \end{aligned} \quad (\text{B.6})$$

PROOF. Take u and v in $\mathcal{D}_\theta(\mathcal{G})$. If \mathcal{O} is bounded then, by the classical Green's formula, we obtain

$$\begin{aligned} \int_{\mathcal{O}} \left(\Delta u(\mathbf{x}) \overline{v(\mathbf{x})} + \nabla u(\mathbf{x}) \cdot \overline{\nabla v(\mathbf{x})} \right) d\mathbf{x} = \\ \int_{\partial \mathcal{O}} (\nabla u(\mathbf{x}) \cdot \mathbf{n}(\mathbf{x})) \overline{v(\mathbf{x})} dS_{\mathbf{x}} + \int_{\partial \mathcal{O} \setminus \partial^\mathcal{G} \mathcal{O}} (\nabla u(\mathbf{x}) \cdot \mathbf{n}(\mathbf{x})) \overline{v(\mathbf{x})} dS_{\mathbf{x}}, \end{aligned}$$

where the last term is null by the quasi-periodicity of the functions. If \mathcal{O} is unbounded, then the statement still holds, upon noticing that both u and v have bounded support. Finally, (B.6) follows trivially from (B.5). \square

By using (B.5), we can extend the definition of the Neumann trace. For $s \in \mathbb{R}$, let

$$H_{\theta,\Delta}^s(\mathcal{O}) := \{u \in H_\theta^s(\mathcal{O}) : \Delta u \in L_\theta^2(\mathcal{O})\}.$$

Then, for $u \in H_{\theta,\Delta}^1(\mathcal{O})$, we define the functional $\gamma_1^i u$ as

$$\langle \gamma_1^i u, v|_\Gamma \rangle_{\partial^\mathcal{G} \mathcal{O}} := \int_{\mathcal{O}} \Delta u(\mathbf{x}) \overline{(\gamma_0^i)^{-1}(v|_\Gamma)(\mathbf{x})} d\mathbf{x} \quad (\text{B.7})$$

$$+ \int_{\mathcal{O}} \nabla u(\mathbf{x}) \cdot \overline{\nabla(\gamma_0^i)^{-1}(v|_\Gamma)(\mathbf{x})} d\mathbf{x}, \quad (\text{B.8})$$

where $v \in \mathcal{D}_\theta(\mathcal{G})$. Clearly, the functional continuously depends only on the boundary values of v , and thus it is well defined. Using the density of $\mathcal{D}_\theta(\mathcal{G})$ in $H_\theta^1(\mathcal{O})$ and since the Dirichlet trace has a continuous right-inverse, we can define the Neumann trace as an element of $H_\theta^{-\frac{1}{2}}(\Gamma)$. Analogously, we can define the exterior Neumann trace, denoted γ_1^e , by integrating over $\mathcal{G} \setminus \overline{\mathcal{O}^\mathcal{G}}$ as follows

$$\langle \gamma_1^e u, v|_\Gamma \rangle_\Gamma := - \int_{\mathcal{G} \setminus \overline{\mathcal{O}^\mathcal{G}}} \Delta u(\mathbf{x}) \overline{(\gamma_0^e)^{-1}(v|_\Gamma)(\mathbf{x})} d\mathbf{x} \quad (\text{B.9})$$

$$- \int_{\mathcal{G} \setminus \overline{\mathcal{O}^\mathcal{G}}} \nabla u(\mathbf{x}) \cdot \overline{\nabla(\gamma_0^e)^{-1}(v|_\Gamma)(\mathbf{x})} d\mathbf{x}. \quad (\text{B.10})$$

From their definitions, it is clear that these operators extend the normal derivative to $H_{\theta,\Delta}^1(\mathcal{O})$.

REMARK B.2. We consider the definition of γ_1^e with a sign difference with respect to that of γ_1^i to ensure $(\gamma_1^i - \gamma_1^e)u = 0$ for $u \in H_{\theta,\Delta}^1(\mathcal{O})$ for a bounded neighborhood containing the boundary Γ . Furthermore, these operators can be extended to local Sobolev spaces (B.2) since their definitions depend only on the behavior of u near the boundary Γ .

Now, one can extend Green's formulas to quasi-periodic Sobolev spaces.

Lemma B.4. Consider $\mathcal{O} \subset \mathcal{G}$ as an open subset whose boundary $\partial^\mathcal{G} \mathcal{O}$ is a finite number of periodic curves of class $\mathcal{C}^{0,1}$ and set \mathbf{n} its unit exterior normal. If $u \in H_{\theta,\Delta}^1(\mathcal{O})$ and $v \in H_\theta^1(\mathcal{O})$, then

$$\int_{\mathcal{O}} \left(\Delta u(\mathbf{x}) \overline{v(\mathbf{x})} + \nabla u(\mathbf{x}) \cdot \overline{\nabla v(\mathbf{x})} \right) d\mathbf{x} = \langle \gamma_1^i u, \gamma_0^i v \rangle_{\partial^\mathcal{G} \mathcal{O}}. \quad (\text{B.11})$$

If u and $v \in H_{\theta, \Delta}^1(\mathcal{O})$, then

$$\int_{\mathcal{O}} \left(\Delta u(\mathbf{x}) \overline{v(\mathbf{x})} - u(\mathbf{x}) \overline{\Delta v(\mathbf{x})} \right) d\mathbf{x} = \langle \gamma_1^i u, \gamma_0^i v \rangle_{\partial^{\mathcal{E}} \mathcal{O}} - \langle \gamma_1^i v, \gamma_0^i u \rangle_{\partial^{\mathcal{E}} \mathcal{O}} \quad (\text{B.12})$$

also holds.

PROOF. Follows from the density of $\mathcal{D}_{\theta}(\mathcal{O})$ on $H_{\theta}^1(\mathcal{O})$, Lemma B.3 and continuity of Dirichlet and Neumann traces (cf. Lemma B.1, (B.7) and (B.10)). \square

B.3. Time-Harmonic wave scattering by periodic surfaces in \mathbb{R}^2

We focus now on finding the field scattered by a grating described by an infinite surface $\tilde{\Gamma}$, with $\Gamma = \tilde{\Gamma} \cap \mathcal{G}$ satisfying Assumption B.1. Following (Elschner & Schmidt, 1998; Nédélec & Starling, 1991; Starling & Bonnet-Bendhia, 1994), this leads to quasi-periodic BIOs. We begin by introducing the Helmholtz equation in periodic domains, stating the appropriate radiation conditions at infinity for such a problem, and finish with an existence and uniqueness result previously found.

We shall only concern ourselves with the half-space above the infinite grating, denoted $\tilde{\Omega}$. We also introduce the periodic cell $\Omega := \tilde{\Omega} \cap \mathcal{G}$, with boundary $\Gamma = \partial^{\mathcal{E}} \Omega$. Let $H \in \mathbb{R}$ be such that $H > \max_{t \in [0, 2\pi]} |z_2(t)|$, where \mathbf{z} is as in Assumption B.1, and let

$$\Omega^H := \{\mathbf{x} \in \Omega \mid x_2 < H\}, \quad \Gamma^H := \{\mathbf{x} \in \mathcal{G} \mid x_2 = H\}.$$

B.3.1. Unbounded wave scattering

We consider the scattering induced by an incident plane wave:

$$u^{(\text{inc})}(\mathbf{x}) = u_0 e^{i(k_1 x_1 + k_2 x_2)}, \quad u_0 \in \mathbb{C}, \quad (\text{B.13})$$

by a grating described by $\tilde{\Gamma}$, where the material above the grating is assumed to be homogeneous and isotropic with wavenumber $k = (k_1^2 + k_2^2)^{\frac{1}{2}} > 0$. Here, we have assumed a

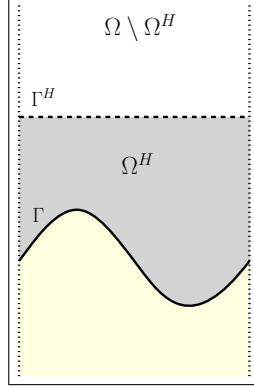


FIGURE B.4. Periodic cell. Dotted and dashed lines represent periodic and fictitious boundaries Γ and Γ_H , respectively. Ω_H is domain enclosed by Γ and Γ_H whereas Ω lies above Γ .

time dependence as $e^{-i\omega t}$ for some frequency $\omega > 0$, where $k := \omega c^{-1}$ and c is the wave speed in the medium above the grating surface.

In this setting, we consider two different sets of scalar boundary value problems:

$$(\text{TM}) \begin{cases} (-\Delta - k^2)u^{(\text{tot})} = 0 \text{ on } \tilde{\Omega}, \\ \gamma_0^i u^{(\text{tot})} = 0 \text{ on } \tilde{\Gamma}. \end{cases} \quad (\text{B.14})$$

$$(\text{TE}) \begin{cases} (-\Delta - k^2)u^{(\text{tot})} = 0 \text{ on } \tilde{\Omega}, \\ \gamma_1^i u^{(\text{tot})} = 0 \text{ on } \tilde{\Gamma}. \end{cases} \quad (\text{B.15})$$

In both (B.14) and (B.15), the total wave is split by linearity into incident and scattered waves, i.e. $u^{(\text{tot})} = u^{(\text{sc})} + u^{(\text{inc})}$. In electromagnetics, they correspond to transverse magnetic (TM) and transverse electric (TE) modes, whereas in acoustics they model sound-soft and -hard problems, respectively.

B.3.2. Quasi-periodicity of the solution and radiation condition

Throughout this section, we fix θ as the only number in $[0, 1)$ such that (cf. (Starling & Bonnet-Bendhia, 1994))

$$\theta = k_1 + n, \text{ for some } n \in \mathbb{Z}.$$

By a translation argument, solutions of (B.14) and (B.15) are not unique. Indeed, if $u \in H_{\text{loc}}^1(\Omega)$ is the scattered solution of either (B.14) or (B.15), then we can consider the following modification:

$$\tilde{u}(\mathbf{x}) := e^{-i2\pi\theta} u(\mathbf{x} + 2\pi\mathbf{e}_1)$$

and build a new solution for either (B.14) or (B.15). In order to ensure uniqueness, we search only for θ -quasi-periodic solutions of (B.14) and (B.15), so that

$$u(\mathbf{x} + 2\pi\mathbf{e}_1) = e^{i2\pi\theta} u(\mathbf{x}). \quad (\text{B.16})$$

We proceed by studying the behaviour of $u^{(\text{sc})}$ for $x_2 \geq H$. The following analysis is performed also in (Bao, 1997; Nédélec & Starling, 1991; Starling & Bonnet-Bendhia, 1994), among others. For $u^{(\text{sc})} \in H_{\theta, \text{loc}}^1(\Omega)$ and $x_2 \geq H$, we may write

$$u^{(\text{sc})}(\mathbf{x}) = \sum_{j \in \mathbb{Z}} u_j^{(\text{sc})}(x_2) e^{ij\theta x_1}, \quad (\text{B.17})$$

where each coefficient $u_j^{(\text{sc})} \in H_{\text{loc}}^1((H, \infty))$ solves

$$-\frac{\partial^2}{\partial x_2^2} u_j^{(\text{sc})}(x_2) - (k^2 - j_\theta^2) u_j^{(\text{sc})}(x_2) = 0, \quad \forall x_2 > H, \quad \forall j \in \mathbb{Z}. \quad (\text{B.18})$$

Since each one of these equations has two independent solutions, we are forced to choose between them as follows:

(i) if $(k^2 - j_\theta^2) < 0$, we select the decaying solution:

$$u_j^{(\text{sc})}(x_2) = u_j^{(\text{sc})}(H) e^{-\sqrt{j_\theta^2 - k^2}(x_2 - H)},$$

(ii) if $(k^2 - j_\theta^2) = 0$, we opt for the constant:

$$u_j^{(\text{sc})}(x_2) = u_j^{(\text{sc})}(H),$$

(iii) if $(k^2 - j_\theta^2) > 0$, one chooses the solution corresponding to an outgoing wave:

$$u_j^{(\text{sc})}(x_2) = u_j^{(\text{sc})}(H) e^{i\sqrt{k^2 - j_\theta^2}(x_2 - H)}.$$

Then, the scattered field has the following form for $x_2 \geq H$

$$u^{(\text{sc})}(\mathbf{x}) = \sum_{j \in \mathbb{Z}} u_j^{(\text{sc})}(H) e^{i\beta_j(x_2-H)} e^{ij_\theta x_1}, \quad (\text{B.19})$$

wherein

$$\beta_j := \begin{cases} \sqrt{k^2 - j_\theta^2} & \text{if } k^2 - j_\theta^2 \geq 0 \\ i\sqrt{j_\theta^2 - k^2} & \text{if } k^2 - j_\theta^2 < 0 \end{cases}. \quad (\text{B.20})$$

REMARK B.3. *Analogous conditions may be constructed as $x_2 \rightarrow -\infty$ if we were considering transmission conditions at the boundary Γ and the wave transmitted into the grating were non-trivial.*

Inspired by the previous analysis, we are now able to introduce an appropriate radiation condition to be satisfied by the scattered field (*cf.* (Bao et al., 1995; Kirsch, 1993; B. Zhang & Chandler-Wilde, 1998) and references therein).

Definition B.15 (Radiation Condition). *We say that $u \in H_{\theta, \text{loc}}^1(\mathcal{G})$ satisfies radiation conditions at infinity if there exists $h > 0$ large enough such that, for all $|x_2| \geq h$, there holds*

$$u^{(\text{sc})}(\mathbf{x}) = \begin{cases} \sum_{j \in \mathbb{Z}} u_j^+ e^{i\beta_j(x_2-h)} e^{ij_\theta x_1} & \text{if } x_2 \geq h, \\ \sum_{j \in \mathbb{Z}} u_j^- e^{i\beta_j(x_2+h)} e^{ij_\theta x_1} & \text{if } x_2 \leq -h, \end{cases}$$

with u_j^+ and $u_j^- \in \mathbb{C}$ for all $j \in \mathbb{Z}$ and β_j as in (B.20).

We may now state the TM and TE equations –including radiation and quasi-periodicity conditions– over the periodic cell:

$$(\text{TM}_\theta) \left\{ \begin{array}{l} (-\Delta - k^2)u^{(\text{tot})} = 0 \text{ on } \Omega, \\ \gamma_0^i u^{(\text{tot})} = 0 \text{ on } \Gamma, \\ u^{(\text{sc})} \text{ is } \theta\text{-quasi-periodic}, \\ u^{(\text{sc})} \text{ satisfies radiation conditions at infinity.} \end{array} \right. \quad (\text{B.21})$$

$$(\text{TE}_\theta) \left\{ \begin{array}{l} (-\Delta - k^2)u^{(\text{tot})} = 0 \text{ on } \Omega, \\ \gamma_1^i u^{(\text{tot})} = 0 \text{ on } \Gamma, \\ u^{(\text{sc})} \text{ is } \theta\text{-quasi-periodic}, \\ u^{(\text{sc})} \text{ satisfies radiation conditions at infinity.} \end{array} \right. \quad (\text{B.22})$$

We can now state both problems on local Sobolev spaces:

PROBLEM B.3.1 (Unbounded TM problem). Find $u^{(\text{sc})} \in H_{\theta, \text{loc}}^1(\Omega)$ such that $u^{(\text{sc})}$ satisfies (B.21).

PROBLEM B.3.2 (Unbounded TE problem). Find $u^{(\text{sc})} \in H_{\theta, \text{loc}}^1(\Omega)$ such that $u^{(\text{sc})}$ satisfies (B.22).

We also introduce an adjoint radiation condition as it will be useful to establish properties of the resulting BIOs later on.

Definition B.16 (Adjoint Radiation Condition). *We say that $u \in H_{\theta, \text{loc}}^1(\mathcal{G})$ satisfies adjoint radiation conditions at infinity if there exists $h > 0$ large enough such that, for all $|x_2| \geq h$, there holds*

$$u^{(\text{sc})}(\mathbf{x}) = \begin{cases} \sum_{j \in \mathbb{Z}} u_j^+ e^{i\tilde{\beta}_j(x_2-h)} e^{ij\theta x_1}, & \text{if } x_2 \geq h, \\ \sum_{j \in \mathbb{Z}} u_j^- e^{i\tilde{\beta}_j(x_2+h)} e^{ij\theta x_1}, & \text{if } x_2 \leq -h, \end{cases},$$

with u_j^+ and $u_j^- \in \mathbb{C}$ for all $j \in \mathbb{Z}$ and

$$\tilde{\beta}_j := \begin{cases} -\sqrt{k^2 - j_\theta^2} & \text{if } k^2 - j_\theta^2 \geq 0, \\ i\sqrt{j_\theta^2 - k^2} & \text{if } k^2 - j_\theta^2 < 0. \end{cases} \quad (\text{B.23})$$

This condition will only be used in the proofs found in Section B.7. In fact, given the time dependence $e^{-i\omega t}$, the adjoint radiation condition corresponds to admitting incoming waves from infinity rather than outgoing waves, as with the radiation condition in Definition B.15.

B.3.3. Dirichlet-to-Neumann (DtN) maps

The standard procedure to solve Problems B.3.1 and B.3.2 requires the use of an appropriate DtN operator at the fictitious boundary Γ^H (cf. (Ammari & Bao, 2008; Nédélec & Starling, 1991; Starling & Bonnet-Bendhia, 1994)).

Definition B.17. Taking the cue from the radiation condition from Definition B.15, we define the DtN operator $\mathcal{T}(k, \theta)$ as

$$\mathcal{T}(k, \theta) := \begin{cases} H_\theta^{\frac{1}{2}}(\Gamma^H) & \rightarrow H_\theta^{-\frac{1}{2}}(\Gamma^H) \\ \sum_{j \in \mathbb{Z}} v_j(H) e^{ij_\theta x_1} & \mapsto \sum_{j \in \mathbb{Z}} i\beta_j v_j(H) e^{ij_\theta x_1} \end{cases}.$$

Definitions of $H_\theta^{\frac{1}{2}}(\Gamma^H)$ and $H_\theta^{-\frac{1}{2}}(\Gamma^H)$ are given in Section B.2.3.

Lemma B.5. The operator $\mathcal{T}(k, \theta) : H_\theta^{\frac{1}{2}}(\Gamma^H) \rightarrow H_\theta^{-\frac{1}{2}}(\Gamma^H)$ is continuous.

PROOF. By straightforward computation, it holds

$$\|\mathcal{T}(k, \theta)v\|_{H_\theta^{-\frac{1}{2}}(\Gamma^H)}^2 = \sum_{j \in \mathbb{Z}} (1 + j^2)^{-\frac{1}{2}} |\beta_j|^2 |v_j|^2 \leq \sup_{j \in \mathbb{Z}} \frac{|\beta_j|^2}{1 + j^2} \|v\|_{H_\theta^{\frac{1}{2}}(\Gamma^H)}^2.$$

By definition of β_j , $\frac{|\beta_j|^2}{1 + j^2} = \frac{|k^2 - j^2 - 2j\theta - \theta^2|}{1 + j^2}$ is bounded in j . □

Lemma B.6 (Proposition 3.1 in (Starling & Bonnet-Bendhia, 1994)). *If u is a solution of either Problem B.3.1 or B.3.2, then the following are equivalent:*

- (i) u satisfies (B.19) (radiation condition at infinity),
- (ii) $\gamma_1^i u = \mathcal{T}(k, \theta) \gamma_0^i u$ on Γ^H .

PROOF. (i) \Rightarrow (ii) can be proved directly from (B.19) considering that the normal derivative in Γ^H is the derivative in x_2 . Conversely, if u is a solution of any of the Helmholtz problems (TM) or (TE), by (B.18) we have that the coefficients u_j have, for $x_2 > H$, the general expression:

$$u_j(x_2) = c_1 e^{i\beta_j(x_2-H)} + c_2 e^{-i\beta_j(x_2-H)},$$

with β_j as in (B.20). By incorporating (ii) as a boundary condition we have that $c_2 = 0$, $c_1 = u_j(H)$. \square

Then, we consider the following modified versions of (TE_θ) and (TM_θ) :

$$(\text{TM}_\theta^H) \left\{ \begin{array}{l} (-\Delta - k^2)u^{(\text{tot})} = 0 \text{ on } \Omega^H, \\ \gamma_0^i u^{(\text{tot})} = 0 \text{ on } \Gamma, \\ \gamma_1^i u^{(\text{sc})} = \mathcal{T}(k_1, k) \gamma_0^i u^{(\text{sc})} \text{ on } \Gamma^H, \\ u^{(\text{sc})} \text{ is } \theta\text{-quasi-periodic.} \end{array} \right. \quad (\text{B.24})$$

$$(\text{TE}_\theta^H) \left\{ \begin{array}{l} (-\Delta - k^2)u^{(\text{tot})} = 0 \text{ on } \Omega^H, \\ \gamma_1^i u^{(\text{tot})} = 0 \text{ on } \Gamma, \\ \gamma_1^i u^{(\text{sc})} = \mathcal{T}(k_1, k) \gamma_0^i u^{(\text{sc})} \text{ on } \Gamma^H, \\ u^{(\text{sc})} \text{ is } \theta\text{-quasi-periodic.} \end{array} \right. \quad (\text{B.25})$$

PROBLEM B.3.3 (Bounded TM problem). Find $u^{(\text{sc})} \in H_\theta^1(\Omega^H)$ such that $u^{(\text{sc})}$ satisfies (B.24).

PROBLEM B.3.4 (Bounded TE problem). Find $u^{(\text{sc})} \in H_\theta^1(\Omega^H)$ such that $u^{(\text{sc})}$ satisfies (B.25).

By Lemma B.6, Problems B.3.3 and B.3.4 are equivalent to Problems B.3.1 and B.3.2, respectively. Lastly, we conclude this chapter by stating an existence and uniqueness result for Problems B.3.3 and B.3.4 proved in (Nédélec & Starling, 1991; Starling & Bonnet-Bendhia, 1994).

Let $K_{\text{sing}}^{(TM)}$ and $K_{\text{sing}}^{(TE)}$ be countable sets of wavenumbers (growing towards infinity) for which non-unique solutions for Problems B.3.3 and B.3.4 may exist, respectively (cf. (Starling & Bonnet-Bendhia, 1994, Section 3.4) and references therein).

Theorem B.8 (Theorems 3.3 and 3.4 in (Starling & Bonnet-Bendhia, 1994) and Theorem 3.3 in (Elschner & Schmidt, 1998)). *There exist solutions for Problems B.3.3 and B.3.4 for every real wavenumber k . However, these may not be unique for $k \in K_{\text{sing}}^{(TE)}$ or $k \in K_{\text{sing}}^{(TM)}$, respectively.*

Actually, a uniqueness result for the Dirichlet problem is available in (Kirsch, 1993) when the grating surface Γ is of class \mathcal{C}^2 for all wavenumbers $k \in \mathbb{R}$. Also see (Alber, 1979; Kirsch, 1993, 1994) and references therein. Moreover, the results in (Elschner & Schmidt, 1998) include the more general transmission problem and a more detailed description of the sets $K_{\text{sing}}^{(TE)}$ and $K_{\text{sing}}^{(TM)}$ in terms of the frequency and incidence angle. We also highlight Theorem 3.2 in (Elschner & Schmidt, 1998), which gives a uniqueness result for any small enough frequency ω . The authors are not aware of similar uniqueness results for the Neumann problem, or for the Dirichlet problem under weaker assumptions such as Lipschitz regularity.

B.4. Boundary integral operators

We now establish the properties of BIOs acting on quasi-periodic Sobolev spaces. We begin by introducing an appropriate Green's function and follow by defining the corresponding operators that arise from it. We shall resume the notation used in Section B.2 for the quasi-periodic shift, i.e. $\theta \in [0, 1)$. Recall that fixing θ as the unique real number in $[0, 1)$ such that

$$\theta = k_1 + n, \text{ for some } n \in \mathbb{Z},$$

will yield BIOs corresponding to the problems considered in the previous section.

Definition B.18 (Quasi-periodic Green's function). *Let $\theta \in [0, 1)$, $k > 0$ such that $|j + \theta| \neq k$, for all $j \in \mathbb{Z}$, and denote by $G^k(\mathbf{x}, \mathbf{y})$ the fundamental solution for the two-dimensional Helmholtz equation with wavenumber k . For \mathbf{x} and \mathbf{y} on $\mathcal{A} := \{\mathbf{x}, \mathbf{y} \in \mathbb{R}^2 \mid \mathbf{x} - \mathbf{y} \neq 2\pi n \mathbf{e}_1, \forall n \in \mathbb{Z}\}$, we define the θ -quasi-periodic Green's function for the Helmholtz problem on a periodic surface as (cf. (Cho & Barnett, 2015; Nédélec & Starling, 1991; Linton, 1998; Liu & Barnett, 2016)):*

$$G_\theta^k(\mathbf{x}, \mathbf{y}) := \lim_{m \rightarrow \infty} \sum_{n=-m}^m e^{-i2\pi n \theta} G_n^k(\mathbf{x}, \mathbf{y}), \quad \forall (\mathbf{x}, \mathbf{y}) \in \mathcal{A}, \quad (\text{B.26})$$

where $G_n^k(\mathbf{x}, \mathbf{y})$ denotes the displaced kernel function:

$$G_n^k(\mathbf{x}, \mathbf{y}) := G^k(\mathbf{x} + 2\pi n \mathbf{e}_1, \mathbf{y}).$$

We make a special mention to the work of C. M. Linton (Linton, 1998), focused on the description of several analytic techniques that allow for a more efficient computation of the quasi-periodic Green's function in comparison to truncating the series in (B.26). Moreover, the series in (B.26) does not converge absolutely but rather as an alternating series.

For the remainder of the article, we assume that $|j + \theta| \neq k$ for all $j \in \mathbb{Z}$. Otherwise, we would be unable to build the θ -quasi-periodic Green's function, as the sum in (B.26) fails to converge (Nédélec & Starling, 1991). Values of k such that $|j + \theta| = k$ for some integer j are known as Rayleigh-Wood frequencies and, while different strategies have been developed to circumvent this issue (e.g. (Bruno & Fernandez-Lado, 2017; Bruno et al., 2017; Cho & Barnett, 2015)), we shall simply avoid them as their treatment lies beyond the scope of this article. We emphasize that Rayleigh-Wood frequencies are not to be mistaken with singular values of Problems B.3.3 and B.3.4.

PROPOSITION B.5. *The following relations hold:*

- (i) $G_\theta^k(\mathbf{x}, \mathbf{y}) = \frac{i}{4\pi} \sum_{j \in \mathbb{Z}} \frac{1}{\beta_j} e^{i\beta_j |x_2 - y_2| - i j \theta (y_1 - x_1)}$ for all \mathbf{x}, \mathbf{y} in \mathbb{R}^2 ,
- (ii) $(-\Delta_{\mathbf{y}} - k^2)G_\theta^k(\mathbf{x}, \mathbf{y}) = \widehat{\delta}_{2\pi, \theta}(\mathbf{x} - \mathbf{y})$ in $\mathcal{D}'_\theta(\mathbb{R}^2)$ for $\mathbf{x} \in \mathbb{R}^2$,

- (iii) $(-\Delta_{\mathbf{y}} - k^2)G_\theta^k(\mathbf{x}, \mathbf{y}) = \widehat{\delta}(\mathbf{x} - \mathbf{y})$ in $\mathcal{D}'_\theta(\mathcal{G})$ for $\mathbf{x} \in \mathcal{G}$,
- (iv) $G_\theta^k(\mathbf{x}, \mathbf{y})$ is C^∞ in \mathcal{A} , and
- (v) $G_\theta^k(\mathbf{x}, \mathbf{y})$ is θ -quasi-periodic in \mathbf{x} , $(1 - \theta)$ -quasi-periodic in \mathbf{y} and satisfies the radiation condition in Definition B.15 on both variables.

PROOF. Item (i) is proved in (X. Chen & Friedman, 1991, Section 3). The rest follow from (i) and (Nédélec & Starling, 1991, Proposition 3.1). \square

We now introduce the quasi-periodic Newton potential for $f \in \mathcal{D}_\theta(\mathcal{O})$.

Definition B.19. For a given $f \in \mathcal{D}_\theta(\mathcal{G})$, we define its quasi-periodic Newton potential $N_\theta^k(f)(\mathbf{x})$, for all $\mathbf{x} \in \mathcal{G}$, as

$$\mathcal{N}_\theta^k(f)(\mathbf{x}) := \int_{\mathcal{G}} G_\theta^k(\mathbf{x}, \mathbf{y}) f(\mathbf{y}) \, d\mathbf{y}.$$

Theorem B.9. The quasi-periodic Newton potential may be extended to a continuous operator from $H_\theta^s(\mathcal{G})$ to $H_{\theta, \text{loc}}^{s+2}(\mathcal{G})$, for $s \in \mathbb{R}$.

PROOF. See Section B.6. \square

We point out that the proof of Theorem B.9 is nothing but the characterization of the Newton potential order when considered as a pseudo-differential operator on the previously defined Sobolev spaces. This result was also previously established in (Lechleiter & Nguyen, 2013, Proposition 4).

Corollary B.2. Let $\mathcal{O} \subseteq \mathcal{G}$. The mapping $\mathcal{N}_\theta^k : \widetilde{H}_\theta^s(\mathcal{O}) \rightarrow H_{\theta, \text{loc}}^{s+2}(\mathcal{G})$ is bounded.

PROOF. Let $f \in \widetilde{H}_\theta^s(\mathcal{O})$. By definition, $\|f\|_{\widetilde{H}_\theta^s(\mathcal{O})} = \|\widetilde{f}\|_{H_\theta^s(\mathcal{G})}$, where \widetilde{f} is the extension by zero of f (cf. Definition B.7). The results follows directly from Theorem B.9. \square

From the integration-by-parts formula (B.12) and the series representation in Proposition B.5, one can show that, for $f \in \widetilde{H}_\theta^{-1}(\mathcal{O})$, the quasi-periodic Newton potential $\mathcal{N}_\theta^k f(\mathbf{x})$

satisfies

$$(-\Delta - k^2)\mathcal{N}_\theta^k f = \tilde{f} \text{ in } \mathcal{G}, \quad (\text{B.27})$$

where (B.27) is to be understood in the sense of $H_\theta^{-1}(\mathcal{G})$. Similarly, one can see that $\mathcal{N}_\theta^k f$ satisfies the appropriate radiation condition at infinity specified in Definition B.15 as $|x_2| \rightarrow \infty$. Indeed, consider H so that $\text{supp } f \subset [0, 2\pi] \times [-H, H]$ and \mathbf{x} such that $x_2 > H$. Then,

$$\begin{aligned} \mathcal{N}_\theta^k(f)(\mathbf{x}) &= \int_{\mathcal{O}} G_\theta^k(\mathbf{x}, \mathbf{y}) f(\mathbf{y}) \, d\mathbf{y} = \int_{\mathcal{O} \cap \text{supp } f} G_\theta^k(\mathbf{x}, \mathbf{y}) f(\mathbf{y}) \, d\mathbf{y} \\ &= \frac{i}{4\pi} \int_{\mathcal{O} \cap \text{supp } f} \sum_{j=-\infty}^{\infty} \frac{e^{i\beta_j |x_2 - y_2|} e^{-i j_\theta (y_1 - x_1)}}{\beta_j} f(\mathbf{y}) \, d\mathbf{y} \\ &= \frac{i}{4\pi} \int_{\mathcal{O} \cap \text{supp } f} \sum_{j=-\infty}^{\infty} \frac{e^{i\beta_j (x_2 - H)} e^{i\beta_j (H - y_2)} e^{-i j_\theta (y_1 - x_1)}}{\beta_j} f(\mathbf{y}) \, d\mathbf{y} \\ &= \sum_{j=-\infty}^{\infty} \frac{i}{4\pi} \frac{e^{i\beta_j (x_2 - H)} e^{i j_\theta x_1}}{\beta_j} \int_{\mathcal{O}} e^{i\beta_j (H - y_2)} e^{-i j_\theta y_1} f(\mathbf{y}) \, d\mathbf{y}. \end{aligned}$$

Integration is to be understood as a duality pairing since we consider $f \in \tilde{H}_\theta^s(\mathcal{O})$. We recall that Γ is assumed to be a periodic curve of class $\mathcal{C}^{r-1,1}$ for some $r \in \mathbb{N}$ (cf. Assumption B.1) and Ω is the open set above Γ (Figure B.4).

Definition B.20 (Single layer potential). *We define the single layer potential on Γ as*

$$\text{SL}_\theta^k := \mathcal{N}_\theta^k \circ (\gamma_0^i)',$$

where $(\gamma_0^i)'$ denotes the adjoint operator of γ_0^i such that, for $\frac{1}{2} < s < \infty$, $u \in H_\theta^s(\Omega)$ and $v \in H_\theta^{-s+\frac{1}{2}}(\Gamma)$

$$\langle \gamma_0^i u, v \rangle_{s-\frac{1}{2}, \Gamma} = \langle u, (\gamma_0^i)' v \rangle_{s, \Omega}.$$

Therein $\langle \cdot, \cdot \rangle_{s-\frac{1}{2}, \Gamma}$ denotes the duality between $H_\theta^{s-\frac{1}{2}}(\Gamma)$ and $H_\theta^{-s+\frac{1}{2}}(\Gamma)$, and $\langle \cdot, \cdot \rangle_{s, \Omega}$ denotes the duality between $H_\theta^s(\Omega)$ and $\tilde{H}_\theta^{-s}(\Omega)$.

Theorem B.10. *Let Γ be of class $\mathcal{C}^{r-1,1}$ with $r \in \mathbb{N}$ and $s \in \mathbb{R}$ be such that*

- $1 - r < s < \frac{1}{2}$ if $r > 1$ or
- $|s| < \frac{1}{2}$ if $r = 1$.

Then, it holds $\text{SL}_\theta^k : H_\theta^{s-\frac{1}{2}}(\Gamma) \rightarrow H_{\theta,\text{loc}}^{s+1}(\mathcal{G})$, is a continuous operator. Moreover, for $f \in \mathcal{D}_\theta(\Gamma)$ we have the representation:

$$\text{SL}_\theta^k(f)(\mathbf{x}) = \int_\Gamma G_\theta^k(\mathbf{x}, \mathbf{y}) f(\mathbf{y}) \, d\mathbf{y}, \quad \forall \mathbf{x} \in \mathcal{G} \setminus \Gamma. \quad (\text{B.28})$$

PROOF. The continuity of the single layer potential follows by Definition B.20 as both the Newton potential and the Dirichlet trace are themselves continuous (cf. Corollary B.2, Theorem B.7 and Lemma B.2). For the representation (B.28), we refer to (McLean, 2000, Section 6.3), specifically to (6.16). \square

Definition B.21 (Double layer potential). *We define the double layer potential on Γ as*

$$\text{DL}_\theta^k := \mathcal{N}_\theta^k \circ (\gamma_1^i)',$$

where $(\gamma_1^i)'$ denotes the interior adjoint of the Neumann trace.

If $f \in \mathcal{D}_\theta(\Gamma)$, we have the representation

$$\text{DL}_\theta^k(f)(\mathbf{x}) = \int_\Gamma \gamma_{1,\mathbf{y}}^i G_\theta^k(\mathbf{x}, \mathbf{y}) f(\mathbf{y}) \, d\mathbf{y}, \quad \forall \mathbf{x} \in \mathcal{G} \setminus \Gamma,$$

wherein $\gamma_{1,\mathbf{y}}^i$ refers to the interior Neumann trace γ_1^i acting on $G_\theta^k(\mathbf{x}, \mathbf{y})$ as a function of \mathbf{y} , for fixed \mathbf{x} . Further properties of DL_θ^k will be studied in the following section.

Theorem B.11 (Integral representation formula). *Let f satisfy*

$$f|_\Omega \in \tilde{H}_\theta^{-1}(\Omega), \quad f|_{\mathcal{G} \setminus \bar{\Omega}^\mathcal{G}} \in \tilde{H}_\theta^{-1}(\mathcal{G} \setminus \bar{\Omega}^\mathcal{G}).$$

Also, let $u \in L_{\theta,\text{loc}}^2(\mathcal{G})$ be such that $u|_\Omega \in H_\theta^1(\Omega)$, $u|_{\mathcal{G} \setminus \bar{\Omega}^\mathcal{G}} \in H_\theta^1(\mathcal{G} \setminus \bar{\Omega}^\mathcal{G})$ and

$$(-\Delta - k^2)u = f \text{ in } \mathcal{G} \setminus \Gamma,$$

along with the radiation condition (B.19). Then, the following representation formula holds

$$u(\mathbf{x}) = \mathcal{N}_\theta^k(f)(\mathbf{x}) + \mathrm{DL}_\theta^k([\gamma_0 u]_\Gamma)(\mathbf{x}) - \mathrm{SL}_\theta^k([\gamma_1 u]_\Gamma)(\mathbf{x}), \quad \forall \mathbf{x} \in \mathcal{G} \setminus \Gamma,$$

with $[\gamma u]_\Gamma := \gamma^i u - \gamma^e u$ for any of the trace operators.

PROOF. The proof resembles that for the standard representation formula (cf. (McLean, 2000, Chapter 7) and (Nédélec & Starling, 1991, Section 3.2)). The proof follows from Proposition B.5, the integration-by-parts formulas in Lemma B.4 and the density of $\mathcal{D}_\theta(\mathcal{G})$ in the considered Sobolev spaces. \square

In particular, for any given $g \in H_\theta^{\frac{1}{2}}(\Gamma)$ consider $u \in H_{\theta,\mathrm{loc}}^1(\Omega)$ such that

$$\begin{cases} (-\Delta - k^2)u = 0 \text{ on } \Omega, \\ \gamma_0^i u = g \text{ on } \Gamma, \\ u \text{ satisfies radiation conditions at infinity,} \end{cases}$$

and its extension by zero to the exterior of Ω as

$$\tilde{u}(\mathbf{x}) = \begin{cases} u(\mathbf{x}) & \text{if } \mathbf{x} \in \Omega, \\ 0 & \text{if } \mathbf{x} \in \mathcal{G} \setminus \overline{\Omega}^\mathcal{G}. \end{cases}$$

By Theorem B.11, we obtain

$$\mathrm{DL}_\theta^k g = \mathrm{SL}_\theta^k \gamma_1^i u - \tilde{u}, \quad \text{on } \Omega.$$

Hence, by the Fredholm alternative and the continuities of the single layer potential and of the interior Neumann trace, one derives

$$\|\mathrm{DL}_\theta^k g\|_{H_\theta^1(\Omega^H)} \leq C(H) \|g\|_{H_\theta^{\frac{1}{2}}(\Gamma)},$$

for all $H > 0$, where $\Omega^H := \{\mathbf{x} \in \Omega \mid x_2 < H\}$. Thus,

$$\mathrm{DL}_\theta^k : H_\theta^{\frac{1}{2}}(\Gamma) \rightarrow H_{\theta,\mathrm{loc}}^1(\Omega),$$

is continuous.

Theorem B.12 (Properties of the BIOs). *Let Γ be a $\mathcal{C}^{r-1,1}$ -periodic curve with $r \in \mathbb{N}$. Then, the layer potentials*

$$\begin{aligned} \text{SL}_\theta^k &: H_\theta^{s-\frac{1}{2}}(\Gamma) \rightarrow H_{\theta,\text{loc}}^{s+1}(\mathcal{G}), \\ \text{DL}_\theta^k &: H_\theta^{s+\frac{1}{2}}(\Gamma) \rightarrow H_{\theta,\text{loc}}^{s+1}(\mathcal{G} \setminus \Gamma), \end{aligned}$$

as well as the BIOs

$$\begin{aligned} \mathbf{V}_\theta^k &:= \gamma_0^i \text{SL}_\theta^k : H_\theta^{s-\frac{1}{2}}(\Gamma) \rightarrow H_\theta^{s+\frac{1}{2}}(\Gamma), \\ \mathbf{W}_\theta^k &:= \gamma_1^i \text{DL}_\theta^k : H_\theta^{s+\frac{1}{2}}(\Gamma) \rightarrow H_\theta^{s-\frac{1}{2}}(\Gamma), \\ \mathbf{K}_\theta^k &:= \gamma_1^i \text{SL}_\theta^k : H_\theta^{s-\frac{1}{2}}(\Gamma) \rightarrow H_\theta^{s-\frac{1}{2}}(\Gamma), \\ \mathbf{K}_\theta^{k'} &:= \gamma_0^i \text{DL}_\theta^k : H_\theta^{s+\frac{1}{2}}(\Gamma) \rightarrow H_\theta^{s+\frac{1}{2}}(\Gamma), \end{aligned}$$

are continuous for $|s| < \frac{1}{2}$ if $r = 1$ and for $1 - r < s < \frac{1}{2}$ for $r \in \mathbb{N} \setminus \{1\}$.

PROOF. See Section B.7. The proof follows by adapting the procedure in (McLean, 2000, Chapters 4 and 6) to the periodic setting. \square

Notice that in the above definitions, trace operators may be taken from either side of Γ giving rise to interior and exterior BIOs in contrast to the standard definitions (McLean, 2000). By Theorem B.12 and their equivalents in (Costabel, 1988), one can show the next results.

Lemma B.7. *Let $\phi \in H_\theta^{\frac{1}{2}}(\Gamma)$ and $\psi \in H_\theta^{-\frac{1}{2}}(\Gamma)$. Then, the following relations hold*

$$[\gamma_0 \text{SL}_\theta^k \psi]_\Gamma = 0, \quad [\gamma_1 \text{SL}_\theta^k \psi]_\Gamma = \psi, \quad [\gamma_0 \text{DL}_\theta^k \phi]_\Gamma = \phi, \quad [\gamma_1 \text{DL}_\theta^k \phi]_\Gamma = 0.$$

Theorem B.13. *The BIOs \mathbf{V}_θ^k and \mathbf{W}_θ^k are coercive on $H_\theta^{-\frac{1}{2}}(\Gamma)$ and $H_\theta^{\frac{1}{2}}(\Gamma)$, respectively.*

The coercivity of V_θ^k was already established in (Ammari & Bao, 2008) for the three dimensional (3D) case. However, the proof presented depends on the smoothness properties of $G_\theta^k - G^0$ and, as such, requires the boundary Γ to be of class \mathcal{C}^2 . A proof for the two dimensional case for Lipschitz curves is, to our knowledge, new. Similarly, the mapping properties of the BIOs were studied in (Schmidt, 2009, 2011), arriving at very similar results to those in Theorem B.12 in the cases that: (i) Γ be infinitely smooth or (ii) Γ be \mathcal{C}^2 -piecewise and such that the angles between adjacent tangents at its corners are strictly between 0 and 2π .

We finish this section by stating uniqueness and existence results for variational problems on the boundary Γ when formulated using BIEs.

Theorem B.14. *Let $k \in \mathbb{R}$ and consider the following set of equations:*

$$\left\{ \begin{array}{l} (-\Delta - k^2)u = 0 \text{ on } \Omega, \\ (-\Delta - k^2)u = 0 \text{ on } \mathcal{G} \setminus \overline{\Omega}^\mathcal{G}, \\ \gamma_0^i u = \gamma_0^e u = 0 \text{ on } \Gamma, \\ u \text{ satisfies radiation conditions at infinity,} \end{array} \right. \quad (\text{B.29})$$

where interior traces are considered from within Ω and exterior traces from $\mathcal{G} \setminus \overline{\Omega}^\mathcal{G}$. Then, for any given $g \in H_\theta^{\frac{1}{2}}(\Gamma)$, there exists a unique $\psi \in H_\theta^{-\frac{1}{2}}(\Gamma)$ such that

$$V_\theta^k \psi = g,$$

if and only if the only $u \in H_{\theta, \text{loc}}^1(\mathcal{G} \setminus \Gamma)$ that satisfies the system (B.29) is $u = 0$. Furthermore, it holds

$$\left\{ \begin{array}{l} (-\Delta - k^2)\text{SL}_\theta^k \psi = 0 \text{ on } \Omega, \\ (-\Delta - k^2)\text{SL}_\theta^k \psi = 0 \text{ on } \mathcal{G} \setminus \overline{\Omega}^\mathcal{G}, \\ \gamma_0^i \text{SL}_\theta^k \psi = \gamma_0^e \text{SL}_\theta^k \psi = g \text{ on } \Gamma, \\ \text{SL}_\theta^k \psi \text{ satisfies radiation conditions at infinity.} \end{array} \right.$$

Theorem B.15. *Let $k \in \mathbb{R}$ and consider the following set of equations:*

$$\left\{ \begin{array}{l} (-\Delta - k^2)u = 0 \text{ on } \Omega, \\ (-\Delta - k^2)u = 0 \text{ on } \mathcal{G} \setminus \overline{\Omega}^{\mathcal{G}}, \\ \gamma_1^i u = \gamma_1^e u = 0 \text{ on } \Gamma, \\ u \text{ satisfies radiation conditions at infinity,} \end{array} \right. \quad (\text{B.30})$$

where interior traces are considered from within Ω and exterior traces from $\mathcal{G} \setminus \overline{\Omega}^{\mathcal{G}}$. Then, for any given $q \in H_{\theta}^{-\frac{1}{2}}(\Gamma)$, there exists a unique $\phi \in H_{\theta}^{\frac{1}{2}}(\Gamma)$ such that

$$W_{\theta}^k \phi = q,$$

if and only if the only $u \in H_{\theta, \text{loc}}^1(\mathcal{G} \setminus \Gamma)$ satisfying the system (B.30) is $u = 0$. Furthermore,

$$\left\{ \begin{array}{l} (-\Delta - k^2)DL_{\theta}^k \psi = 0 \text{ on } \Omega, \\ (-\Delta - k^2)DL_{\theta}^k \psi = 0 \text{ on } \mathcal{G} \setminus \overline{\Omega}^{\mathcal{G}}, \\ \gamma_1^i DL_{\theta}^k \psi = \gamma_1^e DL_{\theta}^k \psi = q \text{ on } \Gamma, \\ DL_{\theta}^k \psi \text{ satisfies radiation conditions at infinity.} \end{array} \right.$$

The proofs of Theorems B.14 and B.15 follow from considering the jump relations of the respective layer potentials, as well as the uniqueness and existence of the volume problems. We emphasize that the equivalence between volume problems and boundary integral equations only hold while assuming that the wavenumber k is not a singular frequency for the volume problem formulated on either domain, Ω or $\mathcal{G} \setminus \overline{\Omega}^{\mathcal{G}}$.

B.5. Concluding remarks

The previous results allow for an analogous extension of the classical theory of BIOs on bounded domains to periodic ones, acting on quasi-periodic Sobolev spaces. It is quite noteworthy that most of the results follow from the definition of the quasi-periodic Sobolev

spaces, the trace theorem for these spaces, and by directly modifying previously established results for the classical integral operators (Costabel, 1988; McLean, 2000; Steinbach, 2007). Future work includes extensions to three dimensional (3D) geometries as well as numerical implementations and analysis of Galerkin low and high order boundary element methods for BIEs as those in Theorems B.14 and B.15.

B.6. Proof of Theorem B.9

In order to prove the boundedness of the quasi-periodic Newton potential, we shall make use of the following lemma.

Lemma B.8. *Let $g \in \mathcal{D}(\mathbb{R})$, and $\xi \in \mathbb{R}$, $|\xi| > 0$. Then, for some $C > 0$, it holds that*

$$\left| \int_0^\infty g(x) \sin(\xi x) dx \right| \leq C \frac{1}{|\xi|}, \quad \left| \int_0^\infty g(x) \cos(\xi x) dx \right| \leq C \frac{1}{|\xi|^2}. \quad (\text{B.31})$$

PROOF. Let $R > 0$ be so that the support of $g(x)$ is contained in $[-R, R]$. Then,

$$\begin{aligned} \int_0^\infty g(x) \sin(\xi x) dx &= \frac{1}{\xi} \int_0^\infty g\left(\frac{t}{\xi}\right) \sin(t) \, dt \\ &= \frac{1}{\xi} \left(g\left(\frac{t}{\xi}\right) \cos(t) \Big|_0^\infty + \int_0^\infty \frac{d}{dt} \left(g\left(\frac{t}{\xi}\right) \right) \cos(t) \, dt \right) \\ &= \frac{1}{\xi} \left(g(0) + \frac{1}{\xi} \int_0^\infty g'\left(\frac{t}{\xi}\right) \cos(t) \, dt \right), \\ \left| \int_0^\infty g(x) \sin(\xi x) dx \right| &= \frac{1}{|\xi|} \left| g(0) + \frac{1}{\xi} \int_0^{R\xi} g'\left(\frac{t}{\xi}\right) \cos(t) \, dt \right| \\ &\leq \frac{1}{|\xi|} \left(|g(0)| + R \max_{t \in [0, R]} |g'(t)| \right). \end{aligned}$$

Also, the second inequality follows by integration-by-parts:

$$\begin{aligned} \int_0^\infty g(x) \cos(\xi x) dx &= g(x) \sin(\xi x) \Big|_0^\infty - \frac{1}{\xi} \int_0^\infty g'(x) \sin(\xi x) dx, \\ &= -\frac{1}{\xi} \int_0^\infty g'(x) \sin(\xi x) dx. \end{aligned} \quad \square$$

We now prove Theorem B.9 by adapting a strategy similar to that used in (Steinbach, 2007, Theorem 6.1).

PROOF OF THEOREM B.9. First, consider $f \in \mathcal{D}_\theta(\mathcal{G})$ for which the expression

$$f(\mathbf{x}) = \sum_{j \in \mathbb{Z}} f_j(x_2) e^{ij_\theta x_1}$$

holds. Since f has compact support in the x_2 -direction, there exists some positive $r \in \mathbb{R}$ such that $f_j(x_2) = 0$ if $|x_2| > r$, for all $j \in \mathbb{Z}$. Fix $R > 0$ and set $u := \mathcal{N}_\theta^k f$. Then, u is a quasi-periodic function on \mathcal{G} by the quasi-periodicity of the Green's function. Consider $\mu \in \mathcal{D}(\mathbb{R})$ such that $\mu(t) = 1$, for all $t \in [0, r + R]$. We define a modified version of u as

$$u_\mu(\mathbf{x}) := \int_{\mathcal{G}} G_\theta^k(\mathbf{x}, \mathbf{y}) \mu(|x_2 - y_2|) f(\mathbf{y}) d\mathbf{y}.$$

Notice that for $\mathbf{x} \in \mathcal{G}^R := \mathcal{G} \cap \{|x_2| < R\}$, $u_\mu(\mathbf{x}) = u(\mathbf{x})$. Hence, u_μ is an extension of u and, from the norm definition for $H_\theta^s(\mathcal{G}^R)$, we find that $\|u\|_{H_\theta^s(\mathcal{G}^R)} \leq \|u_\mu\|_{H_\theta^s(\mathcal{G})}$. We now prove the boundedness of $\|u_\mu\|_{H_\theta^s(\mathcal{G})}$. Since u_μ is also θ -quasi-periodic, it holds

$$\begin{aligned} u_{\mu,j}(x_2) &= \int_0^{2\pi} u_\mu(x_1, x_2) e^{-ij_\theta x_1} d\mathbf{x}_1, \\ \widehat{u}_{\mu,j}(\xi) &= \int_{\mathbb{R}} e^{-i2\pi x_2 \xi} \int_0^{2\pi} u_\mu(x_1, x_2) e^{-ij_\theta x_1} d\mathbf{x}_1 d\mathbf{x}_2 \\ &= \int_{\mathbb{R}} \int_0^{2\pi} \int_{\mathbb{R}} \int_0^{2\pi} e^{-i2\pi x_2 \xi} e^{-ij_\theta x_1} G_\theta^k(\mathbf{x}, \mathbf{y}) \mu(|x_2 - y_2|) f(\mathbf{y}) d\mathbf{y}_1 d\mathbf{y}_2 d\mathbf{x}_1 d\mathbf{x}_2. \end{aligned}$$

Since μ and f have compact support, we can exchange the integration order so as to write

$$\begin{aligned} \widehat{u}_{\mu,j}(\xi) &= \int_{\mathbb{R}} \int_0^{2\pi} \int_{\mathbb{R}} \int_0^{2\pi} e^{-i2\pi x_2 \xi} e^{-ij_\theta x_1} G_\theta^k(\mathbf{x}, \mathbf{y}) \mu(|x_2 - y_2|) f(\mathbf{y}) d\mathbf{x}_1 d\mathbf{x}_2 d\mathbf{y}_1 d\mathbf{y}_2 \\ &= \int_{\mathbb{R}} \int_0^{2\pi} \int_{\mathbb{R}} \int_{-y_1}^{2\pi - y_1} e^{-i2\pi(z_2 + y_2)\xi} e^{-ij_\theta(z_1 + y_1)} G_\theta^k(\mathbf{z}, \mathbf{0}) \mu(|z_2|) f(\mathbf{y}) dz_1 dz_2 d\mathbf{y}_1 d\mathbf{y}_2 \\ &= \int_{\mathbb{R}} \int_0^{2\pi} \int_{\mathbb{R}} \int_0^{2\pi} e^{-i2\pi(z_2 + y_2)\xi} e^{-ij_\theta(z_1 + y_1)} G_\theta^k(\mathbf{z}, \mathbf{0}) \mu(|z_2|) f(\mathbf{y}) dz_1 dz_2 d\mathbf{y}_1 d\mathbf{y}_2, \end{aligned}$$

and where we used the periodicity of $e^{-\imath j_\theta z_1} G_\theta^k(z, 0)$. Then, replacing G_θ^k by its expansion (Proposition B.5) yields

$$\widehat{u}_{\mu,j}(\xi) = \widehat{f}_j(\xi) \frac{1}{\imath \beta_j} \int_{\mathbb{R}} e^{-\imath 2\pi z_2 \xi} e^{\imath \beta_j |z_2|} \mu(|z_2|) \, \mathrm{d}z_2.$$

Observe that

$$\frac{1}{\imath \beta_j} \int_{\mathbb{R}} e^{-\imath 2\pi z_2 \xi} e^{\imath \beta_j |z_2|} \mu(|z_2|) \, \mathrm{d}z_2 = \frac{2}{\imath \beta_j} \int_0^\infty e^{\imath \beta_j z_2} \mu(z_2) \cos(2\pi \xi z_2) \, \mathrm{d}z_2$$

and consider j_θ such that $\beta_j \in \mathbb{R}$, i.e. $j_\theta^2 < k^2$. From Lemma B.8, we get

$$\left| \frac{2}{\imath \beta_j} \int_0^\infty e^{\imath \beta_j |z_2|} \mu(|z_2|) \cos(2\pi \xi z_2) \, \mathrm{d}z_2 \right| \leq C_k \frac{1}{|\xi|^2 + 1}.$$

Furthermore, since β_j is real for a finite number of j , depending only on k and θ , then for all $j \in \mathbb{Z}$ such that $j_\theta < k^2$, yields

$$\left| \frac{2}{\imath \beta_j} \int_0^\infty e^{\imath \beta_j |z_2|} \mu(z_2) \cos(2\pi \xi z_2) \, \mathrm{d}z_2 \right| \leq C_{k,\theta} \frac{1}{1 + |\xi|^2 + j_\theta^2}.$$

Now, let us take $j_\theta^2 > k^2$ so that β_j is imaginary and $e^{\imath \beta_j |z_2|}$ decays as $|z_2|$ increases. Since

$$\frac{\mathrm{d}}{\mathrm{d}z_2} \left(e^{\imath \beta_j z_2} \frac{\xi \sin(\xi z_2) + \imath \beta_j \cos(\xi z_2)}{\xi^2 + \beta_j^2} \right) = e^{\imath \beta_j z_2} \cos(2\pi \xi z_2),$$

integration-by-parts gives

$$\begin{aligned} & \frac{2}{\imath \beta_j} \int_0^\infty e^{\imath \beta_j z_2} \mu(z_2) \cos(2\pi \xi z_2) \, \mathrm{d}z_2 \\ &= \frac{2}{\imath \beta_j} \left(\mu(z_2) e^{\imath \beta_j z_2} \frac{\xi \sin(\xi z_2) + \imath \beta_j \cos(\xi z_2)}{\xi^2 + \beta_j^2} \right) \Big|_0^\infty \\ & \quad - \frac{2}{\imath \beta_j} \int_0^\infty \mu'(z_2) e^{\imath \beta_j z_2} \frac{\xi \sin(\xi z_2) + \imath \beta_j \cos(\xi z_2)}{\xi^2 + \beta_j^2} \, \mathrm{d}z_2 \\ &= \frac{2}{\xi^2 + \beta_j^2} \left(1 - \frac{1}{\imath \beta_j} \int_0^\infty \mu'(z_2) e^{\imath \beta_j z_2} (\xi \sin(\xi z_2) + \imath \beta_j \cos(\xi z_2)) \, \mathrm{d}z_2 \right). \end{aligned}$$

By Lemma B.8, we deduce that

$$\frac{1}{\imath \beta_j} \int_0^\infty \mu'(z_2) e^{\imath \beta_j z_2} (\xi \sin(\xi z_2) + \imath \beta_j \cos(\xi z_2)) \, \mathrm{d}z_2$$

is bounded for all $\xi \in \mathbb{R}$, $j \in \mathbb{Z}$. Hence,

$$\left| \frac{2}{\xi^2 + \beta_j^2} \left(1 - \int_0^\infty \mu'(z_2) e^{\imath \beta_j z_2} (\xi \sin(\xi z_2) + \imath \beta_j \cos(\xi z_2)) dz_2 \right) \right| \quad (\text{B.32})$$

$$\leq C \frac{1}{|\xi|^2 + j_\theta^2 - k^2} \leq C \frac{1}{1 + |\xi|^2 + j_\theta^2}, \quad (\text{B.33})$$

where C depends only on k and μ . Thus, there exists $C > 0$ depending only on k , k_1 , and μ such that for all $s \in \mathbb{R}$,

$$(1 + j_\theta^2 + |\xi|^2)^{\frac{s}{2}} |\widehat{u}_{\mu,j}(\xi)| \leq C |\widehat{f}_j(\xi)| (1 + j_\theta^2 + |\xi|^2)^{\frac{s}{2}-1}. \quad (\text{B.34})$$

Taking the squared L^2 -norm of both sides of (B.34) and adding over $j \in \mathbb{Z}$, we obtain

$$\|u_\mu\|_{H_\theta^s(\mathcal{G})}^2 \leq C \|f\|_{H_\theta^{s-2}(\mathcal{G})}^2 \quad \forall s \in \mathbb{R}.$$

Since $\mathcal{D}_\theta(\mathcal{G})$ is dense in $H_\theta^{s-2}(\mathcal{G})$ (cf. Proposition B.3), the result is proven. \square

B.7. Regularity of solutions and continuity of BIOs

We extend the main results in (McLean, 2000, Chapter 4), introduced by Nečas (Necas, 2011), to the periodic case. We highlight changes needed to replicate the arguments. Our starting point is the result presented in Section B.3. Recall that $\theta \in [0, 1)$, Γ a periodic curve in $\mathcal{G} := [0, 2\pi] \times \mathbb{R}$ and Ω as the open domain above Γ (see Figure B.4).

Lemma B.9 (Lemma 2.3 in (Nédélec & Starling, 1991), and 3.2 in (Starling & Bonnet-Bendhia, 1994)). *Let $u \in H_\theta^1(\Omega^H)$ be such that*

$$\begin{cases} (-\Delta - k^2)u = 0 \text{ on } \Omega^H, \\ \gamma_0^i u = 0 \text{ or } \gamma_1^i u = 0 \text{ on } \Gamma, \\ \gamma_1^i u = \mathcal{T}(k_1, k) \gamma_0^i u, \text{ on } \Gamma^H, \end{cases}$$

with $\mathcal{T}(k_1, k)$ being the DtN operator from Definition B.17. Then, the Fourier coefficients $u_j = 0$ for all j in $J_{k_1}^- := \{j \in \mathbb{Z} \mid k^2 > j_\theta^2\}$.

PROOF. We proceed as in (Nédélec & Starling, 1991, Lemma 2.3),

$$0 = \int_{\Omega^H} (\Delta u \bar{u} - u \overline{\Delta u}) \, d\mathbf{x} = \int_{\Gamma \cup \Gamma_H} (\gamma_1^i u \, \overline{\gamma_0^i u} - \overline{\gamma_1^i u} \, \gamma_0^i u) \, dS_{\mathbf{x}}.$$

The integral over Γ vanishes due to either condition: $\gamma_0^i u = 0$ or $\gamma_1^i u = 0$. Hence, we only need to consider the integration on Γ^H ,

$$\begin{aligned} 0 &= \int_{\Gamma_H} (\gamma_1^i u \, \overline{\gamma_0^i u} - \overline{\gamma_1^i u} \, \gamma_0^i u) \, dS_{\mathbf{x}} \\ &= \int_{\Gamma_H} (\mathcal{T}(k_1, k) \gamma_0^i u \, \overline{\gamma_0^i u} - \overline{\mathcal{T}(k_1, k) \gamma_0^i u} \, \gamma_0^i u) \, dS_{\mathbf{x}}. \end{aligned} \quad (\text{B.35})$$

Recall the Fourier series for u and the DtN operator,

$$u(x_1, H) = \sum_{j \in \mathbb{Z}} u_j(H) e^{ij\theta x_1}, \quad \mathcal{T}(k_1, k)u(x_1, H) = \sum_{j \in \mathbb{Z}} \imath \beta_j u_j(H) e^{ij\theta x_1}.$$

Hence,

$$\int_{\Gamma_H} (\mathcal{T}(k_1, k) \gamma_0^i u \, \overline{\gamma_0^i u}) \, dS_{\mathbf{x}} = \sum_{j \in \mathbb{Z}} \imath \beta_j |u_j(H)|^2,$$

and (B.35) becomes,

$$\int_{\Gamma_H} (\mathcal{T}(k_1, k) \gamma_0^i u \, \overline{\gamma_0^i u} - \overline{\mathcal{T}(k_1, k) \gamma_0^i u} \, \gamma_0^i u) \, dS_{\mathbf{x}} = \sum_{j \in \mathbb{Z}} (\imath \beta_j - \overline{\imath \beta_j}) |u_j(H)|^2 = 0.$$

For $j \notin J_{k_1}^-$, we have $\imath \beta_j \in \mathbb{R}$ and $\overline{\imath \beta_j} - \imath \beta_j = 0$. Thus,

$$0 = \sum_{j \in J_{k_1}^-} (\overline{\imath \beta_j} - \imath \beta_j) |u_j(H)|^2 = \sum_{j \in J_{k_1}^-} 2\beta_j |u_j(H)|^2.$$

Since $\beta_j > 0$ for all $j \in J_{k_1}^-$, $|u_j(H)| = 0$, for all $j \in J_{k_1}^-$. □

PROPOSITION B.6. *Let $k > 0$ and $f \in \widetilde{H}_\theta^{-1}(\Omega)$ with compact support.*

(i) Let $g \in H_{\theta}^{\frac{1}{2}}(\Gamma)$ and $k \notin K_{sing}^{(TM)}$. Then, there is a unique $u \in H_{\theta,loc}^1(\Omega)$ that satisfies

$$\begin{cases} (-\Delta - k^2)u(\mathbf{x}) = f(\mathbf{x}) \text{ on } \Omega, \\ \gamma_0^i u = g \text{ on } \Gamma, \\ u \text{ satisfies radiation conditions at infinity.} \end{cases}$$

Moreover, the solution depends continuously on the data

$$\|u\|_{H_{\theta}^1(\Omega^R)} \lesssim \|f\|_{\tilde{H}_{\theta}^{-1}(\Omega)} + \|g\|_{H_{\theta}^{\frac{1}{2}}(\Gamma)}.$$

(ii) Let $w \in H_{\theta}^{-\frac{1}{2}}(\Gamma)$ and $k \notin K_{sing}^{(TE)}$. Then, there is a unique $u \in H_{\theta,loc}^1(\Omega)$ that satisfies

$$\begin{cases} (-\Delta - k^2)u(\mathbf{x}) = f(\mathbf{x}) \text{ on } \Omega, \\ \gamma_1^i u = w \text{ on } \Gamma, \\ u \text{ satisfies radiation conditions at infinity.} \end{cases}$$

Also, it holds

$$\|u\|_{H_{\theta}^1(\Omega^R)} \lesssim \|f\|_{\tilde{H}_{\theta}^{-1}(\Omega)} + \|w\|_{H_{\theta}^{-\frac{1}{2}}(\Gamma)}.$$

(iii) Let $g \in H_{\theta}^{\frac{1}{2}}(\Gamma)$ and $k \notin K_{sing}^{(TM)}$. Then, there is a unique $u \in H_{\theta,loc}^1(\Omega)$ that satisfies

$$\begin{cases} (-\Delta - k^2)u(\mathbf{x}) = f(\mathbf{x}) \text{ on } \Omega, \\ \gamma_0^i u = g \text{ on } \Gamma, \\ u \text{ satisfies the adjoint radiation condition at infinity.} \end{cases}$$

The next bound holds

$$\|u\|_{H_{\theta}^1(\Omega^R)} \lesssim \|f\|_{\tilde{H}_{\theta}^{-1}(\Omega)} + \|g\|_{H_{\theta}^{\frac{1}{2}}(\Gamma)}.$$

(iv) Let $w \in H_\theta^{-\frac{1}{2}}(\Gamma)$. If $k \notin K_{sing}^{(TE)}$, there is a unique $u \in H_{\theta,loc}^1(\Omega)$ that satisfies

$$\begin{cases} (-\Delta - k^2)u(\mathbf{x}) = f(\mathbf{x}) \text{ on } \Omega, \\ \gamma_1^i u = w \text{ on } \Gamma, \\ u \text{ satisfies the adjoint radiation condition at infinity.} \end{cases}$$

Moreover, the solution is bounded by the data

$$\|u\|_{H_\theta^1(\Omega^R)} \lesssim \|f\|_{\tilde{H}_\theta^{-1}(\Omega)} + \|w\|_{H_\theta^{-\frac{1}{2}}(\Gamma)}.$$

PROOF. For the standard radiation condition (Definition B.15), items (i) and (ii) follow from the Fredholm alternative and Theorem B.8 (see (Starling & Bonnet-Bendhia, 1994, Theorems 3.3 and 3.4)). The same strategy holds if the adjoint radiation condition (see Definition B.16) is used: we just need to show that the equations in items (iii) and (iv) have the same eigenvalues as those in (i) and (ii), which follows from noticing that one can build solutions of the equations with one radiation condition from the other. \square

The last proposition motivates the definition of solution operators. We consider two different cases. Let $k \notin K_{sing}^{(TM)}$ and $g \in H_\theta^{\frac{1}{2}}(\Gamma)$, we set

$$\mathcal{U}_k := \begin{cases} H_\theta^{\frac{1}{2}}(\Gamma) & \rightarrow H_{\theta,loc}^1(\Omega) \\ g & \mapsto u \end{cases},$$

where u is the only element in $H_{\theta,loc}^1(\Omega)$ that satisfies

$$\begin{cases} (-\Delta - k^2)u(\mathbf{x}) = 0 \text{ on } \Omega, \\ \gamma_0^i u = g \text{ on } \Gamma, \\ u \text{ satisfies radiation conditions at infinity.} \end{cases}$$

The corresponding adjoint version is

$$\mathcal{V}_k := \begin{cases} H_{\theta}^{\frac{1}{2}}(\Gamma) & \rightarrow H_{\theta, \text{loc}}^1(\Omega) \\ g & \mapsto v \end{cases},$$

where v is the only element in $H_{\theta, \text{loc}}^1(\Omega)$ that satisfies

$$\begin{cases} (-\Delta - k^2)v(\mathbf{x}) = 0 \text{ on } \Omega, \\ \gamma_0^i v = g \text{ on } \Gamma, \\ v \text{ satisfies the adjoint radiation condition at infinity.} \end{cases}$$

We also consider Steklov-Poincaré operators defined as

$$\gamma_1^i \mathcal{U}_k : H_{\theta}^{\frac{1}{2}}(\Gamma) \rightarrow H_{\theta}^{-\frac{1}{2}}(\Gamma), \quad \gamma_1^i \mathcal{V}_k : H_{\theta}^{\frac{1}{2}}(\Gamma) \rightarrow H_{\theta}^{-\frac{1}{2}}(\Gamma).$$

For a given domain $\mathcal{O} \subset \mathcal{G}$, $k > 0$ and a pair of functions $u, v \in H_{\theta}^1(\mathcal{O})$, we define the following sesquilinear form:

$$\Phi_{\mathcal{O}}^k(u, v) := \int_{\mathcal{O}} (\nabla u(\mathbf{x}) \cdot \nabla \overline{v(\mathbf{x})} - k^2 u(\mathbf{x}) \overline{v(\mathbf{x})}) \, d\mathbf{x}. \quad (\text{B.36})$$

Lemma B.10. *For $g_1, g_2 \in H_{\theta}^{\frac{1}{2}}(\Gamma)$ we have that*

$$\langle \gamma_1^i \mathcal{U}_k g_1, g_2 \rangle_{\Gamma} = \langle g_1, \gamma_1^i \mathcal{V}_k g_2 \rangle_{\Gamma}.$$

PROOF. From the radiation conditions, there is an $R > 0$ such that for $x_2 \geq R$, it holds

$$\mathcal{U}_k g_1(\mathbf{x}) = \sum_{j \in \mathbb{Z}} a_j e^{i\beta_j(x_2 - R)} e^{ij_{\theta} x_1}, \quad \mathcal{V}_k g_2(\mathbf{x}) = \sum_{j \in \mathbb{Z}} b_j e^{i\tilde{\beta}_j(x_2 - R)} e^{ij_{\theta} x_1},$$

with β_j and $\tilde{\beta}_j$ as in (B.20) and (B.23), respectively. Using Lemma B.4 and the definitions of \mathcal{U}_k and \mathcal{V}_k leads to

$$\Phi_{\Omega^R}^k(\mathcal{U}_k g_1, \mathcal{V}_k g_2) = \langle \gamma_1^i \mathcal{U}_k g_1, \gamma_0^i \mathcal{V}_k g_2 \rangle_{\Gamma \cup \Gamma^R},$$

$$\Phi_{\Omega^R}^k(\mathcal{U}_k g_1, \mathcal{V}_k g_2) = \langle \gamma_0^i \mathcal{U}_k g_1, \gamma_1^i \mathcal{V}_k g_2 \rangle_{\Gamma \cup \Gamma^R},$$

with $\Phi_{\Omega^R}^k$ as in (B.36) and $\Gamma^R := \{\mathbf{x} \in \mathcal{G} \mid x_2 = R\}$. Subtracting these last equations, we get

$$\langle \gamma_1^i \mathcal{U}_k g_1, g_2 \rangle_\Gamma = \langle g_1, \gamma_1^i \mathcal{V}_k g_2 \rangle_\Gamma + \langle \gamma_0^i \mathcal{U}_k g_1, \gamma_1^i \mathcal{V}_k g_2 \rangle_{\Gamma^R} - \langle \gamma_1^i \mathcal{U}_k g_1, \gamma_0^i \mathcal{V}_k g_2 \rangle_{\Gamma^R}.$$

In Γ^R we can use the expansions given by the radiation conditions:

$$\langle \gamma_0^i \mathcal{U}_k g_1, \gamma_1^i \mathcal{V}_k g_2 \rangle_{\Gamma^R} - \langle \gamma_1^i \mathcal{U}_k g_1, \gamma_0^i \mathcal{V}_k g_2 \rangle_{\Gamma^R} = - \sum_{j \in \mathbb{Z}} a_j \overline{b_j} (\imath \widetilde{\beta_j} + \imath \beta_j).$$

Then, for j such that β_j is a real number we have that $\widetilde{\beta_j} = -\beta_j$. Hence, $(\imath \widetilde{\beta_j} + \imath \beta_j) = \imath(-\beta_j + \beta_j) = 0$. On the other hand, if β_j is pure imaginary we have that $\widetilde{\beta_j} = \beta_j$ and $(\imath \widetilde{\beta_j} + \imath \beta_j) = \imath(\beta_j + \beta_j) = 0$. Thus, the duality products over Γ^R cancel each other out, yielding

$$\langle \gamma_1^i \mathcal{U}_k g_1, g_2 \rangle_\Gamma = \langle g_1, \gamma_1^i \mathcal{V}_k g_2 \rangle_\Gamma, \quad \langle \gamma_1^i \mathcal{U}_k g_1, g_2 \rangle_{\Gamma^R} = \langle g_1, \gamma_1^i \mathcal{V}_k g_2 \rangle_{\Gamma^R}. \quad \square$$

Following (McLean, 2000, Chapter 4), we now focus on establishing regularity properties of solutions in Ω . If u is a θ -quasi-periodic function defined in Ω , we denote by u^p its θ -quasi-periodic extension. For $h \in \mathbb{R}$ with $|h| < \pi$, we define the following estimators for the partial derivatives

$$\Delta_h^1 u(\mathbf{x}) := h^{-1} (u^p(\mathbf{x} + h \mathbf{e}_1) - u^p(\mathbf{x})), \quad \Delta_h^2 u(\mathbf{x}) := h^{-1} (u(\mathbf{x} + h \mathbf{e}_2) - u(\mathbf{x})).$$

The properties of Δ_h^2 are established in (McLean, 2000, Lemmas 4.13 to 4.15), where $L_2(\mathbb{R}^d)^m$ and $\mathcal{D}(\mathbb{R}^d)^m$ have to be replaced by $L_\theta^2(\mathcal{G})$, and $\mathcal{D}_\theta(\mathcal{G})$, respectively. There are, however, slight differences in the proofs for Δ_h^1 , which are exposed when proving Lemmas B.11 and B.12.

Lemma B.11 (Lemma 4.13 in (McLean, 2000)). *For $\theta \in [0, 1)$, let u be a θ -quasi-periodic function. Then, for $i = 1, 2$, it holds*

$$(a) \text{ If } \partial_i u \in L_\theta^2(\mathcal{G}), \text{ then } \|\Delta_h^i u\|_{L_\theta^2(\mathcal{G})} \leq \|\partial_i u\|_{L_\theta^2(\mathcal{G})} \text{ and } \|\Delta_h^i u - \partial_i u\|_{L_\theta^2(\mathcal{G})} \rightarrow 0 \text{ as } h \rightarrow 0.$$

(b) If there is a constant M such that $\|\Delta_h^i u\|_{L_\theta^2(\mathcal{G})} \leq M$, then, for h small, we have that $\partial_i u \in L_\theta^2(\mathcal{G})$, and $\|\partial_i u\|_{L_\theta^2(\mathcal{G})} \leq M$.

PROOF. The proof for (b) follows Lemma 4.13 in (McLean, 2000). Similarly for (a) for $i = 2$ whereas for $i = 1$, we observe that

$$|\Delta_h^1 u(\mathbf{x})|^2 \leq \int_0^1 |\partial_1 u^p(\mathbf{x} + t h \mathbf{e}_1)|^2 \, dt.$$

Integrating over \mathcal{G} yields,

$$\begin{aligned} \|\Delta_h^1 u(\mathbf{x})\|_{L_\theta^2(\mathcal{G})}^2 &\leq \int_{\mathcal{G}} \left(\int_0^1 |\partial_1 u^p(\mathbf{x} + t h \mathbf{e}_1)|^2 \, dt \right) d\mathbf{x} \\ &= \int_0^1 \left(\int_{\mathcal{G}} |\partial_1 u^p(\mathbf{x} + t h \mathbf{e}_1)|^2 \, d\mathbf{x} \right) dt = \int_0^1 \left(\int_{\mathcal{G} + \mathbf{e}_1(th)} |\partial_1 u^p(\mathbf{y})|^2 \, d\mathbf{y} \right) dt \\ &= \int_0^1 \left(\int_{\{\mathcal{G} + \mathbf{e}_1(th)\} \cap \mathcal{G}} |\partial_1 u(\mathbf{y})|^2 \, d\mathbf{y} + \int_{\{\mathcal{G} + \mathbf{e}_1(th)\} \setminus \mathcal{G}} |\partial_1 u^p(\mathbf{y})|^2 \, d\mathbf{y} \right) dt \\ &= \int_0^1 \left(\int_{\{\mathcal{G} + \mathbf{e}_1(th)\} \cap \mathcal{G}} |\partial_1 u(\mathbf{y})|^2 \, d\mathbf{y} + \int_{\mathcal{G} \setminus \{\mathcal{G} + \mathbf{e}_1(th)\}} |\partial_1 u(\mathbf{y})|^2 \, d\mathbf{y} \right) dt \quad (\text{B.37}) \\ &= \int_0^1 \left(\int_{\mathcal{G}} |\partial_1 u(\mathbf{y})|^2 \, d\mathbf{y} \right) dt = \|\partial_1 u\|_{L^2(\mathcal{G})}^2, \end{aligned}$$

where (B.37) follows from the periodicity of $|\partial_1 u(\mathbf{y})|$. \square

Lemma B.12 (Lemma 4.15 in (McLean, 2000)). *Let u and v belong to $L_\theta^2(\mathcal{G})$, $h \in \mathbb{R}$ such that $|h| < \pi$. Moreover, let $k > 0$ and $\mathcal{O} \subset \mathcal{G}$ be an open bounded set whose boundary is given by two disjoint periodic curves. Assume further that $\text{supp } u \subset \mathcal{O} \cap (\mathcal{O} - h \mathbf{e}_2)$ and $\text{supp } v \subset \mathcal{O} \cap (\mathcal{O} + h \mathbf{e}_2)$. Then,*

- (a) if $u, v \in L_\theta^2(\mathcal{O})$, then $(\Delta_h^i u, v)_{L_\theta^2(\mathcal{O})} = - (u, \Delta_{-h}^i v)_{L_\theta^2(\mathcal{O})}$, $i = 1, 2$.
- (b) if $u, v \in H_\theta^1(\mathcal{O})$, then $\Phi_\theta^k(\Delta_h^i u, v) = -\Phi_\theta^k(u, \Delta_{-h}^i v)$, $i = 1, 2$.

PROOF. For $i = 2$ the result follows verbatim from (McLean, 2000) whereas for $i = 1$, this is deduced directly from the definition of Δ_h^1 and the quasi-periodicity property. \square

Theorem B.16 (Thm. 4.16 in (McLean, 2000)). *Let $\mathcal{O} \subset \Omega$ be a bounded open set, whose boundary is given by two periodic curves and such that $\overline{\mathcal{O}}^\mathcal{G} \subset \Omega$. For $r \geq 0$ and*

$k > 0$, let $f \in H_\theta^r(\Omega)$ and $u \in H_{\theta,\text{loc}}^1(\Omega)$ be such that

$$(-\Delta - k^2)u = f \text{ in } \Omega.$$

Then, $u \in H_\theta^{r+2}(\mathcal{O})$ and for any $R > 0$ such that $\overline{\mathcal{O}^\mathcal{E}} \subset \Omega^R$, we have that

$$\|u\|_{H_\theta^{r+2}(\mathcal{O})} \lesssim \|u\|_{H_\theta^1(\Omega^R)} + \|f\|_{H_\theta^r(\Omega)}.$$

PROOF. We take similar steps to those in the proof of Theorem 4.16 in (McLean, 2000). Set $r = 0$ and consider a function $\chi \in \mathcal{D}_\theta(\Omega^R)$ such that $\chi = 1$ in \mathcal{O} . Define

$$f_1 := (-\Delta - k^2)(\chi u).$$

By direct computation, we obtain that $\|f_1\|_{L_\theta^2(\Omega^R)} \lesssim \|u\|_{H_\theta^1(\Omega^R)} + \|f\|_{L_\theta^2(\Omega^R)}$, so $f_1 \in L_\theta^2(\Omega^R)$. Let $v \in H_{\theta,\text{loc}}^1(\Omega)$ with null trace in $\partial^\mathcal{E}\Omega^R$. Using (B.11), we have that

$$\Phi_{\Omega^R}^k(\chi u, v) = (f_1, v)_{L_\theta^2(\Omega^R)}.$$

Also, by Lemma B.12, we have that for $i = 1, 2$, if $\overline{\text{supp } v^\mathcal{E}} \subset \Omega^R$ and h is sufficiently small, it holds

$$|\Phi_{\Omega^R}^k(\Delta_h^i(\chi u), v)| = |\Phi_{\Omega^R}^k(\chi u, \Delta_{-h}^i v)|.$$

Hence,

$$|\Phi_{\Omega^R}^k(\Delta_h^i(\chi u), v)| = |(f_1, \Delta_{-h}^i v)|.$$

By Lemma B.11 and norm definitions, we have that

$$|\Phi_{\Omega^R}^k(\Delta_h^i(\chi u), v)| \lesssim \|f_1\|_{L_\theta^2(\Omega^R)} \|v\|_{H_\theta^1(\Omega^R)}. \quad (\text{B.38})$$

On the other hand, by the coercivity of the Helmholtz operator, we get

$$\|\Delta_h^i(\chi u)\|_{H_\theta^1(\Omega^R)}^2 \lesssim \|\Delta_h^i(\chi u)\|_{L_\theta^2(\Omega^R)}^2 + \Phi_{\Omega^R}^k(\Delta_h^i(\chi u), \Delta_h^i(\chi u)).$$

Taking $v = \Delta_h^i(\chi u)$ in (B.38) leads to

$$\|\Delta_h^i(\chi u)\|_{H_\theta^1(\Omega^R)}^2 \lesssim \|\Delta_h^i(\chi u)\|_{L_\theta^2(\Omega^R)}^2 + \|f_1\|_{L_\theta^2(\Omega^R)} \|\Delta_h^i(\chi u)\|_{H_\theta^1(\Omega^R)}.$$

Here, we use the inequality $ab \leq \frac{1}{2}(\epsilon a + \epsilon^{-1}b^2)$ for a small ϵ to obtain

$$\|\Delta_h^i(\chi u)\|_{H_\theta^1(\Omega^R)}^2 \lesssim \|\Delta_h^i(\chi u)\|_{L_\theta^2(\Omega^R)}^2 + \|f_1\|_{L_\theta^2(\Omega^R)}^2.$$

Again, by Lemma B.11, $\|\Delta_h^i(\chi u)\|_{L_\theta^2(\Omega^R)} \lesssim \|u\|_{H_\theta^1(\Omega^R)}$ and, by the bound for the norm of f_1 , we retrieve

$$\|\Delta_h^i(\chi u)\|_{H_\theta^1(\Omega^R)}^2 \lesssim \|u\|_{H_\theta^1(\Omega^R)}^2 + \|f\|_{L_\theta^2(\Omega^R)}^2.$$

Finally, by recalling the norm definition on a subset $\mathcal{O} \subset \Omega^R$ and Lemma B.11, it holds

$$\|u\|_{H_\theta^2(\mathcal{O})}^2 \lesssim \|u\|_{H_\theta^1(\Omega^R)}^2 + \|f\|_{L_\theta^2(\Omega^R)}^2.$$

The proof is then achieved by induction, analogously to that of Theorem 4.16 in (McLean, 2000). \square

Now, we establish regularity results up to the boundary.

Theorem B.17 (Thm. 4.18 (McLean, 2000)). *Assume Ω to be a $\mathcal{C}^{r-1,1}$ -domain, with $r \geq 2$. Let $\mathcal{O} \subset \Omega$ be a bounded subset whose boundary is composed of two periodic curves, one of them being $\Gamma = \partial^\mathcal{G}\Omega$. Moreover, let the wavenumber $k > 0$, $f \in H_\theta^{r-2}(\Omega)$ and $u \in H_{\theta,\text{loc}}^1(\Omega)$ be such that*

$$(-\Delta - k^2)u = f \text{ on } \Omega.$$

Then, the following bounds hold

(i) *If $\gamma_0^i u \in H_\theta^{r-\frac{1}{2}}(\Gamma)$, then $u \in H_\theta^r(\mathcal{O})$ and*

$$\|u\|_{H_\theta^r(\mathcal{O})} \lesssim \|u\|_{H_\theta^1(\Omega^R)} + \|\gamma_0^i u\|_{H_\theta^{r-\frac{1}{2}}(\Gamma)} + \|f\|_{H_\theta^{r-2}(\Omega^R)}.$$

(ii) If $\gamma_1^i u \in H_\theta^{r-\frac{3}{2}}(\Gamma)$, then $u \in H_\theta^r(\mathcal{O})$ and

$$\|u\|_{H_\theta^r(\mathcal{O})} \lesssim \|u\|_{H_\theta^1(\Omega^R)} + \|\gamma_1^i u\|_{H_\theta^{r-\frac{3}{2}}(\Gamma)} + \|f\|_{H_\theta^{r-2}(\Omega^R)}.$$

for all $R > 0$ such that $\mathcal{O} \subset \Omega^R$.

PROOF. We bound the derivative $\partial_1 u$ as in Theorem B.16 while bounds for $\partial_2 u$ may be obtained from the boundary value problem:

$$-\partial_2^2 u = f + k^2 u + \partial_1^2 u.$$

The remainder of the proof follows that of (McLean, 2000, Theorem 4.18), requiring only minor modifications to the periodic setting. \square

Corollary B.3 (Thm. 4.21 (McLean, 2000)). *Assume that Ω is a $\mathcal{C}^{r-1,1}$ -domain and $r \geq 2$. Then, for $k \notin K_{\text{sing}}^{(TM)}$, we have that*

(i) For $0 \leq s \leq r - 1$,

$$\mathcal{U}_k : H_\theta^{s+\frac{1}{2}}(\Gamma) \rightarrow H_{\theta,\text{loc}}^{s+1}(\Omega), \quad \mathcal{V}_k : H_\theta^{s+\frac{1}{2}}(\Gamma) \rightarrow H_{\theta,\text{loc}}^{s+1}(\Omega).$$

(ii) For $-r + 1 \leq s \leq r - 1$,

$$\gamma_1^i \mathcal{U}_k : H_\theta^{s+\frac{1}{2}}(\Gamma) \rightarrow H_\theta^{s-\frac{1}{2}}(\Gamma), \quad \gamma_1^i \mathcal{V}_k : H_\theta^{s+\frac{1}{2}}(\Gamma) \rightarrow H_\theta^{s-\frac{1}{2}}(\Gamma).$$

PROOF. We begin by proving (i). The case $s = 0$ is direct from Proposition B.6, while the result for $s = r + 1$ follows from Theorem B.17. For $0 < s < r - 1$, the result is derived by interpolation (McLean, 2000, Appendix B) –interpolation of quasi-periodic spaces in the boundary Γ follows from their definition, inducing an isomorphism to regular Sobolev spaces on closed boundaries (Kress, 2014, Chapter 8)). For (ii), the result for positive s is deduced by similar arguments as those used for (i) whereas the result for $s < 0$ is due to the duality pairing in Lemma B.10. \square

Theorem B.18 (Theorem 4.24 in (McLean, 2000)). *Assume Ω to be Lipschitz. Let $k > 0$, $f \in L^2_\theta(\Omega)$ and $u \in H^1_{\theta,\text{loc}}(\Omega)$ such that*

$$(-\Delta - k^2)u = f \text{ on } \Omega.$$

If $\gamma_0^i u \in H^1_\theta(\Gamma)$ then $\gamma_1^i u \in L^2_\theta(\Gamma)$ and, for R such that $\Gamma \subset \mathcal{G}^R$, we have that

$$\|\gamma_1^i u\|_{L^2_\theta(\Gamma)} \lesssim \|\gamma_0^i u\|_{H^1_\theta(\Gamma)} + \|u\|_{H^1_\theta(\Omega^R)} + \|f\|_{L^2_\theta(\Omega)}.$$

PROOF. First, we assume that $u \in H^2_{\theta,\text{loc}}(\Omega)$ and, following the proof for (McLean, 2000, Theorem 4.24), it can be shown that

$$\|\gamma_1^i u\|_{L^2_\theta(\Gamma \cup \Gamma^R)} \lesssim \|\gamma_0^i u\|_{H^1_\theta(\Gamma \cup \Gamma^R)} + \|u\|_{H^1_\theta(\Omega^R)} + \|f\|_{L^2_\theta(\Omega)}.$$

Now consider a bounded open set $\mathcal{O} \subset \Omega^R$ such that $\overline{\mathcal{O}}^\mathcal{G} \subset \Omega^R$, with $\partial^\mathcal{G} \mathcal{O}$ composed of two periodic curves, one of them being Γ^R . By Theorem B.7 and the definition of the Neumann trace for smooth functions, we have that

$$\|\gamma_0^i u\|_{H^1_\theta(\Gamma^R)} \lesssim \|u\|_{H^{\frac{3}{2}}_\theta(\mathcal{O})} \leq \|u\|_{H^2_\theta(\mathcal{O})},$$

and, for $0 < \epsilon < \frac{1}{2}$, it holds

$$\|\gamma_1^i u\|_{L^2_\theta(\Gamma^R)} \leq \|\gamma_1^i u\|_{H^\epsilon_\theta(\Gamma^R)} \lesssim \|u\|_{H^{\frac{3}{2}+\epsilon}_\theta(\mathcal{O})} \leq \|u\|_{H^2_\theta(\mathcal{O})}.$$

Then, by Theorem B.16, we derive

$$\|u\|_{H^2_\theta(\mathcal{O})} \lesssim \|u\|_{H^1_\theta(\Omega^R)} + \|f\|_{L^2_\theta(\Omega)}.$$

We now take $u \in H^1_{\theta,\text{loc}}(\Omega)$ and assume that Γ can be parametrized as $(x, \zeta(x))$ with $x \in (0, 2\pi)$. Consider a sequence of smooth functions $\{\zeta_n\}_{n \in \mathbb{N}}$ such that

$$\zeta_n \rightarrow \zeta \text{ in } L^\infty((0, 2\pi)), \quad \nabla \zeta_n \rightarrow \nabla \zeta \text{ in } L^p((0, 2\pi)) \text{ for } 1 \leq p < \infty,$$

$$\nabla \zeta_n \text{ is uniformly bounded, } \quad \zeta_n(x) \geq \zeta(x) \text{ for } x \in (0, 2\pi).$$

Then, $\Omega = \{\mathbf{x} \in \mathcal{G} \mid x_2 > \zeta(x)\}$. Define

$$\Omega_n := \{\mathbf{x} \in \mathcal{G} \mid x_2 > \zeta_n(x_1)\}, \quad \Gamma_n := \{\mathbf{x} \in \mathcal{G} \mid x_2 = \zeta_n(x_1)\} = \partial^{\mathcal{G}} \Omega_n.$$

Following the proof of (McLean, 2000, Theorem 4.24), let us define $g(\mathbf{x}) := \gamma_0^i u(x_1, \zeta(x_1))$, where the trace is taken over Γ . Finally, we consider $\lambda > k^2$, $R > 0$ such that $\Gamma \subset \mathcal{G}^R$ and a sequence $\{u_n\}_{n \in \mathbb{N}}$ where each $u_n \in H_\theta^1(\Omega_n)$ satisfies

$$\begin{cases} (-\Delta - k^2 + \lambda)u_n = f + \lambda u \text{ on } \Omega_n^R, \\ \gamma_0^i u_n = \gamma_0 g \text{ on } \Gamma_n, \\ \gamma_0^i u_n = \gamma_0 u \text{ on } \Gamma^R. \end{cases}$$

The elements of the sequence $\{u_n\}_{n \in \mathbb{N}}$ are well defined in $H_\theta^1(\Omega_n^R)$ since the domain is bounded and the associated operator is elliptic. Since Γ_n is smooth, by Theorem B.17, we have that each u_n belongs to $H_\theta^2(\Omega_n^R)$ for all $n \in \mathbb{N}$. Hence, we can use the result for elements of $H_{\theta, \text{loc}}^2(\Omega)$. To conclude, we need to show that a proper extension of u_n converges to u in $H_\theta^1(\Omega^R)$, which is done in (McLean, 2000, Theorem 4.24) for regular Sobolev spaces and extended to quasi-periodic Sobolev spaces with only minor modifications. \square

Corollary B.4 (Theorem 4.25 in (McLean, 2000)). *Assume Ω to be Lipschitz. Let $k \notin K_{\text{sing}}^{(TM)}$. For $|s| \leq \frac{1}{2}$, it holds*

$$\gamma_1^i \mathcal{U}_k : H_\theta^{s+\frac{1}{2}}(\Gamma) \rightarrow H_\theta^{s-\frac{1}{2}}(\Gamma), \quad \gamma_1^i \mathcal{V}_k : H_\theta^{s+\frac{1}{2}}(\Gamma) \rightarrow H_\theta^{s-\frac{1}{2}}(\Gamma).$$

PROOF. The case $s = 0$ is given by Proposition B.6, $s = \frac{1}{2}$ is given by Theorem B.18, and $s = -\frac{1}{2}$ is obtained by the duality relation in Lemma B.10. For all other $|s| < \frac{1}{2}$, the result follows by interpolation. \square

In order to prove the mapping properties of the double layer potential, we need one more auxiliary result. For $k > 0$, we denote by \mathcal{U}_k^- the solution operator in $\Omega^- := \mathcal{G} \setminus \overline{\Omega}^{\mathcal{G}}$, and $\mathcal{U}_k^+ := \mathcal{U}_k$. Given $\lambda \in \mathbb{R}$ such that $k^2 - \lambda > 0$, we set $\mathcal{U}_{k,\lambda}^\pm := \mathcal{U}_{\sqrt{k^2-\lambda}}^\pm$.

Lemma B.13. *Let Ω be Lipschitz and set $k > 0$. Then, there exists $\lambda \in \mathbb{R}$ such that $k^2 - \lambda > 0$ and $\mathcal{U}_{k,\lambda}^+$ as well as $\mathcal{U}_{k,\lambda}^-$ are well defined in $H_{\theta}^{\frac{1}{2}}(\Gamma)$. For $|s| < \frac{1}{2}$, we also have that*

$$\mathcal{U}_{k,\lambda}^+ : H_{\theta}^{s+\frac{1}{2}}(\Gamma) \rightarrow H_{\theta,\text{loc}}^{s+1}(\Omega).$$

PROOF. Since the eigenvalues of the problem in Ω and Ω^- are numerable we can find λ such that $k^2 - \lambda > 0$ and $|\theta + j| \neq \sqrt{k^2 - \lambda}$, for every $j \in \mathbb{Z}$. Then, the following sets of equations

$$\begin{cases} (-\Delta - k^2 + \lambda)u = 0 \text{ on } \Omega, \\ \gamma_0^i u = g \text{ on } \Gamma, \\ u \text{ satisfies radiation conditions at infinity,} \end{cases}$$

$$\begin{cases} (-\Delta - k^2 + \lambda)u = 0 \text{ on } \Omega^-, \\ \gamma_0^i u = g \text{ on } \Gamma, \\ u \text{ satisfies radiation conditions at infinity,} \end{cases}$$

are satisfied by only one element of $H_{\theta,\text{loc}}^1(\Omega)$ and $H_{\theta,\text{loc}}^1(\Omega^-)$, respectively. Then, consider w defined as

$$w := \begin{cases} \mathcal{U}_{k,\lambda}^+ g \text{ on } \Omega, \\ \mathcal{U}_{k,\lambda}^- g \text{ on } \Omega^-. \end{cases}$$

Thanks to the properties of the solution operators, we have

$$w|_{\Omega} \in H_{\theta,\text{loc}}^1(\Omega), \quad w|_{\Omega^-} \in H_{\theta,\text{loc}}^1(\Omega^-), \quad w \in L_{\theta,\text{loc}}^2(\mathcal{G}).$$

By Theorem B.11, it holds

$$w = -\text{SL}_{\theta}^{\sqrt{k^2 - \lambda}}([\gamma_1 w]),$$

with $[\gamma_1 w] := \gamma_1^i w - \gamma_1^e w$. Then, by the continuity of the single layer potential and Corollary B.4, it holds

$$\left\| \text{SL}_\theta^{\sqrt{k^2 - \lambda}} [\gamma_1 w] \right\|_{H_\theta^{s+1}(\Omega^R)} \lesssim \|[\gamma_1 w]\|_{H_\theta^{s-\frac{1}{2}}(\Gamma)} \lesssim \|g\|_{H_\theta^{s+\frac{1}{2}}(\Gamma)}.$$

Thus, we can conclude that

$$\|\mathcal{U}_{k,\lambda}^+ g\|_{H_\theta^{s+1}(\Omega^R)} = \|w\|_{H_\theta^{s+1}(\Omega^R)} \lesssim \|g\|_{H_\theta^{s+\frac{1}{2}}(\Gamma)},$$

from where the result follows. \square

We define operators $\mathcal{V}_{k,\lambda}^\pm$ in a similar fashion to $\mathcal{U}_{k,\lambda}^\pm$ by using the adjoint radiation condition (*cf.* Definition B.16) and repeating the steps presented above. It is easy to check that both operators have the same properties.

PROOF OF THEOREM B.12. Results for SL_θ^k and \mathcal{V}_θ^k can be established directly from their definitions and Theorems B.7 and B.10. Now, consider $\eta, \mu \in \mathcal{D}_\theta(\Gamma)$ and let $\lambda \in \mathbb{R}$ be such that $k^2 - \lambda > 0$ and $\mathcal{V}_{k,\lambda}^+$ is well defined. By the mapping properties of SL_θ^k , we have that

$$((-\Delta - k^2 + \lambda)\text{SL}_\theta^k \eta, \mathcal{V}_{k,\lambda}^+ \mu)_{L_\theta^2(\Omega^R)} = (\lambda \text{SL}_\theta^k \eta, \mathcal{V}_{k,\lambda}^+ \mu)_{L_\theta^2(\Omega^R)}.$$

Applying Lemma B.4 leads to

$$\Phi_{\Omega^R}^{\sqrt{k^2 - \lambda}} (\text{SL}_\theta^k \eta, \mathcal{V}_{k,\lambda}^+ \mu) = \langle \gamma_1^i \text{SL}_\theta^k \eta, \gamma_0^i \mathcal{V}_{k,\lambda}^+ \mu \rangle_{\Gamma \cup \Gamma^R} + (\lambda \text{SL}_\theta^k \eta, \mathcal{V}_{k,\lambda}^+ \mu)_{L_\theta^2(\Omega^R)}.$$

On the other hand, since $(-\Delta - k^2 + \lambda)\mathcal{V}_{k,\lambda}^+ \mu = 0$ in Ω^R , Green's formula yields

$$\Phi_{\Omega^R}^{\sqrt{k^2 - \lambda}} (\text{SL}_\theta^k \eta, \mathcal{V}_{k,\lambda}^+ \mu) = \langle \gamma_0^i \text{SL}_\theta^k \eta, \gamma_1^i \mathcal{V}_{k,\lambda}^+ \mu \rangle_{\Gamma \cup \Gamma^R}.$$

As the single layer potential satisfies the radiation condition in Definition B.15 (*cf.* Proposition B.5) and $\mathcal{V}_{k,\lambda}^+ \mu$ the adjoint version (Definition B.16), we get

$$\langle \gamma_1^i \text{SL}_\theta^k \eta, \gamma_0^i \mathcal{V}_{k,\lambda}^+ \mu \rangle_{\Gamma^R} = \langle \gamma_0^i \text{SL}_\theta^k \eta, \gamma_1^i \mathcal{V}_{k,\lambda}^+ \mu \rangle_{\Gamma^R}$$

by the same arguments as in the proof of Lemma B.10. Then,

$$\langle \gamma_1^i \mathbf{SL}_\theta^k \eta, \gamma_0^i \mathcal{V}_{k,\lambda}^+ \mu \rangle_\Gamma = \langle \gamma_0^i \mathbf{SL}_\theta^k \eta, \gamma_1^i \mathcal{V}_{k,\lambda}^+ \mu \rangle_\Gamma - (\lambda \mathbf{SL}_\theta^k \eta, \mathcal{V}_{k,\lambda}^+ \mu)_{L_\theta^2(\Omega^R)}.$$

The first term in the right-hand side can be bounded as

$$\begin{aligned} |\langle \gamma_0^i \mathbf{SL}_\theta^k \eta, \gamma_1^i \mathcal{V}_{k,\lambda}^+ \mu \rangle_\Gamma| &\leq \|\gamma_0^i \mathbf{SL}_\theta^k \eta\|_{H_\theta^{s+\frac{1}{2}}(\Gamma)} \|\gamma_1^i \mathcal{V}_{k,\lambda}^+ \mu\|_{H_\theta^{-s-\frac{1}{2}}(\Gamma)} \\ &\lesssim \|\eta\|_{H_\theta^{s-\frac{1}{2}}(\Gamma)} \|\mu\|_{H_\theta^{-s+\frac{1}{2}}(\Gamma)}, \end{aligned}$$

where the last inequality follows from the continuity of $\gamma_0^i \mathbf{SL}_\theta^k = \mathbf{V}_\theta^k$ and Corollaries B.4 or B.3 depending on whether Γ is Lipschitz or smoother, respectively. For the second term, it holds

$$\begin{aligned} |(\lambda \mathbf{SL}_\theta^k \eta, \mathcal{V}_{k,\lambda}^+ \mu)_{L_\theta^2(\Omega^R)}| &\lesssim \|\mathbf{SL}_\theta^k \eta\|_{L_\theta^2(\Omega^R)} \|\mathcal{V}_{k,\lambda}^+ \mu\|_{L_\theta^2(\Omega^R)} \\ &\lesssim \|\eta\|_{H_\theta^{s-\frac{1}{2}}(\Gamma)} \|\mu\|_{H_\theta^{-s+\frac{1}{2}}(\Gamma)}, \end{aligned}$$

where the last inequality is due to the continuity of \mathbf{SL}_θ^k , and Lemma B.13. Mapping properties for $\gamma_1^i \mathbf{SL}_\theta^k = \mathbf{K}_\theta^{k'}$ are obtained by density arguments.

For the double layer potential and its traces, pick $g \in \mathcal{D}_\theta(\Gamma)$ and use the representation formula in Theorem B.11 –with $\mathcal{U}_{k,\lambda}^+ g$ extended by zero to Ω^- – to obtain

$$\mathbf{DL}_\theta^k g = \mathcal{U}_{k,\lambda}^+ g + \mathbf{SL}_\theta^k(\gamma_1^i \mathcal{U}_{k,\lambda}^+ g) - \mathcal{N}_\theta^k(-\lambda \mathcal{U}_{k,\lambda}^+ g).$$

Thus, we obtain the estimate

$$\begin{aligned} \|\mathbf{DL}_\theta^k g\|_{H^{s+1}(\Omega^R)} &\lesssim \|\mathcal{U}_{k,\lambda}^+ g\|_{H^{s+1}(\Omega^R)} + \|\mathbf{SL}_\theta^k(\gamma_1^i \mathcal{U}_{k,\lambda}^+ g)\|_{H^{s+1}(\Omega^R)} + \|\mathcal{N}_\theta^k(\mathcal{U}_{k,\lambda}^+ g)\|_{H^2(\Omega^R)}. \end{aligned}$$

By Lemma B.13, the mapping properties of \mathbf{SL}_θ^k and Theorem B.9, we obtain

$$\|\mathbf{DL}_\theta^k g\|_{H^{s+1}(\Omega^R)} \lesssim \|g\|_{H_\theta^{s+\frac{1}{2}}(\Gamma)} + \|\gamma_1^i \mathcal{U}_{k,\lambda}^+ g\|_{H_\theta^{s-\frac{1}{2}}(\Gamma)} + \|\mathcal{U}_{k,\lambda}^+ g\|_{L_\theta^2(\Omega^R)}.$$

Finally, by using Corollary B.4, we have that

$$\|\mathrm{DL}_\theta^k g\|_{H^{s+1}(\Omega^R)} \lesssim \|g\|_{H_\theta^{s+\frac{1}{2}}(\Gamma)}.$$

Bounds for the norms in $\mathcal{G} \setminus \overline{\Omega}^\mathcal{G}$ are derived by using $\mathcal{U}_{k,\lambda}^-$ and repeating the same procedure. The continuity of $\gamma_0^i \mathrm{DL}_k^\theta = \mathbf{K}_\theta^k$ is direct from the trace continuity in Theorem B.7. The Neumann trace can be estimated as follows

$$\begin{aligned} & \|\gamma_1^i \mathrm{DL}_\theta^k g\|_{H_\theta^{s-\frac{1}{2}}(\Gamma)} \\ & \lesssim \|\gamma_1^i \mathcal{U}_{k,\lambda}^+ g\|_{H_\theta^{s-\frac{1}{2}}(\Gamma)} + \|\gamma_1^i \mathrm{SL}_\theta^k(\gamma_1^i \mathcal{U}_{k,\lambda}^+ g)\|_{H_\theta^{s-\frac{1}{2}}(\Gamma)} + \|\gamma_1^i \mathcal{N}_\theta^k(\mathcal{U}_{k,\lambda}^+ g)\|_{L_\theta^2(\Gamma)}. \end{aligned}$$

The first term on the right-hand side is bounded by Corollary B.4 whereas the second one is bounded by the continuity of $\mathbf{K}_\theta^{k'}$. The last term is bounded by the continuity of the Neumann trace, that of the Newton potential and Corollary B.4. \square

APPENDIX C. TECHNICAL RESULTS FOR 3D-SCREEN PROBLEMS.

C.1. Proof of Lemma 4.3

Recall the weakly- and hyper-singular BIOs defined in Section 4.3.1. For $k = 0$ and $\Gamma = \mathbb{D}$, we write

$$\begin{aligned} V_{\mathbb{D}}u(\mathbf{x}) &:= \int_{\mathbb{D}} \frac{1}{4\pi\|\mathbf{x} - \mathbf{x}'\|_2} u(\mathbf{x}') d\mathbf{x}', \\ W_{\mathbb{D}}u(\mathbf{x}) &:= -\gamma_{n,\mathbf{x}} \int_{\mathbb{D}} \gamma_{n,\mathbf{x}'} \frac{1}{4\pi\|\mathbf{x} - \mathbf{x}'\|_2} u(\mathbf{x}') d\mathbf{x}', \end{aligned}$$

These operators have two key properties. First, they are continuous and elliptic so they can be used to define equivalent norms. In fact, by (Sauter & Schwab, 2011, Theorem 3.5.9) we have that

$$\|u\|_{\tilde{H}^{-\frac{1}{2}}(\mathbb{D})}^2 \cong \langle V_{\mathbb{D}}u, u \rangle_{\mathbb{D}}, \quad \|u\|_{\tilde{H}^{\frac{1}{2}}(\mathbb{D})}^2 \cong \langle W_{\mathbb{D}}u, u \rangle_{\mathbb{D}}. \quad (\text{C.1})$$

Secondly, we have a characterization of the eigenvalues of these two operators¹:

$$V_{\mathbb{D}}q_m^l = \frac{1}{4}\Lambda_{l,m}p_m^l, \quad l+m \text{ even}, \quad W_{\mathbb{D}}p_m^l = \frac{1}{\Lambda_{l,m}}q_m^l, \quad l+m \text{ odd}, \quad (\text{C.2})$$

where

$$\Lambda_{l,m} = \frac{\Gamma\left(\frac{l+|m|+1}{2}\right) \Gamma\left(\frac{l-|m|+1}{2}\right)}{\Gamma\left(\frac{l+|m|+2}{2}\right) \Gamma\left(\frac{l-|m|+2}{2}\right)},$$

here Γ denotes the Gamma function and not an screen. Using Gautschi's inequality (Gautschi, 1959), it holds that

$$\frac{1}{l+1} \lesssim \Lambda_{l,m} \lesssim \frac{1}{\sqrt{l+1}}. \quad (\text{C.3})$$

With these elements, we proceed with the proof of Lemma 4.3. Pick any smooth function u on \mathbb{D} and consider its even lifting to \mathbb{S} . Since spherical harmonics are dense on smooth functions defined on the sphere, we can approximate the lifting u by even spherical

¹See (Wolfe, 1971) for the original proof of the weakly-singular BIO and (Ramaciotti & Nédélec, 2017, Theorem 2.7.1) for the hyper-singular case

harmonics. Thus, u can be expanded as

$$u = \sum_{l=0}^{\infty} \sum_{\substack{m=-l \\ m+l \text{ even}}}^l \langle u, q_m^l \rangle p_m^l,$$

now (4.3) follows from the orthogonality relation (4.1). To prove (4.4), we use the density of functions q_l^e in $\tilde{H}^{-\frac{1}{2}}(\mathbb{D})$, i.e.

$$u = \sum_{l=0}^{\infty} \sum_{\substack{m=-l \\ m+l \text{ even}}}^l u_m^l q_m^l,$$

wherein, by orthogonality it holds that $u_m^l = \langle u, p_m^l \rangle$. Hence, computing the norm of u using the equivalence (C.1), the relation (C.2) and the estimate (C.3) yields

$$\|u\|_{Q_e^{-\frac{1}{2}}(\mathbb{D})} \lesssim \|u\|_{\tilde{H}^{-\frac{1}{2}}(\mathbb{D})} \lesssim \|u\|_{Q_e^{-\frac{1}{4}}(\mathbb{D})},$$

which implies the result. Similar ideas are used to show (4.5). \square

C.2. Singular Integrals Analysis

We consider the integrals I^c, I^d, I^e defined in Section 4.4.2.2. These integrals have in common that the singularities occur in specific points in three- or two-dimensional spaces, i.e. when three or two variables take a specific value. In contrast, I^a, I^b , singularities occur when one variable takes a specific value regardless of the other.

C.2.1. General idea

Let us start with the simpler case of an integral which has a singularity in 2D:

$$I := \int_0^1 \int_0^1 \frac{1}{\sqrt{x+y}} dy dx,$$

the integrand has a singularity at $(x, y) = (0, 0)$. Performing the polar change of variables $x = \rho \cos \alpha, y = \rho \sin \alpha$, we have that

$$I = \int_0^{\frac{\pi}{4}} \int_0^{\frac{1}{\cos \alpha}} \frac{\sqrt{\rho}}{\sqrt{\cos \alpha + \sin \alpha}} d\rho d\alpha + \int_{\frac{\pi}{4}}^{\frac{\pi}{2}} \int_0^{\frac{1}{\sin \alpha}} \frac{\sqrt{\rho}}{\sqrt{\cos \alpha + \sin \alpha}} d\rho d\alpha.$$

Moreover, one can fix the integration domain for the ρ variable by doing a linear change of variable

$$I = \int_0^{\frac{\pi}{4}} \int_0^1 \frac{\sqrt{t}}{(\cos \alpha)^{3/2} \sqrt{\cos \alpha + \sin \alpha}} dt d\alpha + \int_{\frac{\pi}{4}}^{\frac{\pi}{2}} \int_0^1 \frac{\sqrt{t}}{(\sin \alpha)^{3/2} \sqrt{\cos \alpha + \sin \alpha}} dt d\alpha.$$

These last two integrals can be straightforwardly computed by using a Jacobi rule in t and Gauss-Legendre in α , resulting in an optimal convergence rate –exponential in this particular case. The idea is in fact very simple: use polar coordinates with the origin in the point where the singularity occurs, transferring the multidimensional singularity to the radial coordinate only. The rest of this section gives the detail on each change of variable that is needed and also proving that the resulting integrals are computed with optimal rates.

C.2.2. Integral I^c

Consider the integral of the form

$$J^c := \int_{\frac{\sqrt{3}}{2}}^1 \int_{\frac{-\pi}{2}}^{\frac{-\pi}{3}} \int_0^{\frac{1}{2}} \frac{\lambda A^2(r, \beta)}{4\pi \|\mathbf{r}(\mathbf{x}) - \mathbf{r}(\mathbf{x} + \lambda A(r, \beta) \mathbf{e}_{\theta+\beta})\|} \frac{r d\lambda d\beta dr}{\sqrt{1-r^2} \sqrt{1 - \|\mathbf{x} + \lambda A(r, \beta) \mathbf{e}_{\theta+\beta}\|^2}}, \quad (\text{C.4})$$

where in comparison to (4.19), we restrict to the first interval for the β variable as the other cases follows similarly, and we have omitted the integral in the θ variable as it is not relevant to the singularity analysis and can be treated with Gauss-Legendre quadrature having not effect on the rate of convergence. Since trial and test polynomials are smooth functions they have also been neglected in the ensuing singularity analysis. Consider the following change of variables: $u^2 = 1 - r^2$, $\cos \beta = v$. Define $d := 4\pi \|\mathbf{r}(\mathbf{x}) - \mathbf{r}(\mathbf{x} + \lambda A(r, \beta) \mathbf{e}_{\theta+\beta})\|$ and use expansion (4.18) so that (C.4) becomes

$$J^c = \int_0^{\frac{1}{2}} \int_0^{\frac{1}{2}} \int_0^{\frac{1}{2}} \frac{\lambda d^{-1} A^2 du dv d\lambda}{\sqrt{1-\lambda} \sqrt{1-v^2} \sqrt{u^2(1+\lambda) - 2\lambda \sqrt{1-u^2} v A}},$$

wherein by definition of $A(r, \beta)$ (see (4.17)), we have that

$$A = \left(\sqrt{u^2 + (1 - u^2)v^2} - \sqrt{1 - u^2}v \right).$$

Apply the first polar change of variables $u = \rho \cos \alpha$, $v = \rho \sin \alpha$ so that

$$A = \rho \left(\sqrt{1 - \rho^2 \cos^2 \alpha \sin^2 \alpha} - \sin \alpha \sqrt{1 - \rho^2 \cos^2 \alpha} \right) =: \rho \tilde{A},$$

and we obtain two integrals

$$J_1^c := \int_0^{\frac{1}{2}} \frac{\lambda}{\sqrt{1-\lambda}} \int_0^{\frac{\pi}{4}} \int_0^{\frac{1}{2\cos\alpha}} \frac{(1 - \rho^2 \sin^2 \alpha)^{-1} \rho^2 d^{-1} \tilde{A}^2 d\rho d\alpha d\lambda}{\sqrt{\cos^2 \alpha (1 + \lambda) - 2\lambda \sqrt{1 - \rho^2 \cos^2 \alpha} \sin \alpha \tilde{A}}}, \quad (\text{C.5})$$

$$J_2^c := \int_0^{\frac{1}{2}} \frac{\lambda}{\sqrt{1-\lambda}} \int_{\frac{\pi}{4}}^{\frac{\pi}{2}} \int_0^{\frac{1}{2\sin\alpha}} \frac{(1 - \rho^2 \sin^2 \alpha)^{-1} \rho^2 d^{-1} \tilde{A}^2 d\rho d\alpha d\lambda}{\sqrt{\cos^2 \alpha (1 + \lambda) - 2\lambda \sqrt{1 - \rho^2 \cos^2 \alpha} \sin \alpha \tilde{A}}}. \quad (\text{C.6})$$

We apply a linear change of variables to fix the integration domain of the ρ variable. For the first integral, it holds that

$$J_1^c = \int_0^{\frac{1}{2}} \frac{\lambda}{\sqrt{1-\lambda}} \int_0^{\frac{\pi}{4}} \int_0^{\frac{1}{2}} \frac{t^2 d^{-1} \tilde{A}^2 \cos \alpha^{-3} dt d\alpha d\lambda}{\sqrt{1 - t^2 \tan^2 \alpha} \sqrt{\cos^2 \alpha (1 + \lambda) - 2\lambda \sqrt{1 - t^2} \sin \alpha \tilde{A}}},$$

wherein $\tilde{A} = \left(\sqrt{1 - t^2 \sin^2 \alpha} - \sin \alpha \sqrt{1 - t^2} \right)$. One can see that this integral converges at the optimal rate when we use the Gauss-Legendre rule for all the variables as neither of the terms inside the square roots vanish in the integration domain. For the second integral we have

$$J_2^c = \int_0^{\frac{1}{2}} \frac{\lambda}{\sqrt{1-\lambda}} \int_{\frac{\pi}{4}}^{\frac{\pi}{2}} \int_0^{\frac{1}{2}} \frac{t^2 d^{-1} \tilde{A}^2 \sin \alpha^{-3} dt d\alpha d\lambda}{\sqrt{1 - t^2} \sqrt{\cos^2 \alpha (1 + \lambda) - 2\lambda \sqrt{1 - t^2} \cot^2 \alpha \sin \alpha \tilde{A}}},$$

and where $\tilde{A} = \left(\sqrt{1 - t^2 \cos^2 \alpha} - \sin \alpha \sqrt{1 - t^2} \cot^2 \alpha \right)$. In contrast to J_1^c , one can easily verify that the integrated has one singularity in $(\lambda, \alpha) = (0, \frac{\pi}{2})$, so further transformations are needed. In particular, we use $z = \cos \alpha$, $x^2 = \lambda$. Thus, we have that

$$J_2^c = \int_0^{1/\sqrt{2}} \frac{2x^3}{\sqrt{1-x^2}} \int_0^{1/\sqrt{2}} \int_0^{\frac{1}{2}} \frac{t^2 d^{-1} \tilde{A}^2 (1 - z^2)^{-2} dt dz dx}{\sqrt{1 - t^2} \sqrt{z^2 (1 + x^2) - 2x^2 \sqrt{1 - z^2} - t^2 z^2 \tilde{A}}},$$

with $\tilde{A} = (\sqrt{1 - t^2 z^2} - \sqrt{1 - z^2 - t^2 z^2})$. Once again we make a polar change of variables $x = \sigma \cos(\phi)$, $z = \sigma \sin(\phi)$, and we obtain two integrals

$$J_{2,1}^c := \int_0^{\frac{1}{2}} \int_0^{\frac{\pi}{4}} \int_0^{1/(\sqrt{2} \cos \phi)} \frac{2(\sigma \cos \phi)^3 t^2 d^{-1} \tilde{A}^2 (1 - (\sigma \sin \phi)^2)^{-2}}{\sqrt{1 - (\sigma \cos \phi)^2} \sqrt{1 - t^2}} \\ \times \frac{d\sigma d\phi dt}{\sqrt{\sin^2 \phi (1 + (\sigma \cos \phi)^2) - 2 \cos^2 \phi \sqrt{1 - (\sigma \sin \phi)^2 (1 + t^2)}} \tilde{A}},$$

$$J_{2,2}^c := \int_0^{\frac{1}{2}} \int_{\frac{\pi}{4}}^{\frac{\pi}{2}} \int_0^{1/(\sqrt{2} \sin \phi)} \frac{2(\sigma \cos \phi)^3 t^2 d^{-1} \tilde{A}^2 (1 - (\sigma \sin \phi)^2)^{-2}}{\sqrt{1 - (\sigma \cos \phi)^2} \sqrt{1 - t^2}} \\ \times \frac{d\sigma d\phi dt}{\sqrt{\sin^2 \phi (1 + (\sigma \cos \phi)^2) - 2 \cos^2 \phi \sqrt{1 - (\sigma \sin \phi)^2 (1 + t^2)}} \tilde{A}},$$

where $\tilde{A} = (\sqrt{1 - t^2 (\sigma \sin \phi)^2} - \sqrt{1 - (\sigma \sin \phi)^2 (1 + t^2)})$. Finally, we take the corresponding change of variables needed to fix the integration domain for the σ variable, and we obtain

$$J_{2,1}^c = \int_0^{\frac{1}{2}} \int_0^{\frac{\pi}{4}} \int_0^{1/\sqrt{2}} \frac{2s^3 t^2 d^{-1} \tilde{A}^2 (1 - (s \tan \phi)^2)^{-2}}{\cos \phi \sqrt{1 - s^2} \sqrt{1 - t^2}} \\ \times \frac{ds d\phi dt}{\sqrt{\sin^2 \phi (1 + s^2) - 2 \cos^2 \phi \sqrt{1 - (s \tan^2 \phi) (1 + t^2)}} \tilde{A}},$$

with $\tilde{A} = (\sqrt{1 - t^2 (s \tan \phi)^2} - \sqrt{1 - (s \tan \phi)^2 (1 + t^2)})$. It is easy to see that the integrand has not singularities and as so it can be integrated with optimum rate using a tensorization of the Gauss-Legendre rule. For the second integral we have

$$J_{2,2}^c = \int_0^{\frac{1}{2}} \int_{\frac{\pi}{4}}^{\frac{\pi}{2}} \int_0^{1/\sqrt{2}} \frac{2(s \cot \phi)^3 t^2 d^{-1} \tilde{A}^2 (1 - s^2)^{-2}}{\sin \phi \sqrt{1 - (s \cot \phi)^2} \sqrt{1 - t^2}} \\ \times \frac{ds d\phi dt}{\sqrt{\sin^2 \phi (1 + (s \cot \phi)^2) - 2 \cos^2 \phi \sqrt{1 - s^2 (1 + t^2)}} \tilde{A}},$$

where $\tilde{A} = (\sqrt{1 - t^2 s^2} - \sqrt{1 - s^2 (1 + t^2)})$. Once again the integrand does not has singularities and the optimum rate of convergence is retrieved.

C.2.3. Integral I^d

As in the previous case we simplify the Integral I^d in (4.20) to the following integral

$$J^d := \int_{\frac{\sqrt{3}}{2}}^1 \int_{-\frac{\pi}{3}}^{\frac{\pi}{3}} \int_0^{\frac{1}{2}} \frac{\lambda A^2(r, \beta)}{4\pi \|\mathbf{r}(\mathbf{x}) - \mathbf{r}(\mathbf{x} + \lambda A(r, \beta) \mathbf{e}_{\theta+\beta})\|} \frac{(1-r^2)^{-\frac{1}{2}} r d\lambda d\beta dr}{\sqrt{1 - \|\mathbf{x} + \lambda A(r, \beta) \mathbf{e}_{\theta+\beta}\|^2}}, \quad (\text{C.7})$$

where we have only take the first interval for the β variable as the other case is similar. We have to make a transformation in λ, r : start by fixing the singularity $(\lambda, r) = (0, 1)$ to the origin of the new variables $r^2 = 1 - u^2$, $v^2 = \lambda$, by doing so we obtain

$$J^d := \int_0^{\frac{1}{2}} \int_{-\frac{\pi}{3}}^{\frac{\pi}{3}} \int_0^{1/\sqrt{2}} \frac{2v^3 d^{-1} A^2 dv d\beta dr}{\sqrt{1-v^2} \sqrt{(u^2(1+v^2) - 2v^2 \sqrt{1-u^2} \cos \beta A)}},$$

where $A = \sqrt{u^2 + (1-u^2) \cos^2 \beta} - \sqrt{1-u^2} \cos \beta$. Now, we make the polar change of variables $u = \rho \cos \alpha$, $v = \rho \sin \alpha$, which leads to

$$\begin{aligned} J_1^d &:= \int_{-\frac{\pi}{3}}^{\frac{\pi}{3}} \int_0^{\arctan(\sqrt{2})} \int_0^{1/(2 \cos \alpha)} \frac{d^{-1} 2(\rho \sin \alpha)^3 A^2}{\sqrt{1 - (\rho \sin \alpha)^2}} \\ &\quad \times \frac{d\rho d\alpha d\beta}{\sqrt{\cos^2 \alpha (1 + (\rho \sin \alpha)^2) - 2 \sin^2 \alpha \sqrt{1 - (\rho \cos \alpha)^2} \cos \beta A}}, \\ J_2^d &:= \int_{-\frac{\pi}{3}}^{\frac{\pi}{3}} \int_{\arctan(\sqrt{2})}^{\frac{\pi}{2}} \int_0^{1/(\sqrt{2} \sin \alpha)} \frac{d^{-1} 2(\rho \sin \alpha)^3 A^2}{\sqrt{1 - (\rho \sin \alpha)^2}} \\ &\quad \times \frac{d\rho d\alpha d\beta}{\sqrt{\cos^2 \alpha (1 + (\rho \sin \alpha)^2) - 2 \sin^2 \alpha \sqrt{1 - (\rho \cos \alpha)^2} \cos \beta A}}, \end{aligned}$$

with $A = \sqrt{(\rho \cos \alpha)^2 + (1 - (\rho \cos \alpha)^2) \cos^2 \beta} - \sqrt{1 - (\rho \cos \alpha)^2} \cos \beta$.

Finally we apply the corresponding linear transformation to fix the ρ integration domain,

$$J_1^d := \int_{-\frac{\pi}{3}}^{\frac{\pi}{3}} \int_0^{\arctan(\sqrt{2})} \int_0^{\frac{1}{2}} \frac{d^{-1} 2(t \tan \alpha)^3 A^2}{\cos \alpha \sqrt{1 - (t \tan \alpha)^2}} \\ \times \frac{dt d\alpha d\beta}{\sqrt{\cos^2 \alpha (1 + (t \tan \alpha)^2) - 2 \sin^2 \alpha \sqrt{1 - t^2} \cos \beta A}},$$

where $A = \sqrt{t^2 + (1 - t^2) \cos^2 \beta} - \sqrt{1 - t^2} \cos \beta$. This integrand is smooth: only possible singularities can occur when $\rho = 0$ but are eliminated by the numerator, and so the rate of convergence is optimal. Similarly for the second part as

$$J_2^d := \int_{-\frac{\pi}{3}}^{\frac{\pi}{3}} \int_{\arctan(\sqrt{2})}^{\frac{\pi}{2}} \int_0^{1/\sqrt{2}} \frac{d^{-1} 2t^3 A^2}{\sin \alpha \sqrt{1 - t^2}} \\ \times \frac{dp d\alpha d\beta}{\sqrt{\cos^2 \alpha (1 + t^2) - 2 \sin^2 \alpha \sqrt{1 - (t \cot \alpha)^2} \cos \beta A}},$$

where the new change of variables leads to

$$A = \sqrt{(t \cot \alpha)^2 + (1 - (t \cot \alpha)^2) \cos^2 \beta} - \sqrt{1 - (t \cot \alpha)^2} \cos \beta.$$

Once again the integrand is smooth and the optimal convergence rate is retrieved.

C.2.4. Integral I^e

Finally, we consider the simplification of I^e defined as in (4.21):

$$J^e := \int_{\frac{\sqrt{3}}{2}}^1 \int_{-\frac{\pi}{2}}^{-\frac{\pi}{3}} \int_{\frac{1}{2}}^1 \frac{\lambda A^2(r, \beta)}{4\pi \|\mathbf{r}(\mathbf{x}) - \mathbf{r}(\mathbf{x} + \lambda A(r, \beta) \mathbf{e}_{\theta+\beta})\|} \frac{rd\lambda d\beta dr}{\sqrt{1 - r^2} \sqrt{1 - \|\mathbf{x} + \lambda A(r, \beta) \mathbf{e}_{\theta+\beta}\|^2}},$$

we have again fixed the value of β to the first interval as other cases are similar. The analysis here follows that of the first part of J_1 (up until the first polar change of variables).

We obtain two integrals, the first one being

$$J_1^e = \int_{\frac{1}{2}}^1 \frac{\lambda}{\sqrt{1 - \lambda}} \int_0^{\frac{\pi}{4}} \int_0^{\frac{1}{2}} \frac{t^2 d^{-1} \tilde{A}^2 \cos^{-3} \alpha dt d\alpha d\lambda}{\sqrt{1 - t^2 \tan^2 \alpha} \sqrt{\cos^2 \alpha (1 + \lambda) - 2\lambda \sqrt{1 - t^2} \sin \alpha \tilde{A}}},$$

with $\tilde{A} = \left(\sqrt{1 - t^2 \sin^2 \alpha} - \sin \alpha \sqrt{1 - t^2} \right)$, and the second one

$$J_2^e = \int_{\frac{1}{2}}^1 \frac{\lambda}{\sqrt{1 - \lambda}} \int_{\frac{\pi}{4}}^{\frac{\pi}{2}} \int_0^{\frac{1}{2}} \frac{t^2 d^{-1} \tilde{A}^2 \sin \alpha^{-3} dt d\alpha d\lambda}{\sqrt{1 - t^2} \sqrt{\cos^2 \alpha (1 + \lambda) - 2\lambda \sqrt{1 - t^2} \cot^2 \alpha \sin \alpha \tilde{A}}},$$

where $\tilde{A} = \left(\sqrt{1 - t^2 \cos^2 \alpha} - \sin \alpha \sqrt{1 - t^2 \cot^2 \alpha} \right)$. Contrary to the first case, these integrands are not smooth due to the term $(1 - \lambda)^{-1}$. However, by using a Jacobi rule in λ one recovers the optimal convergence rate.

APPENDIX D. IMPLEMENTATION DETAILS FOR 3D SPECTRAL SCREEN SOLVER

We have already described a basic implementation of the spectral algorithm for 3d screens explained in Section 4.4.2. However many details were left off and will be explained in the present Appendix. In particular, we will explain some optimizations that were used, and also the overall structure of the associated computer library. This section complements the general description of the algorithm given in Section 4.4.2, is not intended to be self-contained as no details of the underlying mathematical algorithm are explained here.

The implementation was done in c++, the target machines were desktop x64 pcs. In more detail, we will consider that we have at our disposal a multicore processor (CPU), with three cache levels of memory typically around 32kb (L1, per core), 256kb (L2, per core), and 8Mb (L3 shared), working memory (ram) between 8 and 32Gb, and a graphical processor (GPU) with dedicated memory between 1 and 4Gb. We have explicitly detailed the memory available as it is a restriction to our algorithm ¹. We have also considered the option of using single or double-precision arithmetic, as more operations can be carried in parallel in single-precision mode, at cost of lower accuracy.

Now we proceed to detail the main sections of the library, they are described as separate classes of c++.

D.0.1. Screen Class

This class describes the geometry of the problem as a surface parametrized by polar coordinates $r \in [0, 1]$, $\theta \in [0, 2\pi]$. The main method returns the coordinates (in three-dimensional space) of the corresponding point given its r, θ -parameters. This method is callable from the CPU and GPU.

Also included in this class are auxiliary functions that are used for the computation of the hyper-singular operator.

¹If we have more memory available, we could in theory reduce the number of computations by storing results and re-use them. However, this will obviously reduce the size of the problems that can be solved.

D.0.2. Green Function Class

This class implements the Helmholtz fundamental solution ($G_k(\mathbf{x}, \mathbf{y})$). For the weakly-singular operator, the function is separated into a regular part ($R_k(\mathbf{x}, \mathbf{y})$), and a singular part ($S_k(\mathbf{x}, \mathbf{y})$), which are defined as

$$\begin{aligned} R_k(\mathbf{x}, \mathbf{y}) &= \frac{\sin(k\|\mathbf{x} - \mathbf{y}\|)}{4\pi\|\mathbf{x} - \mathbf{y}\|}, \\ S_k(\mathbf{x}, \mathbf{y}) &= \frac{\cos(k\|\mathbf{x} - \mathbf{y}\|)}{4\pi\|\mathbf{x} - \mathbf{y}\|}, \\ G_k(\mathbf{x}, \mathbf{y}) &= R_k(\mathbf{x}, \mathbf{y}) + iS_k(\mathbf{x}, \mathbf{y}). \end{aligned}$$

For the hyper-singular operator, the same functions are used, but they are multiplied by extra factors coming from the expression of the derivatives of the trial and test functions. As the screen class this one can also be instantiated from the cpu or gpu.

D.0.3. Disk Function Class

The Disk Function class is tasked to compute the functions $p_l^o, p_l^e, q_l^o, q_l^e$ defined in 4.2.3. The main part of these functions can be characterized in polar coordinates as the following product

$$P_{|m|}^l(\sqrt{1 - r^2})e^{im\theta},$$

where $P_{|m|}^l$ are the associated Legendre functions. The implementation of the latter is based on the code of the Wigner identities by Hidekazu Ikeno (Ikeno, 2016), which use a two-term recursion formula for the computation.

It is important to mention that the evaluation of the Legendre functions by the recursive formula could potentially lead to overflows. To deal with this, a small factor can be used to scale the terms, then make an iteration of the recursion, and finally re-scale the result. While for our ranges we do not observe this behavior we have included the scale factor (their current value is 1, but commented is the small factor in the case is needed).

As in the geometry and fundamental solution class, the disk functions can be instantiated from the CPU and GPU.

To increase the performance of the evaluation, since the square root of the first few integer values is repetitively used. We have declared a static variable that stores the square root of the first 259 integer values.

D.0.4. Quadratures

The Quadrature file contains a set of auxiliary functions that compute the weights and points of various Gaussian quadratures. The implementations are just an adaptation of John Burkardt codes (Burkardt, 2010).

D.0.5. Integration and Inside Integrator Class

Now we will explain how the integral operators are implemented using the tools provided by the classes that we previously presented. We will focus in the implementation of the weakly-singular operator, as for the hyper-singular only minor modifications are needed (see Section 4.4.2.4 for details). There are two groups of integrals that need to be computed for the implementation of the weakly-singular namely,

$$\begin{aligned}(I_S)_{m',m}^{l',l} &:= \int_{\mathbb{D}} \int_{\mathbb{D}} q_m^l(\mathbf{x}) S_k(\mathbf{r}(\mathbf{x}'), \mathbf{r}(\mathbf{x})) \overline{q_{m'}^{l'}(\mathbf{x}')} d\mathbf{x} d\mathbf{x}', \\ (I_R)_{m',m}^{l',l} &:= \int_{\mathbb{D}} \int_{\mathbb{D}} q_m^l(\mathbf{x}) R_k(\mathbf{r}(\mathbf{x}), \mathbf{r}(\mathbf{x}')) \overline{q_{m'}^{l'}(\mathbf{x}')} d\mathbf{x} d\mathbf{x}',\end{aligned}$$

where (l, m) and (l', m') are the index of trials and test functions, defined as in 4.2.3, \mathbb{D} is the unitary disk, and \mathbf{r} is the parametrization of the underlying open surface. For the second integral (regular case) the strategy is to split it into two 2-dimensional integrals as,

$$(I_R)_{m',m}^{l',l} = \int_0^{2\pi} \int_0^1 r' \overline{q_{m'}^{l'}(r', \theta')} \int_0^{2\pi} \int_0^1 R_k(\mathbf{r}(\mathbf{x}), \mathbf{r}(\mathbf{x}')) r q_m^l(r, \theta) dr d\theta dr' d\theta',$$

where $\mathbf{x} = (r \cos \theta, r \sin \theta)$. We implemented this as a two level integration. The lower level is the inside integrator class, which compute the following general integrals:

$$\begin{aligned} (I_R^1)_m^l &= \int_0^{2\pi} \int_0^1 f(r, \theta) r q_m^l(\mathbf{x}) dr d\theta, \\ (I_R^2)_m^l &= \int_0^{2\pi} \int_0^1 f(r, \theta) r \overline{q_m^l(\mathbf{x})} dr d\theta, \end{aligned}$$

where f is smooth given function. This inside integrator returns a vector for all the combinations $m + l$ even such that $0 \leq l \leq N$, $0 \leq m \leq l$ for a given integer N , the negatives values of m are obtained using the symmetry

$$q_{-m}^l = (-1)^m \overline{q_m^l},$$

and the fact that $R_k(\cdot, \cdot)$ is a real function. The integrals are computed using a tensorization of one dimensional quadrature rules. Notice that our inside integration class requires the evaluation of the functions $r q_m^l(\mathbf{x})$ on the tensorization of the quadrature points regardless of the integrand $f(r, \theta)$. Consequently, we only make this computation one time and stored them, then they can be used for different integrands. To be more precise, we store the multiplication of the previous functions by the quadrature weights, thus the inside integrator class store the following variables

$$(Q_m^l)_{i,j} = w_i^1 w_j^2 x_i^1 q_m^l(x_i^1, x_j^2), \quad 1 \leq i \leq N_q, \quad 1 \leq j \leq N_q^\theta.$$

where N_q, N_q^θ are the number of points for the quadrature rules $(x_i^1, w_i^1)_{i=1}^{N_q}$, and $(x_i^2, w_i^2)_{i=1}^{N_q^\theta}$ respectively. The storage of this evaluations is done in the cpu memory, as typically the gpu memory would not be enough. The higher level is the integrator class, which has two stages. In the first one, we iterate on the quadrature points and call the inside integrator for the function $f(r, \theta) = R_k(\mathbf{r}(\mathbf{x}), \mathbf{r}(\mathbf{x}'))$, where \mathbf{x}' is fixed for each iteration in the loop and \mathbf{x} is determined by the polar coordinates r, θ , which are the integration variable for the inside integrator. We notice that the computations for different \mathbf{x}' are independent, hence the external loop is done in parallel with a combination of CPU and GPU threads.

Once the first stage is finished we use the results as the input for a second call of the inside integrator and obtain the full integral. Again, this results in independent calls to the inside integrator that are done in parallel.

The computation of the singular integrals is more complicated as it involves number of cases and sub-cases with different changes of variables, the details are in Section 4.4.2. In general terms, using the structure of the test functions we can split each singular integral into a one dimensional integration of a three dimension integral as follows,

$$(I_S)_{m',m}^{l',l} = \int_0^{2\pi} e^{-im'\theta'} N_{m',m}^{l',l}(\theta') d\theta',$$

where,

$$N_{m',m}^{l',l}(\theta') := \int \int \int e^{im\theta(x_1,x_2,x_3,\theta')} \widetilde{q}_m^l(r(x_1, x_2, x_3)) \\ F(x_1, x_2, x_3, \theta') \widetilde{q}_{m'}^{l'}(r'(x_1, x_2, x_3)) dx_1 dx_2 dx_3,$$

where the exact range of variables x_1, x_2, x_3 depends of the particular change of variable. The functions \widetilde{q}_m^l are the associated Legendre part of the trial (test) functions, they only depend of the radial coordinate and are real, the exact expression for them are

$$\widetilde{q}_m^l(r) = \sqrt{\frac{(2l+1)(l-|m|)!}{2\pi(l+|m|)!}} \frac{P_{|m|}^l(\sqrt{1-r^2})}{\sqrt{1-r^2}},$$

where again, $P_{|m|}^l$ denotes the corresponding associated Legendre function. The function $F(x_1, x_2, x_3, \theta')$ is real and smooth and is obtained from the singular part of the fundamental solution multiplied by the factors that comes from the corresponding change of variables of the particular case and sub-case, we again refer to 4.4.2, and C.2 for the details. As in the regular case we use a two level strategy. The inside integrator computes the function $N_{m',m}^{l',l}(\theta')$ and the outer integration only iterates in the θ' variable (in parallel).

We remark that the matrix with entries $(I_S)_{m',m}^{l',l}$ is Hermitian, thus only one of the triangular parts has to be computed. Consequently, for a fixed θ' we only need a triangular

part of the function $N_{m',m}^{l',l}(\theta')$. Moreover using that F is a real function and the symmetry

$$\widetilde{q_{-m}^l} = (-1)^m \widetilde{q_m^l}$$

we can further reduce the total computations needed. To be more precise, if a maximum level N is selected. The total number of entries of the function $N_{m',m}^{l',l}(\theta')$ is:

$$\begin{cases} \frac{(N+2)^2((N+2)^2+4)}{32}, & N \text{ even,} \\ \frac{(N+1)(N+3)((N+1)(N+3)+4)}{32}, & N \text{ odd.} \end{cases}$$

In contrast the total entries of the matrix $(I_S)_{m',m}^{l',l}$ is

$$\frac{(N+1)^2(N+2)^2}{4}.$$

This means that our implementation is approximately 8 times faster than a direct computation of all the entries. Another important observation is that the functions r and r' , that are the norm of \mathbf{x} and \mathbf{x}' after the regularization produced by the change of variables, do not depend of θ' . Hence, as in the case of the regular integrator, for every case and sub case we can store the evaluations of the functions $\widetilde{q_m^l}$ and $\widetilde{q_{m'}^{l'}}$ for all the quadrature points on the x_1, x_2, x_3 variables.

When using N_q quadrature points for x_1, x_2, x_3 variables, the most computational intense part of the inside integrator consist of

$$N_q^3 \times \begin{cases} \frac{(N+2)^2((N+2)^2+4)}{32}, & N \text{ even,} \\ \frac{(N+1)(N+3)((N+1)(N+3)+4)}{32}, & N \text{ odd.} \end{cases},$$

multiplications. In half of the cases this can be reduced since radial coordinate of \mathbf{x}' only depends on x_1 , and not of the three quadrature variables x_1, x_2, x_3 . For these cases the

TABLE D.1. Computational cost in terms of number of multiplications.

	Number of Cases	Inside Integrator (C_I)	Total Operations
Regular Integrator	1	$(N_q^\theta N_q) \frac{(N+2)^2}{4}$	$2 C_I$
Singular Integrator 1	14	$N_q^3 \frac{(N+2)^2}{4} + N_q \frac{(N+2^2)((N+2)^2+4)}{32}$	$N_q^\theta C_I$
Singular Integrator 2	14	$N_q^3 \frac{(N+2^2)((N+2)^2+4)}{32}$	$N_q^\theta C_I$

inside integrator split the computations as

$$N_{m',m}^{l',l}(\theta') := \int \widetilde{q}_{m'}^{l'}(r'(x_1)) \widetilde{N}_m^l(x_1) dx_1,$$

$$\widetilde{N}_m^l(x_1) := \int \int e^{im\theta(x_1, x_2, x_3, \theta')} \widetilde{q}_m^l(r(x_1, x_2, x_3)) F(x_1, x_2, x_3, \theta') dx_2 dx_3.$$

And now the most computational intense part of the inside integrator consist of

$$N_q^3 \times \begin{cases} \frac{(N+2)^2}{4}, & N \text{ even}, \\ \frac{(N+1)(N+3)}{4}, & N \text{ odd}. \end{cases},$$

multiplications.

Assuming again that we use N_q quadrature points for x_1, x_2, x_3 variables, and N_q^θ quadrature points for the variable θ' , in the singular case, and N_q, N_q^θ for the corresponding variables x_1, x_2 . If the maximum level of functions, N , is even, the computational cost is summarized in Table D.1. If N is odd we need to replace $\frac{(N+2)^2}{4}$ for $\frac{(N+1)(N+3)}{4}$ in the Inside Integrator column.

The implementation of the Inside Integrator class, for both regular and singular integrator, has two different implementations, one for CPU execution and another for GPU execution (both can be used in parallel). To achieve the best performance possible, the CPU implementation was written in x86-assembly using AVX2 SIMD instructions².

²We have implementations for SSE4 and AVX2, in our current test machine (intel i7-4790K) the first perform better which suggest that the bottleneck is caused by memory operations.